RESEARCH ARTICLE

First report of *Eutrichosomella* Girault (Hymenoptera, Aphelinidae) from China, with description of a new species

Ye Chen[1], Hai-feng Chen[1]

1 *Hebei Key Laboratory of Animal Diversity, College of Life Science, Langfang Normal University, Langfang, 065000, China*

Corresponding author: Hai-feng Chen (chenhaifeng@lfnu.edu.cn)

Citation: Chen Y, Chen H-f (2021) First report of *Eutrichosomella* Girault (Hymenoptera, Aphelinidae) from China, with description of a new species. ZooKeys 1071: 1–9. https://doi.org/10.3897/zookeys.1071.71909

Abstract

The genus *Eutrichosomella* Girault is recorded for the first time from China (Yunnan Province), and *Eutrichosomella yunnanensis* **sp. nov.** (♀, ♂) is described and illustrated. A distribution map of this genus is presented.

Keywords

Aphelininae, Eutrichosomellini, Chalcidoidea, parasitic wasp, taxonomy

Introduction

The genus *Eutrichosomella* Girault, containing 11 valid species, is distributed in the Indomalayan and Australasian regions (Noyes 2019). Hosts of this genus are known for only three species, which were all reared from cockroach oothecae (Girault 1915; Hayat 2014; Hayat and Veenakumari 2016). *Eutrichosomella* differs from other genera of Aphelinidae by the following combination of characters: antenna with 6 antennomeres; mesopleuron convex, large and undivided; axilla large with small interaxillar

distance compared to most other Aphelinidae, and width of axilla at least equal to anterior width of mesoscutellum; axilla not exceeding anterior line of mesoscutellum (Figs 7, 13); scape not or very slightly ventrally expanded, at least 3× as long as wide; clava more than 2.5× as long as wide. Currently, *Eutrichosomella* and five other genera (*Saengella* Kim & Heraty, *Samariola* Hayat, *Mashimaro* Kim & Heraty, *Umairia* Hayat, and *Zubairia* Hayat) belong to the tribe Eutrichosomellini (Kim and Heraty 2012; Hayat 2014). Kim and Heraty (2012) discussed the phylogeny of Aphelininae based on morphological characters, with *Eutrichosomella* as the sister group to *Saengella*, *Samariola*, and *Mashimaro*.

Girault (1915) established *Eutrichosomella* and described three species from Australia: *E. albiclava* Girault, 1915, *E. blattophaga* Girault, 1915, and *E. multifasciata* Girault, 1915, designating *E. albiclava* as the type species. Later, Girault (1923, 1924) described another two Australian species, respectively *E. albifemora* Girault, 1923 and *E. aereiscapus* Girault, 1924. Timberlake (1941) described *E. insularis* Timberlake, 1941 from Nuku Hiva Island. *Eutrichosomella* was treated as an encyrtid (Timberlake 1941; Trjapitzin 1973) for a long time, until Hayat (1983) placed the genus within Aphelinidae. Hayat and Fatima (1990) transferred *Aphelinus voltairei* (Girault, 1921) to *Eutrichosomella*. These seven species described in the last century were all from the Australasian Region. The remaining four species, *E. indica* Singh & Srinivasa, 2010, *E. keralaensis* Manickavasagam & Menakadevi, 2012, *E. veenakumariae* Hayat, 2014 and *E. ibra* Hayat & Veenakumari, 2016 were all described from India.

In the present paper, we describe the twelfth species in the genus, *E. yunnanensis* sp. nov., from the Yunnan Province of China. This is the first report of the genus *Eutrichosomella* from China.

Material and methods

Samples were obtained using a pyrethroid fog generated from a thermal fogger (Swing-fog SN50, Germany, Model 2610E, Series 3). Specimens were dissected and mounted in Canada Balsam on slides, following the method described by Noyes (1982). Prior to slide mounting, specimens in ethanol were photographed with an Axiocam 305 color digital camera attached to a ZEISS Discovery V12 stereomicroscope. Slide-mounted specimens were photographed with a digital CCD camera attached to an Olympus BX53 compound microscope. Images were processed using Helicon Focus 6 and Adobe Photoshop CS5. Absolute measurements were made using Measurement Systems of the ZEISS Discovery V12 stereomicroscope. All measurements are given in micrometers (μm), except body length, which was measured in millimeters (mm). Scale bars are 100 μm except where otherwise indicated. In the descriptions below, measurements/ratios in parentheses after measurement/ratio ranges refer to the measurement/ratio of the holotype. The distribution map was generated with the SimpleMappr software (Shorthouse 2010) and ArcMap 10.4.1. All specimens listed below are deposited in Langfang Normal University (LFNU), Langfang, China.

Terminology follows the Hymenoptera Anatomy Consortium (2021) for most body parts except the linea calva, which follows Hayat (1998).

The following abbreviations are used in the text:

F1–3   funicle segments 1–3;
Gt$_1$, Gt$_2$ etc. tergites 1, 2, etc. of gaster.

Taxonomy

Eutrichosomella yunnanensis sp. nov.
http://zoobank.org/BE0EB460-BB33-446B-9FF0-958AC43FF96B
Figs 1–15

Type material. *Holotype*: CHINA • 1♀; Yunnan Province; Xishuangbanna; Mengla County; Menglun Town; 21°53.72'N, 101°17.08'E; 611m a.s.l.; 22 Aug. 2020; Y. Chen, H.-f. Zhao, Y.-g. Qin, Z.-g. Chen, leg.; LFNU A-Eut202101 [on slide]. *Paratypes*: 1♂; same data as holotype; LFNU A-Eut202102 [on slide]. 1♀; Yunnan Province; Xishuangbanna; Mengla County; Menglun Town; 21°54.28'N, 101°16.75'E; 629m a.s.l.; 25 Jun. 2019; Z.-l. Bai, Z.-g. Chen, Y.-j. Lin, C. Wang, Y.-f. Tong, H. Yu leg.; LFNU A-Eut202103 [on slide]. 1♀; Yunnan Province; Xishuangbanna; Mengla County; Menglun Town; 21°54'N, 101°16.9'E; 561m a.s.l.; 27 Jun. 2019; Z.-l. Bai, Z.-g. Chen, C. Wang, Y.-f. Tong, H. Yu leg.; LFNU A-Eut202104 [on slide].

Diagnosis. Females of *Eutrichosomella yunnanensis* sp. nov. can be distinguished from females of other species in this genus by the following combination of characters: dark brown gaster; characteristically pigmented forewing as in Figs 2, 8; long pedicel and F3 as in Fig. 6; linea calva broadening from the anterior forewing margin to the posterior forewing margin; long postmarginal vein, almost as long as the stigma vein (Fig. 8, inset) and location of setae on mesoscutellum as in Fig. 7.

Description. Female. Body length 1.18–1.63 mm (1.48 mm).

Coloration (Figs 1, 2). Head with face and malar space pale, vertex orange yellow and with dark setae, occiput pale. Eyes yellow, ocelli dark brown. Antenna with scape pale yellow and with ventral surface brown, pedicel pale brown to brown, funicle brown, clava with basal half to two thirds brown and remainder parts yellow. Mandible pale with apex dark. Pronotum yellow. Mesosoma mostly orange yellow, with lateral lobe of mesoscutum paler; propodeum with two brown patches interior to each spiracle. Mesopleuron pale. Forewing (Fig. 8) largely infuscated, with hyaline parts as follows: submarginal vein, a curved band adjacent to stigmal vein and apex narrowly. Hindwing (Fig. 9) infuscated medially and apically. Legs generally yellow and suffused with brown on tibiae and tarsomeres. Metasoma with petiole pale yellow, gaster mostly dark brown and with blue reflections, Gt$_1$ and third valvula brown yellow.

Head (Fig. 5), in frontal view, scaly reticulated, with the reticulation becoming elongate laterally. Frontovertex 0.3× head width, vertex with about 30 brown setae. Ocellar tri-
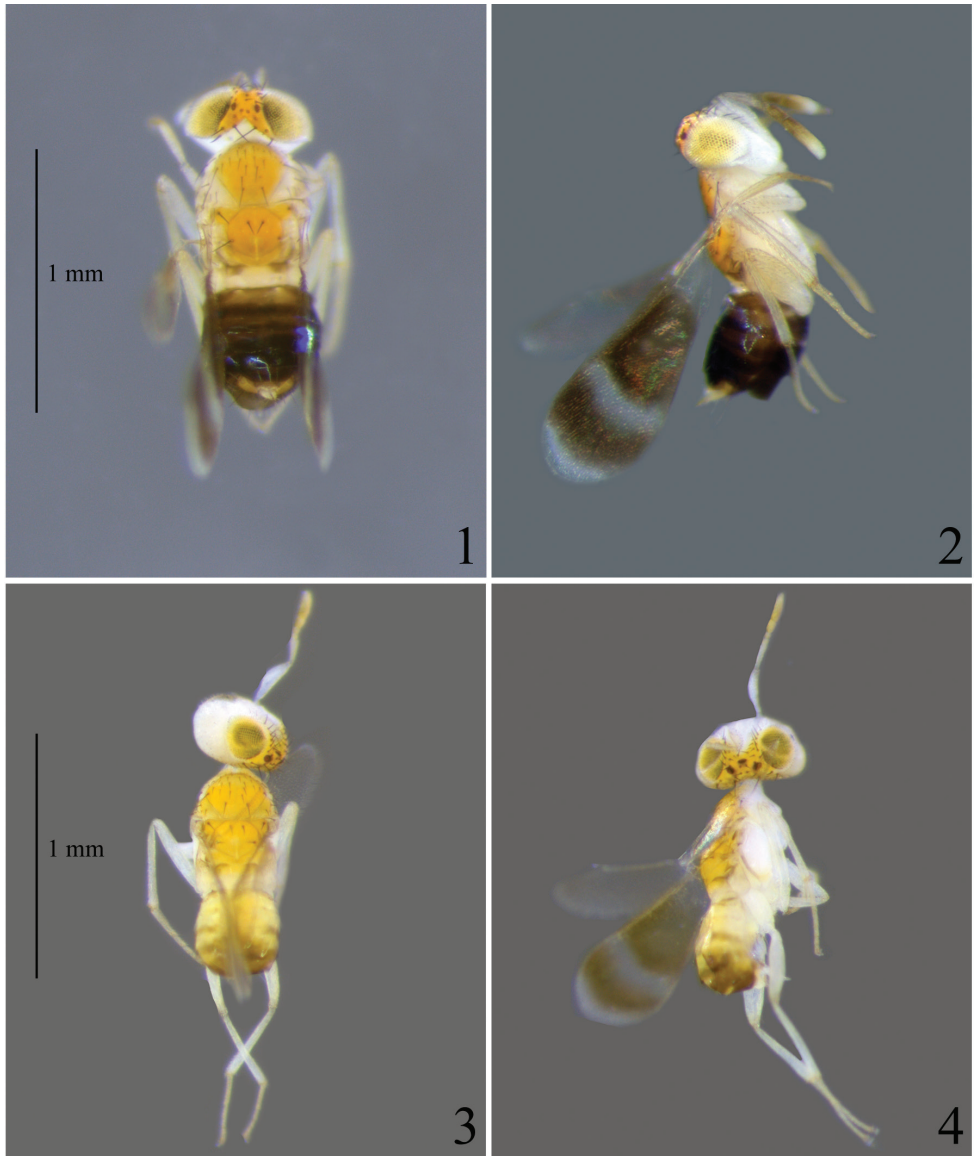
Figure 1–4. *Eutrichosomella yunnanensis* sp. nov., paratypes **1** body (♀), dorsal view **2** body (♀), lateral view **3** body (♂), dorsal view **4** body (♂), lateral view.

angle with apical angle acute. Mandible with two teeth and a truncation. Antenna (Fig. 6) with scape 4.3–4.6× (4.5×) as long as wide; pedicel 3.2–3.6× (3.6×) as long as wide, about as long as funicle segments combined; an anellus (Fig. 6, inset) is present between pedicel and F1; F1 transverse, with ventral margin a little longer than dorsal margin, 0.7–0.9× (0.9×) as long as wide; F2 quadrate, 1.2× as long as F1; F3 1.5–1.8× (1.8×) as long as wide, 1.3× as long as F1 and F2 combined; clava 3.0–3.7× (3.7×) as long as wide, 0.8× length
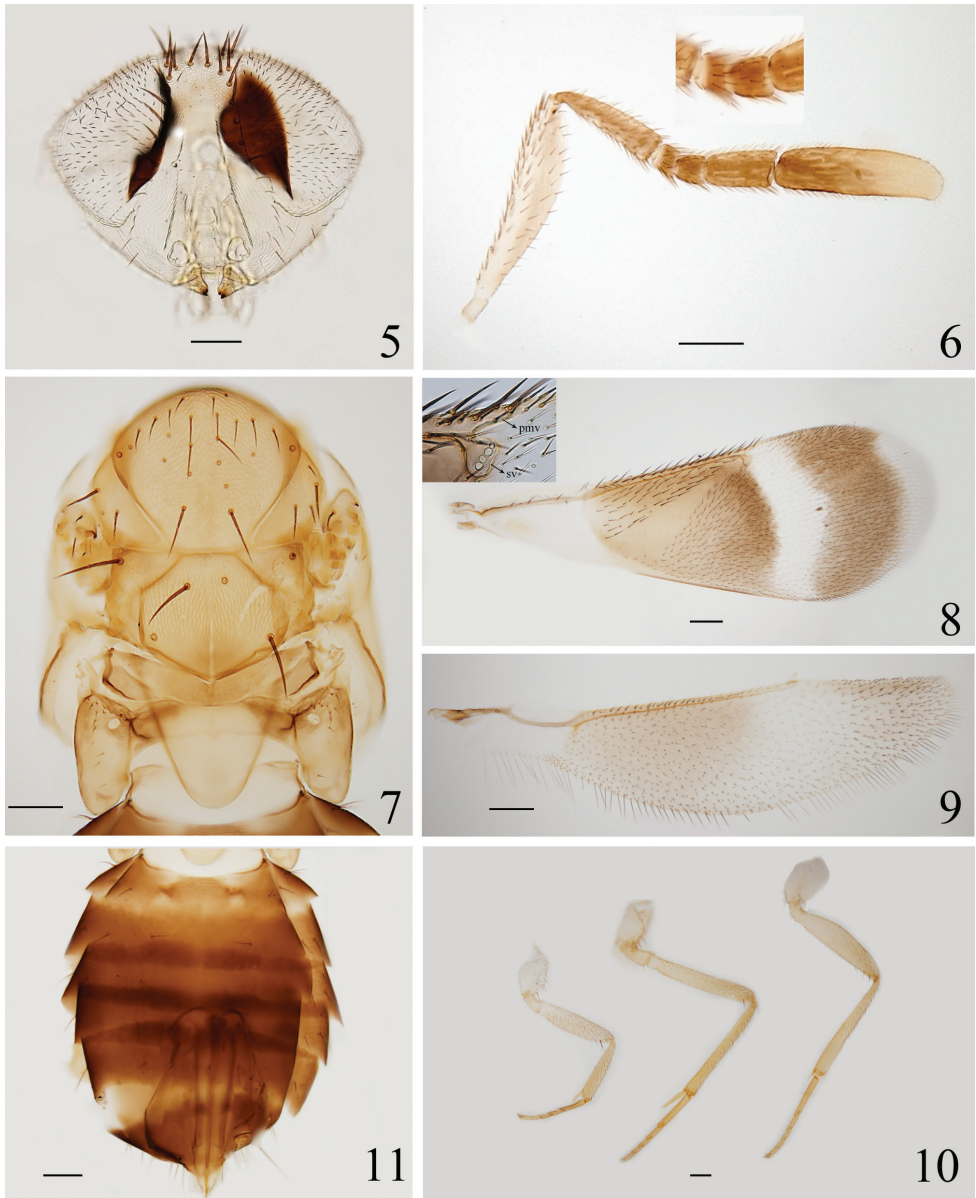
Figure 5–11. *Eutrichosomella yunnanensis* sp. nov., holotype **5** head **6** antenna **7** mesosoma **8** forewing, inset shows postmarginal vein (pmv) and stigma vein (sv) **9** hindwing **10** legs **11** gaster.

of scape, and 2.5–2.6× (2.6×) as long as F3. F3 and clava with 4 and 16 longitudinal sensilla, respectively. Measurements of holotype, length (width): scape, 320.9 (70.7); pedicel, 171.4 (47.6); F1, 37.0 (42.0); F2, 42.8 (42.8); F3 101.7 (57.3); clava, 256.4 (69.7).

Mesosoma (Fig. 7). Dorsum of mesoscutum polygonal reticulate, with the sculpture of lateral lobe of mesoscutum elongate on inner side; mesoscutellum mostly re-
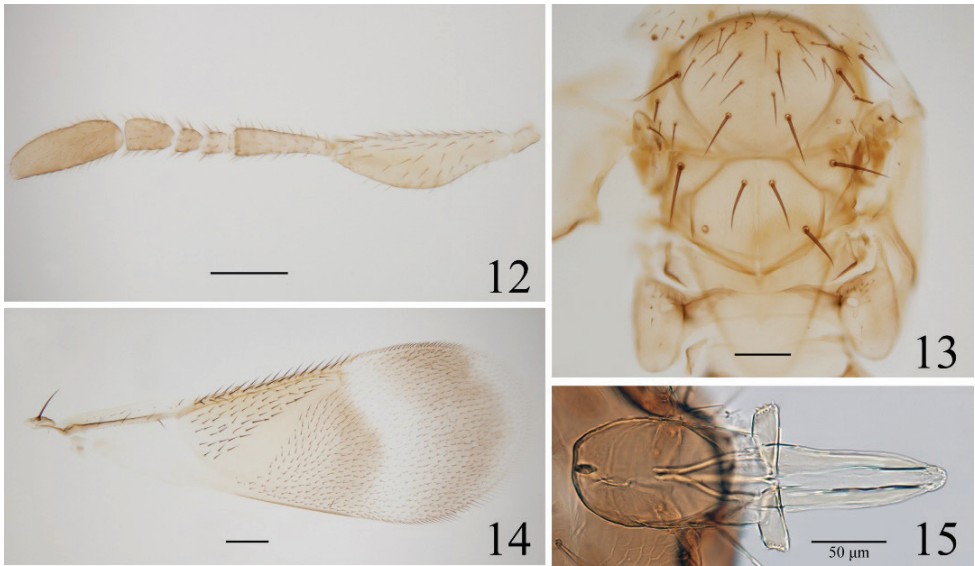
Figure 12–15. *Eutrichosomella yunnanensis* sp. nov., paratype (♂) **12** antenna **13** mesosoma **14** forewing **15** genitalia.

ticulate, smooth posteriorly, and with a pale longitudinal groove medially; metanotum reticulate on median region; propodeum smooth, but with finely polygonal reticulate sculpture on lateral sides. Pronotum with 4–5 rows of setae, the row along the posterior margin longer. Midlobe of mesoscutum 0.8× as long as wide, with 21–24 (24) setae, the seta on the anterolateral corner and the apical pair of setae long. Lateral lobe of mesoscutum with 3 or 4 setae. Axilla with 1 long seta, its width 1.3× anterior width of mesoscutellum. Mesoscutellum hexagonal, as long as wide, with two pairs of long setae located in anterior part and posterior part, respectively. Distance between anterior pair of scutellar setae 0.4× that between posterior pair. Placoid sensilla located in median region of mesoscutellum; distance between sensilla 0.5× that between posterior scutellar setae. Metanotum 0.7× as long as propodeum in median length. Propodeum with 13–15 (15) short setae (Fig. 7) proximal to spiracle, and with a digital projection on median area posteriorly.

Wings. Forewing (Fig. 8) 2.8× as long as wide. Costal cell 0.8× length of marginal vein, with 12 fine setae; submarginal vein with 5 setae; parastigma with 1 seta; marginal vein with 14 setae along anterior margin; postmarginal vein long, about as long as stigmal vein; stigmal vein swollen posteriorly and with 3 big and 1 small sensilla arranged nearly in a line (Fig. 8, inset). Linea calva becoming broader posteriorly, not closed. Hindwing (Fig. 9) 4.2× as long as wide, with longest marginal fringe 0.2–0.3× (0.3×) wing width. Measurements of holotype, length (width): forewing, 1441.6 (529.4); costal cell, 350; marginal vein, 460; postmarginal vein, 40; stigmal vein, 40; hindwing 1189.7 (282.4).

Legs (Fig. 10). Mesotibial spur 0.7× as long as corresponding basitarsus. Length measurements of holotype: mesotibia, 564.4; mesotibial spur, 147.1; mesobasitarsus, 216.

Metasoma (Fig. 11). Dorsum of metasoma generally smooth, except median area of Gt_1 and lateral sides of gasteral tergites with fine reticulations. Ovipositor originating from Gt_2 to apex of Gt_3, 0.8–0.9× (0.8×) as long as mesotibia and slightly exerted. Second valvifer 2.7× as long as third valvula; third valvula 0.6× as long as mesobasitarsus. Length measurements of holotype: ovipositor, 465.2; second valvifer, 340.7; third valvula, 124.5.

Male. Body length 1.16 mm. Similar to female except as follows. Forewing (Figs 4, 14) with the infuscate patches a little paler than in the female. Legs paler. Gaster (Fig. 3) with Gt_1 and Gt_2 yellow, Gt_3 mostly yellow and with a transverse short brown band on each lateral side, Gt_4 brown posteriorly, Gt_5–Gt_7 brown.

Head with ocellar triangle with apical angle obtuse. Antenna (Fig. 12) with scape expanded ventrally, 3.4× as long as wide; F1 and F2 subequal in length and width, F3 about as long as F1 and F2 combined. F3 and clava with 2 and 7 longitudinal sensilla, respectively. Genitalia (Fig. 15) with paramere 1.8× as long as wide; each digitus 0.3× length of paramere, with two short denticles and a fine seta at apex; aedeagus 1.5× as long as paramere and 1.2× as long as mesobasitarsus. Measurements, length (width): scape, 230.7 (67); pedicel, 122.1 (37); F1, 28.5 (30.5); F2, 31 (31); F3, 57.5 (42.3); clava, 149 (50); forewing 1185.2 (426.7); hindwing 1010 (210); mesotibia, 431.3; mesotibial spur, 96.9; mesobasitarsus, 168.6; genitalia, 245.3; paramere, 132.5; aedeagus, 198.8.

Host. Unknown.

Etymology. Named after the locality of type specimen.

Distribution. China (Xishuangbanna Dai Autonomous Prefecture of Yunnan Province).

Comments. This species does not run to any couplet in the key to Indian species of *Eutrichosomella* (Hayat & Veenakumari 2016), and differs from the four Indian species (*E. ibra*, *E. indica*, *E. keralaensis*, and *E. veenakumariae*) by the following combination of characters: antenna mostly brown with scape and apical of clava pale yellow to yellow (vs. antenna white to yellow, or antenna dark brown with a subapical band on scape and most of clava white; cf. fig. 3 in Manickavasagam and Menakadevi 2012), F3 1.5–1.8× as long as wide (vs. less than 1.4× as long as wide), forewing largely infuscated, with the following parts hyaline: the area below the submarginal vein, a curved band adjacent to the stigmal vein and apex narrowly (vs. forewing with broad or narrow infuscation below margin vein, without hyaline band adjacent to stigmal vein; forewing of *E. keralaensis* similar to the new species but with a large suboval hyaline spot in the median infuscate area; cf. fig. 6 in Manickavasagam and Menakadevi 2012), postmarginal vein of forewing long, about as long as stigmal vein (vs. absent, or three-fourths of stigmal vein), two pairs of setae on mesoscutellum located in anterior part and posterior part, respectively (vs. both located in posterior part; cf. fig. 4 in Hayat 2014, except *E. keralaensis*). Apart from the above differences, the new species can be distinguished from *E. keralaensis* by having scape 4.3–4.6× as long as wide (vs 3.1×), F1 a little wider than long and F2 quadrate (vs. F1 and F2 both 0.5× as long as wide), and propodeum with 13–15 setae proximal to spiracle (vs. at least 3, possibly 4, setae according to redescription of Hayat 2014).
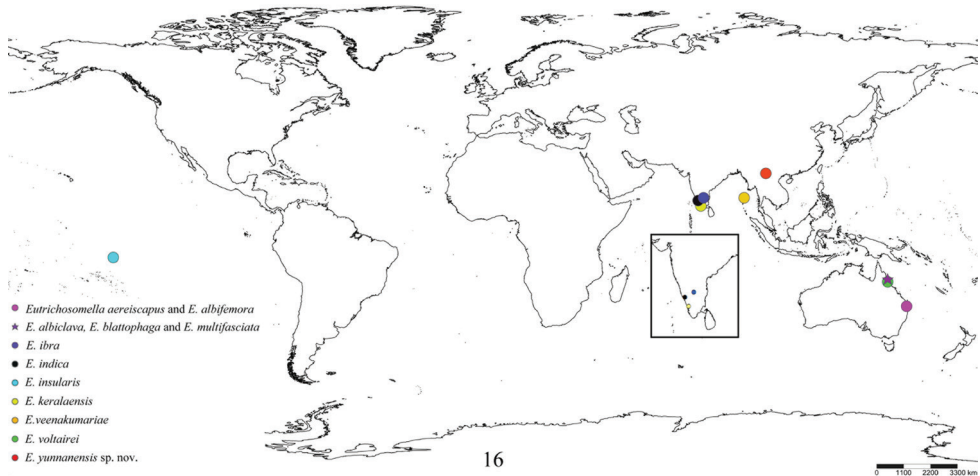
Figure 16. Distribution of all species of *Eutrichosomella* Girault 1915. Inset shows distributions of *E. ibra*, *E. indica*, and *E. keralaensis*.

Eutrichosomella yunnanensis sp. nov. seems morphologically close to *E. albiclava*. Based on Girault's description and images (QMDIU_03328–QMDIU_03335 from the Queensland Museum), *E. yunnanensis* differs from *E. albiclava* by following characters: color of gaster apparently darker than mesosoma in slide-mounted specimen (vs. nearly the same according to QMDIU_03330 and QMDIU_03331), pedicel about as long as funicle segments combined (vs. two thirds), F3 1.5–1.8× as long as wide (vs. a little longer than wide), forewing infuscated below marginal vein and subapically (vs. only infuscated below marginal vein, without any distal pigmentation, cf. QMDIU_03332).

Acknowledgements

References

Girault AA (1915) Australian Hymenoptera Chalcidoidea-VII. The family Encyrtidae with descriptions of new genera and species. Memoirs of the Queensland Museum 4: 1–184.

Girault AA (1921) Miscellaneous species of chalcid-flies from Australia (Hymenoptera, Chalcididae). Insecutor Inscitiae Menstruus 9: 186–191.

Girault AA (1923) Microscopitis, womanitis and new hexapods 7 pp. (private publication).

Girault AA (1924) Notes and description of Australian chalcid flies. I. Insecutor Inscitiae Menstruus 12: 1–9.

Hayat M (1983) The genera of Aphelinidae (Hymenoptera) of the World. Systematic Entomology 8: 63–102. https://doi.org/10.1111/j.1365-3113.1983.tb00467.x

Hayat M (2014) Eutrichosomellini (Hymenoptera: Chalcidoidea: Aphelinidae) from India, with description of two new genera. Zootaxa 3821(4): 425–442. http://dx.doi.org/10.11646/zootaxa.3821.4.2

Hayat M, Veenakumari K (2016) Description of three new species of Aphelinidae (Hymenoptera: Chalcidoidea) with some records from India. Journal of Insect Systematics 2(2): 106–119.

Hymenoptera Anatomy Consortium (2021) Hymenoptera Anatomy Ontology Portal. http://glossary.hymao.org [accessed 7 October 2021]

Hayat M, Fatima K (1990) Taxonomic studies on *Aphelinus* (Hymenoptera: Aphelinidae) 1. The Australian species described by A.A. Girault. Oriental Insects 24: 247–252. https://doi.org/10.1080/00305316.1990.11835539

Kim JW, Heraty J (2012) A phylogenetic analysis of the genera of Aphelininae (Hymenoptera: Aphelinidae), with a generic key and descriptions of new taxa. Systematic Entomology 37: 479–549. https://doi.org/10.1111/j.1365-3113.2012.00625.x

Manickavasagam S, Menakadevi C (2012) A new species of *Eutrichosomella* Girault (Chalcidoidea: Aphelinidae) from India, with additional records of chalcids. Madras Agricultural Journal 99(10–12): 877–881.

Noyes JS (1982) Collecting and preserving chalcid wasps (Hymenoptera: Chalcidoidea). Journal of Natural History 16: 315–334. https://doi.org/10.1080/00222938200770261

Noyes JS (2019) Universal Chalcidoidea Database. http://www.nhm.ac.uk/chalcidoids [accessed July 2021]

Shorthouse DP (2010) SimpleMappr, an online tool to produce publication-quality point maps. https://www.simplemappr.net [accessed 10 July 2021]

Singh S, Srinivasa YB (2010) Description of a new species of the genus *Eutrichosomella* Girault (Hymenoptera: Chalcidoidea: Aphelinidae) from the Western Ghats, India. Annals of Entomology 28(2): 1–5.

Timberlake PH (1941) Encyrtidae of the Marquesas and Society Islands (Hymenoptera, Chalcidoidea). Occasional Papers of the Bernice Pauahi Bishop Museum 16(9): 215–230.

Trjapitzin VA (1973) Classification of the parasitic Hymenoptera of the family Encyrtidae (Chalcidoidea). Part II. Subfamily Encyrtinae Walker, 1837. Entomologicheskoe Obozrenie 52(2): 416–429.

RESEARCH ARTICLE

ZooKeys

A peer-reviewed open-access journal

Launched to accelerate biodiversity research

A review of tangle-veined flies (Nemestrinidae, Diptera) in Egypt

Arafa Elsayed El-Hashash[1,2], Haitham Badrawy Mousa Badrawy[3], Ayman Mohyie-Eldin Ibrahim[1]

1 *Department of Taxonomy, Plant Protection Research Institute, Agricultural Research Centre, Dokki-Giza, Egypt* **2** *Plant Protection Department, Agricultural Faculty, Peoples' Friendship University of Russia, Moscow, Russia* **3** *Department of Entomology, Faculty of Science, Ain Shams University, Abbassia-Cairo, Egypt*

Corresponding author: Arafa Elsayed El-Hashash (arafa.Elhashash@yahoo.com)

Citation: El-Hashash AE, Badrawy HBM, Ibrahim AM-E (2021) A review of tangle-veined flies (Nemestrinidae, Diptera) in Egypt. ZooKeys 1071: 11–42. https://doi.org/10.3897/zookeys.1071.70743

Abstract

The Egyptian fauna of the genus *Nemestrinus* Latreille, 1802 is revised. In 1967, Steyskal and El-Bialy listed 12 species from the region, but only six species are now recognized. The primary type specimens of the species *N. aegyptiacus* (Wiedemann, 1828), *N. rufipes* (Olivier, 1810), and *N. lateralis* Wiedemann, 1828 (*N. lateralis* being a synonym of *N. rufipes*) deposited in the Museum für Naturkunde, Berlin, Germany were examined. Two species (*N. abdominalis* Olivier, 1811 and *N. fascifrons* (Bigot, 1888) are placed as new synonyms of *N. ater* (Olivier, 1811), and *N. ruficornis* Macquart, 1840 is synonymized with *N. rufipes* (Olivier, 1811). *Nemestrinus jullieni* (Efflatoun, 1925) is confirmed as a synonym of *N. aegyptiacus*. Furthermore, three species (*N. caucasicus* Fischer, 1806, *N. pallipes* (Olivier, 1811), and *N. persicus* Lichtwardt, 1909) have been removed and are doubtful records from Egypt. A key to the species, lists of specimens examined, and Illustrations and distributions for each species are provided. The status of species of doubtful occurrence in Egypt is discussed.

Keywords

Distribution, Egypt, Nemestrinus, taxonomy

Introduction

Nemestrinidae (tangle-veined flies) are a small dipteran family belonging to the suborder Brachycera-Orthorrhapha and occur all over the world, but are most abundant and diverse in the Palaearctic, Australian and Afrotropical Regions (Richter 1997; Pape et al. 2011). The family is classified into five subfamilies and comprises approximately 300 species worldwide in 23 genera, while 77 species in eight genera are known from the Palaearctic region (Richter 1997; Narchuk 2007; Papavero and Bernardi 2009; Pape et al. 2011).

The Nemestrininae comprise *ca.* 175 species worldwide in six genera (Bernardi 1973; Papavero and Bernardi 2009). In the Palaearctic Region, the Nemestrininae currently include approximately 67 species in two genera (*Nemestrinus* Latreille, and *Stenopteromyia* Lichtwardt) according to the last published catalogue by Richter (1988).

The genus *Nemestrinus* was described by Latreille in 1802 based on specimens collected from Egypt and Syria. It comprises 66 species in the Palaearctic Region (Bernardi 1973; Richter 1988, 1997; Narchuk 2007) and is characterized by the wing venation: The apical part of the wing occasionally has supernumerary transverse veins, R_3 is present, R_{3+4} and R_5 are free, M_1 and M_2 are free, the diagonal vein reaches the wing margin, and the proboscis is well developed and longer than the head. One of the important tools to separate nemestrinid species is the genitalia, composed of the well-developed hypandrium, partly fused with the gonocoxites with a linguiform apical projection bearing numerous hairs; and the elongate gonocoxal apodemes, which are sinuate and fused medially forming a dorsal bridge (Richter and Ovtshinnikova 1996; Richter 1997).

Nemestrinus is primarily distributed along the arid desert belt of the Palaearctic Region where several species occur in North Africa (Morocco, Algeria, Tunisia, Libya, and Egypt) and the Middle East (Arabia, Israel, Iran), east to Central Asia, as far as Mongolia and southern Russia, and in addition southern Europe (Bulgaria, Romania, Ukraine, France, Spain, and Turkey). The genus penetrates south into the Saharan part of the Afrotropical Region, being recorded from Sudan and Ethiopia (Bernardi 1973; Richter 1988, 1997). The type localities of seven species are situated in Egypt: *N. abdominalis* Olivier, 1811, *N. aegyptiacus* (Wiedemann, 1828), *N. ater* (Olivier, 1811), *N. fasciatus* (Olivier, 1811), *N. reticulatus* Latreille, 1802, *N. ruficornis* Macquart, 1840, and *N. rufipes* (Steyskal and El-Bialy 1967; Bernardi 1973; Richter 1988).

Two catalogues cover the nemestrinid fauna of Egypt: the monograph of Sack (1933) lists ten species and one variety [*Nemestrellus abdominalis*, *N. ater*, *N. exalbidus* (Lichtwardt, 1907), *N. fascifrons*, *N. ruficornis*, *N. rufipes*, *Nemestrinus aegyptiacus*, *Ne. a. var. jullieni*, *Ne. persicus*, *Ne. reticulatus*, and *Rhynchocephalus fasciatus*] in three genera (*Nemestrellus*, *Nemestrinus*, *Rhynchocephalus*), while Steyskal and El-Bialy (1967) list eleven species and one variety in the same three genera, adding *R. caucasicus* to Sack's monograph. There are also outdated works (e.g., Bequaert 1932, 1938) on the taxonomic status of the genus. Bernardi (1973) reviewed the world genera, and Richter (1988) presented the Palaearctic catalogue of Nemestrinidae; both listed ten species in Egypt, removing the same two species (*Nemestrinus caucasicus* and *N. persicus*) listed by Steyskal and El-Bialy (1967). Bernardi (1973) and Richter (1988) added *N. pallipes* that was not listed in Steyskal and El-Bialy (1967) as Egyptian species.

There is no modern comprehensive work identifying and cataloguing the Egyptian nemestrinine fauna. The subfamily in Egypt has never been monographed, and the genus is very much in need of a modern revision. This study was undertaken to revise, update, and clarify the taxonomic status of the species of genus *Nemestrinus* Latreille in the Egyptian fauna.

Materials and methods

Specimens examined in this study are deposited in the following collections:

ASUC   Entomology Department, Faculty of Science, Ain Shams University
AZUC   Faculty of Agriculture, Alfieri, Al Azhar University
CUC   Entomology Department, Faculty of Science, Cairo University
ESEC   Entomological Society of Egypt
MAC   Department of Taxonomy, Plant Protection Institute, Ministry of Agriculture
NHMW Naturhistorisches Museum Wien, Austria

The Museum für Naturkunde, Germany, Berlin (**ZMHB**) is the depository of type specimens of *N. aegyptiacus*, *N. rufipes*, and *N. lateralis* Wiedemann, 1828 (the latter is a synonym of the second species). We obtained this information by personal communication with Mr. Sven Marotzke and Ms. Elena Grigoryeva.

We could not access the types of other species because some are missing, as in the Egyptian Society of Entomology, wherein type specimens of the species *N. jullieni* have apparently been destroyed, and it is not known where the other types are. We examined and revised the original descriptions of all Egyptian nemestrinid species.

The Smithsonian National Museum of Natural History (**USNM**) has specimens of Nemestrinidae from Egypt: *N. abdominalis*, *N. aegyptiacus*, and *N. rufipes* that have all been identified by Dr. Torsten Dikow using our key. Redescriptions are based on series of specimens of each of these species and body measurements include genitalia.

Morphological terms follow McAlpine et al. (1981), Richter and Ovtshinnikova (1996), Richter (1997) and Cumming and Wood (2017). Line drawings of body parts were made by using a stereomicroscope at a magnification of 40×. We have access to the photographs by Ms. Elena Grigoryeva, Mr. Sven Marotzke, and Bernhard Schurian of the types that were downloaded at https://doi.org/10.7479/4wgc-dv22.

Taxonomic account

Nemestrinus

Nemestrinus Latreille, 1802: 437. Type species: *Nemestrinus reticulatus* Latreille, 1802: 437.
Rhynchocephalus Fischer, 1806: 219–220.

Andrenomyia Rondani, 1850: 189.
Heminemestrinus Bequaert, 1932: 21.
Symmictoides Bequaert, 1932: 105.
Nemestrellus Sack, 1933: 7.
Nemestrina Rondani, 1850: 189, 197: incorrect subsequent spelling of *Nemestrinus* Latreille, 1802 or subsequent usage of *Nemestrina* Blanchard, 1845: 468.

Remarks. Currently there are six species the Egyptian fauna (*N. aegyptiacus*, *N. ater*, *N. exalbidus*, *N. fasciatus*, N. *reticulatus*, and *N. rufipes*). The type specimens of *N. jullieni* deposited in ESEC have been destroyed by dermestid beetles and the types of the species *N. aegyptiacus* and *N. rufipes* and the type of latter's synonym *N. lateralis* are deposited in ZMHB.

Three species (*N. caucasicus N. pallipes*, and *N. persicus*) have been treated as doubtful since there is no evidence of their occurrence in Egypt. This is based on their known distributions as listed in the world catalogue by Bernardi (1973), the Palaearctic catalogue by Richter (1988), and the Systema Dipterorum (Thompson and Pape 2021). Additionally, the type localities of *N. caucasicus* and *N. persicus* are in the Caucasus, Iran, and Jaffa (Israel) respectively, not in Egypt.

Key to the Egyptian species of Nemestrinus

1 Wing without supernumerary transverse veins (Fig. 65)...................***N. fasciatus***
– Wing with supernumerary transverse veins, resulting in reticulate venation (Fig. 8) **2**
2 Small cells extending forward posterior to R1 (Fig. 27); frons shiny black with a transverse white band..***N. ater***
– Small cells extending forward posterior to R2 (Fig. 18); frons entirely pollinose or with a shiny spot...**3**
3 Small cells restricted between R2 and hind margin (Fig. 85); abdomen entirely black or grey with transverse black stripes **4**
– Small cells restricted between R2 and M1 or M2 (Figs 46, 90); abdomen orange with a longitudinal black vitta (Figs 57, 101) **5**
4 Abdomen entirely black (Fig. 1); frons entirely pollinose (Figs 4, 5) ....
   ....***N. aegyptiacus***
– Abdomen gray with incomplete transverse black stripes (Fig. 84); frons with a shiny spot (Figs 80, 81)...***N. reticulatus***
5 Frons yellowish black; vertex black; venter of abdomen black with yellowish incisions...***N. pallipes***
– Frons yellow or grey; vertex black or brown; venter of abdomen entirely orange or with black sides **6**
6 Frons yellow pollinose; tergum II with a transverse white band (Figs 2, 3, 91); venter of abdomen orange and black laterally......................................***N. rufipes***
– Frons grey pollinose; tergum II without a transverse white band (Fig. 47); venter of abdomen entirely orange...***N. exalbidus***

Nemestrinus aegyptiacus Wiedemann, 1828
Figures 1, 4–22

Nemestrinus aegyptiacus Wiedemann, 1828: 249.
Nemestrinus tripolitana Lichtwardt, 1907: 443.
Nemestrinus jullieni Efflatoun, 1925: 357.

Type material. *Nemestrinus aegyptiacus*: Syntype female, without date, Egypt (ZMHB) (pers. comm., Mr. Sven Marotzke). *Nemestrinus jullieni*: Type W. Hoff 29°53'02.6"N, 31°18'42.2"E , 15.iii.1922, Helwan 29°50'37.6"N, 31°19'05.0"E , 20.iii.1925; Lectotype male "W. Hoff 29°53'02.6"N 31°18'42.2"E, 23.iii.1922", Egypt (formerly ESEC, destroyed by dermestid beetles).

Specimens examined. *N. aegyptiacus*: Burg El-Arab 30°54'12.7"N, 29°33'13.7"E, 25.iii.1927 (1 f#), 25.iii.1934 (1 m#); Helwan 29°50'37.6"N, 31°19'05.0"E, 17.iii.1934 (1 f#), 16.iii.1935 (1 f#); W. dar El Maskhara 29°47'02.9"N, 31°24'59.9"E , 11.iv.1927 (1 f#); W. Garawi 29°47'43.9"N 31°25'54.9"E, 22.iii.1930 (1 f#), 31.iii.1930 (1 m#); W. Hoff 29°53'02.6"N, 31°18'42.2"E, 10.iii.1930 (2 m#) (AZUC); Abu Rawash 30°04'30.7"N, 31°11'59.7"E, 7.iii.1955 (9 m#), 8.iii.1955 (3 m# & 1 f#), 13.iii.1955 (4 m# & 3 f#), 17.iii.1955 (5 m# & 4 f#), 20.iii.1955 (2 m# & 5 f#); Giza 30°00'40.0"N, 31°11'31.4"E, 22.iii.1954 (1 m#), 17.v.1955 (1 m#); Helwan 29°50'37.6"N, 31°19'05.0"E, 17.iii.1934 (1 m#), 20.iii.1934 (1 m#), 3.iv.1934 (1 f#); Ogret El-Sheik 29°52'50.1"N, 31°18'27.8"E , 25.ii.1927 (1 m#); W. Garawi 29°47'43.9"N 31°25'54.9"E, 25.iii.1932 (1 f#); W. Rishrash 29°27'51"N, 31°22'2"E, 29.iii.1935 (1 f#); W. Silly Helwan 29°50'37.6"N, 31°19'05.0"E, 19.iii.1926 (1 f#); Ain Mousa 29°52'22.0"N, 32°39'00.7"E , 16.iii.1925 (2 f#) (CUC); Asyut (Lentil) 27°23'00.0"N, 31°44'38.0"E, 3.iii.1965 (2 m# & 6 f#); Ogret El-Sheik 29°52'50.1"N, 31°18'27.8"E, 21.iii.1926 (2 f#); Burg El-arab 30°54'12.7"N, 29°33'13.7"E, 25.iii.1927 (1 m#), 9.iii.1928 (1 m#); Kafr Hakim 30°04'39.7"N, 31°06'46.3"E, 24.iii.1924 (1 m#); Gerga (Eg. Lupia) 26°20'23.2"N, 31°53'21.3"E , 2.iv.1965 (2 f#); W. Hoff 29°53'02.6"N, 31°18'42.2"E, 21.iii.1922 (1 f#), 22.iii.1927 (1 m#); W. Morrah 22°22'39.1"N, 33°46'00.3"E, 25.iii.1921 (1 m#); W. Silly Helwan 29°50'37.6"N, 31°19'05.0"E, 23.iii.1926 (1 m#), 25.iii.1927 (2 f#) (MAC); Abu Mena 30°50'28"N, 29°39'49"E, 15.iii.1953 (1 m#), 8.iv.1954 (3 m#); Gabal Asfar 30°12'05.7"N 31°21'19.7"E, 9.iii.1951 (1 f#), 19.iii.1951 (1 f#); Kerdasa 30°01'32.1"N, 31°06'27.5"E, 14.iv.1951 (1 f#), 20.iii.1952 (1 f#) (ASUC); (1 m#), without data (NHMW) sent by Dr. Peter Sehnal; Egypt (1 f#), without date, (ZMHB) sent by Mr. Sven Marotzke and Bernhard Schurian; Cairo, Shoubra, 30°4'27.1632"N, 31°14'53.9844"E, 28.iii.1921 (1 m#), specimen number USNMENT01371555 (USNM) (identified by Dr. Torsten Dikow).

Specimens previously identified as *N. julieni:* Abu Rawash 30°04'30.7"N, 31°11'59.7"E, 7.iii.1955 (1 m#), 8.iii.1955 (1 m#), 13.iii.1955(1 m#); Burg El-Arab 30°54'12.7"N, 29°33'13.7"E, 25.iii.1934 (4 m# & 4 f#); W. Garawi 29°47'43.9"N, 31°25'54.9"E, 25.iii.1932 (2 f#), 21.iii.1930 (1 f#); W. Hoff 29°53'02.6"N, 31°18'42.2"E, 28.ii.1927 (1 m#); W. Um Elek 29°52'59.9"N, 31°31'00.1"E, 21.iii.1924 (1 f#) (CUC); Ain Mousa 29°52'22.0"N, 32°39'00.7"E , 16.iii.1925 (2

Figure 1. *Nemestrinus aegyptiacus*, female syntype **A** dorsal view **B** lateral view **C** frontal view **D** ventral view **E** labels (ZMHB).
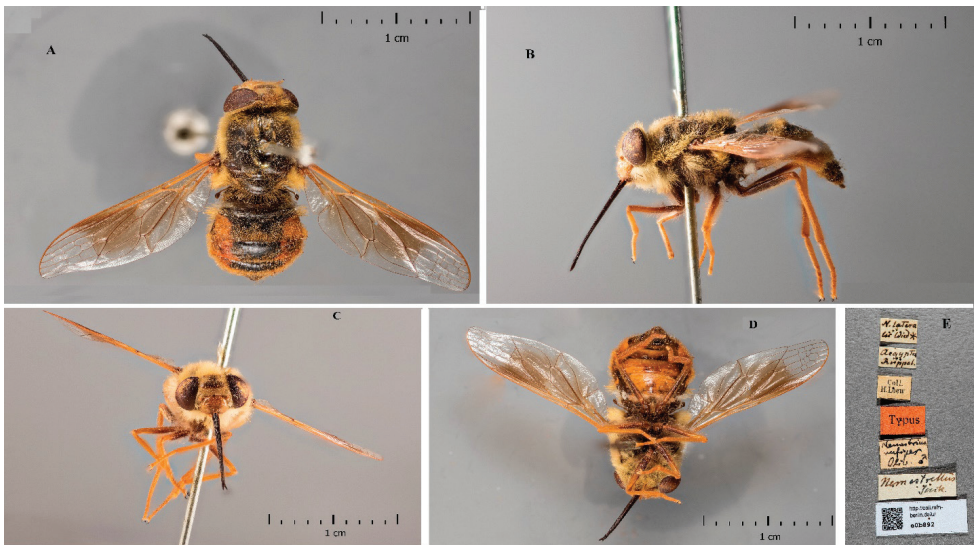

Figure 2. *Nemestrinus rufipes*, male type **A** dorsal view **B** lateral view **C** frontal view **D** ventral view **E** labels (ZMHB).

f#); Asyut (Lentil) 27°23'00.0"N, 31°44'38.0"E, 3.iii.1965 (1 m# & 2 f#); Burg El-Arab 30°54'12.7"N, 29°33'13.7"E, 14.iv.1920 (1 m#), 16.ii.1922 (1 f#),12.iv.1923 (1 f#),11.iv.1925 (1 m#), 18.iv.1925 (1 f#); Kafr Hakim 30°04'39.7"N, 31°06'46.3"E, 20.iv.1925 (1 f#); W. Garawi 29°47'43.9"N, 31°25'54.9"E, 14.iv.1928 (1 f#); W. Mor-
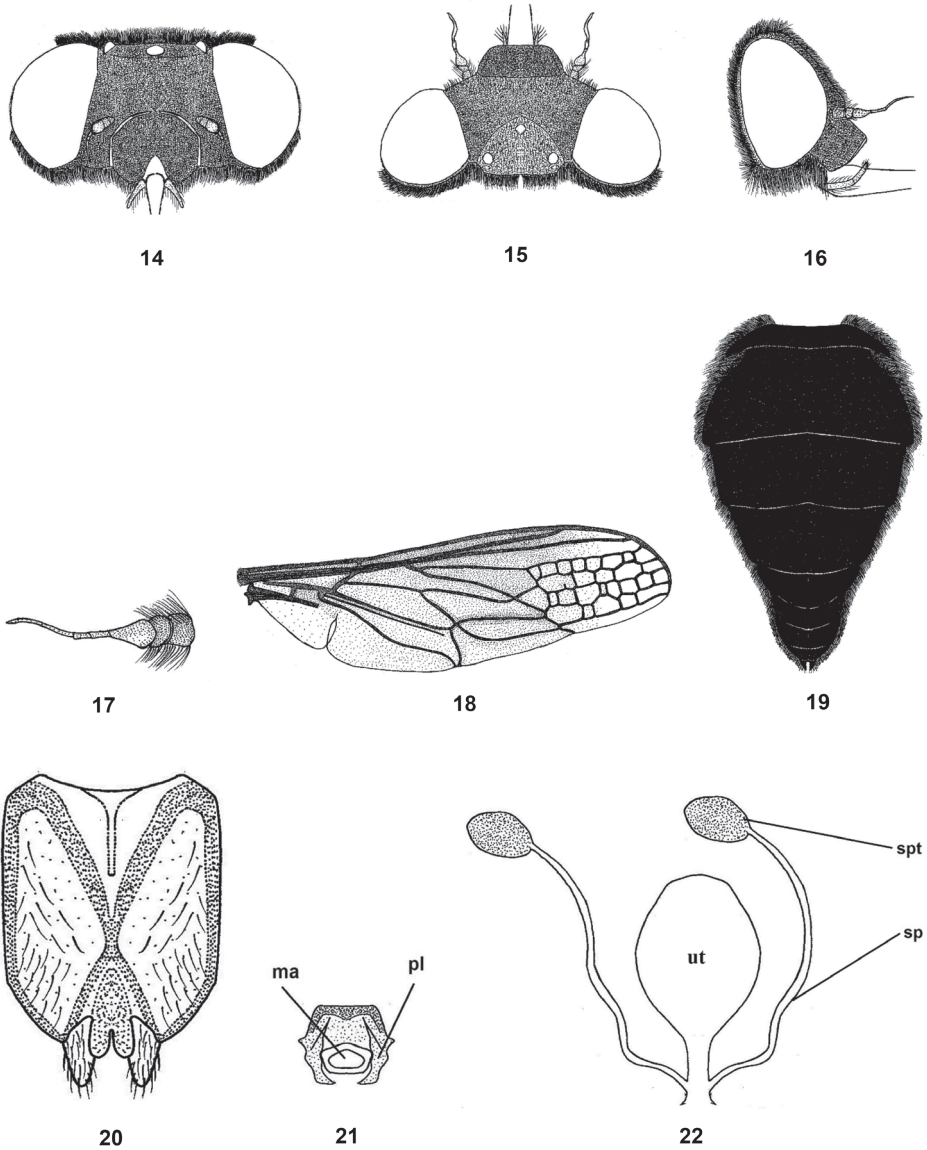
Figure 3. *Nemestrinus lateralis* (synonym), female syntype **A** dorsal view **B** lateral view **C** frontal view **D** Ventral View **E** Labels.

rah 22°22'39.1"N, 33°46'00.3"E, 25.iii.1927 (1 f#), W. Silly Helwan 29°50'37.6"N, 31°19'05.0"E, 19.iii.1926 (2 f#), 22.iii.1926 (1 f#), W. Um Elek 29°52'59.9" N, 31°31'00.1"E, 21.iii.1924 (1 f#) (MAC); Kosseir 26°06'26.2"N, 34°16'38.8"E, 24.ii.1965 (1 m#); W. Digla 29°59'00.1"N, 31°19'41.2"E, 5.iv.1952 (1 f#), 13.iii.1955 (1 m#); W. Natroun 30°25'58.2"N, 30°14'39.2"E, 13.iii.1955 (3 f# & 1 m#), (2 m# & 1 f#), without data (ASUC).

Diagnosis. Frons and face entirely yellow or grayish pollinosity; thorax completely shiny black with yellowish hairs; wing with many small cells restricted between R2 and hind margin; abdomen entirely black with short erect hairs. Male genitalia with only outer gonocoxal process; gonocoxal apodemes long, narrow, sinuate, fused medially and forming a narrow dorsal bridge; gonostyli wider than gonocoxal processes, ventrally with a cleft and small projection. Aedeagal complex with tapered aedeagus and lateral parameres, which are usually separated apically, fused with basal part of the aedeagus; parameral apodeme rather long; ejaculatory apodeme long and broad.

Redescription. Length: male body 14–17 mm, wing 13.5–15 mm. Female body 14–20 mm, wing 13.5–16.5 mm. Head wider than thorax; frons with yellow or grayish yellow pollinosity, with rather long hairs, at antennal elevation frons wide but narrowing toward vertex; face relatively shorter than high, with dull pollinosity, its hairs similar to those of the frons (Figs 4–6, 14–16); antenna entirely blackish brown to black, scape and pedicel with long hairs (Figs 7, 17). Thorax shiny black; mesonotum with dense pale yellow hairs but rather long; pleurae with tuft-like hairs. Leg hairy,

Figures 4–13. Male of *Nemestrinus aegyptiacus*, head, frontal (**4**), head, dorsal (**5**), head, lateral (**6**), antenna (**7**), wing (**8**), abdomen (**9**). **10–13** male genitalia: epandrium, proctiger, and cerci (**10**), gonocoxite with gonostylus, ventral (**11**), aedeagal complex, lateral (**12**) and dorsal (**13**). Abbreviations: aedg. aedeagus, aec. aedeagal complex, aedg tn. aedeagal tine A2. anal vein, al. alula, ant. Antenna, bm. basal medial cell, br. basal radial cell, c. cerci, C. costa, CuA1,2, CuP. cubital veins, d. discal cell, db. dorsal bridge, DV. diagonal vein, e. epandrium, ej. ejaculatory apodeme, enaedg pr. endoaedeagal process, fc. Face, 1st fl. first flagellomere, fr. Frons, gap. gonocoxal apodeme, gc. gonocoxite, gpr. gonocoxal process, gs. gonostylus, h. hypandrium, h. humeral cross vein, lat ej pr. lateral ejaculatory process, m3. third medial cell, pm. parameres, pm ap. parameral apodeme, pr. proctiger, pt. phallic plate, M1, M2, M3. medial veins, m-cu. cross vein between medial and cubital veins, pd, pedicel, plp. Palpus, R1, R2, R3+4, R5,Rs. radial veins, r-m. cross vein between redial and medial veins, Sc. subcostal vein, sc. Scape, st. stylus, vt. vertex.

yellowish brown with black femora. Wing smoky brown, except apex and posterapical margin clear and transparent (Figs 8, 18). The differences in cell number and structure on the wing is continuous variation and inconsistently different between

14   15   16

17   18   19

20   21   22

Figures 14–22. Female of *Nemestrinus aegyptiacus*, head, frontal (**14**), head, dorsal (**15**), head, lateral (**16**), antenna (**17**), wing (**18**), and abdomen (**19**). **20–22** female genitalia: subgenital plate (**20**), genital furca (**21**), and spermathecae (**22**). Abbreviations: ma. median aperture, pl. posterolateral projection, sp. spermatheca, spd. spermathecal duct, ut. uterus.

males and females. Abdomen entirely shiny black, covered with yellowish pubescence except the venter is blackish, which is rather short and erect, excluding dorsal side of two basal segments and on lateral margins of second segment where it is much longer and tufted, also on hind margin of each segment appear as narrow light bands (Figs 9, 19). Male genitalia with only outer gonocoxal process; gonocoxal apodemes long, nar-

row, sinuate, fused medially, and forming a narrow dorsal bridge; gonostyli wider than gonocoxal processes, ventrally with a cleft and small projection (Figs 10, 11). Aedeagal complex with tapered aedeagus and lateral parameres, which are usually separated apically, fused with basal part of aedeagus; parameral apodeme rather long; ejaculatory apodeme long and broad (Figs 12, 13). Female genitalia with subgenital plate rectangular with two hairy lobes (Fig. 20); genital furca free, narrow, with broadened ends of posterior projections, bent medially; median aperture of genital furca nearly triangular (Fig. 21); uterus rounded, with two narrow and rather long spermathecae (Fig. 22).

Local distribution. Coastal strip, Lower Nile.

Geographical distribution. Algeria, Egypt, Libya, Morocco, Italy (Sicily), and Tunisia (Sack 1933; Bernardi, 1973; Richter 1988).

Remarks. After examining the female type specimen of *Nemestrinus aegyptiacus* (Fig. 1) and comparing it with a large series of specimens identified as *Nemestrinus jullieni* Efflatoun (some specimens were by seen by him but it is not clear who determined the identification), we confirm this identification, and it is clear that both are the same species. Hence, *N. jullieni* is placed as a synonym instead of a subspecies based on examination of the series of specimens and dissections of genitalia of both *N. aegyptiacus and N. jullieni* and the female type specimen of *N. aegyptiacus*, and comparisons with the genitalia figures of Bernardi's (1973: figs 54–56) *N. aegyptiacus*.

Nemestrinus ater Olivier, 1811
Figures 23–41

Nemestrinus ater Olivier, 1811: 171.
*Nemestrinus abdominalis* Olivier, 1811: 171. Syn. nov.
Nemestrinus nigra Wiedemann, 1828: 560.
Nemestrinus osiris Wiedemann, 1828: 561.
Nemestrina fascifrons Bigot, 1888: 8. Syn. nov.

Type locality. Egypt.

Specimens examined. Abu Rowash 30°04'30.7"N, 31°11'59.7"E, 24.ii.1926 (1 f#), 26.ii.1927 (1 f#); Rafah 31°17'03.0"N, 34°14'18.0"E , 25.iv.1921 (1 f#); W. Garawi 29°47'43.9"N, 31°25'54.9"E, 31.iii.1930 (1 f#) (AZUC); W. Garawi 29°47'43.9"N, 31°25'54.9"E, 22.iii.1930 (1 f#), 31.iii.1930 (1 f#) (CUC); Abu Qir 31°18'42.4"N, 30°03'37.3"E, 26.iii.1915 (1 f#); (Noaman Bey) Alexandria 31°10'03.5"N, 29°51'56.2"E, (1 f#, without date); Dekheila 31°07'32.0"N, 29°48'37.3"E, 4.iii.1928 (1 f#); Dekheila Mariut 31°07'32.0"N, 29°48'37.3"E, 24.v.1925 (1 f#); Burg El-Arab 30°54'12.7"N, 29°33'13.7"E, 19.iv.1928 (1 f#); Gabal Abu Rowash 30°04'30.7"N, 31°11'59.7"E, 13.ii.1924 (1 f#); 19.iii.1924 (1 f#); Kafr Hakim 30°04'39.7"N, 31°06'46.3"E, 24.iii.1925 (1 f#), 20.iii.1926 (1 f#); Man-
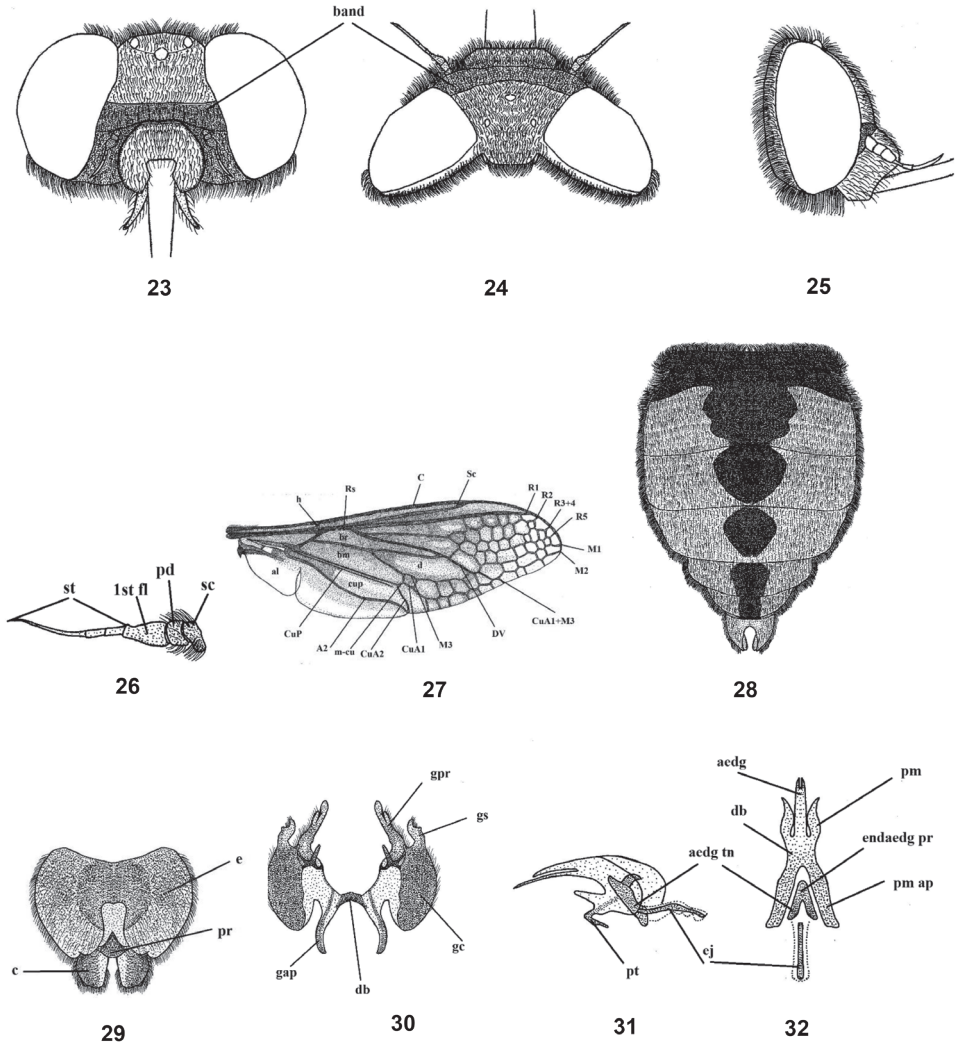
Figures 23–32. Male of *Nemestrinus ater*, head, frontal (**23**), head, dorsal (**24**), head, lateral (**25**), antenna (**26**), wing (**27**), and abdomen (**28**). **29–32** male genitalia: epandrium, proctiger, and cerci (**29**), gonocoxite with gonostylus, ventral (**30**), aedeagal complex, lateral (**31**) and dorsal (**32**). Abbreviations: aedg. aedeagus, aec. aedeagal complex, aedg tn. aedeagal tine A2. anal vein, al. alula, bm. basal medial cell, br. basal radial cell, c. cerci, C. costa, CuA1,2, CuP. cubital veins, d. discal cell, db. dorsal bridge, DV. diagonal vein, e. epandrium, ej. ejaculatory apodeme, endaedg pr. endoaedeagal process, 1st fl. first flagellomere, gap. gonocoxal apodeme, gc. gonocoxite, gpr. gonocoxal process, gs. gonostylus, h. hypandrium, h. humeral cross vein, lat ej pr. lateral ejaculatory process, m3. third medial cell, pm. parameres, pm ap. parameral apodeme, pr. proctiger, pt. phallic plate, M1, M2, M3. medial veins, m-cu. cross vein between medial and cubital veins, pd. pedicel, R1, R2, R3+4, R5,Rs. radial veins, r-m. cross vein between redial and medial veins, Sc. subcostal vein, sc. Scape, st. stylus.

souriah 29°58'05.3"N, 31°08'51.9"E, 4.iii.1934 (2 f#); Burg El-Arab 30°54'12.7"N, 29°33'13.7"E, 18.iv.1925 (1 f#); Marsa Matrouh 31°11'04.1"N, 27°15'42.4"E, 17.iii.1933 (2 f#); Suize 29°58'09.6"N, 32°32'59.8"E, 5.iv.1927 (1 f#); Sinai N.E. 31°15'49.4"N, 34°10'15.8"E, 19.iv.1928 (1 f#); W. Silly Helwan 29°50'37.6"N, 31°19'05.0"E, 22.iii.1926 (1 f#) (MAC); Abu Rawash 30°04'30.7"N, 31°11'59.7"E, 26.iii.1952 (1 f#); Gabal Asfar 30°12'05.7"N, 31°21'19.7"E, 9.iii.1951 (1 f#); Mansoura 31°02'43.1"N, 31°22'54.9"E, 2.iii.1955 (1 f#); Mansouriah 29°58'05.3"N, 31°08'51.9"E, 12.iii.1952 (1 f#); Pyramids 30°04'39.8"N, 31°00'53.4"E, 12.iii.1951 (1 f#); W. Natroun 30°25'58.2"N, 30°14'39.2"E, 2.iv.1951 (1 f#) (ASUC).

Specimens previously identified as *N. fascifrons:* Abu Rowash 30°04'30.7"N, 31°11'59.7"E, 6.ii.1926 (2 m#); Helwan 29°50'37.6"N, 31°19'05.0"E, 18.iii.1927 (1 m#), 7.iii.1930 (1 m#); Mansouriah 29°58'05.3"N,31°08'51.9"E , 18.ii.1926 (1 m#); Mariut 31°08'32.5"N, 29°54'10.5"E , 5.iv.1921 (1 m#); W. Garawi 29°47'43.9"N, 31°25'54.9"E, 22.iii.1930 (1 m#), 31.iii.1930 (1 f#); W. Morrah 22°22'39.1"N, 33°46'00.3"E, 26.iii.1927 (1 m#) (AZUC); Kafr Hakim 30°04'39.7"N, 31°06'46.3"E, 20.iii.1926 (1 m#); Mansouriah 29°58'05.3"N, 31°08'51.9"E, 13.ii.1926 (1 m#), 2.iii.1927 (1 m#); W. Garawi 29°47'43.9"N, 31°25'54.9"E, 22.iii.1930 (1 m#), 31.iii.1930 (2 m#) (CUC); Dekheila 31°07'32.0"N, 29°48'37.3"E, 4.ii.1928 (2 m#), 4.iii.1928 (1 m#); Burg El-Arab 30°54'12.7"N, 29°33'13.7"E, 19.iv.1923 (1 m#); Kerdasa 30°01'32.1"N, 31°06'27.5"E, 15.ii.1923 (1 m#), 10.ii.1925 (1 m#); Mansouriah 29°58'05.3"N, 31°08'51.9"E, 13.ii.1926 (1 m#), 6.iii.1926 (1 m#); Burg El-Arab 30°54'12.7"N, 29°33'13.7"E, 27.iv.1923 (1 m#), 18.iv.1925 (5 m#); (Six Towers) Suize Road 29°59'45.9"N, 32°29'34.4"E , 26.iii.1926 (1 m#); Gabal Asfar 30°12'05.7"N, 31°21'19.7"E, 9.iii.1951 (1 m#); Mansoura 31°02'43.1"N, 31°22'54.9"E, 2.iii.1955 (1 m#) (ASUC).

Specimens previously identified as *N. abdominalis:* Egypt (1 f#), without date, specimen number USNMENT01371553 (USNM) (previously identified by W. Wirth as *N. abdominalis* but as *N. ater* by Dr. Torsten Dikow using our key).

Diagnosis. Frons shiny black with a transverse white band; wing with small cells extending forward from R1 to hind margin; abdomen orange with longitudinal black vitta in male but entirely black in female.

Redescription. Length: male body 10–16 mm, wing 9–15 mm. Female body 14–21 mm, wing 10–13 mm. Male: Frons shiny black with transverse white band; face rather short, snout-like, sides with grayish yellow pollinosity (Figs 23–25). Antenna blackish and pollinose (Fig. 26).

Thorax black or blackish brown, with blackish to yellowish brown hairs, pleurae with long and dense black hairs; leg blackish or dark yellow; claws well developed; pulvilli almost rudimentary. Wing blackish brown, but apex and postero-apical margin pale brown; wing with many small cells extend forward from R1 to hind margin (Fig. 27). Abdomen short, wide, reddish to orange with longitudinal black strip that is narrow posteriorly and sometimes absent at apex (Fig. 28). Male genitalia with gonocoxite having two processes, inner process short and slender, whereas the outer process is longer, thicker and subapically curved; gonostyli longer than the inner gonocoxal processes but shorter than the outer one, with subapical cleft and small projection (Figs
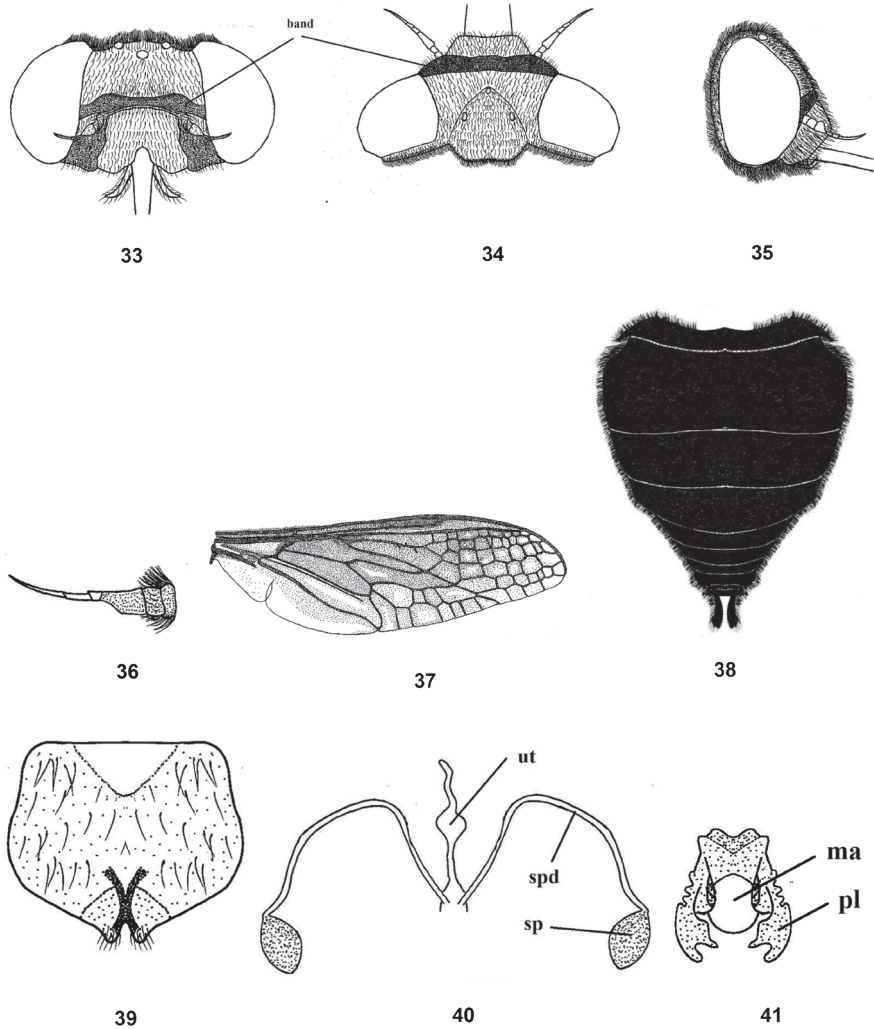
Figures 33–41. Female of *Nemestrinus ater*, head, frontal (**33**), head, dorsal (**34**), head, lateral (**35**), antenna (**36**), wing (**37**), and abdomen (**38**). **39–41** female genitalia: subgenital plate (**39**), genital furca (**40**), and spermathecae (**41**). Abbreviations: ma. median aperture, pl. posterolateral projection, sp. spermatheca, spd. spermathecal duct, ut. uterus.

29, 30); aedeagus free, narrow distally and fused proximally with parameres; parameres slightly sinuate; parameral apodeme a long, while aedeagal tine is short; ejaculatory apodeme slender and narrow (Figs 31, 32). Female. Similar as male (Figs 33–37), except: eyes widely separated more than in male. Abdomen entirely black or at least with reddish black lateral margins (Fig. 38). Head in male slightly wider than thorax but in female narrower than thorax. Female genitalia with quadrate subgenital plate, bilobed distally (Fig. 39); genital furca with furcated arms and serrated laterally (Fig. 40); uterus small, with terminal accessory process; spermathecal ducts narrow and long with oval medium spermathecae (Fig. 41).
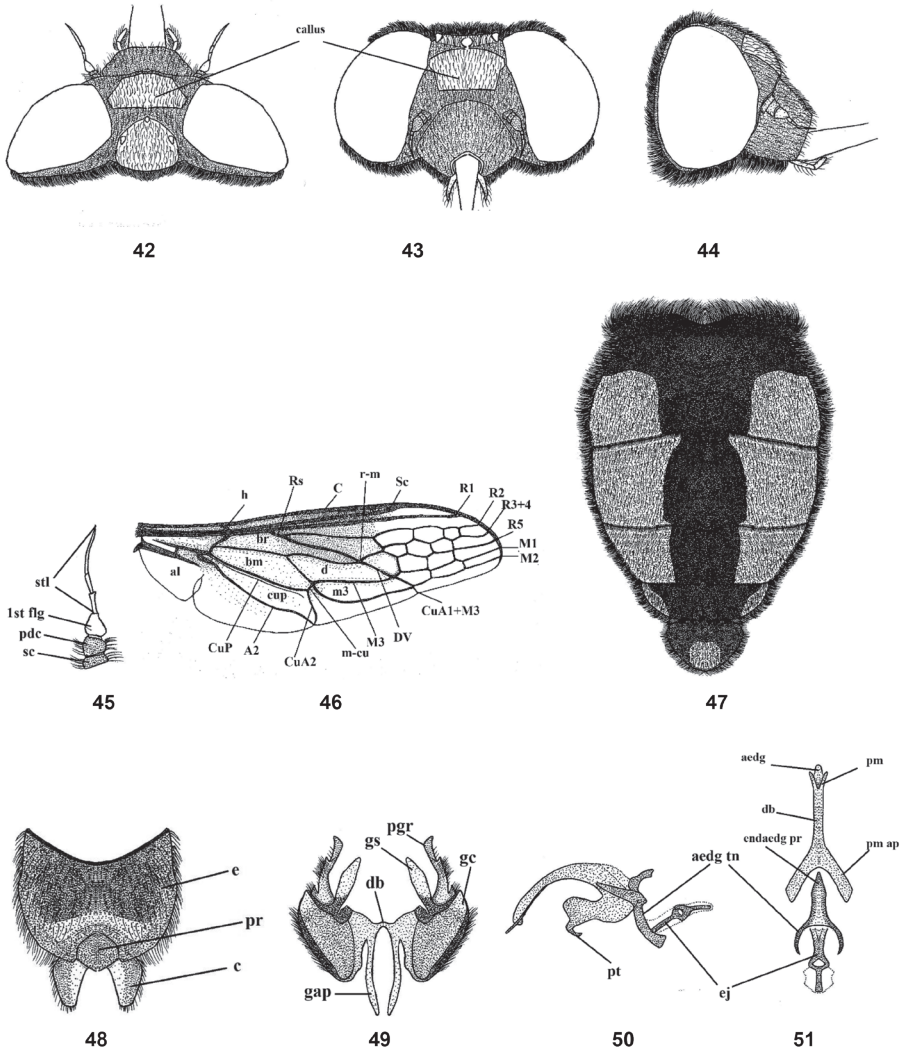
Figures 42–51. Male of *Nemestrinus exalbidus*, head, frontal (**42**), head, dorsal (**43**), head, lateral (**44**), antenna (**45**), wing (**46**), and abdomen (**47**). **48–51** male genitalia: epandrium, proctiger, and cerci (**48**), gonocoxite with gonostylus, ventral (**49**), aedeagal complex, lateral (**50**) and dorsal (**51**). Abbreviations: aedg. aedeagus, aec. aedeagal complex, aedg tn. aedeagal tine A2. anal vein, al. alula, bm. basal medial cell, br. basal radial cell, c. cerci, C. costa, CuA1,2, CuP. cubital veins, d. discal cell, db. dorsal bridge, DV. diagonal vein, e. epandrium, ej. ejaculatory apodeme, endaedg pr. endoaedeagal process, 1st fl. first flagel-lomere, gap. gonocoxal apodeme, gc. gonocoxite, gpr. gonocoxal process, gs. gonostylus, h. hypandrium, h. humeral cross vein, lat ej pr. lateral ejaculatory process, m3. third medial cell, pm. parameres, pm ap. parameral apodeme, pr. proctiger, pt. phallic plate, M1, M2, M3. medial veins, m-cu. cross vein between medial and cubital veins, pd, pedicel, R1, R2, R3+4, R5,Rs. radial veins, r-m. cross vein between redial and medial veins, Sc. subcostal vein, sc. Scape, st. stylus.

Local distribution. Coastal strip, Lower Nile.

Geographical distribution. Algeria, Egypt, Ethiopia, Israel, Spain, and Tunisia (Sack 1933; Bernardi, 1973; Richter 1988).

Remarks. *Nemestrinus abdominalis* and *N. fascifrons* are newly synonymized with *N. ater*. The earlier works of Lichtwardt (1909, 1919), Villeneuve (1912), and Bequaert (1938) suggested that *N. ater*, *N. abdominalis*, and *N. fascifrons* were closely related to each other based on Egyptian, Tunisian, and Palestinian material. We observed that *N. ater* has sexually dimorphic abdominal color. We also discovered that all the specimens previously identified by Efflatoun as *N. fascifrons* are males and we confirm these identifications. We also confirm that all the specimens that were previously identified by the same author as *N. ater* are females and confirmed by us as *N. fascifrons*. The two "species" of Efflatoun were captured from approximately the same locality and time of year by the same collector, i.e., "Efflatoun collected males at W. Garawi on 22.iii.1930 and 31.iii.1930 and females at W. Garawi on 22.iii.1930 and 31.iii.1930"; both are deposited in the Cairo University collection. We observed the sexual dimorphism and regard them as representing the same species.

Nemestrinus exalbidus (Lichtwardt, 1907)
Figures 42–60

Nemestrina exalbidus Lichtwardt, 1907: 441. Type locality: Israel (Jerusalem).

Specimens examined. W. Dar El-Maskhara 29°47'02.9"N, 31°24'59.9"E, 12.iv.1930 (1 f#); W. Hodein South Eastern Desert 23°5'14'"N, 35°19'45"E, 17.iii.1928 (1 m#); W. Hoff 29°53'02.6"N, 31°18'42.2"E, 12.iv.1921 (1 f#), 24.iii.1930 (1 m#); W. Zohleiga 26°07'59.9"N, 33°45'00.0"E, 27.iii.1925 (1 f#) (AZUC); Abu Rowash 30°04'30.7"N, 31°11'59.7"E, 16.iii.1927 (1 f#); Ogret El-Sheikh 29°52'50.1"N, 31°18'27.8"E, 31.iii.1926 (1 f#); W. Hoff 29°53'02.6"N, 31°18'42.2"E, 24.iii.1930 (1 m#); W. Rishrash 29°27'51"N, 31°22'2"E, 29.iii.1935 (7 m# & 4 f#) (CUC); Ogret El-Sheikh 29°52'50.1"N, 31°18'27.8"E, 14.iii.1927 (1 m#); W. Hoff 29°53'02.6"N, 31°18'42.2"E, 30.iii.1928 (1 m#); W. Zohleiga 26°07'59.9"N, 33°45'00.0"E, 25,29.iii.1925 (1 f#) (MAC); Etaka 29°26'19.1"N, 32°28'07.2"E , 22.ii.1951(1 f#), 26.iii.1951 (1 m#); Kerdasa 30°01'32.1"N, 31°06'27.5"E, 14.iv.1951 (3 f#); Mansouriah 29°58'05.3"N, 31°08'51.9"E, 25.iv.1957 (1 m#); W. Kaber 23°26'29"N, 25°50'23"E, 1.iv.1994 (1 f#) (ASUC).

Diagnosis. Frons covered with dense gray pollinosity except shiny black oval callus below ocellar triangle; wing hyaline, except slightly brownish along anterior margin, with a few small cells extending forward from R2+3 to M1 or M2. Abdomen orange or reddish with longitudinal median black vitta.

Redescription. Length: male body 14–17 mm, wing 12.5–14.5 mm. Female body 18 mm, wing 15.5 mm. Head shiny black with white hairs; frons covered with dense gray pollinosity except shiny black oval callus below ocellar triangle; face rather conical
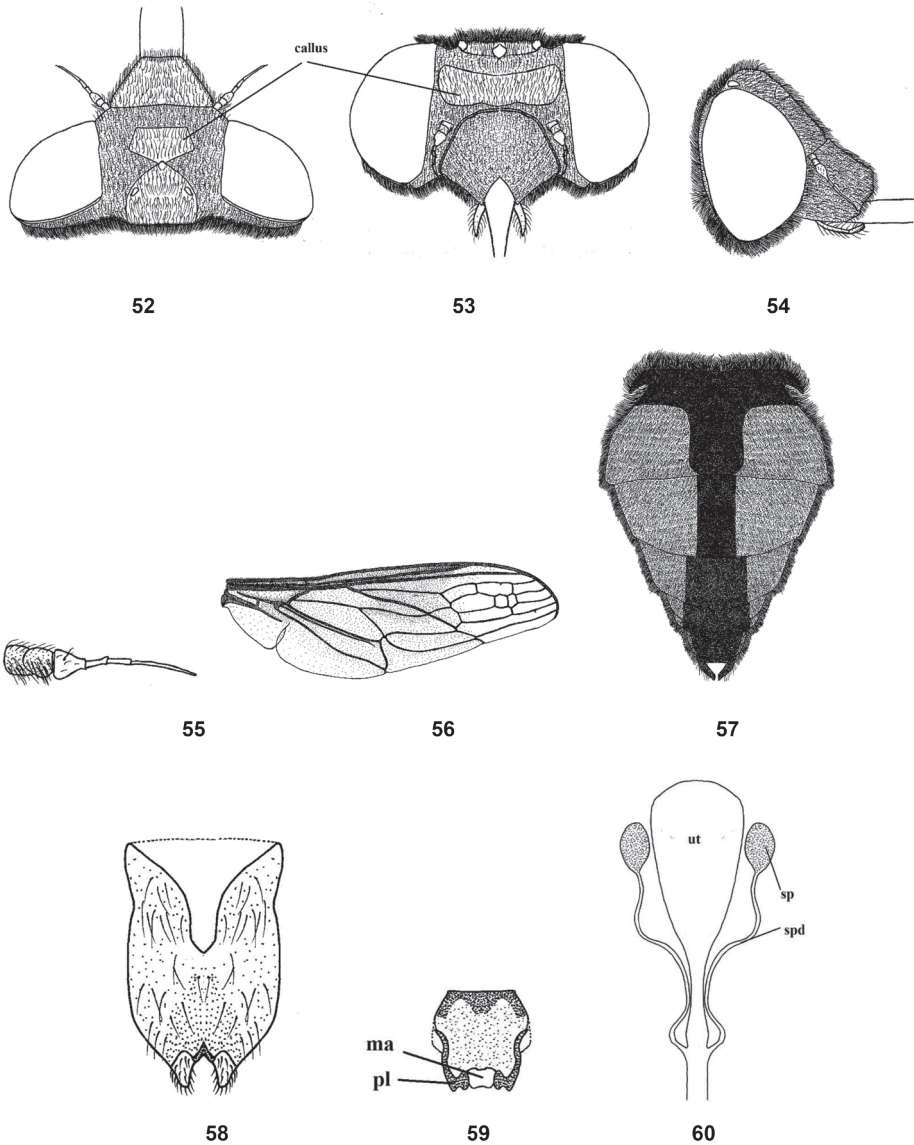
Figures 52–60. Female of *Nemestrinus exalbidus*, head, frontal (**52**), head, dorsal (**53**), head, lateral (**54**), antenna (**55**), wing (**56**), and abdomen (**57**). **58–60** female genitalia: subgenital plate (**58**), genital furca (**59**), and spermathecae (**60**). Abbreviations: ma. median aperture, pl. posterolateral projection, sp. spermatheca, spd. spermathecal duct, ut. uterus.

(Figs 42–44, 52–54). Thorax shiny black with dense whitish hairs laterally and a few dorsally. Leg orange, but femora black. Wing hyaline, except pale brownish anterior margin, with just a few small cells extending forward from R2+3 to M1 or M2 (Figs 46, 56). The differences in cell number and structure on the wing is continuous variation and inconsistently different between males and females. Abdomen orange or reddish with longitudinal black median vitta; base of abdomen covered with dense, short,

yellowish gray hairs, lateral margins of subsequent segments with dense white hairs; venter of abdomen entirely orange (Figs 47, 57). Gonocoxite with only inner gonocoxal process, tapered apically (Figs 48, 49); distiphallus narrow; parameral apodeme rather short, aedeagal tine narrow and curved, forming semicircle, pointed distally; ejaculatory apodeme distally broader (Figs 50, 51). Female differentiated from male by the eyes that are more dichoptic. Female genitalia with rectangular subgenital plate, excavated proximally to approx. 1/2 length of plate (Fig. 58); genital furca with small genital aperture, between projections with broad ends, and curved posteromedially with small curve on upper and lower margins (Fig. 59); uterus large and flatted, spermathecae long (Fig. 60).

   Local distribution. Eastern Desert, Lower Nile.

   Geographical distribution. Egypt, Iran, and Israel (Sack 1933; Bernardi, 1973; Richter 1988).

Nemestrinus fasciatus (Olivier, 1811)
Figures 61–79

Nemestrina fasciata Olivier, 1811: 171–172. Type locality: Egypt.
Specimens examined. Burg El-Arab 30°54'12.7"N, 29°33'13.7"E, 6.v.1926 (1 m#); Burg El-Arab, 2.v.1921 (10 m#) (AZUC); Burg El-Arab 30°54'12.7"N, 29°33'13.7"E, 5.v.1926 (1 f#) (CUC); Burg El-Arab 30°54'12.7"N, 29°33'13.7"E, 10.v.1927 (1 m#), 19.iv.1928 (6 m# & 6 f#); King Mariut 30°57'27.2"N, 29°38'51.0"E, 14.iv.1915 (1 m#), 23.v.1925 (1 m#); Burg El-Arab 30°54'12.7"N, 29°33'13.7"E, 2.v.1924 (1 f#) (MAC); Max 31°09'50.5"N, 29°51'47.7"E, 21.iv.1952 (1 f#) (ASUC).
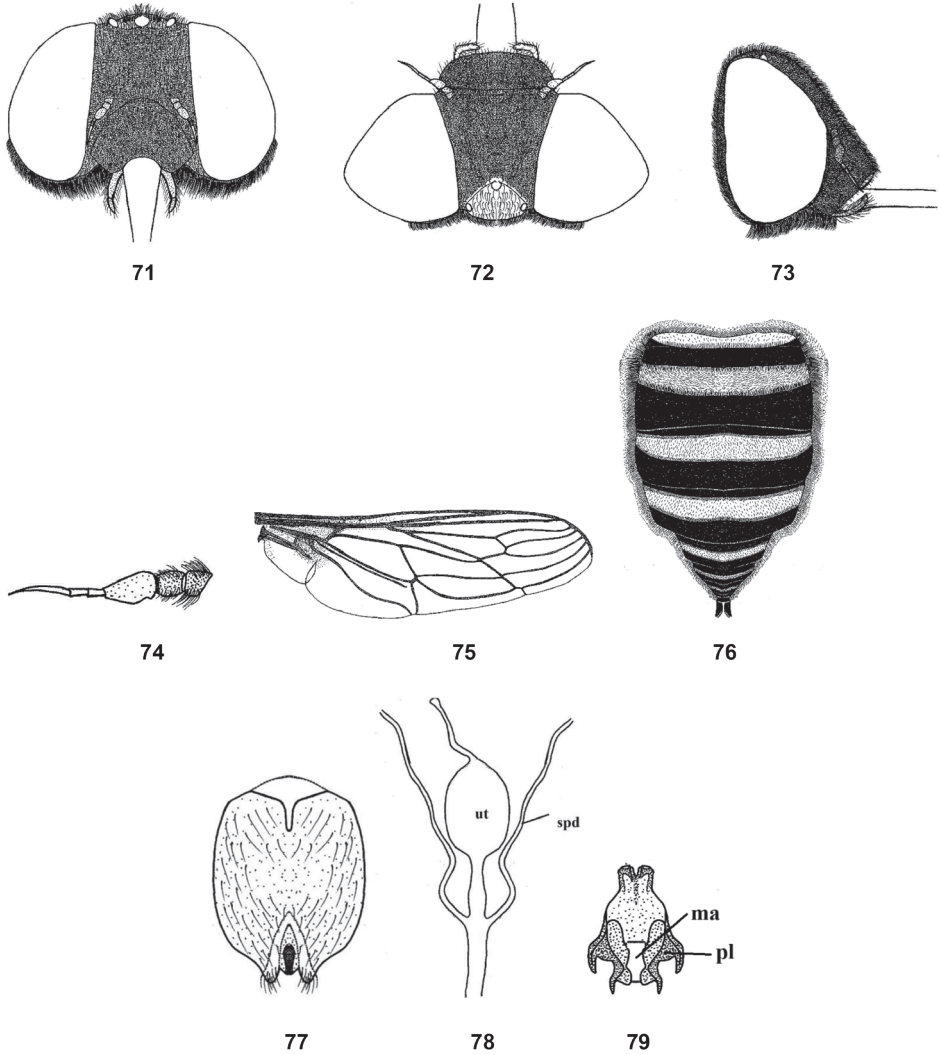
   Diagnosis. Frons and face with dense whitish hairs and pollinose; inner ends of transverse suture with two white spots; wing hyaline with brownish base, veins yellowish, without additional small cells; abdomen black with transverse white bands, slightly curved medially; gonocoxite with inner and outer processes, the inner tapered apically, outer slightly curved subapically; gonostyli broader than gonocoxal processes with broad subapical projection; aedeagal complex narrow, aedeagus slightly broader distally.

   Redescription. Length: male body 13–16.5 mm, wing 1–12 mm. Female) body 12–19.5 mm, wing 1–13 mm.

   Head triangular in profile, ventrally with dense, short, whitish hairs; frons and face with dense whitish hairs and pollinosity (Figs 61–63, 71–73); antenna distinctly jointed, stylus is brown (Figs 64, 74). Thorax slightly shiny black; inner parts of transverse suture with two white spots; scutellum and mesonotum with grayish yellow hairs; pleurae with long white hairs. Leg with blackish femora covered with whitish hairs; tibiae and tarsi brown with brownish red hairs; pulvilli orange, nearly as long as claws. Wing hyaline with brownish infuscate base; veins yellowish, without additional small cells (Figs 65, 75). Abdomen black with transverse white bands, whi slightly curved medially; basal segments with long yellowish hairs but subsequent segments with white hairs; venter of abdomen with dense white hairs that fold on the lateral
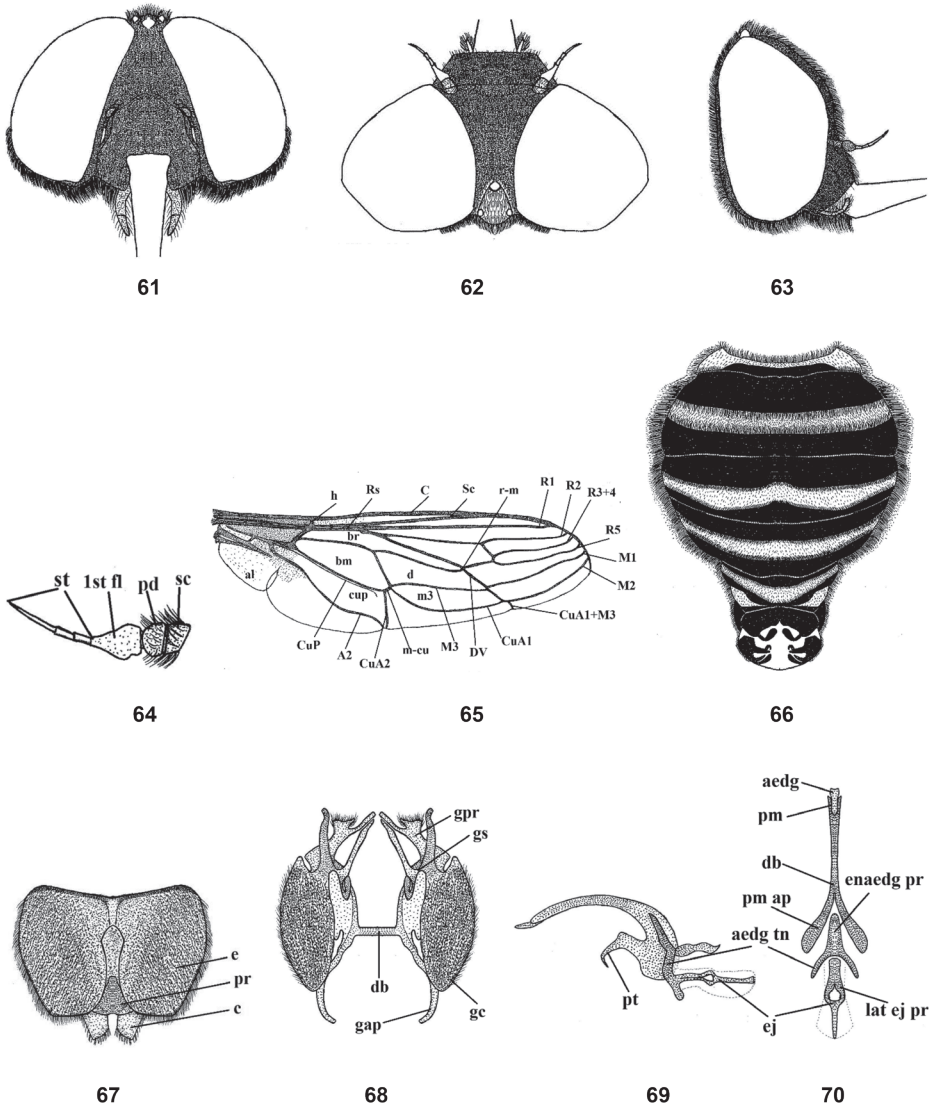
Figures 61–70. Male of *Nemestrinus fasciatus*, head, frontal (**61**), head, dorsal (**62**), head, lateral (**63**), antenna (**64**), wing (**65**), and abdomen (**66**). **67–70** male genitalia, epandrium, proctiger and cerci (**67**), gonocoxite with gonostylus, ventral (**68**), aedeagal complex, lateral (**69**) and dorsal (**70**). Abbreviations: aedg. aedeagus, aec. aedeagal complex, aedg tn. aedeagal tine A2. anal vein, al. alula, bm. basal medial cell, br. basal radial cell, c. cerci, C. costa, CuA1,2, CuP. cubital veins, d. discal cell, db. dorsal bridge, DV. diagonal vein, e. epandrium, ej. ejaculatory apodeme, enaedg pr. endoaedeagal process, 1st fl. first flagellomere, gap. gonocoxal apodeme, gc. gonocoxite, gpr. gonocoxal process, gs. gonostylus, h. hypandrium, h. humeral cross vein, lat ej pr. lateral ejaculatory process, m3. third medial cell, pm. parameres, pm ap. parameral apodeme, pr. proctiger, pt. phallic plate, M1, M2, M3. medial veins, m-cu. cross vein between medial and cubital veins, pd, pedicel, R1, R2, R3+4, R5,Rs. radial veins, r-m. cross vein between redial and medial veins, Sc. subcostal vein, sc. Scape, st. stylus.

Figures 71–79. Female of *Nemestrinus fasiciatus*, head, frontal (**71**), head, dorsal (**72**), head, lateral (**73**), antenna (**74**), wing (**75**), and abdomen (**76**). **77–79** female genitalia: subgenital plate (**77**), genital furca (**78**), and spermathecae (**79**). Abbreviations: ma. median aperture, pl. posterolateral projection, sp. spermatheca, spd. spermathecal duct, ut. uterus.

margins (Figs 66, 76). Gonocoxite with inner and outer processes, inner tapered apically, outer slightly curved subapically; gonostyli broader than gonocoxal processes with broad projection subapically (Figs 67, 68); aedeagal complex narrow, aedeagus slightly broader apically (Figs 69, 70).

Female: eyes separated in both sexes but considerably broader than in male at vertex; genitalia with sub-rectangular subgenital plate (Fig. 77); genital furca narrower

anteriorly with four incurved posterolateral projections (Fig. 78); uterus with terminal accessory process; spermathecae rather long (Fig. 79).

Local distribution. Coastal strip.

Geographical distribution. Algeria, Egypt, Morocco, Israel, and Syria (Sack 1933; Bernardi, 1973; Richter 1988).

Nemestrinus reticulatus Latreille, 1802
Figures 80–85

Nemestrinus reticulatus Latreille, 1802: 437. Type locality: not given but according to
    Latreille (1809: 307), it is Egypt and Syria.
Rhynchocephalus latreillei Fischer, 1812: 195.
Nemestrina cinctus Macquart, 1840: 16.
Nemestrina kindermanni Bischof, 1905: 172.

Diagnosis. Frons with shiny yellow or black spot below ocelli; mesonotum with two gray spots at inner ends of the transverse suture, between them there is a thin longitudinal stripe; wing hyaline in posterior 1/2 and apex but brownish on anterior 1/2 and slightly infuscate at base; wing with small cells that extend forward from R_2 to hind margin; abdomen gray, matte, with incomplete transverse black stripes; tergite II bears shiny black spots divided in the middle by a transverse longitudinal gray strip; black spots on tergites III–V more or less fused into bands with an emargination along the posterior margin; on tergite III, gray emargination varies from very deep to nearly absent; abdominal venter with dense gray pollinosity, the second sternite with central black spot.

Description. Length: body 14–15 mm. Head black with dense gray pollinosity and whitish hairs; frons with shiny yellow or black spot below ocelli, in male frons at vertex nearly as wide as eye width (Figs 80, 83), while in female nearly twice as eye width (Fig. 81); antenna with orange scape and pedicel, first flagellomere brown to blackish brown with some gray pollinosity (Fig. 82), basal two segments of stylus subequal in length and segment III 2/3 × longitudinal eye diameter; palpi yellow or brown with black apices. Thorax pale black with yellowish white or grayish white hairs, but longer and denser on scutellum and pleurae; mesonotum with two gray spots at inner ends of transverse suture and between them is a thin longitudinal stripe. Leg rusty red; in females, only hind tarsi blackish or hind leg entirely blackish; in males, all femora black; hind tibiae and tarsi blackish. Wing hyaline over posterior 1/2 and at apex, but somewhat brown over anterior 1/2 and slightly infuscate at base; wing with small cells that extend forward from R_2 to hind margin (Fig. 85). Abdomen gray, matte, with incomplete transverse black stripes; tergite II with shiny black spots divided in the middle by a transverse longitudinal gray strip; black spots on tergites III–V are more or less fused into bands with an emargination along the posterior margin; on tergite III, gray emargination varies from very deep to nearly absent; abdominal venter with dense gray pollinosity, sternite II with black central spot (Fig. 84).
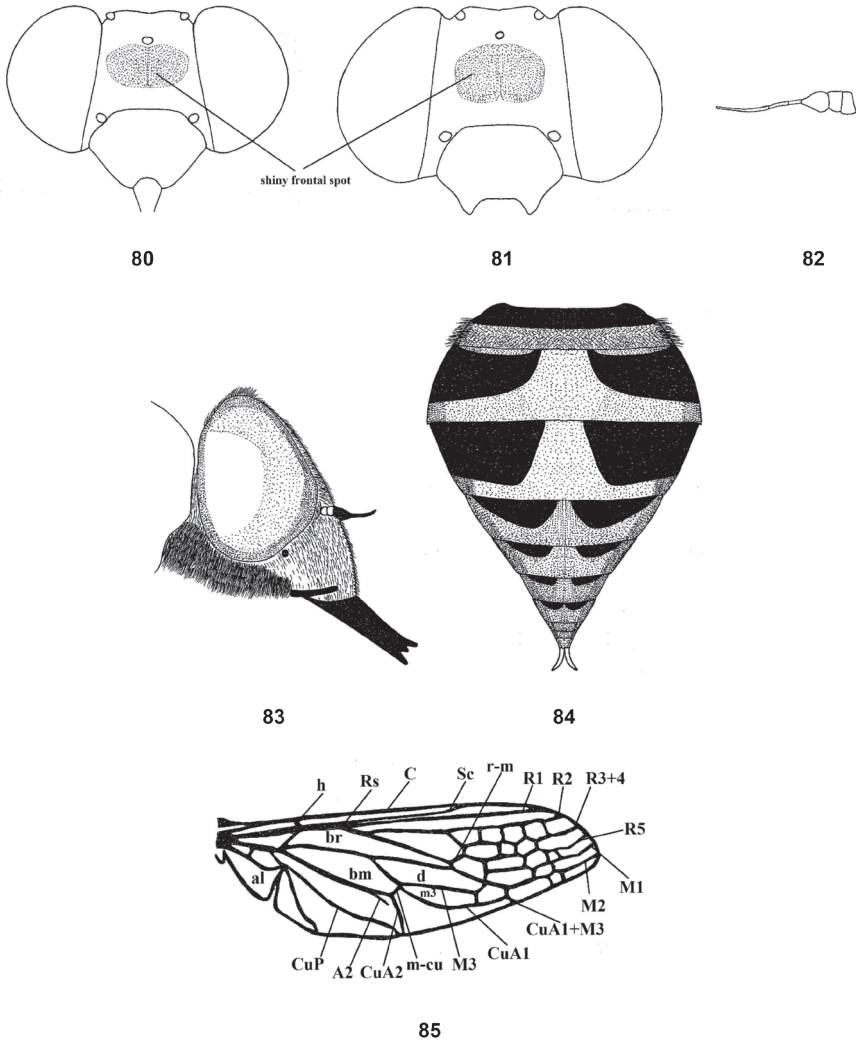
Figures 80–85. *Nemestrinus reticulatus*, male head, frontal (**80**), female head, frontal (**81**), male antenna (after Bequaert, 1938) (**82**), male head, lateral (**83**), female abdomen (after Sack 1933) (**84**), and wing (after Seguy, 1926) (**85**). Abbreviations: A2. anal vein, al. alula, bm. basal medial cell, br. basal radial cell, C. costa, CuA1,2, CuP. cubital veins, d. discal cell, DV. diagonal vein, h. humeral cross vein, m3. third medial cell, M1, M2, M3. medial veins, m-cu. cross vein between medial and cubital veins, R1, R2, R3+4, R5,Rs. radial veins, r-m. cross vein between redial and medial veins, Sc. subcostal vein.

Local distribution. Unknown.

Geographical distribution. Armenia, Egypt, Greece, Russia (Caucasus), Saudi Arabia, Syria, and Turkey (Sack 1933; Bernardi, 1973).

Remarks. This species is not represented in Egyptian collections nor in the field. We include the species here and in the key below as it has been recorded from Egypt (Sack 1933 & Bernardi, 1973 & Richter 1988); future research might reveal its presence in this part of Africa.

Nemestrinus rufipes (Olivier, 1811)
Figures 1, 2, 86–104

Nemestrina rufipes Olivier, 1811: 171.
Nemestrina lateralis Wiedemann, 1828: 560.
Nemestrina ruficornis Macquart, 1840: 15. Syn. nov.

Type material. *Nemestrinus rufipes*: Type male, "Aegypten", Egypt (ZMHB) (pers. comm. Mr. Sven Marotzke). *Nemestrina lateralis*: Type female, "Aegypten", Egypt (ZMHB) (pers. comm. Mr. Sven Marotzke).

Specimens examined. Ezbet El-Nakhl 30°08'22.6"N, 31°19'27.8"E, 20.iv.1921 (1 m# & 3 f#); Helwan 29°50'37.6"N, 31°19'05.0"E, 8.iv.1932 (2 f#); W. Morrah 22°22'39.1"N, 33°46'00.3"E, 26.iii.1927 (1 m#) (AZUC); Abu Rawash 30°04'30.7"N, 31°11'59.7"E, 13.iii.1955 (3 m# & 4 f#), 17.iii.1955 (1 m#); Kerdasa 30°01'32.1"N, 31°06'27.5"E, 11.iv.1926 (1 m#); Giza 30°00'40.0"N, 31°11'31.4"E, 7.v.1955 (1 m#), 2.iii.1927 (1 m#); Helwan 29°50'37.6"N, 31°19'05.0"E, 8.iv.1932 (2 f#), 3.iv.1934 (1 m# & 3 f#), 8.iv.1934 (6 f#), 17.iii.1934 (1 f#), 17.iv.1934 (1 f#), 23.iv.1935 (3 f#); W. Garawi 29°47'43.9"N, 31°25'54.9"E, 31.iii.1930 (1 f#) (CUC); Abu Rawash 30°04'30.7"N, 31°11'59.7"E, 11.iv.1925 (1 m#), 17.iv.1925 (2 m# & 1 f#), 3.iv.1926 (1 m# & 1 f#),12.iii.1936 (1 f#), 4.iv.1961 (3 f#); (Noaman Bey) Alexandria 31°10'03.5"N, 29°51'56.2"E, (1 f#, without date); Assyut 27°23'00.0"N, 31°44'38.0"E, 2.iv.1917 (1 f#); Bent Suef 29°04'N, 31°05'E, iii.1965 (1 m#); Dakhla Mout 25°32'41.4"N, 28°55'44.0"E, 17.iii.1934 (1 m#); El-Mallah 30°00'37.7"N, 31°09'34.0"E , 14.v.1927 (1 m#); Gabal El-Halal 30°39'10.8"N, 34°01'43.9"E, 25.iv.1924 (1 m# & 1 f#); Gabal El-Sanadiq, 5.iv.1934 (1 f#); 12.iv.1924 (1 m#); Kafr Hakim 30°04'39.7"N, 31°06'46.3"E, 7.iv.1924 (1 m#), 14.iv.1925 (1 m#), 20.iv.1925 (1 m# & 1 f#); Mansouriah 29°58'05.3"N, 31°08'51.9"E, 28.iv.1926 (1 f#), 4.iii.1934 (1 m#); Marg, 1.iv.1923 (1 f#); Marsa Matrouh 31°11'04.1"N, 27°15'42.4"E, 19.i.1933 (1 m#), 17.iii.1933 (1 m#), 1.iv.1961 (1 f#); W. Garawi 29°47'43.9"N, 31°25'54.9"E, 3.iii.1925 (1 f#); W. Um Elek 29°52'59.9"N, 31°31'00.1"E, 28.iii.1918 (1 f#); W. Zohleiga 26°07'59.9"N, 33°45'00.0"E, 25–29.iii.1925 (1 f#) (MAC); W. Digla 29°59'00.1"N, 31°19'41.2"E, 5.iv.1952 (1 m#) (ASUC). Aegypten (1 m# & 1f#), without date (ZMHB) sent by Mr. Sven Marotzke and Bernhard Schurian; Dakahlia, Mansuriya 31.1656° N, 31.4913°E 31.iii.1964 (1 m# & 1 f#) specimen numbers: male: USNMENT01371563, female: USNMENT01371564, Cairo, Marg 30.1543°N, 31.3484°E (1 f#), without date, specimen number USNMENT01371561 (USNM) (identified by Dr. Torsten Dikow).

Diagnosis. Frons covered with dense orange yellow pollinosity except with shiny blackish brown transverse oval callus below dark orange ocellar triangle; wing with yellowish brown band in the middle, but clear in apical part and along posterior margin; wing with small cells extending forward from R2 to M1 or M2. Abdomen orange to reddish orange with longitudinal black median vitta; first tergite entirely black, ter-
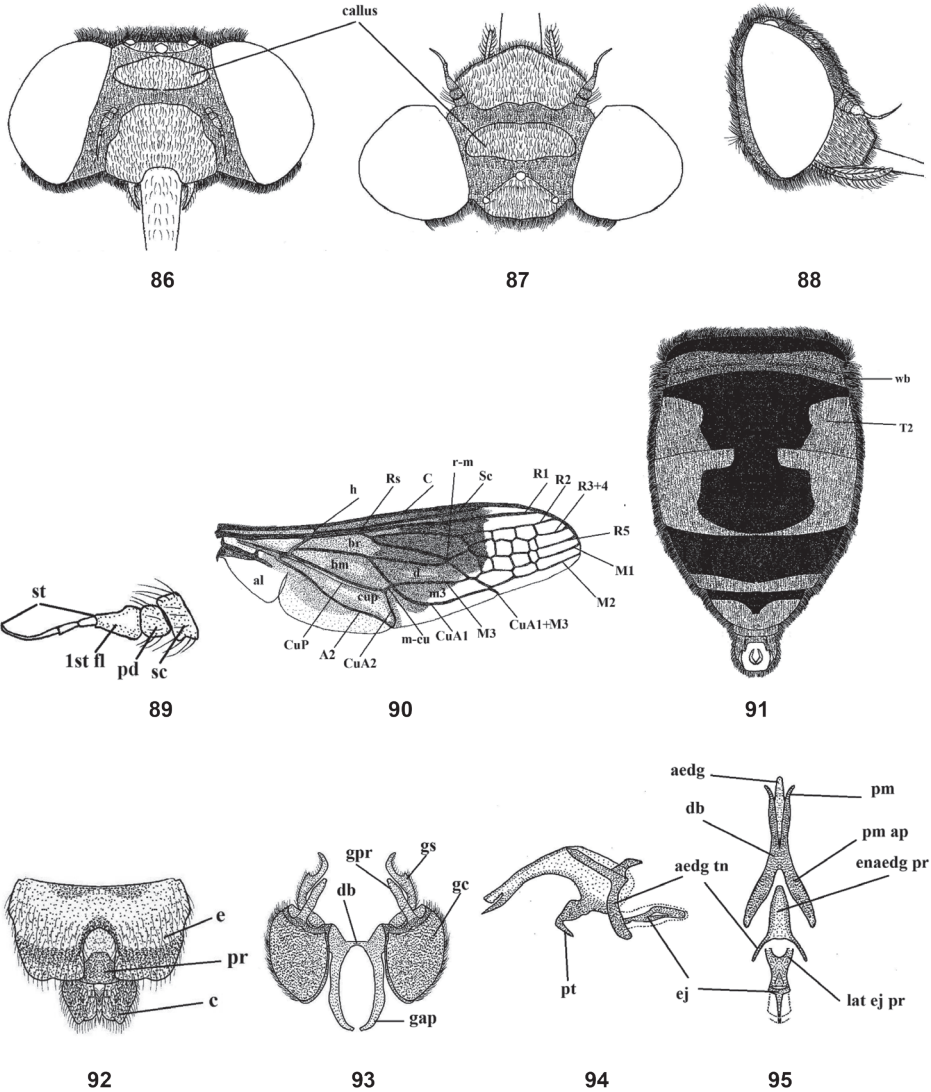
Figures 86–95. Male of *Nemestrinus rufipes*, head, frontal (**86**), head, dorsal (**87**), head, lateral (**88**), antenna (**89**), wing (**90**), and abdomen (**91**). **92–95** male genitalia: epandrium, proctiger and cerci (**92**), gonocoxite with gonostylus, ventral (**93**), aedeagal complex, lateral (**94**) and dorsal (**95**). Abbreviations: aedg. aedeagus, aec. aedeagal complex, aedg tn. aedeagal tine A2. anal vein, al. alula, bm. basal medial cell, br. basal radial cell, c. cerci, C. costa, CuA1,2, CuP. cubital veins, d. discal cell, db. dorsal bridge, DV. diagonal vein, e. epandrium, ej. ejaculatory apodeme, enaedg pr. endoaedeagal process, 1st fl. first flagel-lomere, gap. gonocoxal apodeme, gc. gonocoxite, gpr. gonocoxal process, gs. gonostylus, h. hypandrium, h. humeral cross vein, lat ej pr. lateral ejaculatory process, m3. third medial cell, pm. parameres, pm ap. parameral apodeme, pr. proctiger, pt. phallic plate, M1, M2, M3. medial veins, m-cu. cross vein between medial and cubital veins, pd, pedicel, R1, R2, R3+4, R5,Rs. radial veins, r-m. cross vein between redial and medial veins, Sc. subcostal vein, sc. Scape, st. stylus, T2. tergite 2, wb. White band.
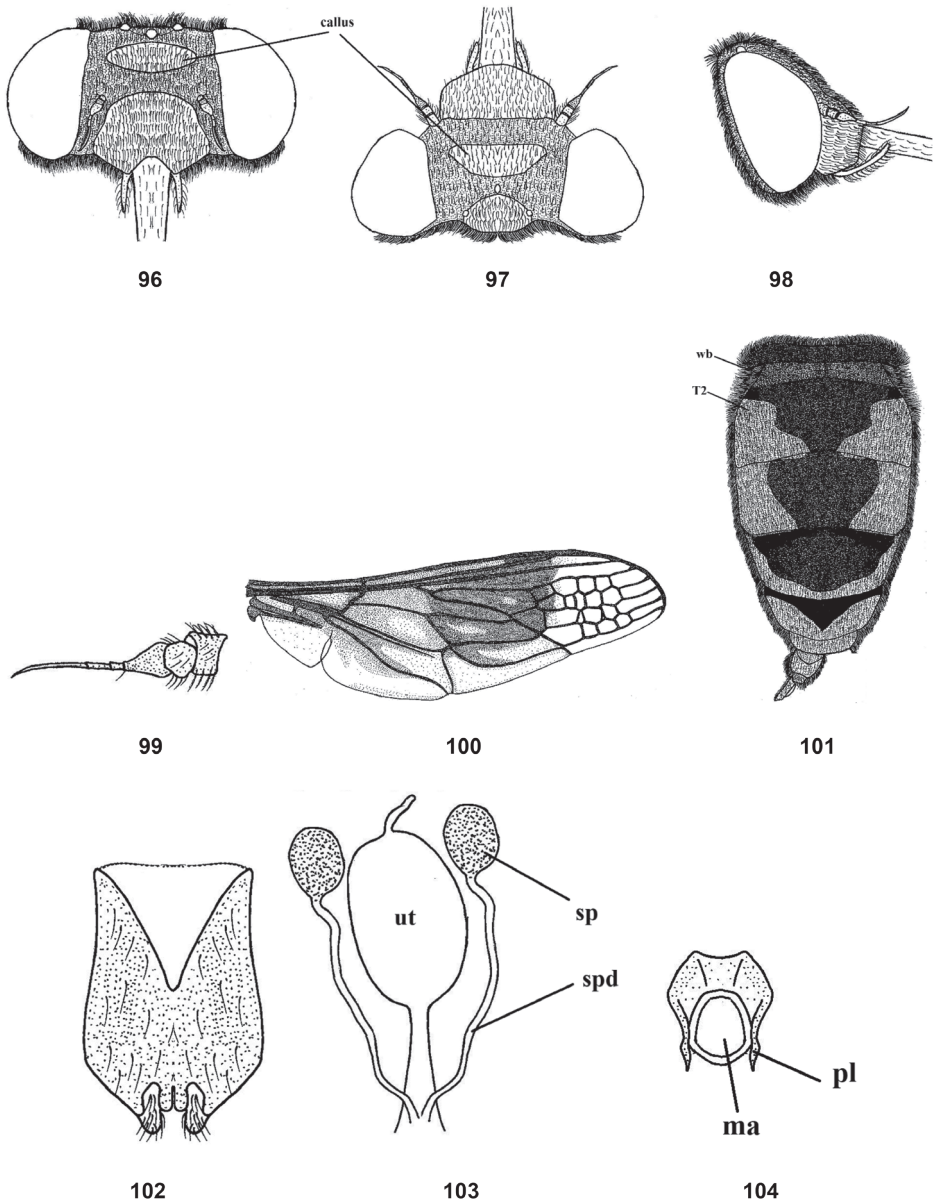
Figures 96–104. Female of *Nemestrinus rufipes*, head, frontal (**96**), head, dorsal (**97**), head, lateral (**98**), antenna (**99**), wing (**100**) and abdomen (**101**). **102–104** female genitalia: subgenital plate (**102**), genital furca (**103**), and spermathecae (**104**). Abbreviations: ma. median aperture, pl. posterolateral projection, sp. spermatheca, spd. spermathecal duct, ut. uterus, T2. tergite 2, wb. White band.

gite II on anterior margin with transverse white band. Gonocoxite with inner process slightly tapered; gonostyli longer than gonocoxal process, curved subapically with small projection; aedeagus fused proximally with parameres and separated distally, parameres and aedeagus with small indentations distally in lateral view.

Redescription. Length: male body 13.5–18.5 mm, wing 11.5–16 mm. Female body 14–21 mm, wing 12–17.5 mm. Head short, wider than thorax; frons covered with dense orange-yellow pollinosity except with shiny blackish brown transverse oval callus (Figs 86–88, 96–98); face shiny brownish orange with short yellow hairs; antenna orange (Figs 89, 99); proboscis black, as long as thorax, upper surface of base with short yellow hairs; palpi orange. Thorax shiny black with yellow hairs, longer and denser on the sides and in front; mesonotum with indistinct spots at inner ends of transverse suture. Leg orange, coxae and base of femora somewhat brown, pulvilli light yellow and nearly 1/2 length of claw. Wing with yellowish brown band in the middle, but clear apically and along posterior margin; wing with small cells extending forward from R2 to M1 or M2 (Figs 90, 100). Halter brown with light yellow pedicel. Abdomen orange to reddish orange with longitudinal black median vitta; tergite I entirely black, tergite II with transverse white band; abdomen with short and golden yellow hairs but longer laterally; abdominal venter orange and with black lateral margins (Figs 91, 101). Gonocoxite with inner process slightly tapered; gonostyli longer than gonocoxal process, curved subapically with small projection (Fig. 93); aedeagus fused proximally with parameres and separated distally, parameres and aedeagus with small indentations distally in lateral view (Figs 94, 95). Female genitalia: rectangular subgenital plate with large curve (Fig. 102); genital furca with large aperture surrounded by narrow and slightly curved posterolaterally projections (Fig. 103); uterus with small terminal accessory; spermathecae nearly as long as the uterus (Fig. 104).

**Local distribution.** Coastal strip, Lower Nile, Upper Nile, Sinai.

Geographical distribution. Algeria, Egypt, and Syria (Sack 1933; Bernardi, 1973; Richter 1988).

Remarks. Bernardi (1973) and Richter (1988) considered *N. rufipes* and *N. ruficornis* to be valid species but, in contrast, Lichtwardt (1909) and Bequaert (1938) synonymized the two. We agree with this decision based on a comparison of the original description of *N. ruficornis* (no material was examined) with the male type specimen of *N. rufipes* (Fig. 2) and the female type specimen of *N. lateralis* (Fig. 3), both in ZMHB, in addition to both sexes of many old Egyptian specimens of *N. rufipes*. Thus, we confirm that *N. rufipes* and *N. ruficornis* are conspecific and the first is the valid name, and *Nemestrinus ruficornis* is here synonymized with *N. rufipes*.

List of doubtful species. In the present study, three species are treated as doubtful and are excluded from the list of Egyptian Nemestrinidae: *Nemestrinus caucasicus*, *Nemestrinus pallipes*, and *Nemestrinus persicus*.

Discussion

As a result of this revision, we can confirm six species of *Nemestrinus* present in Egypt. This is lower than the 12 taxa (eleven species and one subspecies) listed by Steyskal and El-Bialy (1967) but three species are treated as doubtfully occurring including *N. pallipes* added by Bernardi (1973) and Richter (1988) as Egyptian species and three species that are newly synonymized (*N. abdominalis*, *N. fascifrons*, and *N. ruficornis*).
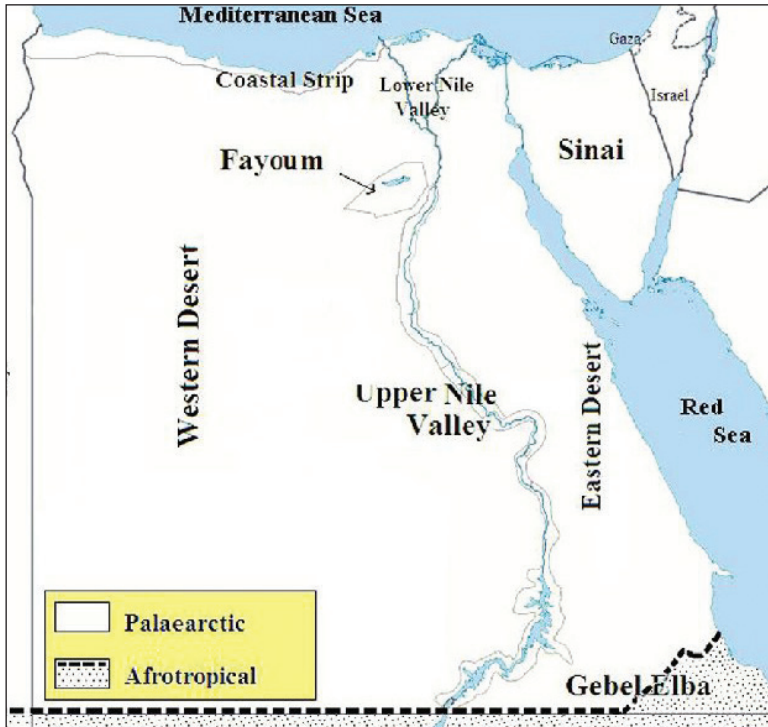
Map 1. Map of Egypt showing the ecological zones (after elhawagry and gilbert 2014).

Map 2. Distribution of the species *N. aegyptiacus* in Egypt.

Map 3. Distribution of the species *N. ater* in Egypt.

Map 4. Distribution of the species *N. exalbidus* in Egypt.

Map 5. Distribution of the species *N. fasciatus* in Egypt.

Map 6. Distribution of the species *N. rufipes* in Egypt.

Furthermore, *N. jullieni*, a subspecies designated by Steyskal and El-Bialy (1967), is confirmed as a synonym of *N. aegyptiacus*.

The first species (*N. caucasicus*) does not occur in Egypt according to Sack (1933), Bequaert (1938), Bernardi (1973), Richter (1988), Narchuk (2007), or Kocak and Kemal (2013), whereas Paramonov (1951) reported it from North Africa but without examining any Egyptian material. It is also listed by Steyskal and El-Bialy (1967) citing the literature but not represented in the Egyptian reference collections.

The second species (*N. pallipes*) is not represented in Egyptian collections. This species was previously considered to be an Egyptian species based on an erroneous interpretation of its type locality (Java) by Bequaert (1932), Bernardi (1973), and Richter (1988), for reasons unknown. The type locality was given by Olivier (1811) in his original description as Java, while describing seven new species from Egypt, although two of them were from Arabia and around the Caspian Sea. Olivier (1811) based his paper on material collected from different areas in the Middle East and his "Java" evidently refers to a place near Tel-Aviv in Israel currently known as Jaffa, not an Egyptian locality. We communicated with managers in Tel Aviv museum (Steinhardt museum), Diptera collection (Dr. Elizabeth Morguilis and Dr. Ariel-Leib Frieman), who checked the nemestrinid group and they do not have any specimens of this species in their collections. This species is also not mentioned in the list of Steyskal and El-Bialy (1967). Although it is believed that this species does not occur in Egypt, it may yet be found and recorded from the country.

The third species (*N. persicus*) is reported in Sack (1933) and Paramonov (1945) as an Egyptian species, but without any listing of Egyptian material. It is also mentioned as an Egyptian species by Steyskal and El-Bialy (1967) but is not represented in Egyptian reference collections; however, Bequaert (1932), Bernardi (1973), and Richter (1988) excluded it as an Egyptian species. The type locality in the original description was given as Iran by Lichtwardt (1909) and, consequently, this species is excluded from the Egyptian fauna.

Nemestrinus reticulatus is stated here as not having any specimens in Egyptian collections and is not excluded from the Egyptian fauna in our study because we trust the descriptions of Latreille (1809) who originally reported the species in Egypt. Our drawings of this species are reproduced from Bequaert (1938), Sack (1933), and Seguy (1926).

As we observed on the maps there are similarities in the distributions of *N. aegyptiacus* and *N. rufipes*, which are longitudinally scattered from Lower to Upper Egypt and the western and eastern deserts, while *N. faciatus* is concentrated only in some localities on the coastal strip in Alexandria. *Nemestrinus exalbidus* is dispersed around the lower Egyptian delta and a few localities in the western and eastern deserts. *Nemestrinus ater* has a crosswise distribution in the northern area of Egypt including Sinai, and the lower and upper Nile valley (see Map 1), and one record in the eastern desert, in addition to one locality near Libya.

The species of *Nemestrinus* are concentrated in the semiarid areas around the Nile delta, especially around Lower Egypt and in some arid areas in western, eastern, and the Egyptian Sinai deserts. The wider geographical distribution of *Nemestrinus* in the

adjacent countries includes North Africa (Algeria, Libya, Morocco, and Tunisia) which all have a large percentage of the arid deserts that these nemestrinid species prefer. And at nearly the same latitude are Israel, Saudi Arabia, and Syria which also have arid areas (deserts) and may support species.

We found based that the seasonal imago flight activity of all *Nemestrinus* species in Egypt is in the spring season (March, April, and May) and only the species *N. ater* and *N. exalbidus* may also be activate in February.

Acknowledgements

References

Bequaert J (1932) The Nemestrinidae (Diptera) in the V.v. Röder collection. Zoologischer Anzeiger 100: 13–33.

Bequaert J (1938) Sur quelques Nemestrinides palaearctiques, particulièrement d l'Iran. Annales de la Société entomologique de Belgique 78: 292–310.

Bernardi N (1973) The genera of the Family Nemestrinidae (Diptera: Brachycera). Arquivos de Zoologia 24(4): 211–318. https://doi.org/10.11606/issn.2176-7793.v24i4p211-318

Bigot J (1888) Enumeration des diptères recueillis en Tunisie dans la Mission de 1884 par M. Valery Mayet. Exploration scientifique de la Tunisie, Zoologie, Diptères. Imprimerie nationale, Paris, 11 pp. https://doi.org/10.5962/bhl.title.53767

Bischof J (1905) Neuropteren und Dipteren. In: Penther A, Zederbauer E (Eds) Ergebnisse einer naturwissenschaftlichen Reise zum Erdschias-Dagh (Kleinasien). Annalen des Naturhistorischen Hofmuseums, Wien 20: 170–179.

Blanchard CE (1845) Histoire des insectes, traitant de leurs moeurs et leurs métamorphoses en général et comprenant une nouvelle classification fondée sur leurs rapports naturels. Coléoptères, orthoptères, thysanoptères, névroptères, lépidoptères, hémiptères, aphaniptères, strepsiptères, diptères, anoplures et thysanures 2: e20. https://doi.org/10.5962/bhl.title.35820

Efflatoun HC (1925) A new species of Nemestrina (Dipt. Nemestrinidae) from Egypt. Bulletin de la Société Entomologique d'Egypte 8: 357–360.

ElHawagry M, Gilbert F (2014) Zoogeographical affinities and faunal relationships of bee flies (Diptera: Bombyliidae) in Egypt. Zoology in the Middle East 60(1): 50–56. https://doi.org/10.1080/09397140.2014.892339

Cumming JM, Wood DM (2017) Manual of Afrotropical Diptera. In: Diversity of Life, South African National Biodiversity Institute 1: 89–133.

Fischer G (1806) Observation d'un nouveau genre d'une nouvelle famille de diptères du Caucase. Mémoires de la Société impériale des naturalistes de Moscou 1: 217–227.

Fischer G (1812) Observation d'un nouveau genre de diptéres. Lue a la séance du 17 janvier 1806, avec des additions de l'année 1811. Mémoires de la Société impériale des naturalistes de Moscou 1(2): 184–198.

Koçak AÖ, Kemal M (2013) Diptera of Turkey. Priamus Supplement, Ankara, 411pp.

Latreille PA (1802) Histoire naturelle, genérale et particulière, des crustacés et des insectes. Ouvrage faisant suite à l'histoire naturelle générale et particulière, composée par Leclerc de Buffon, et rédigée par C.S. Sonnini, membre de plusieurs sociétés savantes. Tome Troisième. F. Dufart, Paris, 467. https://doi.org/10.5962/bhl.title.15764

Latreille PA (1809) Genera crustaceorum et insectorum secundum ordinem naturalem in familias disposita, iconibus exemplisque plurimis explicata. Tomus quartus et ultimus. A. Koenig, Parisiis and Argentorati [= Paris & Strasbourg], 399 pp.

Lichtwardt B (1907) Uber die Dipteren-Gattung Nemestrina Latr. Zeitschrift für systematische hymenopterologie und dipterologie 7: 433–451.

Lichtwardt B (1909) Beitrag zur Kenntniss der Nemestriniden. Deutsche entomologische Zeitschrift 1: 113–127. https://doi.org/10.1002/mmnd.48019090117

Lichtwardt B (1919) Die Nemestriniden des Ungarischen National Museums in Budapest. Annales historico-naturales Musei nationalis hungarici 17: 24–27.

Macquart J (1840) Diptères exotiques nouveaux ou peu connus. Tome deuxième (1). Mémoires de la Société royale des sciences, de l'agriculture et des arts de Lille, Paris, 135 pp.

Teskey HJ (1981) Nemestrinidae. In: McAlpine JF, Peterson BV, Shewell GE, Teskey HJ, Vockeroth JR, Wood DM (Eds) Manual of Nearctic Diptera. Research Branch, Agriculture Canada Monograph, 585–588.

Narchuk EP (2007) Nemestrinid flies (Diptera, Nemestrinidae) in the Fauna of Eastern Europe and the Caucasus. Entomological Review 87(8): 1076–1085. https://doi.org/10.1134/S0013873807080143

Olivier GA (1811) Insectes [i. e., Arthropoda), Pt.5]. Société de Gens de Savans et d'Artistes, Encyclopédie méthodique, Histoire Naturelle 8: 170–172.

Papavero N, Bernardi N (2009) Manual of Neotropical Diptera, Nemestrinidae. In: Depto. de Biologia – FFCLRP Universidade de São Paulo Ribeirão Preto, SP, Brazil 8: 1–11.

Paramonov SJ (1945) Bestimmungstabelle der Palaearktischen Nemestrinus-Arten (Nemestrinidae: Diptera). Revista Española de Entomología 21(3/4): 279–295.

Paramonov SJ (1951) Bestimmungstabelle der palaearktischen Arten der Gattung Rhynchoce-phalus (Nemestrinidae: Diptera). Zoologischer Anzeiger 146(5–6): 18–127.

Pape T, Blagoderov B, Mostovski BM (2011) Order Diptera Linnaeus, 1758. In: Zhang Z-Q (Ed.) Animal biodiversity: An outline of higher-level classification and survey of taxonomic richness. Zootaxa, Magnolia Press, Auckland 3148: 223–237. https://doi.org/10.11646/zootaxa.3148.1.42

Richter VA (1988) Family Nemestrinidae. In: Soós, Á. & Papp, L. (eds.), Catalogue of Palae-arctic Diptera 5: 171–181.

Richter VA (1997) Contributions to a Manual of Palaearctic Diptera. Vol. 2. Family Nemes-trinidae. In: Science Herald, Budapest, 459–468.

Richter VA, Ovtshinnikova OG (1996) On the structure of male and female genitalia in Pal-aearctic nemestrinids (Diptera, Nemestrinidae). International Journal of Dipterological Research 7(4): 241–249.

Rondani C (1850) Osservazioni sopra alquante specie di esapodi ditteri del Museo Torinese. Nuovi Annali delle Scienze Naturali e Rendiconto delle Sessioni della Società Agraria e dell'Accademia delle Scienze dell'Istituto di Bologna 2(3): 165–197.

Sack P (1933) Die Fliegen der palaearktischen Region, Nemestrinidae. In: Lindner E (Ed.) Stuttgart. Vol. 4 (22): 1–42.

Steyskal GC, El-Bialy S (1967) A list of Egyptian Diptera with a bibliography and key to fami-lies. Ministry of Agriculture Technical Bulletin 3: e37.

Thompson FC, Pape T (2021) Systema Dipterorum. http://www.diptera.org/ [accessed August 2021]

Villeneuve J (1912) Notes synonymiques. Wiener Entomologische Zeitung 31: 1–97.

Wiedemann CRW (1828) Aussereuropaische zweiflugelige Insekten. Zuerst theil. Schulz, Hamm, 608 pp.

COMMENTARY

Diagnosing diagnoses – can we improve our taxonomy?

Art Borkent[1]

1 *691-8ᵗʰ Ave. SE, Salmon Arm, British Columbia, V1E 2C2, Canada*

Corresponding author: Art Borkent (artborkent@telus.net)

Citation: Borkent A (2021) Diagnosing diagnoses – can we improve our taxonomy?. ZooKeys 1071: 43–48. https://doi.org/10.3897/zookeys.1071.72904

Abstract

Taxonomic diagnoses should be clear but minimal statements that precisely distinguish a given specimen from other taxa at the same stage of development (e.g., pupa, adult female, egg). Presently, most diagnoses are of uncertain value. It is a great advantage for readers to be able to simply and confidently confirm their identifications after using a key.

Keywords

Taxonomy, keys, identification

There are numerous features that are important components of systematic treatments. The description of species, a functional key, portrayal of distributions, and discussion of associated taxonomic issues are standard in such publications. Additionally, many authors provide a diagnosis of the taxon at hand. These diagnoses, however, strongly vary in what is included.

In most publications during the past decades, diagnoses are often, at least within literature dealing with Diptera, a set of features that an author deems valuable or interesting in portraying a given taxon. Often, they are a summary of various character states without any specific purpose or only some of which distinguish the taxon. Whether authors desire to include such a summary or not, many diagnoses are not diagnostic, at least as defined by the Oxford dictionary: "the distinctive characterization in precise terms of a genus, species, or phenomenon" [one of two definitions]. Ernst Mayr (1969) in his book 'Principles of Systematic Zoology' defines a diagnosis as "in

taxonomy, a formal statement of the characters (or most important characters) which distinguish a taxon from other similar or closely related coordinate taxa". In 'Phylogenetics, the Theory and Practice of Phylogenetic Systematics', Wiley (1981) states that a diagnosis is "a brief listing of those characters which differentiate a taxon from related and/or similar taxa". In the English glossary of the International Code of Zoological Nomenclature (4th edition) a diagnosis is "A statement in words that purports to give those characters which differentiate the taxon from other taxa with which it is likely to be confused." Dubois (2017) provides a more restricted understanding of the use of diagnoses, noting "the most widespread understanding of the term 'diagnosis' in taxonomy can be put as 'list of taxonomic criteria allowing one to distinguish two different taxa' when the latter are compared". A comparison of only two taxa is often insufficient in groups with many taxa.

Rather than being a mix of character states of uncertain value in recognizing a taxon, it would therefore be a valuable contribution to every taxonomic paper to include a definitive diagnosis that allows a reader to confirm, in the simplest manner, the identification of a specimen at hand (after perhaps running it through a key). If there are further diagnostic features, the author can easily state that the taxon is unique in possessing character states 1+2+3 or character states 2+3+4, etc.

Brown et al. (2009, 2011) presents a comprehensive compendium allowing for the identification of all genera of Central America Diptera in a family-by-family treatment. Each family chapter provides a purported diagnosis, but the purpose of such diagnoses is unclear. The Culicidae (mosquitoes), for example, has the following lengthy diagnosis of the adult stage: "Adults slender (Fig. 1), 3–8 mm long (from anterior margin of clypeus to end of abdomen), 1–2 mm high (from upper margin of scutum to base of coxae). Head small, ovoid. Ocelli absent. Eye reniform, occupying most of side of head. Antenna with short, ringlike scape, enlarged globular pedicel, and 13-flagellomeres, usually more plumose in male. Proboscis long, slender, external part (labium) covered with scales. Thorax with patches of scales, as well as patches or rows of setae; setae usually coalesced on scutum into three paired, longitudinal rows: acrostical, dorsocentral, and supra-alar setae. Wing elongate, rounded apically, with scales along length of veins, microtrichia on membrane. Abdomen 10 segmented, segments 1–9 at least partly covered with scales in Culicinae bare in Anophelinae." It is unclear whether the reader needs to check each of these features to be certain of the family identification of a specimen run through the family key. In fact, all extant adult Culicidae can be recognized by checking only two character states: an elongate proboscis, equal or longer than the antenna, and the presence of scales on the wing. These two features in combination are diagnostic within the order. If the reader had this knowledge, she/he could easily confirm the identification of the specimen being studied. In this instance, both sexes can be recognized using these features. Further to this, in each diagnosis, it should be clear what semaphoront (life stage) is being discussed, so that in this case the statement, "Male and female:" should precede the diagnostic features. If male and female features are otherwise both included in a single diagnosis, as in "Male with curved parameres, female with spherical spermatheca", it would actually mean that

features of both sexes are required for confirmation of the identification. As such, males and females generally need to be diagnosed separately, especially at the species level.

Diagnoses need to be restricted to the group under study. As such, the diagnosis of a given species in a generic study need only supply those features that are a unique combination <u>within</u> that genus. To be clear, a statement indicating the group considered should be provided, as in the example of *Corethrella* Coquillett species below. If authors provided such accurate diagnoses, students of our group would be more confident in identifying at every level of classification. They would clearly know, as they studied the literature, that an adult insect they collected in the Nearctic was a Diptera (the only order of insect worldwide with metathoracic halters), a Chaoboridae (the only family of Diptera worldwide with scales on the posterior margin of the wing, mouthparts shorter than the antenna, and wing vein R_1 extending to near the apex of R_2), a *Mochlonyx* Loew (the only Nearctic genus of Chaoboridae with the first tarsomere of each leg shorter than the second), and *Mochlonyx cinctipes* (Coquillett) (the only species of *Mochlonyx* in the Holarctic region with patterned wings).

In a revision of the genus *Corethrella* (Borkent 2008), a diagnosis for each of the 97 extant species was provided. In some instances, males and females could be diagnosed together because the unique set of features was present in both sexes. *Corethrella nippon* Miyagi was diagnosed as follows: *"Male and female adults*: only extant Old World species of *Corethrella* with a plain wing (no pattern of pigmentation), the scutum paler than the dark brown pleura, and the base of the hind tibia without pigmentation (equal to the apex of the hind femur)." In other species the males and females could not be diagnosed together and therefore were distinguished as in the following example of *Corethrella blandafemur* Borkent: "*Male adult*: only extant species of *Corethrella* with a stout, elongate, and apically expanded bristle on flagellomere 6. *Female adult*: only extant species of *Corethrella* in the New World with a circular head (in anterior view), with flagellomere 1 moderately elongate, sensilla coeloconica present only on flagellomeres 1, 9–13 and with only a single sensillum coeloconicum on each of 9–13, wing with only setae, with uniformly pigmented wing, scutum, katepisternum (with or without a very narrow dorsal pale band), and legs." Supportive illustrations were provided and cited in the original diagnoses so that the reader can easily check features.

In many publications, systematic treatments are regional, or knowledge is more limited, and authors therefore may need to modify their diagnoses within a regional context, as in the *Corethrella* examples above, where identification of *Corethrella blandafemur* depends in part on where the features are considered distinctive (i.e., in the New World). If regional treatments can be sure of features being unique in a broader area, this should be stated as such: a Nearctic generic treatment should, if the author can present this, provide the features of a species as being unique worldwide. If restricted to the Nearctic, it would present the possibility to the reader that it may not be distinguishable using those character states from a Palaearctic species or an invasive from elsewhere.

Regardless whether the reader agrees with the statements above or not regarding diagnoses, there remains a need to help the users of our taxonomic work to confirm identifications as easily as possible. As taxonomists we want our work to be as clear and

useful as possible. The keys we write are not for ourselves but for others who follow and who are uncertain of identifications (or they would no be using the key in the first place). When keying material of unfamiliar groups, it is a nearly universal emotion to feel some level of uncertainty in coming to a particular name. We all wish the author of the key could confirm the specimen identification we have determined. In the absence of teleporting, a diagnosis is the author's opportunity to provide such affirmation. This is especially true in cases where keys are long and character states finely defined.

One reviewer pointed out that a diagnosis may hide the presence of further new species and that adding numbers of character states in a diagnosis helps the reader to avoid this. However, it appears to me that the opposite is true. If another researcher recognizes two taxa which both share a single published diagnosis, it provides clear evidence that one of the species is undescribed (or previously unknown from the area if the published study is restricted geographically). Otherwise, a reader who wants to examine other character states of a species can turn to the description for further details.

Some may argue that dichotomous keys provide the diagnostic features for a given taxon and although true, it is mostly a more complicated set of character states that needs to be considered. Taking the example of the Culicidae from above, this family keys out to one of the alternatives in couplet 8 in the family key in the Manual of Central American and couplet 15 of the Manual of Nearctic Diptera. For both, a number of other features need to be examined to arrive at this family. It is true that some diagnoses, with the minimum number of features allowing identification, are actually a sum of the features present in the key. However, in such instances (the minority) it is useful for the reader to know that all the features, already presented in the key, need to be checked for confirmation.

The increasing use of DNA barcodes has paved the way for describing new species characterized by a sequence shown or believed to be unique, and in some cases devoid of morphologically based diagnoses (e.g., Sharkey et al. 2021). For some, this is a panacea to deal with the often-overwhelming diversity present in some tropical habitats and/or hyperdiverse genera noted for small or miniscule morphological differences. There are, however, serious challenges that indicate the questionable interpretation of such results (Ahrens et al. 2021; Meier et al. 2021). What remains, however, is that there are currently some groups of species which are so morphologically similar that it is not possible to either key them and, by extension, provide a diagnosis. The evidence for treating them as species may be entirely behavioral or genetic (so that the diagnosis can only be a sequence). Further to this, it is clear that some life stages may not be diagnosable (e.g., the eggs of many species), with the evidence for treating them as separate species for some being present in only one stage. In such instances, it is most clear to state this in the diagnosis section of the systematic treatment (e.g., "Female adult not diagnosable to species"). Of course, future research may discover character states that do allow diagnosis of a given life stage. Regardless, such statements can make it clear to the reader as to which semaphoronts can or cannot be identified.

I have not, in this paper, compiled statistics on how many systematic treatments provide accurate diagnoses. However, experience with a few large systematic projects in Dipterology (the study of flies), reviewing more than 30 manuscripts per year for sev-

eral decades (mostly taxonomic), and counseling students in their systematic projects, I diagnose a strong majority of diagnoses either to not to be diagnostic at all or to have diagnostic features included among a much larger array of character states. Further to this, among both students and colleagues, I have repeatedly encountered differences in opinion regarding the nature of diagnoses of species, genera, and other taxa. It would be beneficial, in my opinion, to re-examine our concepts of diagnoses and perhaps refine our presentation of this aspect of our taxonomic publications. I would also encourage editors of systematic papers to introduce more rigor in what is expected in a diagnosis for submitted papers.

Acknowledgments

References

Ahrens D, Ahyong ST, Ballerio A, Barclay MVL, Eberle J, Espeland M, Huber BA, Mengual X, Pacheco TL, Peters RS, Rulik B, Vaz-De-Mello F, Wesener T, Krell F (2021) Is it time to describe new species without diagnoses? – A comment on Sharkey et al. (2021) Zootaxa 5027 (2): 151–159. https://doi.org/10.11646/zootaxa.5027.2.1

Borkent A (2008) The Frog-Biting Midges of the World (Corethrellidae: Diptera). Zootaxa 1804: 1–456. https://doi.org/10.11646/zootaxa.1804.1.1

Brown BV, Borkent A, Cumming JM, Wood DM, Woodley NE, Zumbado MA (Eds) (2009) Manual of Central American Diptera. Volume 1. National Research Council Press, Ottawa, Canada, 714 pp.

Brown BV, Borkent A, Cumming JM, Wood DM, Woodley NE, Zumbado MA (Eds) (2011) Manual of Central American Diptera. Volume 2. National Research Council Press, Ottawa, Canada, xvi + 715–1442.

Dubois A (2017) Diagnoses in zoological taxonomy and nomenclature. Bionomina 12: 63–85. https://doi.org/10.11646/bionomina.12.1.8

Mayr E (1969) Principles of Systematic Zoology. McGraw Hill, New York and London, 428 pp.

Meier R, Blaimer BB, Buenaventura E, Hartop E, vonRintelen T, Srivathsan A, Yeo D (2021) A re-analysis of the data in Sharkey et al.'s (2021) minimalist revision reveals that BINs do not deserve names, but BOLD Systems needs a stronger commitment to open science. Cladistics (2021) 1–12. https://doi.org/10.1111/cla.12489

Sharkey MJ, Janzen DH, Hallwachs W, Chapman EG, Smith MA, Dapkey T, Brown A, Ratnasingham S, Naik S, Manjunath R, Perez K, Milton M, Hebert P, Shaw SR, Kittel RN, Solis MA, Metz MA, Goldstein PZ, Brown JW, Quicke DLJ, van Achterberg C, Brown BV, Burns JM (2021) Minimalist revision and description of 403 new species in 11 subfamilies of Costa Rican braconid parasitoid wasps, including host records for 219 species. ZooKeys 1013: 1–665. https://doi.org/10.3897/zookeys.1013.55600

Wiley EO (1981) Phylogenetics, the theory and practice of phylogenetic systematics. Wiley & Sons, New York, 439 pp.

RESEARCH ARTICLE

Another Laurasian connection in the Early Eocene of India: *Myrmecarchaea* spiders (Araneae, Archaeidae)

Hannah M. Wood¹, Hukam Singh², David A. Grimaldi³

1 *Department of Entomology, National Museum of Natural History, Smithsonian Institution, Washington, DC 20560, USA* **2** *Birbal Sahni Institute of Palaeosciences, Lucknow 226007, India* **3** *Division of Invertebrate Zoology, American Museum of Natural History, New York, NY 10024-5192, USA*

Corresponding author: Hannah M. Wood (woodh@si.edu)

Abstract

The first fossil Archaeidae in Cambay amber from India, of Eocene age, is documented. The inclusion is a spider exuvium and is placed as *Myrmecarchaea* based on the presence of elongated legs, a slightly elongated pedicel with lateral spurs, and a diastema between coxae III and IV that is similar to *M. antecessor* from Oise amber. The previous occurrences of the genus are from Baltic and Oise amber, both of Eocene age. Because most spiders, including Archaeidae, only molt as juveniles, the exuvium does not have adult features nor have distinct species-specific features, and a new taxon is not erected. This new record further extends the distribution of the family and genus to India 50–52 million years ago. *Myrmecarchaea* in Indian Cambay amber provides additional evidence that India in the Early Eocene had affinities with the Palearctic mainland rather than showing Gondwanan insularity.

Introduction

Archaeidae Koch & Berendt, 1854 was initially described from fossils in Baltic amber of Eocene age. Decades later, extant species were discovered in the forests of Madagascar (Pickard-Cambridge 1881), and then were also found and documented from South Africa and Australia (Forster and Platnick 1984). The number of extant species contin-

ues to grow due to taxonomic revision, some recent (e.g., Lotz 2015; Wood and Scharff 2018). Yet thus far, the extant clades remain known only from these three areas. The fossil record has also expanded, not only in new species, but from new deposits from different parts of the world. Presently archaeid species have been described from the following deposits, ordered chronologically in geological time: Bitterfeld amber, age controversial, but likely middle Eocene (Wolfe et al. 2016; Dunlop et al. 2018); Baltic amber from the "Blue Earth" stratum (which yields much but not all commercial Baltic amber) is of mid-Eocene (Lutetian) age (Ritzkowski 1997); French Oise amber of lower Eocene age (Nel et al. 1999); Burmese amber of Late Cretaceous age (Shi et al. 2012); compression fossils from Inner Mongolia of Late Jurassic age (Huang 2019), and from Kazakhstan dated as Late Jurassic (Doludenko et al. 1990). The fossil record for archaeids is extensive compared to most other spiders, spanning deep geological time and large geographical distances. Many of the archaeid fossils are preserved in amber, which captures exquisite morphological details and thus provides more evidence about evolutionary relationships. While the northern lineages have gone extinct, the southern lineages have persisted, making Archaeidae an intriguing group for understanding ancient biogeography patterns and faunal turnover through deep time.

Herein, we report on the first archaeid documented from Cambay amber, from western India, dated at 50–52 Ma (Rust et al. 2010). The amber piece contains a spider exuvium, and this record extends the known distribution of archaeids to include India. India was once a part of Gondwana and break-up of this landmass started in the Middle Jurassic (Rabinowitz et al. 1983), with India breaking away from Madagascar in the Late Cretaceous (Storey et al. 1995) and traveling northward until colliding with Asia at an age hypothesized to be around 50 Ma (Garzanti et al. 1987; Rowley 1996). Cambay amber documents the Indian biota at a time when it had a tropical, broad-leaved paleoenvironment and around the time of collision with Asia.

Materials and methods

Fossiliferous amber from the Eocene of India comes from the Cambay and Kutch Basins and is dated as mid- to early-Ypresian (50–52 Ma). The specimen reported here occurs in Cambay amber from the Tadkeshwar lignite mine, approximately 30 km NE of Surat, 21°21.400'N, 073°04.532'E, Gujarat state, India. The stratigraphy of the mines and locations of amber-bearing strata are presented in Rust et al. (2010). The archaeid is the only specimen of the family among the several thousand arthropod inclusions screened thus far in bulk, unprocessed Cambay amber. There is a diversity of other spiders and arachnids in this amber.

The amber piece contains an archaeid exuvium (Fig. 1). Following Henningsmoen's criteria for recognizing exuviae (1975), the position of the different pieces of the exuvium and the sutures where the exuvium are broken are in line with what is expected when a spider molts and removes its soft body from the molt. In spiders, first, the cephalothorax breaks laterally, starting near the clypeus and then extending posteriorly

until the carapace lifts off; next, the lateral tears extend to the anterior of the abdomen (opisthosoma); lastly, the spider extracts its body out of the lower portion of the exuvium (Foelix 2011). In the majority of spiders, molting only occurs until the adult stage (Foelix 2011), and this has also been observed for archaeids (H.M.W. personal observation). In fact, the cylindrical carapace is fully fused in adult archaeid specimens, completely encircling the cheliceral bases (Wood et al. 2012), and this configuration would likely prevent molting in adult specimens. Thus, the exuvium does not have adult features, but the size of the exuvium, with most adult archaeids being 2–4 mm in size, suggests this may have been the shed skin of a penultimate female that became an adult.

The more sclerotized portions of the exuvium are the chelicerae, sternum, coxae, pedicel, and anterior-most portion of the abdomen, and these structures retain what is probably much of their original pre-molting shape. Some parts of the legs are deformed, containing bends or shriveling, and since most of the abdomen is less sclerotized, it is also deformed. The exuvium has all parts remaining (chelicerae, lower half of the cephalothorax, and abdomen) except for the carapace and some distal parts of the legs. The exuvium is resting on what appears to be a spider web or silk mesh (Fig. 1B). Archaeids do not construct webs for catching prey, and are instead active hunters specialized to prey on other spiders (Millot 1948; Legendre 1961; Wood et al. 2012). But archaeids do construct silk snares and draglines that they hang from while molting (H.M.W. personal observation). This is not likely the case though for the silk observed in this amber piece because the dorsum of the exuvium is resting on the silk rather than the ventral portion, which would be expected during molting. Instead, it could be that after molting the exuvium was carried in the wind or dropped from above and was captured by the web and/or tree resin. There are other unknown, circular bundles, nearby, possibly of debris.

The amber piece was trimmed and polished, then embedded in EpoTek301-2 synthetic resin, followed by additional trimming and polishing. The specimen was observed with a Leica 205C and an Olympus SZX10 microscope. Photographs were taken as a series of stacks using a Canon EOS T6i digital camera mounted to the Leica microscope. Image stacks were assembled into one combined image using ZereneStacker (Zerene Systems, LLC). All measurements are in millimeters (mm).

Systematic paleontology

Superfamily Palpimanoidea sensu Wood et al. (2012)
Family Archaeidae Koch & Berendt, 1854

Genus *Myrmecarchaea* Wunderlich, 2004

Remarks. The presence of a cheliceral gland mound, peg teeth running along the inner cheliceral margin, cuticle texture with scales and/or tubercles (in this case, having both), and the lack of leg spines indicate Palpimanoidea. The following characters
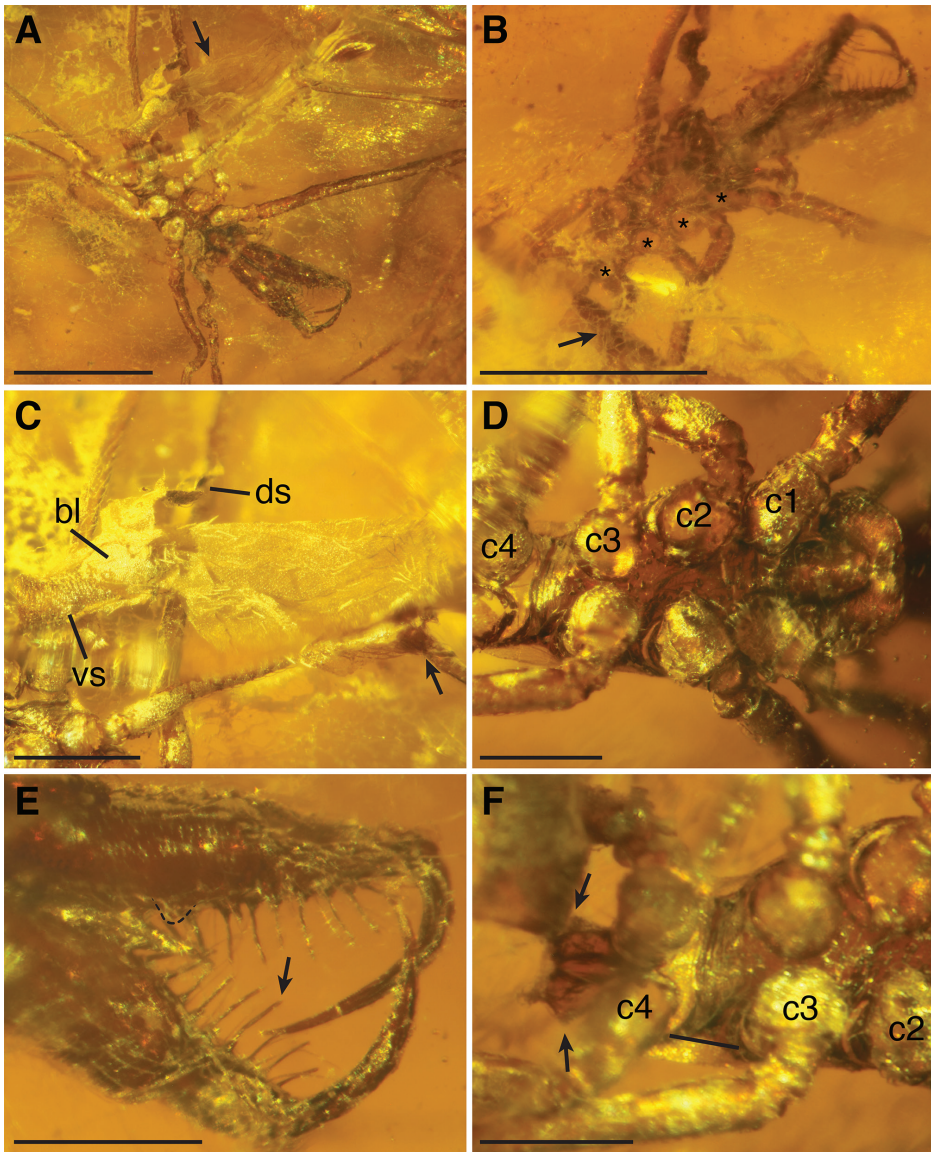
Figure 1. Images of *Myrmecarchaea* sp. (BSIP 41985) from Cambay amber **A** exuvium, ventral; arrow pointing to dorsal of abdomen **B** cephalothorax, dorsal; asterisks denote the coxal openings on the right side where the legs were pulled out of the ventral portion of the exuvium; arrow pointing to some silk threads that is part of a mesh that covers the dorsum of the exuvium **C** abdomen, lateral; arrow pointing at spinnerets; 'ds' showing the anterior dorsal abdominal sclerite, which is folded back as part of the molting process when the spider freed its body from the exuvium; 'bl' marking the booklung cover that is attached to the anterior ventral abdominal sclerite (labeled 'vs') **D** anterior portion of cephalothorax, ventral; for reference, the coxae on the right side are numbered and labeled (c = coxa) **E** distal portion of chelicerae, posterior; dashed line outlines the cheliceral gland mound on the right chelicera; arrow points to one peg tooth **F** posterior portion of cephalothorax, ventral; for reference, the coxae on the left side are numbered and labeled (c = coxa); arrows show the lateral spurs on the pedicel; black line shows the diastema between coxa III and coxa IV. Scale bars: 1 mm (**A, B**); 0.25 mm (**C–F**).

indicate Archaeidae: setal bases on tubercles on the sternum, the shape of the sternum (narrow throughout, not shield shaped), the elongated chelicerae, the shape of the gland mound (pointed, positioned close to fang tip), the blunt setae on the abdomen (rather than tapering), the presence of a bump on the dorsal, basal surface of the femora, and the presence of a curve in femur IV. The specimen is referred to as *Myrmecarchaea* based on having a slightly elongated pedicel and greatly elongated legs (Wunderlich 2004). Specifically, elongated legs are defined here as femur I being at least four times as long as the carapace length. Another diagnostic character for the genus may be the presence of a spur on each lateral side of the pedicel, adjacent to the anterior of the abdomen (Fig. 1F). The presence of lateral spurs is also observed in *M. petiolus* Wunderlich, 2004, and *M. pediculus* Wunderlich, 2004 (Fig. 2; pedicel is obscured in the single known specimen of *M. antecessor* Carbuccia et al., 2020). There are other palpimanoid genera with elongated legs, including both extinct (e.g., *Planarchaea* Wunderlich, 2015) and extant members (e.g., *Eriauchenius workmani* Pickard-Cambridge, 1881, although with only leg I elongated). However, these other taxa do not also have an elongated pedicel, nor a pedicel with lateral spurs.

Myrmecarchaea is comprised of three species: *M. petiolus*, *M. pediculus*, and *M. antecessor*. The exuvium shows similarities to *M. antecessor* in having a diastema between coxae III and IV (compare Fig. 1D, F with fig. 2 from Carbuccia et al. 2020). The pedicel seems slightly longer than in non-*Myrmecarchaea* archaeids, but not as extreme as the pedicel of *M. petiolus* and *M. pediculus*. The ratio of cephalothorax length to pedicel length can be used to compare these shape differences: *M. pediculus* = 1.2; *M. petiolus* = 1.4; *M. antecessor* = 2.3 (estimated from figures in Carbuccia et al. 2020); *E. workmani* = 4.3. This ratio should be treated with caution because measurements were taken from different views for the different species out of necessity due to inconsistencies in fossil preservation. The exuvium from Cambay amber has a ratio of 4.0, and does not present a remarkably long pedicel. The adult ratio may be closer to that of *M. antecessor*, but because this exuvium is from a juvenile, it cannot be determined whether this is *M. antecessor* or a new species.

Myrmecarchaea sp.

Material examined. single specimen, voucher number BSIP41985 (collection details above), deposited in Birbal Sahni Institute for Palaeosciences in Lucknow, India.

Description. Body length from endites to abdomen: 2.4 mm, but abdominal portion of exuvium is partially deformed (Fig. 1C). Carapace missing. Chelicerae texture with scales and also tubercles present at setal bases (Fig. 1E). Sternum and chelicerae setae white and thickly plumose. Posterior sternum tubercle absent (Fig. 1F). Sternum not fused to intercoxal sclerites, with thin suture separating the two. Intercoxal sclerites large, filling up the intercoxal space. Sternum length 0.52 mm and width 0.21 mm, narrow throughout (longer than wide) and not shield shaped (Fig. 1D). Pedicel 0.21 mm long and 0.18 mm wide. Spur on each lateral side of pedicel (Fig. 1F). Posterior of cephalothorax elongated with a large space (0.084 mm) between coxae
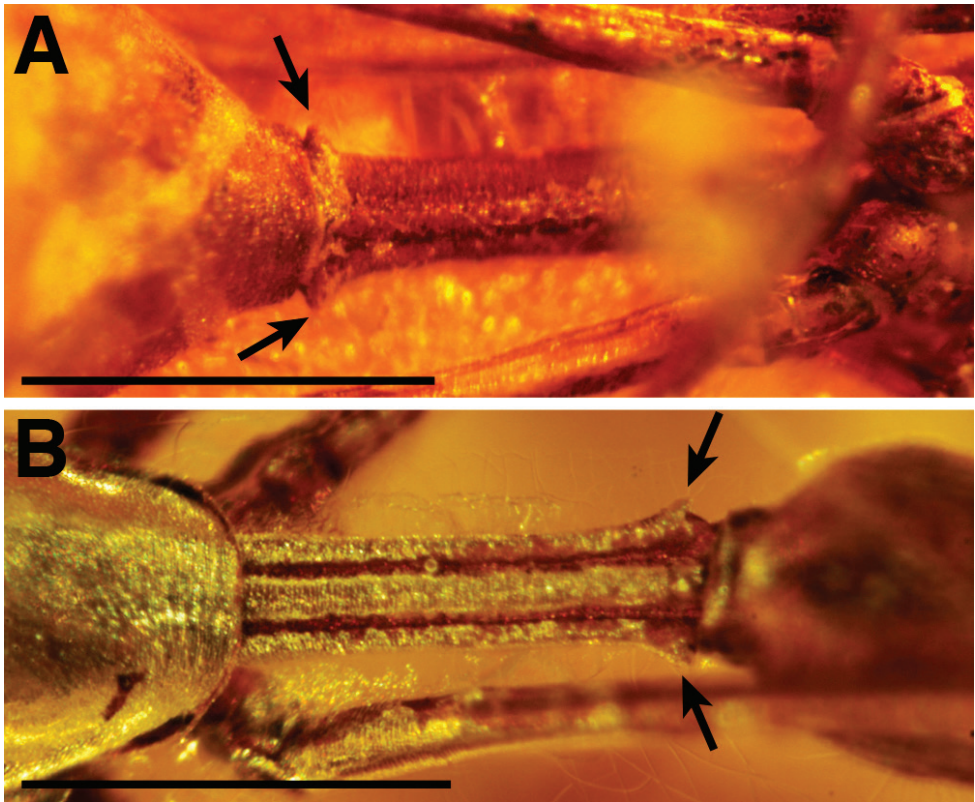
Figure 2. Pedicel of different *Myrmecarchaea* species from Baltic amber, arrows marking lateral spurs **A** *M. pediculus* Wunderlich, 2004, pedicel, ventral, holotype specimen, No. S3907/4338, from Geologisch Paläontologisches Institute und Museum (GPIH) **B** *M. petiolus* Wunderlich, 2004, pedicel, dorsal, holotype specimen, No. S3999/4337, from GPIH. Scale bars: 0.5 mm.

III and IV compared to spaces between other coxae (e.g., 0.048 mm between coxae II and III), roughly twice the length (Fig. 1F). Labium with narrow, v-shaped notch at tip, not fused to sternum. Endite shape slightly convergent, following line of the labium, then converging at distal end around labium (Fig. 1D). Endites elongated to at least half the length of the cephalothorax, pointing downward around 45°, extending beyond the coxae. Patella IV with retrolateral bulge, unclear if present on other patella. Large tubercles absent on legs, leg texture with scales. Femur IV with distinct bend. Dorsal surface of femora with bump. Leg IV patella/tibia juncture straight, not hyperextended. Femur I base the same thickness as other femora (Fig. 1D). Femur I longest (2.05 mm), followed by femur II (1.60 mm), femur IV (1.37 mm), then femur III (1.05 mm). Trochanters entire. Leg spines absent. Chelicerae 0.80 mm long and 0.17 mm wide (at midpoint), anterior surface smooth, i.e., lacking spine, protuberance, or cluster of setae. Basal edge of chelicerae splayed out rather than with parallel edges. Slight constriction at basal edge just distal to splayed edge. 8–9 visible peg

teeth present only on cheliceral promargin, peg teeth uneven lengths, not showing a pattern (e.g., short, long, short, long), with blunt tips rather than tapering (Fig. 1E). Longer peg teeth present, close to gland mound, and at least one peg tooth present that is anterior to main promargin row. Four teeth on cheliceral retromargin. Cheliceral stridulatory striae present, occurring in the basal 1/3 of chelicera, with a regular edge forming an oval patch. Stridulatory cusps present on pedipalpal femora, two visible on basal right femur and one on basal left, with distal remainder of femora obscured. Distal portion of chelicerae curved laterad, with distal tip tapering, rather than blunt (Fig. 1E). Cheliceral gland mound present, a pointed bulge on retromargin close to where closed fang tip would meet cuticle (Fig. 1E). Fangs evenly rounded, lacking increased curvature at tip. Abdomen 1.35 mm long, exuvium shape suggests abdomen was smoothly rounded, elongate, and lacks dorsal tubercles. Abdomen hairs thick, plumose, with tips blunt and club-like (Fig. 1C). Anterior lateral, posterior lateral, and posterior median spinnerets developed (Fig. 1C). Large sclerotized pits on abdomen absent. Dorsal and ventral sclerotization on abdomen anterior, forming a sclerotized circle around pedicel, with dorsal sclerite folded back due to molting process (Fig. 1C). Pedipalpal tarsus lacking prolateral and retrolateral brush of setae, and spines.

Discussion and conclusions

Taxonomic placement and distribution

The fossil from Cambay amber is the first record of an archaeid from India. *Myrmecarchaea* is comprised of three species and was originally diagnosed based on having an elongated pedicel and elongated legs (Wunderlich 2004). We include an additional diagnostic feature for the genus of having lateral spurs on the posterior of the pedicel (Figs 1F and 2). The distribution of *Myrmecarchaea* is expanded to include the following deposits: Baltic amber, French Oise amber, and Indian Cambay amber. These three deposits are all from the Eocene, with Cambay and Oise amber older, dated Ypresian, and most of the commercially sold Baltic amber containing inclusions, dated Lutetian. The Cambay amber specimen is morphologically the most similar to *M. antecessor* from Oise amber, but is separated from that deposit today by over 6000 km.

The widespread nature of Archaeidae in general, and *Myrmecarchaea* specifically, shows a formerly more widespread distribution. One scenario for widespread distributions is the global hothouse climate in the Paleogene, due to the Paleocene-Eocene Thermal Maximum (PETM) and the Early Eocene Climatic Optimum (EECO) (Pearson et al. 2001; Jahren 2007). Indeed, the Cambay amber was formed in coastal, monsoonal, humid dipterocarp forests around this time, with mangroves close by (Rust et al. 2010). Present-day tropical taxa that occurred in northern latitudes during the Paleogene may have retreated southward with the tropical forests when the Earth cooled from late in the Eocene to the Neogene. Today, extant archaeids are considered microendemics (Rix and Harvey 2012; Wood et al. 2015), often occurring on a single

mountain top. The specimen from Cambay amber may be a new, undocumented species or may be *M. antecessor*. Future discovery of more specimens hopefully will resolve this issue.

Myrmecarchaea are rare in collections, with species only known from 1 or 2 specimens. Only one adult male has ever been documented, that of *M. antecessor* whose male pedipalps (secondary genitalia) show remarkable similarity to the fossil archaeid *Archaea paradoxa*: "The general structure of the male palp is . . . very similar to *Archaea* . . . with the same general shape of the palpal bulb, the same orientation and shape, including a spiral of the embolus, and also with tegular apophyses in similar positions" (Carbuccia et al. 2020; compare fig. 3 with fig. 7). *Archaea* is comprised of four species and occurs in Baltic and Bitterfeld amber (Dunlop et al. 2020), and *A. paradoxa* is the only species of the genus where adult male specimens have been documented. While *A. paradoxa* and *M. antecessor* have different somatic features, the morphology of the male pedipalps is conserved. This scenario is similar to what has been observed in the extant Madagascan "workmani-group" and the "vadoni-group", where genitalic differences are subtle, but non-sexual, somatic features, such as carapace shape and abdomen color, are distinct (Wood and Scharff 2018). The diagnostic features of *Myrmecarchaea* argue for monophyly of the genus, but the conserved genitalia suggest shared common ancestry for *Myrmecarchaea* and *Archaea*. The somatic differences between species in these genera suggest substantial divergence in ecology.

Natural history and trait evolution

The cephalic area of archaeid spiders is highly modified compared to most other spiders: the carapace is elevated and tubular, and encircles the cheliceral bases, and the chelicerae are greatly elongated. This morphology relates to their specialized behavior of actively searching for and preying on other spiders, and allows the elongated chelicerae to be extended 90° away from the body in order to attack spider prey at a distance (Millot 1948; Legendre 1961; Wood et al. 2012). The degree of elevation in the cephalic area and chelicerae has served as the basis for historical classifications of archaeid spiders and their closest relatives (Legendre 1970; Forster and Platnick 1984). However, it has since been shown that elongation of the cephalic area and chelicerae has evolved independently within the family (Wood et al. 2007). There has also been a shift in elevation of the cephalic area through time: in general, fossil archaeids have less elevated carapaces and chelicerae, occupying a unique region of morphospace, whereas the extant clades have more elevated carapaces and chelicerae (Wood 2017). *Myrmecarchaea* and *Archaea* have relatively shorter carapaces and chelicerae compared to the extant clades, especially those from Madagascar and Australia. The Cambay amber fossil exuvium is missing the carapace, but is likely similar in elevation to the carapaces of other *Myrmecarchaea* and *Archaea* based on its cheliceral structure. Future discovery of additional specimens will provide insight into evolution of carapace and cheliceral shape.

Biogeography

In Archaeidae, the northern lineages have gone extinct and the southern lineages have persisted, producing a pattern where the extant lineages are confined to the Southern Hemisphere, and fossil lineages are known only from the Northern Hemisphere. Phylogenetic and divergence dating analyses, that include fossils together with extant taxa as terminal tips, suggest distinct northern and southern faunas, and that the split between them is congruent with the timing of Pangaea breaking into Gondwana and Laurasia in the Jurassic (Wood et al. 2013). Along these lines, examination of the spider fossil record revealed that Palpimanoidea, to which Archaeidae belongs, began diversifying in the Mesozoic, and Palpimanoidea and Synspermiata were the dominant spider fauna in the Mesozoic, until faunal turnover in the Cenozoic when they were replaced by Araneoidea and the RTA-clade (Magalhães et al. 2020). Thus, archaeids were at one time more widespread, a more dominant part of the spider fauna, and with diversification patterns showing congruence with the break-up of Pangaea. The discovery of *Myrmecarchaea* in Cambay amber adds another piece of evidence suggesting a distinct Laurasian fauna, specifically with Eocene connections between the Baltic region, Oise, France, and western India.

Among the taxa preserved in Cambay amber that have been studied thus far, some show a Laurasian connection among both living and extinct lineages. The main amber deposits for comparison are the Baltic amber of northern Europe (Lutetian), Oise amber from France (Ypresian), and Fushun amber of northeast China (Ypresian). Laurasian taxa include the following: melikertine bees from both Baltic and Cambay amber (Engel et al. 2013); some long-proboscid fungus gnats (Lygistorrhinidae, Sciaroidea) from both Baltic and Cambay amber (Stebner et al. 2017a); biting midges (Diptera, Ceratopogonidae) from Baltic, Fushun, and Cambay amber, and from the Recent (Stebner et al. 2017b); and termites from Baltic and Cambay amber (Engel et al. 2011a). However, there are a few Cambay amber arthropods showing Gondwanan connections, specifically: a webspinner (Embiodea, Scelembiidae) which occurs today in Africa and South America (Engel et al. 2011b); and a whip spider (Amblypygi, *Paracharonopsis*), apparently closely related to the monotypic, relict African genus *Paracharon* (Engel and Grimaldi 2014). There are even two examples of Cambay amber taxa where each has connections to the Recent and Miocene (Dominican Republic amber) of the Neotropical Region: Leptosaldinae bugs (Heteroptera, Leptopodidae) (Grimaldi et al. 2013b), and some dusky-wing lacewings (Neuroptera, Coniopterygidae, *Spiloconis*) (Grimaldi et al. 2013a). These examples show that the Cambay amber has disparate connections to other regions of the world, signaling widespread affinities. Thus far there is no evidence that, at the time of formation of Cambay amber, the Indian subcontinent was biotically isolated, as might be seen for example in the Recent fauna of Madagascar and Australia. Given the range in the ages that India is thought to have docked with mainland Asia, from the earliest Paleogene to the Miocene based on geophysical scenarios (Zhu et al. 2005; Ali and Aitchison 2008; Najman et al. 2010; White and Lister 2012), the paleontological evidence supports the earlier end of this spectrum, probably Paleocene.

Acknowledgements

References

Ali JR, Aitchison JC (2008) Gondwana to Asia: Plate tectonics, paleogeography and the biological connectivity of the Indian sub-continent from the Middle Jurassic through latest Eocene (166–35 Ma). Earth Science Reviews 88: 145–166. https://doi.org/10.1016/j.earscirev.2008.01.007

Carbuccia B, Wood HM, Rollard C, Nel A, Garrouste R (2020) A new *Myrmecarchaea* (Araneae: Archaeidae) species from Oise amber (earliest Eocene, France). BSGF-Earth Sciences Bulletin 191: 24. https://doi.org/10.1051/bsgf/2020023

Doludenko M, Sakulina G, Ponomarenko A (1990) Geologicheskoye stroyenie rayona unikalnogo mestonakhozhdenia posdnejurskoy fauny i flory aule, (Karatau, southern Kazakhstan). Geologicheskii Institut AN SSSR, Moskva.

Dunlop JA, Kotthoff U, Hammel JU, Ahrens J, Harms D (2018) Arachnids in Bitterfeld amber: A unique fauna of fossils from the heart of Europe or simply old friends? Evolutionary Systematics 2: 31–44. https://doi.org/10.3897/evolsyst.2.22581

Dunlop JA, Penney D, Jekel D (2020) A summary list of fossil spiders and their relatives. In: World Spider Catalog Natural History Museum Bern. http://wsc.nmbe.ch [version 20.5, accessed on July 19, 2021]

Engel MS, Grimaldi DA (2014) Whipspiders (Arachnida: Amblypygi) in amber from the Early Eocene and mid-Cretaceous, including maternal care. Novitates Paleoentomologicae 9: 1–17. https://doi.org/10.17161/np.v0i9.4765

Engel MS, Grimaldi DA, Nascimbene PC, Singh H (2011a) The termites of Early Eocene Cambay amber, with the earliest record of the Termitidae (Isoptera). Zookeys 148: 105–123. https://doi.org/10.3897/zookeys.148.1797

Engel MS, Grimaldi DA, Singh H, Nascimbene PC (2011b) Webspinners in Early Eocene amber from western India (Insecta, Embiodea). Zookeys 148: 197–208. https://doi.org/10.3897/zookeys.148.1712

Engel MS, Ortega-Blanco J, Nascimbene P, Singh H (2013) The bees of Early Eocene Cambay amber (Hymenoptera: Apidae). Journal of Melittology 25: 1–12. https://doi.org/10.17161/jom.v0i25.4659

Foelix RF (2011) Biology of spiders. 3rd edn. Oxford University Press, New York.

Forster RR, Platnick NI (1984) A review of the archaeid spiders and their relatives, with notes on the limits of the superfamily Palpimanoidea (Arachnida, Araneae). Bulletin of the American Museum of Natural History 178: 1–106.

Garzanti E, Baud A, Mascle G (1987) Sedimentary record of the northward flight of India and its collision with Eurasia (Ladakh Himalaya, India). Geodinamica Acta 1: 297–312. https://doi.org/10.1080/09853111.1987.11105147

Grimaldi D, Engel MS, Singh H (2013a) Coniopterygidae (Neuroptera: Aleuropteryginae) in amber from the Eocene of India and the Miocene of Hispaniola. American museum novitates 2013: 20–39. https://doi.org/10.1206/3770.2

Grimaldi DA, Engel MS, Singh H (2013b) Bugs in the biogeography: Leptosaldinae (Heteroptera: Leptopodidae) in amber from the Miocene of Hispaniola and Eocene of India. Journal of the Kansas Entomological Society 86: 226–243. https://doi.org/10.2317/JKES130128.1

Henningsmoen G (1975) Moulting in trilobites. Fossils and Strata 4: 179–200.

Huang D (2019) Jurassic integrative stratigraphy and timescale of China. Science China Earth Sciences 62: 223–255. https://doi.org/10.1007/s11430-017-9268-7

Jahren AH (2007) The Arctic forest of the middle Eocene. Annual Review of Earth and Planetary Sciences 35: 509–540. https://doi.org/10.1146/annurev.earth.35.031306.140125

Koch CL, Berendt GC (1854) Die im Bernstein befindlichen Crustaceen, Myriapoden, Arachniden und Apteren der Vorwelt. In: Berendt GC (Ed.) Die im Bernstein befindlichen organischen Reste der Vorwelt gesammelt in Verbindung mit mehreren bearbeitet und herausgegeben. Berlin, In Commission der Nicolaischen Buchhandlung, 1–124.

Legendre R (1961) Études sur les *Archaea* (Aranéides). – II. La capture des proies et la prise de nourriture. Bulletin of the Zoological Society of France 86: 316–319.

Legendre R (1970) Arachnides-Araignées-Archaeidae. Faune de Madagascar 32: 1–50.

Lotz LN (2015) A new species of *Afrarchaea* (Araneae: Archaeidae) from South Africa. African Invertebrates 56: 409–414. https://doi.org/10.5733/afin.056.0211

Magalhães IL, Azevedo GH, Michalik P, Ramírez MJ (2020) The fossil record of spiders revisited: implications for calibrating trees and evidence for a major faunal turnover since the Mesozoic. Biological Reviews 95: 184–217. https://doi.org/10.1111/brv.12559

Millot J (1948) Faits nouveaux concernant les *Archaea* (Aranéides). Mémoires L'Institut Scientifique de Madagascar, Série A 1: 3–14.

Najman Y, Appel E, Boudagher-Fadel M, Bown P, Carter A, Garzanti E, Godin L, Han J, Liebke U, Oliver G (2010) Timing of India-Asia collision: Geological, biostratigraphic, and palaeomagnetic constraints. Journal of Geophysical Research: Solid Earth 115: B12416. https://doi.org/10.1029/2010JB007673

Nel A, de Plöeg G, Dejax J, Dutheil D, de Franceschi D, Gheerbrant E, Godinot M, Hervet S, Menier J-J, Augé M (1999) An exceptional Sparnacian locality with plants, arthropods and vertebrates (Earliest Eocene, MP7): le Quesnoy (Oise, France). Comptes Rendus de l'Academie des Sciences Series IIA Earth and Planetary Science 1: 65–72. https://doi.org/10.1016/S1251-8050(99)80229-8

Pearson PN, Ditchfield PW, Singano J, Harcourt-Brown KG, Nicholas CJ, Olsson RK, Shackleton NJ, Hall MA (2001) Warm tropical sea surface temperatures in the Late Cretaceous and Eocene epochs. Nature 413: 481–487. https://doi.org/10.1038/35097000

Pickard-Cambridge O (1881) On some new genera and species of Araneidea. Proceedings of the Zoological Society of London 49: 765–775. https://doi.org/10.1111/j.1096-3642.1881.tb01333.x

Rabinowitz PD, Coffin MF, Falvey D (1983) The separation of Madagascar and Africa. Science 220: 67–69. https://doi.org/10.1126/science.220.4592.67

Ritzkowski S (1997) K-ar-altersbestimmungen der bernsteinführenden sedimente des samlandes (paläogen, bezirk kaliningrad). Metalla (Sonderheft) 66: 19–23.

Rix MG, Harvey MS (2012) Phylogeny and historical biogeography of ancient assassin spiders (Araneae: Archaeidae) in the Australian mesic zone: evidence for Miocene speciation within Tertiary refugia. Molecular Phylogenetics and Evolution 62: 375–396. https://doi.org/10.1016/j.ympev.2011.10.009

Rowley DB (1996) Age of initiation of collision between India and Asia: A review of stratigraphic data. Earth and Planetary Science Letters 145: 1–13. https://doi.org/10.1016/S0012-821X(96)00201-4

Rust J, Singh H, Rana RS, McCann T, Singh L, Anderson K, Sarkar N, Nascimbene PC, Stebner F, Thomas JC, Solórzano Kraemer M, Williams CJ, Engel MS, Sahni A, Grimaldi D (2010) Biogeographic and evolutionary implications of a diverse paleobiota in amber from the early Eocene of India. Proceedings of the National Academy of Sciences 107: 18360–18365. https://doi.org/10.1073/pnas.1007407107

Shi G, Grimaldi DA, Harlow GE, Wang J, Wang J, Yang M, Lei W, Li Q, Li X (2012) Age constraint on Burmese amber based on U–Pb dating of zircons. Cretaceous Research 37: 155–163. https://doi.org/10.1016/j.cretres.2012.03.014

Stebner F, Singh H, Rust J, Grimaldi DA (2017a) Lygistorrhinidae (Diptera: Bibionomorpha: Sciaroidea) in early Eocene Cambay amber. PeerJ 5: e3313. https://doi.org/10.7717/peerj.3313

Stebner F, Szadziewski R, Singh H, Gunkel S, Rust J (2017b) Biting midges (Diptera: Ceratopogonidae) from Cambay amber indicate that the Eocene fauna of the Indian subcontinent was not isolated. PLoS ONE 12: e0169144. https://doi.org/10.1371/journal.pone.0169144

Storey M, Mahoney JJ, Saunders AD, Duncan RA, Kelley SP, Coffin MF (1995) Timing of hot spot—related volcanism and the breakup of Madagascar and India. Science 267: 852–855. https://doi.org/10.1126/science.267.5199.852

White LT, Lister GS (2012) The collision of India with Asia. Journal of Geodynamics 56: 7–17. https://doi.org/10.1016/j.jog.2011.06.006

Wolfe AP, McKellar RC, Tappert R, Sodhi RN, Muehlenbachs K (2016) Bitterfeld amber is not Baltic amber: Three geochemical tests and further constraints on the botanical affinities of succinite. Review of Palaeobotany and Palynology 225: 21–32. https://doi.org/10.1016/j.revpalbo.2015.11.002

Wood HM (2017) Integrating fossil and extant lineages: an examination of morphological space through time (Araneae: Archaeidae). The Journal of Arachnology 45: 20–29. https://doi.org/10.1636/JoA-S-16-039.1

Wood HM, Gillespie RG, Griswold CE, Wainwright PC (2015) Why is Madagascar special? The extraordinarily slow evolution of pelican spiders (Araneae, Archaeidae). Evolution 69: 462–481. https://doi.org/10.1111/evo.12578

Wood HM, Griswold CE, Gillespie RG (2012) Phylogenetic placement of pelican spiders (Archaeidae, Araneae), with insight into evolution of the "neck" and predatory behaviours of the superfamily Palpimanoidea. Cladistics 28: 598–626. https://doi.org/10.1111/j.1096-0031.2012.00411.x

Wood HM, Griswold CE, Spicer GS (2007) Phylogenetic relationships within an endemic group of Malagasy 'assassin spiders' (Araneae, Archaeidae): ancestral character reconstruction, convergent evolution and biogeography. Molecular Phylogenetics and Evolution 45: 612–619. https://doi.org/10.1016/j.ympev.2007.07.012

Wood HM, Matzke NJ, Gillespie RG, Griswold CE (2013) Treating fossils as terminal taxa in divergence time estimation reveals ancient vicariance patterns in the palpimanoid spiders. Systematic Biology 62: 264–284. https://doi.org/10.1093/sysbio/sys092

Wood HM, Scharff N (2018) A review of the Madagascan pelican spiders of the genera *Eriauchenius* O. Pickard-Cambridge, 1881 and *Madagascarchaea* gen. n. (Araneae, Archaeidae). Zookeys 727: 1–96. https://doi.org/10.3897/zookeys.727.20222

Wunderlich J (2004) Fossil and extant spiders (Araneae) of the superfamily Eresoidea s.l., with special reference to the Archaeidae and remarks on some higher taxa of the superfamily Araneoidea. In: Wunderlich J (Ed.) Beiträge zur Araneologie, 747–808.

Wunderlich J (2015) On the evolution and the classification of spiders, the Mesozoic spider faunas, and descriptions of new Cretaceous taxa mainly in amber from Myanmar (Burma). In: Wunderlich J (Ed.). Beiträge zur Araneologie, 21–408.

Zhu B, Kidd WS, Rowley DB, Currie BS, Shafique N (2005) Age of initiation of the India-Asia collision in the east-central Himalaya. The Journal of Geology 113: 265–285. https://doi.org/10.1086/428805

RESEARCH ARTICLE

Helen's twins in the Balkans: discovery of two new *Paraptychoptera* Tonnoir, 1919 species closely related to *P. helena* Peus, 1958, with systematic revision of the "lacustris" group (Diptera, Ptychopteridae)

Lujza Keresztes[1], Jürgen Kappert[2], Mária Henning[1], Edina Török[3]

1 *Hungarian Department of Biology and Ecology, Center of Systems Biology, Biodiversity and Bioresources, Advanced Hydrobiology and Biomonitoring Lab, Babeş-Bolyai University, 400006 Cluj-Napoca, Romania* **2** *Forsthaus 1, D-363 94, Sinntal, Germany* **3** *"Lendület" Landscape and Conservation Ecology, Institute of Ecology and Botany, Centre for Ecological Research, 2163 Vácrátót, Hungary*

Corresponding author: Lujza Keresztes (keresztes2012@gmail.com)

Citation: Keresztes L, Kappert J, Henning M, Török E (2021) Helen's twins in the Balkans: discovery of two new Paraptychoptera Tonnoir, 1919 species closely related to P. helena Peus, 1958, with systematic revision of the "lacustris" group (Diptera, Ptychopteridae). ZooKeys 1071: 63–81. https://doi.org/10.3897/zookeys.1071.58598

Abstract

Ptychoptera castor Keresztes & Kappert, **sp. nov.** and *P. pollux* Keresztes & Török, **sp. nov.** both belong to the subgenus *Ptychoptera (Paraptychoptera)* Tonnoir (1919) and are described from boggy headwaters in the south Balkan area. These new species are closely related to the range-restricted *P. helena* Peus, 1958, which is known only from Oiti village, Mount Oeta, Phthioitis region, Greece and, together with *P. lacustris*, forms a morphologically well-defined unit in the subgenus *Paraptychoptera*. Based on cladistic analyses of 53 different morphological characters using the male antenna, wing, and genital structures, a general revision of the "lacustris" group is proposed with a dichotomous key of *Paraptychoptera* species.

Introduction

Ptychopteridae or phantom crane flies are medium- to large-sized flies with slender shiny black body, sometimes with yellow or reddish markings, and long legs with tipuloid appearance, however they differ by several characters including their having a small membranous lobe at the base of the halter (Stubbs 1993; Andersson 1997). Ptychopteridae are remnants of a small, archaic family of Diptera with less than 85 recent species distributed worldwide, but they are absent from Australasia and Oceana (Fasbender 2014; Eskov and Lukashevich 2015).

Extant representatives are classified in two subfamilies, Ptychopterinae with a single genus, *Ptychoptera* (about 70 species) and Bittacomorphinae with two other genera, *Bittacomorpha* (with only 2 species) and *Bittacomorphella* (8 species) (Fasbender 2014). Only sixteen *Ptychoptera* species are present in Europe (Török et al. 2015), from which the monophyletic western Palaearctic *Paraptychoptera* group was proposed first by Tonnoir (1919), sharing a conspicuous invaginated auxiliary sexual organ on the male abdominal sternite III. Later, the group was synonymised by Alexander (1927) and included between the more widespread *Ptychoptera* and, consequently, was ignored in important revisions and contributions to the European Ptychopteridae (Freeman 1959; Peus 1958; Zitek-Zwyrtek 1971; Deliné-Draskovits 1983; Krzeminski 1986; Rozkosny 1997; Krzeminski and Zwick 1993). *Paraptychoptera* was recovered only recently as a subgenus of *Ptychoptera* (Zwick and Starý 2003; Fasbender 2014) and also referred to by Ujvárosi et al. (2011). Strong morphological and molecular support to monophyly of *Paraptychoptera* were added in a reference contribution of the world Ptychopteridae species (Fasbender 2014). In his milestone work on modern Ptychopteridae research, Fasbender (2014) recovered *Ptychoptera* (*Paraptychoptera*) Tonnoir (1919) as a monophyletic group sharing a series of common diagnostic features in male genital structures, such as the poorly sclerotised epandrial claspers, without basal lobes, but variable ventral lobes, the well-developed tongue-like hypoproct, gonostylus with basal lobe divided into knoblike anterior lobe and sickle-like medial lobe, and the presence of a conspicuous invaginated auxiliary sexual organ on sternite III.

Paraptychoptera is a monophyletic western Palaearctic group of Ptychopteridae, largely European in distribution, and with only a few species being present in Western Asia and North Africa. Only ten species are considered here, following Fasbender (2014): *P.* (*Paraptychoptera*) *lacustris* Meigen, 1930; *P. longicauda* Tonnoir, 1919; *P. paludosa*, Meigen 1804 has wider European distribution while *P. handlirschi* Czizek, 1919 and *P. silvicola*, Zwyrtek & Rozkosny, 1967 are restricted to Central or Southern Europe. Another five species, however, have a more restricted distribution: *P. (P.) agnes* Krzeminski & Zwick, 1993 is an endemic species that is described from the Pilis mountains, in the Transdanubian Mountains, Hungary (Krzeminski and Zwick 1993), *P. (P.) delmastroi* Zwick & Stary, 2003 from Villafranca municipality in the City of Turin, and Cantarana municipality (both are in the region of Piemonte), northern Italy (Zwick and Starý 2003) and Tunisia (Paramonov, 2013) while *P. (P.) helena* Peus, 1958 is known only from a single site, Oiti village, Mount Oeta, Phthiotis region, Greece (Peus 1958).

Also considered, are two extra-European species that belong to the subgenus *P. resseli* Theischinger, 1978 from the vicinity of Noshahr city, Noshahr region, Mazandaran Province, Iran and *P. (P.) surcoufi* Seguy, 1925 from Algeria (Fasbender 2014).

Among *Paraptychoptera,* the lacustris group was first proposed by Tonnoir (1919), as species having less developed, but recognisable, auxiliary sexual organs in the male sternite III, and was also referred to by Stubbs (1993) and Zwick and Starý (2003), and included the following species*: P. lacustris, P. longicauda, P. paludosa.* In the present paper we describe two new species of the *Ptychoptera (Paraptychoptera) lacustris* from the South Balkans, and provide a key of the revised lacustris group, within which the two new species belong. Material of the range-restricted North African *P. surcoufi* were not available throughout the present investigation, and a detailed description of morphological features has not been published since its summary description in Seguy (1926).

Materials and methods

The type material of *Paraptychoptera* that was used in this study was acquired through field collections by the present authors. Seventy (70) male specimens belonging to nine different species originating from different parts of Europe were investigated (Fig. 1, Table 1).

Low resolution photos of the whole fly and the wings were taken with a stereomicroscope (Zeiss Stemi 2000-C) and a consumer digital SLR camera (Cannon 1100D). Photos of different genital structure parts were taken with a compound microscope (Motic 310 BA) that was equipped with standard plan-achromatic objectives and additionally with objectives from the inverse microscope of the same manufacturer, for work on glycerol without coverslip. The camera was of the high-resolution USB CCD type (Imaging Source Europe GmbH DFK 51AU02). As stacking software, we used the Hugin suite (SourceForge.net). Male genitalia were left overnight in 10% potassium hydroxide (KOH) and for one hour in undiluted glacial acetic acid, to neutralise and wash out the soap that was created from the soft tissues. The male genitalia were then transferred to a larger amount of glycerol to wash out the acid. Afterwards, they were transferred to a drop of glycerol on a slide with rounded excavation. The genitals were dissected, the parts were oriented using the stereomicroscope, and then the slide was carefully transferred to the compound microscope for the taking of photos. Finally, the parts were washed again in 100% isopropanol and embedded permanently in artificial Canada Balsam (Malinol), whereby high resolution photos were taken. Stacking results in general consist of 5-10 single exposures with the stereomicroscope and of 10-50 exposures with the compound microscope.

The types of *P. castor* sp. nov. and *P. pollux* sp. nov. are deposited in the Diptera collection of the Faculty of Biology and Geology, Babeş-Bolyai University, Cluj-Napoca (UBB), Romania (DCFGB). The study of *P. helena* was based on a paratype male from the Zoological Research Museum Alexander Koenig (*ZFMK*), Bonn, Germany, Museum-Id ZFMK-DIP-00015966.
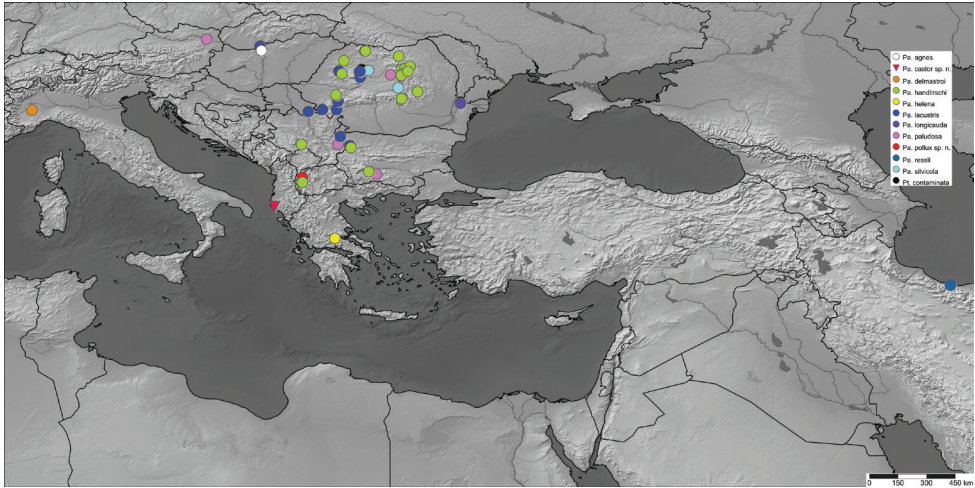
Figure 1. Distribution of different *Paraptychoptera* species used in the present study.

Paraptychoptera agnes Krzeminski & Zwick, 1993, *P. delmastroi* Zwick & Stary, 2003, and *P. ressli* Theischinger, 1978 were not available during the present study, but the detailed morphological description of wing and male terminalia, based on Krzeminski and Zwick (1992) and Zwick and Starý (2003), were used to evaluate discrete details on male terminalia. A comprehensive morphological dataset of the world Ptychopteridae published recently by Fasbender (2014) was also used as a source for morphological details of the male terminalia in species where fresh material were not available to us during the study. Terminology of wing venation and genitalic morphology of *Paraptychoptera* Tonnoir, 1919 follows Fasbender (2014). Cladistic analyses of 53 morphological characters on antennae, wing and male terminalia were analysed (Table 2).

Morphological characters were selected based on the world phylogenetic revision of Ptychopteridae (Fasbender, 2014), but completed with new morphological data. *Ptychoptera* (*Ptychoptera*) *contaminata* was considered as an outgroup taxon. Missing data were coded as '?'. The list of morphological characters is presented in Table 3.

The morphological data matrix was managed with Mesquite 3.5 (Maddison and Maddison 2019). Maximum parsimony analysis of the morphological data was performed using a parsimony programme: "Tree Analysis using New Technologies" (TNT) version 1.5 (Goloboff and Catalano 2016). A "traditional" search based on 1000 replicates of Wagner trees, through 'tree bisection reconnection' (TBR) branch swapping holding 100 trees by the collapsing rule: 'min. length=0'. Subsequently, we selected the best tree, in terms of species topology and population phylogeographical clades, and resampled with 10000 replicates using a standard bootstrap procedure (Felsenstein 1985). Values at nodes represented absolute frequencies and frequency differences (GC, Group present/Contradicted).

Table 1. List of taxa used in this study.

Taxa	Nr. ind	Source of material	Coordinates	Collectors
P. (Pa.) agnes Krzeminski & Zwick, 1993	0	literature data: Krzeminski & Zwick, 1993, Fasbender, 2014	–	–
P. (Pa.) castor sp. nov.	1	Albania, Vlora, Tragjas, Repet y Izvorit, 17 m, 30.iv.2019	40.323132°N, 19.510031°E	leg. Henning, M.
P. (Pa.) delmastroi Zwick and Starý, 2003	0	literature data: Zwick and Starý, 2003 , Fasbender, 2014	–	–
P. (Pa.) handlirschi (Czizek, 1919)	3	Romania, Baia Sprie, Gutin Mts., 955 m, 15.v.2014	47.698860°N, 23.794682°E	leg. Keresztes L.
P. (Pa.) helena Peus, 1958	1	paratype, NMBG Germnay	–	–
P. (Pa.) lacustris Meigen, 1830	1	Bulgaria, Berkovitsa, small brook, 616 m, 28.v.2013	43.218602°N, 23.071343°E	leg. Keresztes L.
	4	Bulgaria, Dabravka, Dabravka lake shore, 364 m, 30.iv.2012	43.651059°N, 22.628539°E	leg. Török E.
	1	Bulgaria, Velingrad, Rhodope Mts., 870 m, 12.vi.2008	41.986014°N, 23.971926°E	leg. Keresztes L.
	7	Hungary, Szobi, Ipolytölgyes, Börzsönyi Mts., 358 m, 2.vi.2016	47.910624°N, 18.821948°E	leg. Török E.
	1	Romania, Cluj, Gilău Mts., Pecica brook, 443 m, 16.iv.2016	46.733137°N, 23.552135°E	leg. Keresztes L.
	3	Romania, Poiana Mărului, Şureanu Mts., 1444 m, 16.vi.2008	45.316562°N, 22.517324°E	leg. Keresztes L.
	1	Romania, Rimetea, Bedeleuilui Mts., 531 m, 28.V.2007	46.448873°N, 23.570063°E	leg. Keresztes L.
	8	Romania, Sasca Română, Almașului Mts., 266 m, 8.v.2009	44.926365°N, 21.782738°E	leg. Keresztes L.
	9	Romania, Valea Iadului, Bihor Mts., Leșu lake, 691 m, 21.v.2006	46.745951°N, 22.556599°E	leg. Keresztes L.
	2	Serbia, Voivodina, Šušara, Deliblatska Peščara, 111 m, 10.vii.2013	44.831943°N, 21.111992°E	leg. Török E.
P. (Pa.) longicauda (Tonnoir, 1919)	3	Romania, Luncvița, Măcin Mts., 151 m, 1.vi.2006	45.221240°N, 28.320892°E	leg. Keresztes L.
P. (Pa.) paludosa Meigen, 1804	1	Austria, Wien, Hermannskoegel, 326 m, 21.v.2013	48.261830°N, 16.302293°E	leg. Graf, W.
	3	Bulgaria, Fotinovo, Rhodope Mts., 1495 m, 16.vii.2012	41.870489°N, 24.344398°E	leg. Keresztes L.
	4	Hungary, Nagybörzsöny, Börzsönyi Mts., 350 m, 1.v.2016	47.939197°N, 18.859785°E	leg. Török E.
	8	Hungary, Szobi, Ipolytölgyes, Börzsönyi Mts., 358 m, 2.vi.2016	47.910624°N, 18.821948°E	leg. Török E.
	2	Romania, Sândominic, Hăghimaş Mts., Babos Laka, 809 m, 9.vi.2019	46.573520°N, 25.822180°E	leg. Keresztes L.
	1	Romania, Voşlobeni, După Luncă peat bog, 757 m, 6.vi.2017	46.670458°N, 25.659906°E	leg. Keresztes L.
	2	Serbia, Fruška Gora National Park, Čerević, 501 m, 5.vii.2018	45.156725°N, 19.738838°E	leg. Keresztes L.
P. (Pa.) pollux sp. nov.	1	North Macedonia, Novo Selo, Mavrovo lake, 990 m, 29.vi.2017	41.721355°N, 20.830103°E	leg. Török E.
P. (Pa.) resseli Theischinger, 1978	0	literature data: Fasbender, 2014	–	–
P. (Pa.) silvicola Zwyrtek & Rozkosny, 1967	3	Romania, Voşlobeni, După Luncă peat bog, 757 m, 6.vi.2006	46.670458°N, 25.659906°E	leg. Keresztes L.
P. (Pa.) surcoufi Seguy, 1925	0	literature data: Fasbender, 2014	–	–
P. (Pt.) contaminata (Linnaeus, 1758)	3	Romania, Floreşti, marshy area, Someşul Mic, 370 m, 18.v.2019	46.749129°N, 23.476040°E	leg. Keresztes L.
	2	Bulgaria. Primorsko, Ropotamo Nature Reserve, 9 m. 11.vii.2018	42.301909°N, 27.727464°E	leg. Keresztes L.
Total	**75**			

Table 2. Morphological characters of male *Paraptychoptera* specimens used in the phylogenetic analyses.

1   Antennal segments: (0), segment 3 equal with segments 4+5; (1) segment 3 shorter than segments 4+5
2   Wing R2+3+4: oblique straight (0); curved or angled in the middle (1)
3   Wing: R2+3+4 length: (0) > 2 × length of rm; (1) < 2 × length of rm
4   Male auxiliary sexual organ on abdominal sternite III: only cluster of setae (0); cluster of setae and distal lobes (1)
5   Male auxiliary sexual organ, distal lobe: absent or weakly developed (0), well developed, ventrally projected outer lip depressed in the middle (1)
6   Male auxiliary sexual organ, distal lobe: outer lip truncate or straight: (0) absent; (1) present
7   Median sclerotized strip of the auxiliary sexual organ with a transverse ornamentation: (0) absent; (1) present
8   Epandrial clasper: well sclerotized with squared basal lobe and complex ventral lobe (0); poorly sclerotized without basal lobe (1)
9   Epandrial clasper configuration: (0), simple cylindrical; (1), cylindrical with additional subterminal ventral lobes
10 Epandrial clasper configuration: (0), simple cylindrical; (1), cylindrical with basal lobes
11 Epandrial clasper apex: rounded (0), pointed and curved (1)
12 Epandrial subapical process: absent (0); present (1)
13 Epandrial subapical process bilobate: absent (0); present (1)
14 Epandrial subapical process bilobate, inferior arm chitinous and curved: (0) absent; (1) present
15 Epandrial subapical process bilobate, superior arm laterally compressed, lobate, inferior arm truncate: (0) absent; (1) present
16 Epandrial subapical process bilobate, both arms chitinous and curved: (0) absent; (1) present
17 Epandrial subapical process bilobate, superior arm beak-shaped, inferior arm triangular: (0) absent; (1) present
18 Epandrial subapical process with chitinous process having curved apex: (0) absent; (1) present
19 Epandrial subapical process with a rounded apex, and strong basal thorn, longer than subapical process: (0) absent; (1) present
20 Epanadrial subapical process with rounded aped and strong basal thorns, shorter than subapical process: (0) absent; (1) present
21 Hypoproct: reduced to paired rectangular plates in subepandrial membrane (0); hypoproct well developed, triangular or tongue like (1)
22 Hypoproct short triangular lobe with rounded apex: (0) absent; (1) present
23 Hypoproct long, tongue like process: (0) absent (1) present
24 Hypoproct long, tongue like process, apex covered with dense hear: (0) absent (1) present
25 Hypoproct long, tongue like process, apex glabrous and bilobate: (0) absent (1) present
26 Hypoproct long, tongue like process, apex pointed, harpoon-shaped: (0) absent (1) present
27 Hypoproct long, tongue like process, apex truncate or slightly depressed: (0) absent (1) present
28 Gonostylus, shape of anterior lobule: (0) scythe-like; (1), lobe-like with rostrum
29 Gonostylus, shape of medial lobule: lobe like (0); scythe-like (1)
30 Gonostylus, apical stylus of gonostylus apex with strong spines: absent (0); present (1)
31 Gonostylus, apical stylus or gonostylus: simple (0); inflated (1)
32 Gonostylus, secondary lobe of apical stylus: present (0); absent (1)
33 Hypandrium apex terminal division spade like, without trichoid sensilla: (0) present; (1) absent;
34 Hypandrium apex terminal division wide spade like, with trichoid sensilla (0) absent; (1) present
35 Hypandrium apex terminal division long lobe like process, with rounded apex: (0) absent; (1) present
36 Hypandrium apex terminal division long lobe like process with bilobate apex: (0) absent; (1) present
37 Hypandrium eversible sac extended anteriorly nearly to margin: (0), absent; (1), present
38 Hypandrium basal scale: (0), absent; (1) present
39 Hypandrium basal scale chitinous, hat shape: (0), absent; (1) present
40 Hypandrium basal scale chitinous, hat shape, with medial lobe (0), absent; (1) present
41 hypandrium: basal scale lobe like, well developed (0), absent; (1) present
42 Hypandrium basal scale lobe like, weakly developed (0), absent; (1) present
43 Aedeagus: ejaculatory apodeme size: (0), larger, than sperm sac; (1), subequal
44 Aedeagus subapical plate wide spatulate: (0) present; (1) absent
45 Aedeagus subapical plate narrow, apex rounded or pointed: (0) present; (1) absent
46 Aedeagus subapical plate narrow, apex depressed: (0) present; (1) absent
47 Paramere apical lobes filiform process: (0) present; (1) absent
48 Paramere apical lobes with a notch in the middle: (0) present; (1) absent
49 Paramere apical lobes tip pointed: (0) present; (1) absent
50 Paramere apical lobes tip rounded: (0) present; (1) absent
51 Paramere lateral arms reduced: (0) present; (1) absent
52 Paramere lateral arms long, beak shaped: (0) present; (1) absent
53 Paramere lateral arms short, truncate: (0) present; (1) absent

Table 3. Matrix of the 53 morphological items of data used in the phylogenetic analyses. For the description of characters and character states see text. Missing data were coded as '?'.

	1	2	3	4	5	6	7	8	9	10	11	12	13	14	15	16	17	18	19	20	21	22	23	24	25	26
contaminata	0	0	0	0	0	0	0	0	0	0	0	0	0	0	0	0	0	0	0	0	0	0	0	0	0	0
agnes	?	1	1	1	?	?	?	1	1	0	0	1	1	1	0	0	0	0	0	0	1	0	1	1	0	0
castor sp. nov.	1	1	1	1	0	1	0	1	0	0	0	1	0	0	0	0	0	0	0	1	1	0	1	0	0	1
delmastroi	?	?	?	?1	1	0	1	0	1	0	1	0	0	0	0	0	0	1	0	0	1	1	0	0	0	0
handlirschi	1	1	1	1	1	0	1	1	0	1	0	1	1	1	0	1	0	0	0	0	1	1	0	0	0	0
helena	1	1	1	1	0	1	0	1	0	0	0	1	0	0	0	0	0	0	1	0	1	0	1	0	1	0
lacustris	1	1	1	1	0	1	0	1	0	0	0	1	0	0	0	0	0	0	0	0	1	1	0	0	0	0
longicauda	1	1	1	1	1	0	1	1	0	1	0	1	0	0	0	0	0	1	0	0	1	1	0	0	0	0
paludosa	1	1	1	1	1	0	1	1	0	1	0	1	1	0	0	1	0	0	0	0	1	1	0	0	0	0
pollux sp. nov.	1	1	1	1	0	1	0	1	0	0	0	1	0	0	0	0	0	0	1	0	1	0	1	0	0	0
resseli	?	?	?	?	0	?	?	1	0	0	1	1	0	0	0	0	0	1	0	0	1	0	1	1	0	0
silvicola	1	1	1	1	1	0	1	1	0	1	0	1	1	0	0	0	1	0	0	0	1	1	0	0	0	0

	27	28	29	30	31	32	33	34	35	36	37	38	39	40	41	42	43	44	45	46	47	48	49	50	51	52	53
contaminata	0	0	0	0	0	0	0	0	0	0	0	0	0	0	0	0	0	0	0	0	0	0	0	0	0	0	0
agnes	0	1	1	0	1	0	1	1	0	0	1	1	0	0	0	1	1	1	1	0	1	1	0	0	1	0	1
castor sp. nov.	0	1	1	1	0	0	1	0	1	0	1	0	0	0	1	1	1	1	0	1	1	0	1	0	1	0	1
delmastroi	0	1	1	0	0	0	1	1	0	0	0	0	1	0	0	1	1	1	1	0	1	1	0	0	1	1	0
handlirschi	0	1	1	0	0	0	1	1	0	0	0	0	1	0	0	1	1	1	1	0	1	1	0	0	1	1	0
helena	0	1	1	1	0	0	1	0	1	0	1	0	0	0	1	1	1	1	0	1	1	0	1	0	1	0	1
lacustris	0	1	1	0	0	0	1	0	1	0	1	0	0	1	0	1	1	1	1	0	1	0	1	0	1	0	1
longicauda	0	1	1	0	1	0	1	0	0	1	1	1	0	0	0	1	1	1	1	0	1	0	1	0	1	1	0
paludosa	0	1	1	0	0	1	1	1	0	0	0	0	1	0	0	1	1	1	1	0	1	1	0	0	1	1	0
pollux sp. nov.	1	1	1	1	0	0	1	0	1	0	1	0	0	0	1	1	1	1	0	1	1	0	1	0	1	0	1
resseli	0	1	1	0	0	0	1	1	0	0	0	0	0	1	0	1	1	1	1	0	1	0	0	1	1	1	0
silvicola	0	1	1	0	0	0	1	1	0	0	0	0	1	0	0	1	1	1	1	0	1	1	0	0	1	1	0

Results

Taxonomic account

Ptychoptera (Paraptychoptera) castor Keresztes & Kappert, sp. nov.
http://zoobank.org/D43DA29E-1941-4B33-BBE9-A3D88D80F277
Figure 2

Type material. *Holotype*. male, Albania: Tragjas municipality, Rrepet e Izvorit, Vlora district, sweeping the vegetation near a limnocren karst spring with large basin and muddy shore with reeds, 30.iv, 2019, 17 m, leg. M. Henning, 40.323132°N, 19.510031°E. Institutional id for specimen is DCFBG-PT-0002.

Diagnosis. *Ptychoptera (Paraptychoptera) castor* sp. nov. is known only from a single male collected near a limnocrene karst spring with muddy shore invaded by rich vegetation at Repet y Izvorit, Tragjas, Albania (Fig. 3). Male general habitus, wing venation and spots are highly similar to *P. helena* (Fig. 4a, b, c). However, the male epandrium has a unique design, differentiated from all other members of *Paraptychoptera*, but close to *P. helena* (Fig. 4d, e). In contrast to *P. helena*, the finger-like subapical
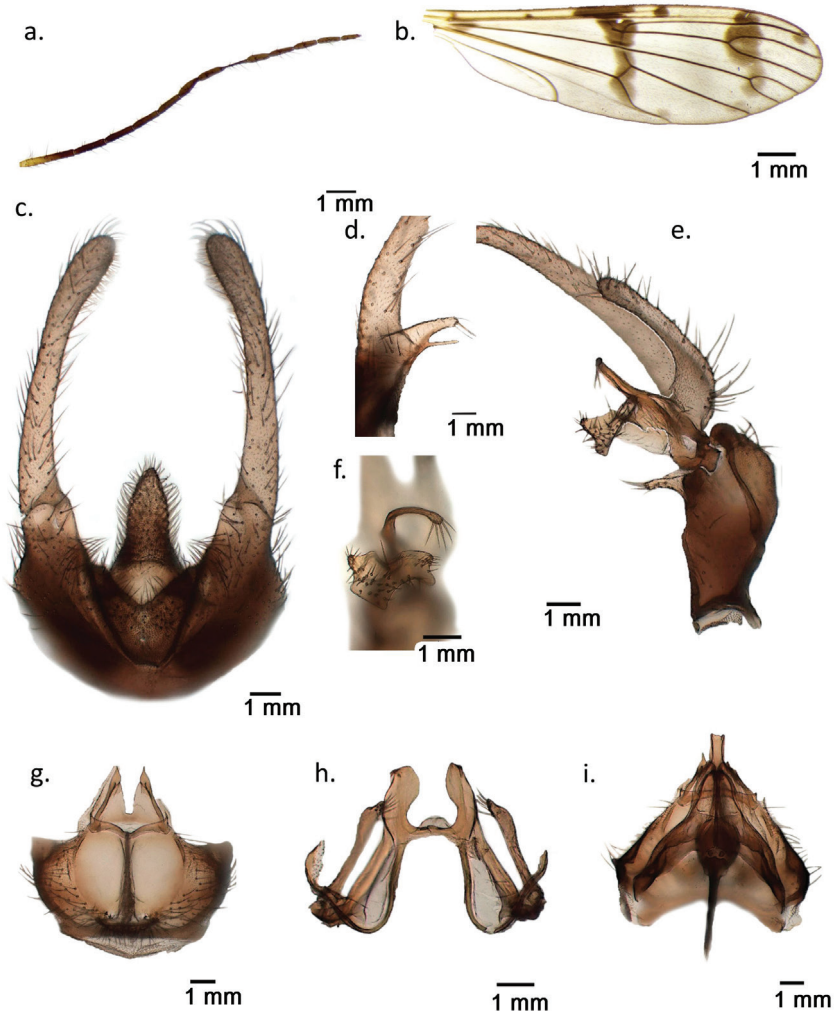
Figure 2. *Ptychoptera castor* sp. nov. **a** flagellum of antennae **b** right wing **c** epandrium, dorsal **d** subapical lobe of epandrium, ventral **e** left gonocoxite with gonocoxite lobes **f** anterior and medial lobules, details **g** hypandrium, caudal **h** paramere, ventral **i** aedeagal complex, dorsal.

process on its ventral side is well developed, with a basal chitinous process, equal in length with subapical lobe, which is much shorter in *P. helena* (Fig. 2d) and the conspicuous long harpoon-shaped apex of the hypoproct (Fig. 2c) which is bilobate in *P. helena* (Fig. 4d). Gonostylus apical stylus is long, twice as long as the secondary lobe (Fig. 2e), which differentiates it well from *P. helena*, where such a process is subequal. Gonostylus anterior lobule with a short finger-like vental process (Fig. 2f), while in *P. helena* such a process is much longer and curved at tip (Fig. 4g). Hypandrium apex lacking a narrow-lobe-like terminal division (Fig. 2g) which is present in *P. helena* (Fig. 4h), and well developed in all other *Paraptychoptera* species, in addition with a series of fine differences in male aedeagal complex and paramere (Fig. 2h, i).

Figure 3. Habitat of *Ptychoptera castor* sp. nov., south-western Albania, Tragjas, Repet y Izvorit.

Description. Medium-sized species, body length 7.3 mm, wing length 8 mm. Head and thorax shiny black, almost glabrous, pleuron almost uniformly brownish, some obvious pale setae only above halter. Head shiny brownish, labrum pale brownish to yellow. Antennae with 15 segments. Scape elongate cylinder, pedicel globular, yellowish, as the half of the first flagellar segment. Remainder flagellomeres blackish brown (Fig. 2a). First flagellar segment shorter than the following two segments together, the others successively shorter and thinner. Each flagellar segment with several long straight black setae and dense pelt of short dark hairs. Eye large, finely faceted, bare; no ocelli. Large, oval, clypeus, convex, terminal labrum yellowish. Large labellum, very long maxillary palpus with whip-like fifth segment pale yellow.

Thorax dorsally black with metallic blue shining, narrow pronotum, base of postnotum and large parts of episternum, epimeron, and metapleuron pale brownish. Coxae and legs yellowish, apex of femur, narrow base and apex of tibia, tarsal segments brownish. Wing with three transverse bands of well-developed confluent dark spots close to anterior margin on basal, middle and distal part of otherwise clear or pale yellowish membrane. Additionally, isolated dark spots are present on both sides of the middle dark band at the level of Sc and at the distal end of R3 (Fig. 2b). Wing membrane with macrotrichia. Prehalter and halter pale yellow.

First abdominal tergite blackish to dark brown with metallic shining, only a narrow yellow stripe near the distal, tergite 2 large part yellowish with brown spot in the middle, distal part shiny black, tergite 3 brownish, tergite 4 and all distal tergites
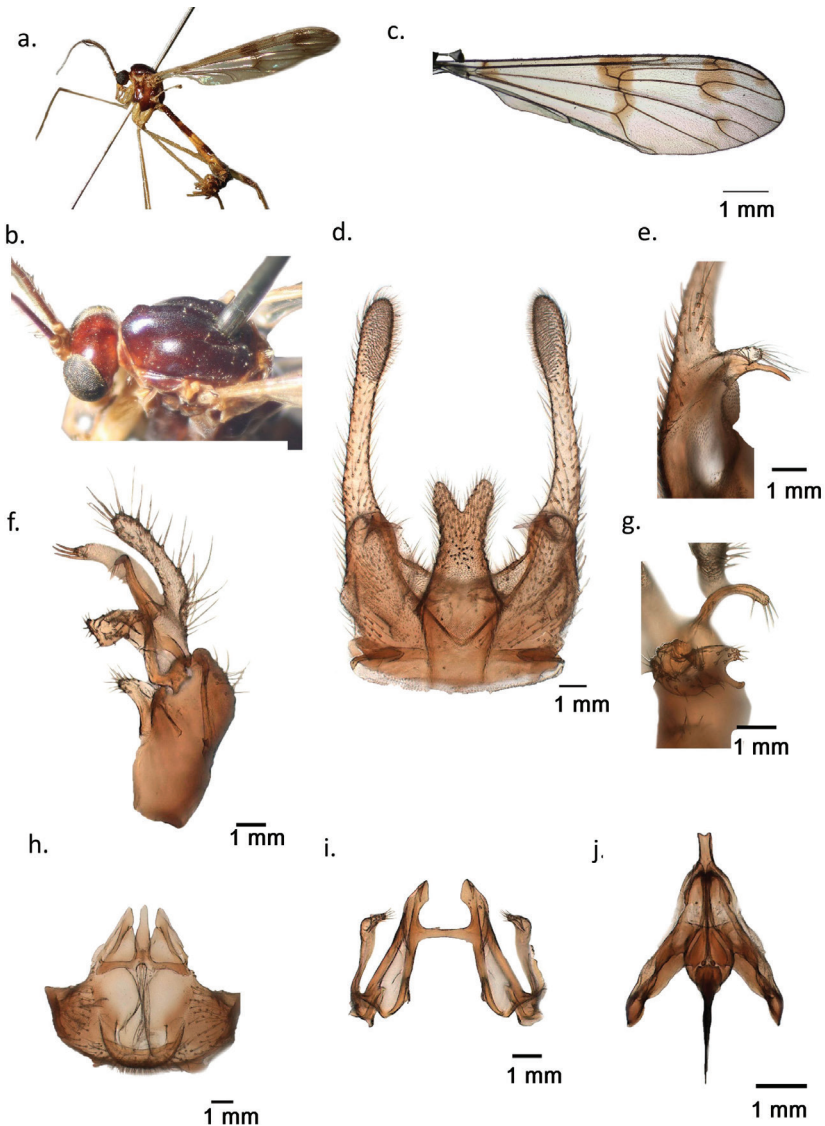
Figure 4. *Ptychoptera helena*, paratype male (ZFMK) **a** habitus male **b** head and thorax dorsal **c** right wing **d** epandrium, dorsal **e** subapical lobe of epandrium, ventral **f** gonocoxite and gonostylus complex, dorsal **g** gonostylus anterior and medial lobules, caudal **h** hypandrium, caudal **i** paramere, ventral **j** aedeagal complex, dorsal.

brownish black. Genitalia pale brown. Narrow sternites pale brown at base, becoming yellowish towards the auxiliary sexual organ on segment III. Sternites 4-7 medially reduced to a narrow band with a deep notch in the middle at proximal margins.

Auxiliary sexual organ less developed than in the other members of *Paraptychoptera*, excepting *P. lacustris* and *P. helena*. Sternite 3 with thin long golden hair fringes on

sides; its bare middle part lacking the transversally sculptured median sclerite, but distal brownish patch is present at distal end, close to the deep pouch of the auxiliary sexual organ. Distally sternite 3 with deep pouch of the auxiliary sexual organ. Two caudal lips of the pouch less developed, one smooth lateral lobe on each side, covered with dense hair fringe in their interior part. Lateral lips separated by a deep furrow leading to a small oval sclerite inside the pouch and two lateral lobes covered with fine sculptures.

Male terminalia. Epandrium with distinct collar, deeply and widely emarginated behind, hypoproct long lobe-like and densely hairy (Fig. 2c). Hypoproct lobe harpoon shaped, tapering at apex. Epandrium lobes long, slightly widened apically. Subapical process of epandrium with a finger-like ventral projection with basal thorn equal in length with the digitiform process (Fig. 2d). Apex of subapical lobe with long macrotrichia (Fig. 2d). Gonocoxite simple, with its medial appendage as a simple curved pilose lobe. Gonostylus apical lobe short, finger-like, fringe of setae at apex, secondary lobe similar shape, but twice as long as the apical lobe (Fig. 2e). Gonostylus anterior lobules divided into a dorsal triangular process and a ventral part with a short finger-like rostrum. Middle lobe strong sclerotised sickle-like rounded at apex, long fine hairs at tip (Fig. 2f). Hypandrium wide, hemispherical, long, elongate crests in the middle, including a narrow slit between them, from which the eversible sac protrudes. The transverse scale at the base of the slit is less developed, tongue-like, rounded apically, membranous and densely pilose. Hypandrium apex terminal division process missing (Fig. 2g). Aedeagal complex highly similar to other *Paraptychoptera* species. Paramere lateral arms well developed, widened towards a sloping apex. Well-developed setae close to the apex of the paramere arms. Apical processes of paramere well developed, rounded, with a recurring thorn-like formation (Fig. 2h). Apex of aedeagus blunt, depressed medially, subapical lobe of aedeagus pointed (Fig. 2i).

Female unknown.

Etymology. The specific epithet is named after Castor, a god from Greek mythology, the twin brother of Helena, because of its close morphological similarity with *P. helena*.

Ptychoptera (Paraptychoptera) pollux Keresztes & Török, sp. nov.

http://zoobank.org/59BAE5BD-BB77-4D24-AB52-A9AB130FD5B9
Figure 5

Type material. *Holotype*. male, North Macedonia: Mavrovo, Novo Selo, sweeping the vegetation near a small outflow from Mavrovo Lake, 29. vi, 2017, 990 m, leg. E. Török, 41.721355°N, 20.830103°E. Institutional id for specimen is DCFBG-PT-0003.

Diagnosis. *Paraptychoptera pollux* sp. nov. is known only from a single male collected near a small overflow of the Mavrovo Lake with muddy shore invaded by rich vegetation (Fig. 6). The male general habitus and wing venation with spots are highly similar to *P. helena* and *P. castor* sp. nov., but the wing spots tend to be reduced, mostly the basal spot and distally band which is divided into two distinct patches. Further differences are in male epandrium: The less developed finger-like subapical process is
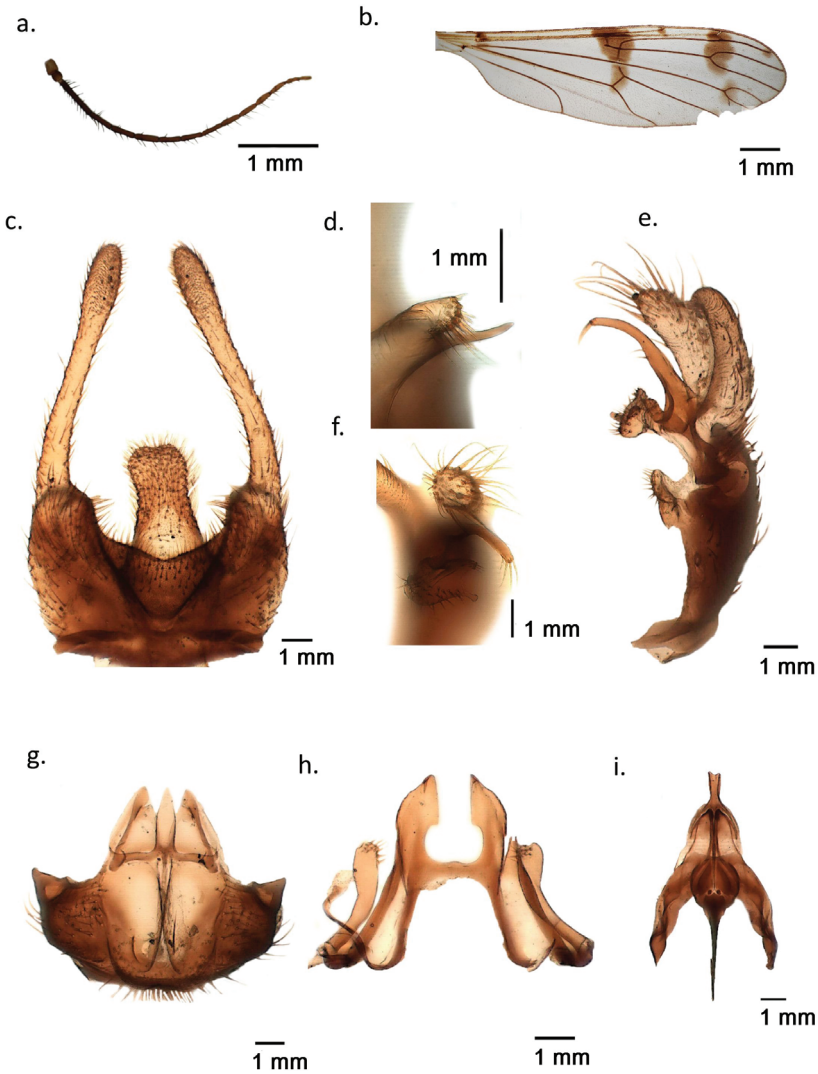
Figure 5. *Ptychoptera pollux* sp. nov. **a** flagellum of antennae **b** right wing **c** epandrium, dorsal **d** subapical lobe of epandrium, ventral **e** gonocoxite and gonostylus complex, dorsal **f** gonostylus anterior and medial lobules, caudal **g** hypandrium, caudal **h** paramere, ventral **i** aedeagal complex, dorsal.

unique to *P. helena*, *P. castor* sp. nov., and *P. pollux* sp. nov. (Figs 2d, 4e, 5d). However, in *P. pollux* sp. nov., this process is much shorter than in *P. castor*, but comparably longer than in *P. helena*, with blunt apex and divergent from the basal thorn. However, there is an important difference in the basal thorn orientation. In *P. pollux*, the basal thorn is oriented upward, while in *P. helena* the thorn is curved downward. Hypopygium shape with its rounded and slightly inflated apex is the second most distinctive character of *P. pollux* sp. nov., which differentiates it from both *P. castor* and *P. helena*, as well as from other *Paraptychoptera* species (Figs 2c, 4d, 5c). Paramere lateral arms of *P. pollux* are

Figure 6. Habitat of *Ptychoptera pollux* sp. nov., north Macedonia, Novo Selo village, Mavrovo lake outflow.

similar to *P. castor* sp. nov. and *P. helena*, but are shorter and gradually widened at tip and rounded (Fig. 5h). The rest of the characters, such the gonocoxite and gonostylus complex, hypandrium and the aedeagus are highly similar to *P. helena* (Fig. 4g, i).

Description. Medium-sized species, highly similar to its sibling species, *P. castor* sp. nov. and *P. helena.* Body length 7.9 mm, wing length 8.5 mm. Head and thorax similar to *P. castor*. Antennae with 15 segments. Scape elongate, cylindrical, yellowish brown, pedicel globular, pale brown, flagellar segments uniformly dark brown (Fig. 5a). First flagellar segment shorter than the following two segments together, the others successively shorter and thinner. Each flagellar segment with several long straight black setae and a dense pelt of short dark hairs. Head shining black. Eye large, finely faceted, bare; no ocelli. Clypeus large, elongate, rectangular, flattened, labrum pale brownish. Labellum large, yellowish, maxillary palpus very long with a whip-like fifth segment pale yellow.

Thorax dorsally brownish black with metallic blue shining, narrow pronotum, base of postnotum and large parts of episternum, epimeron and metapleuron pale brownish. Coxae orange, legs yellowish, apex of femur, narrow base and apex of tibia, tarsal segments brownish. Wing with three transverse bands of well-developed confluent dark spots in the anterior part of base, middle and distal part of otherwise clear or pale yellowish membrane. Basal spot of the wing more reduced. Distal band interrupted close to ventral edge. Isolated dark spots are present at distal end of Sc and R3 (Fig. 5b). Wing membrane with macrotrichia. Halter and prehalter yellow.

First abdominal tergite blackish to dark brown with a metallic blue shining, narrow yellow stripe close to distal end, well developed yellow band in tergite 2 with a black spot in the middle. Tergite 3 black, covered with yellow setae, the remaining tergites brownish black. Genitalia pale brown. Narrow sternites pale brown at base, becoming

yellowish towards the auxiliary sexual organ on segment III. Sternites 4-7 medially reduced to a narrow band with a deep notch in the middle at proximal margins.

Auxiliary sexual organ highly similar to *P. castor* sp. nov. and *P. helena*. Male terminalia. Epandrium with distinct collar, deeply and widely emarginated behind, hypoproct long tongue-like and furry (Fig. 5c). Hypoproct lobe widened at apex, rounded, with a shallow notch in the middle. Epandrium lobe long, slightly widened apically. Subapical process of epandrium with a digitiform ventral projection with basal thorn and curved upward, longer, than the blunt digitiform process (Fig. 5c, d). Apex of the digitiform process with long macrotrichia. Gonocoxite simple, cylindrical. Gonostylus with an anterior lobule divided into a dorsal triangular process, ventral part with a small rostrum (Fig. 5f). Middle lobe strong sclerotised sickle-like curved process, with long fine hairs at the end (Fig. 5e, f). Gonostylus apical lobe narrow fleshly process, subequal with secondary lobe (Fig. 5e). Secondary lobe slightly curved at apex, with strong erect spines. Hypandrium wide, long and elongate crests in the middle, including a narrow slit between them, from which the eversible sac protrudes. The transverse scale at the base of the slit is less developed, with two lateral wings and a triangular process in the middle, membranous and densely pilose. Hypandrium apex terminal division less developed, but distinct as a narrow band with pointed apex (Fig. 5g). Paramere lateral arms less developed, rounded apically and widened with less-developed setae close to the interior of the apex. Apical processes of paramere well developed, rectangular, with a recurring thorn-like formation (Fig. 5h). Aedeagal complex highly similar to other *Paraptychoptera* species. Apex of aedeagus concave, with a depression in the middle, subapical lobe of aedeagus rounded (Fig. 5i).

Female unknown.

Etymology. The specific epithet is named after Pollux, the twin brother of Castor in Greek mythology, known together as the Dioscuri, both twin brothers of Helena, because together with *P. castor* they share close morphological similarity with *P. helena* and all together they form a distinct monophyletic unit among *Paraptychoptera*, as was recovered by our cladistic analysis (Fig. 7).

Cladistic analyses. The parsimony analyses of the 53 different morphological characters selected in the present study resulted in a single most parsimonious tree (Fig. 7).

As shown in our parsimony analyses (Fig. 7.), the eleven different *Paraptychoptera* species are divided into two major monophyletic clades, with a highly divergent monophyletic unit, including five species, *P. agnes*, *P. lacustris*, *P. helena*, *P. castor* sp. nov., and *P. pollux* sp. nov. This monophyletic unit is supported by common morphological features, such as the soft and lobe-like basal scale, hypandrium with a long, but not bilobate narrow ribbon-like process or reduced and the simpler lateral arms of paramere (characters 36, 52).

Among this group, a distinct lineage is represented by *P. agnes*, highly different from all other members of the clade by the presence of a conspicuous epandrial lobe, with a ventral lobe close to the base, and a transverse projection with a comb of long setae, unique only to this species, in addition to the particularly shaped hypoproct and epandrial subapical process, and also by the uniquely shaped secondary lobe of the apical stylus inflated and globulose at apex, besides the details of hypandrium and parameres (characters 8, 12, 13, 23, 30, 37, 47).
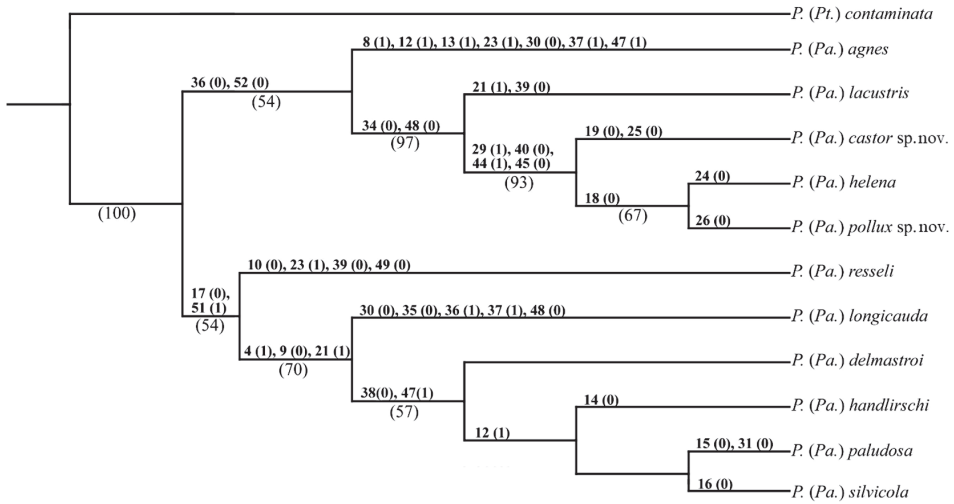
Figure 7. Single most parsimonious tree (1392 steps) based on 53 morphological characters. Bootstrap (B) values over 50% are noted above the corresponding branches, respectively. Branch support was calculated by bootstrap with 10000 replicates. Character states are shown above branches.

The present cladistic analyses recovered the "lacustris" species group as a monophyletic unit, which was also noted by Stubbs (1993) and Zwick and Starý (2002), but in a restricted sense, containing only four species: *P. lacustris, P. helena, P. castor* sp. nov. *and P. pollux* sp. nov. Further, the previously considered *P. loncicauda* and *P. paludosa* were excluded and mostly based on a weekly developed auxiliary sexual organ in "lacustris" group, but well developed in later species, and a weakly developed and reduced subhemispherical membranous basal scale in "lacustris" group in contrast with the well-developed and chitinous scale in *P. longicauda* and *P. lacustris*. There was also the presence of the stripe-like and bifurcate or cross-shaped terminal division of the hypandrium apex in *P. longicauda and P. paludosa*, in contrast with the weakly developed terminal division of hypandrium apex in "lacustris" group. This latter was missing in *P. lacustris* or reduced to a tapering ribbon-like protrusion in *P. helena* and allies (characters 38, 48). However, within the "lacustris" group the subapical lobes of epandrium have a conspicuously similar shape in *P. castor* sp. nov., *P. helena* and *P. pollux* sp. nov., while in *P. lacustris* such a formation is totally absent. *Ptychoptera lacustris* is also divergent from the three closely-related Balkan species by the presence of a small triangular hypoproct and rounded subspherical basal scale of the hypandrium (characters 21, 39). *Ptychoptera helena* and the two newly discovered species of the "lacustris" group are morphologically highly similar, but deeply divergent from all other *Paraptychoptera* species, having unique epandrial clasper lobes that are slightly divergent toward the tip, and epandrial subapical lobes reduced to a finger-like short

projection with a basal chitinous thorn, hypandrium apex terminal division that is highly reduced, finger-like, with pointed apex, lacking laterally directed spines, but thin hairs are sometimes present (only in *P. castor* such a process is absent). Further, the aedeagus tip has a unique shape, with a small depression in the middle (characters 29, 40, 44, 45). *Ptychoptera helena* and *P. pollux* sp. nov. are highly similar, but minor differences are present in the shape of the hypopygium, and the design of the subapical lobe of the epandrium (characters 24, 26). Further, they are distinctly different from *P. castor* sp. nov. by the presence of a long subapical epandrial lobe (character 19), which is as long as its basal chitinous thorn, as well as the long harpoon-like hypoproct, unique only to this species (character 25).

Discussion

According to Fasbender (2014), and also supported by the cladistic analyses of the present work, the following morphological diagnostic characters are important to discriminate the *Paraptychoptera* species from all other Ptychopteridae: the presence of well-articulated, but poorly sclerotised epandrial claspers, the apical stylus of gonostylus mostly membranous, with a secondary lobe present, hypandrium well developed, sub-hemispherical, an eversible sac is present, parameres and gonocoxal lobes fused to a supra-aedeagal membrane, paramere lateral arms well developed, and aedeagus having an elliptical ejaculatory apodeme. Within *Paraptychoptera*, the presence of a well differentiated morphologically divergent "lacustris" group was recovered by our cladistic analyses, but excluded *P. longicauda* and *P. paludosa* which were considered in this work based on data in the literature (Freeman 1959; Stubbs 1993; Zwick and Starý 2003). Based on our morphological analyses, the two new species that are described in the present study, *P. castor* sp. nov. and *P. pollux* sp. nov., both belong to the "lacustris" group, and together with *P. helena* they form a well differentiated, range-restricted South Balkan clade, that is highly distant from the more widespread *P. lacustris* and this highlights the importance of the Balkans as an important refuge and genetic hotspot for *Paraptychoptera* in Europe.

A key to the *Paraptychoptera* species was recently provided by Fasbender in 2014 in his global revision of the world Ptychopteridae, including only four *Paraptychoptera* species, instead of the twelve currently known from the Western Palaearctic area. The present key is mostly based on his comprehensive morphology data, but incorporates additional morphological details from the remainder of the *Paraptychoptera* species, including the two newly described species, *P. castor* sp. nov. and *P. pollux* sp. nov. The North African *P. surcoufi* is not included the key because no material was available for the current investigation, nor was there any detailed information in the literature to the best of our knowledge, but its distinctness from the *P. helena* and related species is obvious according to Peus (1958).

Key to *Paraptychoptera* species (males)

1 Apical stylus of gonostylus reduced .... *P. ressli* **Theischinger, 1978**
– Apical stylus of gonostylus well developed...**2**
2 Epandrial clasper lacking lateral swelling, basal division of hypandrium with a weakly developed membranous basal scale **3**
– Epandrial clasper with lateral swelling (mostly reduced in *P. longicauda*), basal division of hypandrium with a well-developed, chitinous projection of different shapes **7**
3 Epandrial clasper lobes complex, with a transverse projection with a comb of long setae at apex and the presence of a subterminal ventral extension, secondary lobe of the apical stylus expanded into a large balloon-shaped structure.....................
....*P. agnes* **Krzeminski & Zwick, 1993**
– Epandrial lobes simple, apical stylus simple, with apex tapering and rounded.....**4**
4 Subapical sclerite present at base of epandrial clasper, hypoproct long, tongue-like... **5**
– Subapical sclerite absent, hypoproct short, triangular ....
.... *P. lacustris* **Meigen, 1930**
5 Hypoproct furcate apically ....*P. helena* **Peus, 1958**
– Hypoproct not furcate apically...**6**
6 Hypoproct apex rounded, with a shallow depression in the middle, apical stylus and secondary lobe subequal in length .....*P. pollux* **Keresztes & Török, sp. nov.**
– Hypoproct apex tapered with pointed apex, apical stylus twice as long as the secondary lobe... *P. castor* **Keresztes & Kappert, sp. nov.**
7 Epandrial clasper lobe very long, more than twice as long as epandrium length. Apical stylus of gonostylus pendulant, apex of terminal division of hypandrium elongate ribbon-like projection with bifurcate tip, basal scale of hypandrium with no medial triangular projection ....*P. longicauda* **Tonnoir, 1919**
– Epandrial clasper lobe short, shorten than epandrium length. Apical stylus of gonostylus not pendulant, apex of terminal division of hypandrium widened, spatulate, basal scale of hypandrium with medial triangular projection **8**
8 Secondary lobe of apical stylus absent ....*P. paludosa* **Meigen 1804**
– Secondary lobe of apical stylus present **9**
9 Subapical sclerite hook-like .... *P. delmastroi* **Zwick & Stary, 2003**
– Subapical sclerite with a paddle-like ventrally projected division **10**
10 Subapical sclerite with the paddle-like ventrally projected division inflated at apex. With a short hook subterminally and dorsally projected division triangular ....
....*P. silvicola* **Zwyrtek & Rozkosny, 1967**
– Subapical sclerite with ventrally projected arms paddle-like, rounded at apex, without subterminal hooks, dorsally projected division rectangular....................
....*P. handlirschi* **Czizek, 1919**

Acknowledgements

References

Alexander CP (1927) Diptera: Fam. Ptychopteridae. Genera Insectorum 188: 1–13.

Andersson H (1997) Diptera Ptychopteridae, Phantom Crane Flies. Aquatic Insects of North Europe – A taxonomic Handbook. Volume 2 (ed. Nilsson, A. N). Apollo Books,193–207.

Deliné-Draskovits Á (1983) Redős szúnyogok – Ptychopteridae. Fauna Hungariae, XIV. Diptera I. Akadémiai Kiadó, Budapest, 88 pp.

Eskov KY, Lukashevich ED (2015) On the history of ranges of two relict nematoceran families, Ptychopteridae and Tanyderidae (Insecta: Diptera): a biogeographical puzzle. Russian Entomological journal 24(3): 257–270. https://doi.org/10.15298/rusentj.24.3.08.

Fasbender A (2014) Phylogeny and diversity of the phantom crane flies (Diptera: Ptychopteridae). PhD Thesis, Iowa State University, Ames, 855 pp.

Felsenstein J (1985) Confidence limits on phylogenies: an approach using the bootstrap. Evolution 39: 783–791. https://doi.org/10.2307/2408678

Freeman P (1959) Diptera: Culicidae subfamily Dixidae, Anisopodidae and Ptychopteridae. Ruwenzori Expedition 1952(2): 37–42.

Goloboff PA, Catalano SA (2016) TNT version 1.5, including a full implementation of phylogenetic morphometrics. Cladistics 32(3): 221–238. https://doi.org/10.1111/cla.12160

Krzemiński W (1986) Ptychopteridae of Poland (Diptera, Nematocera). Polskie Prismo Entomologiczne 56: 105-132.

Krzemiński W, Zwick P (1993) New and little known Ptychopteridae (Diptera) from the Palaearctic Region. Aquatic Insects 15: 65–87. https://doi.org/10.1080/01650429309361504

Maddison WP, Maddison DR (2019) Mesquite: a modular system for evolutionary analysis. Version 3.61. http://www.mesquiteproject.org

Paramonov N (2013) New records of Ptychopteridae (Diptera) from Europe, North Africa and Asia Minor. Studia Dipterologica 20(2): 279-283.

Peus F (1958) Liriopeidae. In Lindner E (Ed.) Die Fliegen der Palaearktischen Region, 10–44.

Rozkošný R (1997) Family Ptychopteridae. In: Papp L, Darvas B (Eds) Contributions to a Manual of Palaearctic Diptera, Volume 2. Nematocera and Lower Brachicera. Science Herald, Budapest, 291–296.

Séguy E (1926) description d'un nouveau*Paraptychoptera*. In: Encyclopédie Entomologique. Série B, Mémoires et Notes DIPTERA Recueil d'études biologique et systématiques sur les Dipéres du Globe 2(1925–1926): 22.

Stubbs AE (1993) Provisional atlas of the Ptychopterid craneflies (Diptera: Ptychopteridae) of Britain and Ireland. Huntingdon, Biological Records Centre, 34 pp.

Tonnoir A (1919) Notes sur les Ptychopteridae (Dipt.). Annales Societe Entomologique de Belgique 59: 115–122.

Török E, Kolcsár L-P, Dénes A-L, Keresztes L (2015) Morphologies tells more than molecules in the case of the European widespread *Ptychoptera albimana* (Fabricius, 1787) (Diptera, Ptychopteridae). North Western Journal of Zoology 11(2): 304–315.

Ujvárosi L, Kolcsár P.-L, Török E (2011) An annotated list of Ptychopteridae (Insecta, Diptera) from Romania, with notes on the individual variability of *Ptychoptera albimana* (Fabricius, 1787). Entomologica Romanica 16: 39–45.

Zitek-Zwyrtek K (1971) Czechoslovak species of the family Ptychopteridae (Diptera). Acta Entomologica Bohemoslovaka 68: 416–426.

Zwick P, Starý J (2003) *Ptychoptera delmastroi* sp. nov. (Diptera: Ptychopteridae) from Italy. Aquatic Insects 25(3): 241–246. https://doi.org/10.1076/aqin.25.3.241.15262

RESEARCH ARTICLE

Out of *Xanthopygus* (Coleoptera: Staphylinidae): escape from polyphyly

Stylianos Chatzimanolis[1]

1 *Department of Biology, Geology and Environmental Science, University of Tennessee at Chattanooga, 615 McCallie Ave., Dept. 2653, Chattanooga, TN, USA*

Corresponding author: Stylianos Chatzimanolis (stylianos-chatzimanolis@utc.edu)

Citation: Chatzimanolis S (2021) Out of *Xanthopygus* (Coleoptera: Staphylinidae): escape from polyphyly. ZooKeys 1071: 83–107. https://doi.org/10.3897/zookeys.1071.75947

Abstract

Xanthopygus as currently defined is the largest genus in the subtribe Xanthopygina (Coleoptera: Staphylinidae: Staphylininae) with 40 described species. However, the genus is poorly defined, morphologically heterogeneous and previous studies have questioned whether it is a natural group. A morphological (51 characters) Bayesian phylogenetic analysis was performed to test whether *Xanthopygus* is a monophyletic group. The analysis indicated that *Xanthopygus* was polyphyletic, and therefore species were split into four different genera. *Xanthopygus nigricornis* Scheerpeltz was transferred to *Oligotergus* as *Oligotergus nigricornis* **comb. nov.** and *Xanthopygus skalitzkyi* (Bernhauer) was transferred to *Styngetus* as *Styngetus skalitzkyi* **comb. nov.** A new genus, *Photinopygus* **gen. nov.** was erected to accommodate the majority of the species previously in *Xanthopygus* and *Xanthopygus* sensu novo is used in a new restricted sense to accommodate the remaining species. Diagnostic features are provided to distinguish species in the genera *Photinopygus* and *Xanthopygus* from each other and all other Xanthopygina genera.

Keywords

New genus, phylogeny, Staphylininae, Staphylinini, Xanthopygina

Introduction

Recently, Chatzimanolis and Brunke (2019) produced a comprehensive phylogeny of the subtribe Xanthopygina using morphological and molecular data and established several lineages within Xanthopygina. Catapulting from that work was the description of several new genera of Xanthopygina (Chatzimanolis 2019; Chatzimanolis and Hightower 2019; Chatzimanolis and Brunke 2021) that were placed in a phylogenetic framework. And while description of new genera is always exciting, many problems still exist with genera that have received little taxonomic attention over the last 200 years. One of the most problematic areas within Xanthopygina is the *Xanthopygus* lineage (briefly summarized in the next paragraphs), a group that includes *Elecatopselaphus* Scheerpeltz, *Phanolinus* Sharp, *Triacrus* Nordmann, *Xanthopygus* Kraatz, *Xenopygus* Bernhauer, along with *Gastrisus nitidus* Bernhauer and Genus 1 (a potentially undescribed new genus).

Phanolinus is perhaps one of the most charismatic taxa within Xanthopygina, and even Staphylinidae, with bright metallic coloration covering the whole body. However, many species were described solely based on the differences in coloration and many of them are potential synonyms (Chatzimanolis unpublished data). *Elecatopselaphus* was recovered as the sister group of *Phanolinus* (Chatzimanolis and Brunke 2019) and whether or not it should be treated as a separate genus or *Phanolinus* is still a matter of investigation. *Xenopygus* was revised by Caron et al. (2016) and Chatzimanolis and Caron (2016) provided clarifications and additions, but it is doubtful that the two species groups currently recognized in *Xenopygus* form a monophyletic group (Chatzimanolis and Brunke 2019; and this paper). *Gastrisus nitidus* and Genus 1 may belong to the same (new) genus, but more data and analyses are needed to clarify their position. *Triacrus* was shown to be nested within *Xanthopygus* (Chatzimanolis & Brunke 2019) but without support.

Xanthopygus (Fig. 1) as currently defined (referred to as *Xanthopygus* sensu Herman to include all taxa of *Xanthopygus* as presented in Herman's 2001 catalogue) is the most speciose genus in Xanthopygina with 40 valid species. The name *Xanthopygus* refers to the bright yellow or orange coloration of segments 7 and 8. Notes on the biology of adults and larvae are known for *Xa. cognatus* Sharp (Quezada et al. 1969) but the biology of the remaining species of the genus is largely unknown. Since there is no comprehensive taxonomic treatment of *Xanthopygus*, there are no good characters to define the genus, which has been typically diagnosed with a combination of the following: superior marginal line of pronotal hypomeron not continuing to anterior margin, postcoxal process present, and tergites 3–5 with arch-like carina (e.g., Hayashi 1997; Navarrete-Heredia et al. 2002; Navarrete-Heredia 2004; Rodríguez et al. 2012). Unfortunately, these three character states are not unique for *Xanthopygus* and have arisen multiple times within the subtribe (Chatzimanolis and Brunke 2019; and this paper), and as early as 2014; Chatzimanolis (2014) hypothesized that *Xanthopygus* is not monophyletic.

Xanthopygus was described by Kraatz (1857) and included the species that Erichson (1839; 1840) listed in '*Staphylinus* Fam. VII and *Philonthus* Erichs. pro parte' (Herman 2001). Species in Fam. VII included (in the order listed by Erichson) *Staphylinus sapphirinus* Er., *St. calidus* Er., *St. hilaris* Er., *St. tepidus* Er., *St. iopterus* Er., *St. cyanelytrius* Er., *St. chrysopygus* Er., *St. pyraster* Er., (a junior synonym of *St. haemorrhoidalis* Germar also listed by Erichson), *St. chrysurus*, and *St. faustus* Er. Kraatz (1857, p. 540) listed the species *Philonthus xanthopygus* (Nordmann), *Ph. herilis* Er., *Ph. analis* Er., *Ph. bicolor* (Laporte), and *Ph. mirabilis* Er. as those he intended to move from '*Philonthus* Erichs. pro parte' to *Xanthopygus*. As stated by Herman (2001), all included species in a group must be cited by available names according to Article 67.2.1 of the ICZN (ICZN, 1999). Thus, the first included species in *Xanthopygus* were those cited by Gemminger and Harold (1868) who included in *Xanthopygus* all the species listed above and used *X. abdominalis* Gemminger and Harold as a replacement name (without justification) for *X. Xanthopygus* (Nordmann). *Xanthopygus abdominalis* has been treated as junior synonym of *X. xanthopygus* (Nordmann) by all subsequent authors. Sharp (1876) added several more species to *Xanthopygus* and was the first one to recognize that the genus (as proposed by Kraatz) was morphologically heterogeneous. Later, Sharp (1884) established the genus *Lampropygus* Sharp to include *L. xanthopygus* (Nordmann), *L. cognatus* (Sharp), *L. analis* (Er.) and *L. bicolor* (Er.). Unfortunately, the characters (ligula less emarginate, pronotum anterolaterally restricted) provided by Sharp (1884) to establish the concept of *Lampropygus* are present in *Xanthopygus* as well. In 1906, Bernhauer (1906) placed the last two species (*analis* and *bicolor*) in the genus *Xenopygus* Bernhauer. Based on his publications (e.g., Bernhauer 1905, 1906, 1917, 1927), Bernhauer agreed with Sharp on the concepts of *Xanthopygus* and *Lampropygus* as established by Sharp, although neither Sharp nor Bernhauer provided clear diagnostic characters for these genera. Bernhauer (1906) established the subgenus *Heteropygus* Bernhauer for two particularly large species, *L. giganteus* Bernhauer and *L. oliveirae* (Lynch) in *Lampropygus*. Lucas (1920) designated *L. xanthopygus* as the type species of *Lampropygus*. Blackwelder (1943) seemingly ignored the generic concepts that had been established by Sharp and Bernhauer for *Lampropygus* and *Xanthopygus*, and designated *L. xanthopygus* (Nordmann) as the type species of *Xanthopygus*, which resulted in *Lampropygus* becoming a junior synonym of *Xanthopygus*. This nomenclatural act established the concept of *Xanthopygus* as it stands today before the results of this paper. Perhaps to his credit, Blackwelder (1943; p.450 footnote) realized that he was giving a new meaning to *Xanthopygus* and suggested that new generic assignments would be needed in the future for some of the species in *Xanthopygus*.

While it is rather obvious from the taxonomic history above that *Xanthopygus* is not homogeneous, the goal of this paper is to use a phylogenetic framework to show that *Xanthopygus* sensu Herman can be confidently split into two or more taxa. Additionally, I seek to define diagnostic characters that can easily separate the various groups within *Xanthopygus*.

Materials and methods

Taxon sampling

The focus of this paper was to determine whether the species currently in *Xanthopygus* sensu Herman form a monophyletic group. Thus, the analysis conducted focused on this goal rather than attempting to decipher the exact placement of all the different *Xanthopygus* species groups within Xanthopygina. For the ingroup, I included 21 species from *Xanthopygus*, comprising all the different species groups in that genus (Chatzimanolis unpublished data). *Xanthopygus borealis* Hatch was listed as a valid species of *Xanthopygus* by Herman (2001) but that species is a junior synonym of *Tympanophorus puncticollis* (Erichson). I also included 14 species as outgroup taxa, which included representatives of all genera belonging in the *Xanthopygus* lineage except *Elecatopselaphus*. From the *Xanthopygus* lineage I included the following taxa: *Gastrisus nitidus*, an undescribed taxon referred to as Genus 1 (Chatzimanolis and Brunke 2019), *Phanolinus colombinus* Bernhauer, *Triacrus dilatus* Nordmann, and four species of *Xenopygus*, representing both species groups within *Xenopygus*. In addition to the taxa of the *Xanthopygus* lineage, I included species from *Gastrisus* Sharp, *Oligotergus* Bierig and *Styngetus* Sharp since the overall habitus of these taxa is sometimes confused with that of *Xanthopygus*, and *Philothalpus* Kraatz (as distant outgroup). I examined the type specimens of all ingroup taxa included in the analyses, except for *Xa. cyanelytrius* (Perty), *Xa. oliveirae* Lynch and *Xa. pexus* (Motschulsky) that are considered lost. Specimens were examined from the following collections: the American Museum of Natural History (AMNH), the Natural History Museum of London (BMNH); the Canadian National Collection of Insects, Arachnids and Nematodes (CNC), the Field Museum (FMNH); the Naturhistorisches Museum Wien (NMW); the Natural History Museum of Denmark (NHMD), the Senckenberg Deutsches Entomologisches Institut (SDEI), the Snow Entomological Collection, Biodiversity Institute, University of Kansas (SEMC), the University of Tennessee at Chattanooga Insect Collection (UTCI), and the Museum für Naturkunde der Humboldt-Universität (ZMHB). A DarwinCore format file with the voucher numbers for all the material examined can be found as Suppl. material 1. Because not all specimens had catalogue numbers, I added a new label to every specimen examined to serve as the voucher number; these labels had the following format: '*Xanthopygus* phylogeny voucher SC-123'. In addition to the specimens listed in the Supp. File 1, I have access to virtually all specimens of *Xanthopygus* sensu Herman since I have borrowed materials from museums around the world for the revisions, and I had the ability to check a wide range of specimens for characters that are difficult to observe.

Specimen preparation

Specimens were examined using an Olympus ZX10 stereomicroscope either as dry mounts or disarticulated in glycerin. Photographs of species were taken using a Canon 40D camera equipped with a MP-E 65 mm macro lens on a Cognisys StackShot 3X macro rail and controller (https://cognisys-inc.com/stackshot-macro-rail-package.

html). Images were automontaged using Helicon Focus Pro v.7.7.4 (http://www.heliconsoft.com/heliconsoft-products/helicon-focus/) and post-processed in Adobe Photoshop v.22.3. Tree diagrams were first processed using FigTree v.1.4.4 (http://tree.bio.ed.ac.uk/software/figtree/) and then edited in Adobe Illustrator v.25.2.

List of morphological characters

In total, 51 morphological characters were scored in Mesquite v.3.61 (Maddison and Maddison 2019). Some characters were derived from Chani-Posse et al. (2018) or Chatzimanolis and Brunke (2019) but several are novel for Staphylinini phylogenetics. All characters were treated as unordered and neither invariant nor autapomorphic characters were included in the analyses. Figures from this manuscript are cited as Fig. #; figures from other citations are cited as follows: Fig. CA#: Chatzimanolis and Ashe (2005); Fig. CB#: Chatzimanolis and Brunke (2019); Fig. CC#: Chatzimanolis and Caron (2016); Fig. CH#: Chatzimanolis (2017); Fig. CP#: Chani-Posse et al. (2018); Fig. CT#: Chatzimanolis (2015a); Fig. L#: Li and Zhou (2011); Fig. S#: Smetana and Davis (2000). An * denotes novel character for Staphylinini phylogenetics.

1*. Antennae, antennomere 1 in comparison to antennomere 2: (0) less than twice as long; (1) twice as long or longer.

2. Antennae, antennomere 4, tomentose pubescence: (0) absent (Fig. 1D); (1) present (Fig. 1A–C, E, F).

3. Antennae, antennomere 4: (0) elongate (Fig. 1A, F); (1) subquadrate (Fig. 1D).

4. Antennae, antennomere 5: (0) elongate (Fig. 1A, F); (1) subquadrate (Fig. 1D, E); (2) transverse (Fig. CT2).

5. Antennae, antennomere 6: (0) elongate (Fig. 1F); (1) subquadrate (Fig. 1C); (2) transverse (Fig. CT2).

6. Antennae, antennomere 7: (0) elongate (Fig. 1F); (1) subquadrate (Fig. 1A); (2) transverse (Fig. CT2).

7. Head, length in comparison to pronotum: (0) shorter (Fig. 1A–C, E, F); (1) subequal (Fig. 1D).

8. Head, width in comparison to pronotum: (0) narrower (Fig. CC1–2); (1) subequal (Fig. 1A–C, F); (2) wider (Fig. 1D–E).

9*. Head, shape, posterior margin: (0) slightly extended posteriad on each side of the neck (Fig. 1A–C); (1) more or less at same level with neck border (Fig. 1D–F).

10. Head, eye size relative to length of head (length of head measured from anterior margin of clypaeus to posterior margin of head): (0) small (less than 2/5 length of head) (Fig. 1D); (1) medium (between 2/5 and 2/3 length of head) (Fig. 1B); (2) large (more than 2/3 length of head) (Fig. CC1–2).

11. Labrum, emargination, shape: (0) V-shaped, lobes moderately separated; (1) broadly U-shaped, lobes strongly separated (Fig. 1B–C); (2) narrow, lobes separated by a thin channel.

12. Head, deep punctures demarcating raised postmandibular ridge dorsolaterally: (0) absent (Fig. CT3); (1) present (Fig. S81).

13. Hypostomal cavity (hc): (0) hc moderately delimited (i.e., cavity surface without microsculpture or punctation different from rest of nearby head surface) (Figs S8, S10); (1) hc slightly delimited (cavity distinct only laterally, its surface with same microsculpture or punctuation as rest of nearby head surface).

14. Mandible, curvature: (0) more or less straight, except tip of mandible (Fig. 1D); (1) curved from apical (distal) half (Fig. 1B–C, E–F).

15. Mandible, left, teeth structure (excludes tip of mandible): (0) one tooth (Fig. CA14); (1) two teeth, separated by deep emargination (Fig. 1D); (2) one bicuspid tooth (Fig. 1C); (3) one tooth and one bicuspid tooth (in the same proximodistal succession; Fig. CT2).

16. Neck, disc (i.e., dorsal surface of neck not including dorsolateral areas): (0) punctures absent or rather sparse (Fig. 1A, C–D, F); (1) with dense, moderately coarse punctures (Figs CC1–2).

17*. Pronotum, microsculpture: (0) polygon shaped; (1) with transverse lines (seen easily at 70× magnification); (2) with dense micropunctures (Figs CA30, 32,38); (3) with sparse micropunctures (but no transverse lines visible at 70× magnification).

18. Prothorax, disc of pronotum, distribution of punctures: (0) median part of pronotum with punctation beyond midlength (Fig. 1); (1) median part of pronotum with punctation not continuing beyond midlength (Fig. SB2: *Gastrisus*).

19. Prothorax, disc of pronotum, distribution of punctures if punctures continue beyond midlength: (0) more or less homogeneous (i.e., punctures are separated by same distance; Fig. 1A); (1) with large impunctate areas between punctures (i.e., punctures not equally distributed; Fig. 1B–C).

20. Prothorax, hypomeron, inferior marginal line (iml), development: (0) iml not continued as a separate entity beyond anterior pronotal angles (Fig. S42–44); (1) iml continued as a separate entity beyond anterior pronotal angles and curving around them (Fig. S53).

21. Prothorax, hypomeron, superior marginal line: (0) continuous to anterior margin (Fig. 2A); (1) not continuous to anterior margin (Fig. 2B).

22*. Prothorax, hypomeron, angles of superior and inferior marginal lines: (0) superior and inferior line produce anterolateral angles parallel to one other (Fig. 2A); (1) superior and inferior line produce anterolateral angles not parallel to one other (Fig. 2B).

23. Prothorax, postcoxal process: (0) absent; (1) present (Fig. S53).

24. Prothorax, basisternum (bs), length relative to length of furcasternum (fs) (bs/fs, measured laterally): (0) bs slightly to moderately longer than fs (bs/fs ratio up to 1.5); (1) bs distinctly longer than fs (bs/fs ratio >> 1.5) (Fig. CP8A).

25. Prothorax, basisternum, position of pair of macrosetae (ms, if present) in relation to anterior margin of prosternum (amp) and the sternacostal suture (ss): (0) ms situated close to amp (i.e., not farther than one fourth the distance between amp and the ss along midline) (Fig. S86); (1) ms situated far from amp (i.e., farther than one fourth the distance between amp and the ss along midline) (Fig. L11A, B, E, F).

26. Mesothorax, elytra, with contiguous polygon-shaped meshed microsculpture (elytra appearing matt): (0) absent; (1) present (Fig. SB2: *Gastrisus*).

27. Mesothorax, mesocoxae: (0) Mesocoxae contiguous, intercoxal area distinctly recessed compared to mesoventrital and metaventrital processes (Fig. S158); (1) Mesocoxae moderately separated, intercoxal area distinctly recessed compared to mesoventrital process only (Fig. S87); (2) Mesocoxae strongly separated, intercoxal area on approximately same plane as both meso and metaventrital processes (Fig. S117).

28. Mesothorax, mesoscutellum, dense micropunctures: (0) absent (Fig. 2D); (1) present (Fig. 2C).

29. Mesoventrite, intercoxal process, apex: (0) narrow and pointed (Fig. S60); (1) broad and rounded; (2) narrow and rounded (Fig. 2E); (3) broad and pointed (Fig. 2F).

30*. Metathorax, metepisternum, punctures: (0) dorsal 1/3 of metepisternum without punctures throughout its length (Fig. 3A); (1) metepisternum covered with punctures or impunctate area less than 1/3 (Fig. 3B).

31*. Metathorax, relative width of metepimeron in comparison to metepisternum near posterior border: (0) metepimeron subequal or slightly wider than metepisternum (Fig. 3A); (1) metepimeron twice as wide as metepisternum (Fig. 3B).

32*. Metathorax, metacoxae, spines on the posterior surface: (0) 4 or less (Fig. 3C); (1) more than 4 (Fig. 3D). This character is difficult to observe and sometimes spines may have been broken off.

33*. Metathorax, metafemora, upper posterior margin: (0) crenulate (Fig. 3G); (1) not crenulate.

34. Metathorax, metatarsi, tarsomere 3, dorsal surface, chaetotaxy: (0) developed only at margins, dorsal surface of tarsomeres glabrous (or with 1–2 setae) along midline (Fig. 3E); (1) tarsomeres dorsally setose (setae not restricted to marginal series) (Fig. 3F).

35. Abdomen, tergites 3 and 4, anterior basal transverse carina (ABTC), pair of accessory ridges: (0) absent (Fig. 4D); (1) present (Fig. CA1–9).

36. Abdomen, tergite 3, curved carina (arch-like) on disc: (0) absent; (1) present (Fig. 4D).

37. Abdomen, tergite 3, punctation medially: (0) absent; (1) present (Fig. 4D).

38. Abdomen, tergite 5, curved carina (arch-like) on disc (if curved carina present on tergite 3): (0) absent; (1) present (Fig. 4D).

39. Abdomen, sternite 3, basal transverse carina, medial area: (0) straight to arcuate (Fig. L18C); (1) acutely pointed medially (Fig. L18A, D).

40. Abdomen, sternite 5, dense, meshed microsculpture anterolaterally, appearing different in texture to posterior portion (microsculpture more obvious than normal punctures): (0) absent; (1) present (Fig. CH23–34).

41*. Abdomen, sternite 6, two anterior transverse lines: (0) absent; (1) present (Fig. 4C).

42. Abdomen, sternite 7, punctation laterally (excluding micropunctures): (0) sparse (each row of punctures separated by more than two puncture width from other rows) (Fig. 4A); (1) dense (punctures contiguous or rows separated by less than two puncture width) (Fig. 4B).

43. Male, abdomen, sternite 7, emargination of posterior margin (in comparison to female sternite 7): (0) absent; (1) present (Fig. 4A–C).

44. Male, abdomen, sternite 7, degree of emargination of posterior margin if present: (0) broad and shallow (Fig. 4B–C); (1) narrower and more pronounced (Fig. 4A).

45. Male, abdomen, sternite 7, porose structure: (0) absent (Fig. 4A, C); (1) present (Fig. 4B).
46. Male, abdomen, sternite 7, shape of porose structure (if present): (0) circular and pit-like, typically with few modified setae (Fig. CA19); (1) broad and brush-like, with many modified setae (Fig. 4B).
47. Male, abdomen, sternite 8, emargination: (0) shallow (just a notch) (Fig. 4A); (1) U-shaped; (2) deep U-shaped (1/3–1/4 length of segment) (Fig. 4B).
48. Male, aedeagus, median lobe, apical tooth: (0) absent; (1) present (Fig. CT5).
49. Male, aedeagus, tip of median lobe in dorsal view: (0) pointed (Fig. CA53); (1) rounded (Fig. CA112); (2) broadly expanded (Fig. CA71).
50*. Male, aedeagus, median lobe, serrated apical carina: (0) absent; (1) present (Fig. 4E).
51*. Male, aedeagus, median lobe, hook-like carina: (0) absent; (1) present (Fig. 4F).

Phylogenetic analysis

Bayesian analysis were conducted in MrBayes v.3.2.7 (Ronquist et al. 2012) running on the CIPRES Science Gateway v3.3 (https://www.phylo.org). Convergence was assessed by examining the Potential Scale Reduction Factor (PSRF) and Average Standard Deviation of Split Frequency values (ASDSF) in the MrBayes output. The matrix (Suppl. material 2) was treated as a single partition and the analyses were performed using the Mkv model with gamma distribution and correction for ascertainment bias, with two runs of four chains each, default temperature (temp = 0.1) and 10,000,000 generations. I used the 'trace all characters' analysis in Mesquite to map all character states on the tree and the results of this analysis are presented as Suppl. material 3. A maximum parsimony analysis was not performed since Bayesian analysis outperforms parsimony for analysis of discrete morphological data (e.g., Wright and Hillis 2014; O'Reilly et al. 2016).

Results

Phylogenetic analysis

The Bayesian analysis (Fig. 5) of the morphological matrix converged after 10 million generations with ASDSF = 0.001 and all PSRF values = 1.000. The analysis strongly supported the monophyly of the Xanthopygina (PP = 1) but most of the backbone clades were either weakly supported or not supported. Species from *Xanthopygus* sensu Herman appeared in four different parts of the phylogenetic tree (see below for details), and based on these results, *Xa. skalitzkyi* is transferred to *Styngetus* as *Styngetus skalitzkyi* comb. nov., *Xa. nigricornis* is transferred to *Oligotergus* as *Oligotergus nigricornis* comb. nov., a large group of *Xanthopygus* species are transferred to a new genus, named here *Photinopygus* gen. nov. (see Table 2 for details on the taxonomy) and the remaining taxa are left in *Xanthopygus* sensu nov.

In a tree rooted by *Philothalpus*, all other taxa were placed in four different clades in a polytomy. The first clade contained *Phanolinus colombinus*, and the second clade

Table 1. List of *Xanthopygus* species sensu Herman and their current name based on this paper. Bold type font on the first column indicates taxa included in the phylogenetic analysis. Taxa not included in this analysis but transferred to *Photinopygus* have all the diagnostic features of *Photinopygus*. Similarly, taxa that remained in *Xanthopygus* but were not included in the analysis have all the diagnostic features of *Xanthopygus* sensu novo.

Name sensu Herman 2001	Current status
Xanthopygus alienus Bernhauer, 1905	*Photinopygus alienus* (Bernhauer, 1905); comb. nov.
Xanthopygus apicalis Sharp, 1876	*Photinopygus apicalis* (Sharp, 1876); comb. nov.
Xanthopygus borealis Hatch, 1957	junior synonym of *Tympanophorus puncticollis* (Erichson, 1840); (Moore & Legner 1975)
Xanthopygus cacti Horn, 1968	junior synonym of *Xanthopygus xanthopygus* (Nordmann, 1837); (Newton et al. 2000)
Xanthopygus calidus (Erichson, 1839)	*Photinopygus calidus* (Erichson, 1839); comb. nov.
Xanthopygus chapareanus Scheerpeltz, 1969	*Photinopygus chapareanus* (Scheerpeltz, 1969); comb. nov.
Xanthopygus chrysopygus (Nordmann, 1837)	*Photinopygus chrysopygus* (Nordmann, 1837); comb. nov.
Xanthopygus chrysurus (Nordmann, 1837)	*Photinopygus chrysurus* (Nordmann, 1837); comb. nov.
Xanthopygus cognatus Sharp, 1876	*Xanthopygus cognatus* Sharp, 1876
Xanthopygus collaris Bernhauer, 1925	*Photinopygus collaris* (Bernhauer, 1925); comb. nov.
Xanthopygus corcovadoensis Scheerpeltz, 1969	*Photinopygus corcovadoensis* (Scheerpeltz, 1969); comb. nov.
Xanthopygus cyanelytrius (Perty, 1830)	*Photinopygus cyanelytrius* (Perty, 1830); comb. nov.
Xanthopygus cyanipennis Sharp, 1876	*Photinopygus cyanipennis* (Sharp, 1876); comb. nov.
Xanthopygus depressus Sharp, 1876	*Photinopygus depressus* (Sharp, 1876); comb. nov.
Xanthopygus dimidiatus Bernhauer, 1917	*Photinopygus dimidiatus* (Bernhauer, 1917); comb. nov.
Xanthopygus elegans Bernhauer, 1905	*Photinopygus elegans* (Bernhauer, 1905); comb. nov.
Xanthopygus faustus (Erichson, 1839)	*Photinopygus faustus* (Erichson, 1839); comb. nov.
Xanthopygus flohri Sharp, 1884	*Photinopygus flohri* (Sharp, 1884); comb. nov.
Xanthopygus giganteus (Bernhauer, 1906)	*Xanthopygus giganteus* (Bernhauer, 1906)
*Xanthopygus grimmeri*ᵃ Duvivier, 1883	*nomen dubium*; (Herman 2001)
Xanthopygus haemorrhoidalis (Germar, 1824)	*Photinopygus haemorrhoidalis* (German, 1823); comb. nov.
Xanthopygus hilaris (Erichson, 1839)	*Photinopygus hilaris* (Erichson, 1839); comb. nov.
Xanthopygus iopterus (Erichson, 1939)	*Photinopygus iopterus* (Erichson, 1939); comb. nov.
Xanthopygus janthinipennis (Blanchard, 1842)	*Photinopygus janthinipennis* (Blanchard, 1842); comb. nov.
Xanthopygus luctuosus (Blanchard, 1842)	*Xanthopygus luctuosus* (Blanchard, 1842)
Xanthopygus major (Bernhauer, 1917)	*Xanthopygus major* (Bernhauer, 1917)
Xanthopygus max Blackwelder, 1944	*Xanthopygus max* Blackwelder, 1944
Xanthopygus mirabilis (Erichson, 1840)	*Photinopygus mirabilis* (Erichson, 1840); comb. nov.
Xanthopygus morosus Sharp, 1884	*Photinopygus morosus* (Sharp, 1884); comb. nov.
Xanthopygus nigricornis Scheerpeltz, 1969	*Oligotergus nigricornis* (Scheerpeltz, 1969); comb. nov.
Xanthopygus nigripes Sharp, 1876	*Photinopygus nigripes* (Sharp, 1876); comb. nov.
Xanthopygus oliveirae Lynch, 1884	*Xanthopygus oliveirae* Lynch, 1884
Xanthopygus pexus (Motschulsky, 1858)	*Xanthopygus pexus* (Motschulsky, 1858)
Xanthopygus punctatus Bernhauer, 1905	*Photinopygus punctatus* (Bernhauer, 1905); comb. nov.
Xanthopygus puncticollis Sharp, 1884	*Photinopygus puncticollis* (Sharp, 1884); comb. nov.
Xanthopygus rufipennis Sharp, 1884	*Photinopygus rufipennis* (Sharp, 1884); comb. nov.
Xanthopygus sapphirinus (Erichson, 1839)	*Photinopygus sapphirinus* (Erichson, 1839); comb. nov.
Xanthopygus skalitzkyi (Bernhauer, 1906)	*Styngetus skalitzkyi* (Bernhauer, 1906); comb. nov.
Xanthopygus tepidus (Erichson, 1839)	*Photinopygus tepidus* (Erichson, 1839); comb. nov.
Xanthopygus violaceipennis Bernhauer, 1927	*Photinopygus violaceipennis* (Bernhauer, 1927); comb. nov.
Xanthopygus violaceus Sharp, 1876	*Photinopygus violaceus* (Sharp, 1876); comb. nov.
Xanthopygus viridipennis Sharp, 1876	*Photinopygus viridipennis* (Sharp, 1876); comb. nov.
Xanthopygus xanthopygus (Nordmann, 1837)	*Xanthopygus xanthopygus* (Nordmann, 1837)

ᵃ: The species was listed as *nomen dubium* by Herman (2001), and was originally described as distributed in Austria, which is peculiar given that no Xanthopygina are known from the Palearctic. I have contacted the Curator of Coleoptera in the Natural History Museum of Graz, Austria, where the Grimmer collection is housed and no taxa matching this name exist in the collection (Hausl-Hofstätter personal communication). It is unlikely that any specimens exist that can be attached to this name.

is composed of the sister groups *Gastrisus* sp. and *Gastrisus mimetes* (PP = 1). The third clade was unsupported (called here the *Xanthopygus* clade); it contained several species (*Gastrisus nitidus*, *Triacrus dilatus*, Genus 1 and the fours species of *Xenopygus*) and a

Table 2. List of taxonomic characters that distinguish species of *Xanthopygus* from *Photinopygus*. Numbers next to characters refers to the numbers in the data matrix. For a full list of characters and character states see Material and Methods, and for the mapping of the characters on the phylogenetic tree see Suppl. material 3.

Characters	*Photinopygus*	*Xanthopygus*
4. Antennae, antennomere 5	(0) elongate (Figs. 1A, F).	(1) subquadrate (Figs. 1D–E).
8. Head, width in comparison to pronotum	(1) subequal (Figs. 1A–C).	(2) wider[1] (Figs. 1D–E) (apomorphy).
9. Head, shape, posterior margin	(0) slightly extended posteriad on each side of the neck[2] (Figs. 1A–C) (apomorphy).	(1) more or less at same level with neck border (Figs. 1D–E).
10. Head, eye size relative to length of head	(1) medium (between 2/5 and 2/3 length of head) (Fig. 1B).	(0) small (less than 2/5 length of head) (Fig. 1D) (apomorphy).
15. Mandible, left, teeth structure	(2) one bicuspid tooth (Fig. 1C).	(1) two teeth, separated by deep emargination (Fig. 1D) (apomorphy).
17. Pronotum, microsculpture	(3) with sparse micropunctures (but no transverse lines visible at 70× magnification) (apomorphy).	(1) with transverse lines (seen easily at 70× magnification)[3].
22. Prothorax, hypomeron, angles of superior and inferior marginal lines	(0) superior and inferior line produce anterolateral angles parallel to one other (Fig. 2A).	(1) superior and inferior line produce anterolateral angles not parallel to one other (Fig. 2B) (apomorphy).
28. Mesothorax, mesoscutellum, dense micropunctures	(0) absent (Fig. 2D) (apomorphy).	(1) present (Fig. 2C).
29. Mesoventrite, intercoxal process, apex	(2) narrow and rounded (Fig. 2E) (apomorphy).	(1) broad and rounded; or (3) broad and pointed (Fig. 2F).
30. Metathorax, metepisternum, punctures	(1) metepisternum covered with punctures or impunctate area less than 1/3[4] (Fig. 3B).	(0) dorsal 1/3 of metepisterstum without punctures throughout its length (Fig. 3A) (apomorphy).
32. Metathorax, metacoxae, spines on the posterior surface	(0) 4 or less (Fig. 3C).	(1) more than 4[5] (Fig. 3D).
34. Metathorax, metatarsi, tarsomere 3, dorsal surface, chaetotaxy	(1) tarsomeres dorsally setose (setae not restricted to marginal series) (Fig. 3F) (apomorphy).	(0) developed only at margins, dorsal surface of tarsomeres glabrous (or with 1–2 setae) along midline (Fig. 3E).

[1] It should be noted that head size is sexually dimorphic in *Xanthopygus* (but always wider than pronotum) and head size can vary drastically among specimens of the same species similarly to what has been observed in *Smilax* (Chatzimanolis 2016) and *Triacrus dilatus* (Chatzimanolis 2015a; Marlowe et al. 2015); [2] Except *Ph. mirabilis* and *Ph. corcovadoensis* (9:1); [3] Except *Xa. giganteus* (17:0); [4] Except *Ph. mirabilis* (30:0); [5] Except *Xa. xanthopygus* (32:0).

large portion of the *Xanthopygus* species. The species of *Xanthopygus* in this clade formed a monophyletic group that was strongly supported (PP = 0.92) and will be treated as the *Xanthopygus* sensu nov. (for details see below on the Taxonomy section). Taxa included here were the ones placed in the genus *Lampropygus* by early taxonomists. *Xanthopygus giganteus* was the sister group of *Xa. oliveirae* (PP = 0.99) and together were the sister group of *Xa. major* but without support. This clade was placed in a polytomy with *Xa. xanthopygus*, *Xa. cognatus*, *Xa. pexus* and *Xa. max*. For a list of characters that support *Xanthopygus* sensu nov. see the Taxonomy section below and Table 2.

The fourth clade (called here the *Photinopygus* clade) included *Xanthopygus* taxa in three different subclades. *Xanthopygus skalitzkyi* was placed as the sister group of *Styngetus deyrollei* (Solsky) with weak support (PP = 0.80) and supported by a unique synapomorphy present in all *Styngetus* species: (character 33:0 and matrices in Suppl. material 2, 3) upper posterior margin of metafemur crenulate. *Xanthopygus nigricornis* was placed as the sister group of *Oligotergus fasciatus* (Nordmann) with strong support (PP = 0.97) and two unique (for Xanthopygina) synapomorphies (1:0) antennomere 1 less than twice as long as antennomere 2; and (15:0) left mandible with a single tooth (character state also present in *Philothalpus*).

The remaining taxa in the fourth clade all belonged in *Xanthopygus* sensu Herman and were strongly supported as a monophyletic group (PP = 0.99). *Xanthopygus punctatus* was recovered as the sister group of *Xa. flohri* but without support (PP = 0.74) and together as the sister group of *Xa. sapphirinus* (PP = 0.65). That clade was placed in a polytomy with *Xa. mirabilis*, *Xa. cyanelytrius*, *Xa. puncticollis*, *Xa. calidus*, and a strongly supported clade (PP = 0.90) of *Xa. chapareanus* + *Xa. faustus* (PP = 0.95) as the sister group of *Xa. rufipennis* + *Xa. dimidiatus* (PP = 0.93). All these taxa previously in *Xanthopygus* are transferred to a new genus, *Photinopygus* gen. nov. and the apomorphies supporting this new genus are given below in the Taxonomy section and in Table 2.

Taxonomy

Oligotergus Bierig, 1937

Type species. *Philothalpus* (*Oligotergus*) *oculatus*, fixed by monotypy (Herman 2001).
    Species included. The genus includes 20 species listed in Newton (2021) and *Oligotergus nigricornis* comb. nov. based on the results of the phylogenetic analysis presented in this paper. For a complete taxonomic history of the genus see Herman (2001).
    Diagnosis. The genus is not revised so the following characters (in combination) should be considered only as a partial list: left mandible with single tooth; antennomere 1 less than twice as long as antennomere 2; eyes large; pronotum with dense micropunctures (not in all species).
    Remarks. The type species was not available for the phylogenetic analysis. A formal revision of the genus is forthcoming (Chatzimanolis in preparation) where all species belonging to this genus will be treated and illustrated.

Styngetus Sharp, 1884
Fig. 1F

Type species. *Philonthus viduus* Erichson, fixed by subsequent designation by Blackwelder (1952) (Herman 2001).
    Species included. The genus includes 16 species listed in Newton (2021) and *Styngetus skalitzkyi* comb. nov. based on the results of the phylogenetic analysis presented in this paper. For a complete taxonomic history of the genus see Herman (2001).
    Diagnosis. The genus is not revised so the following characters (in combination) should be considered only as a partial list: left mandible with bicuspid tooth; protarsi without ventral pale macrosetae (not present in all taxa); metafemur with upper posterior margin crenulate; sternites 3–5 with arch-like carina.
    Remarks. The type species was not available for the phylogenetic analysis. A formal revision of the genus is forthcoming (Chatzimanolis in preparation) where all species belonging to this genus will be treated and illustrated.
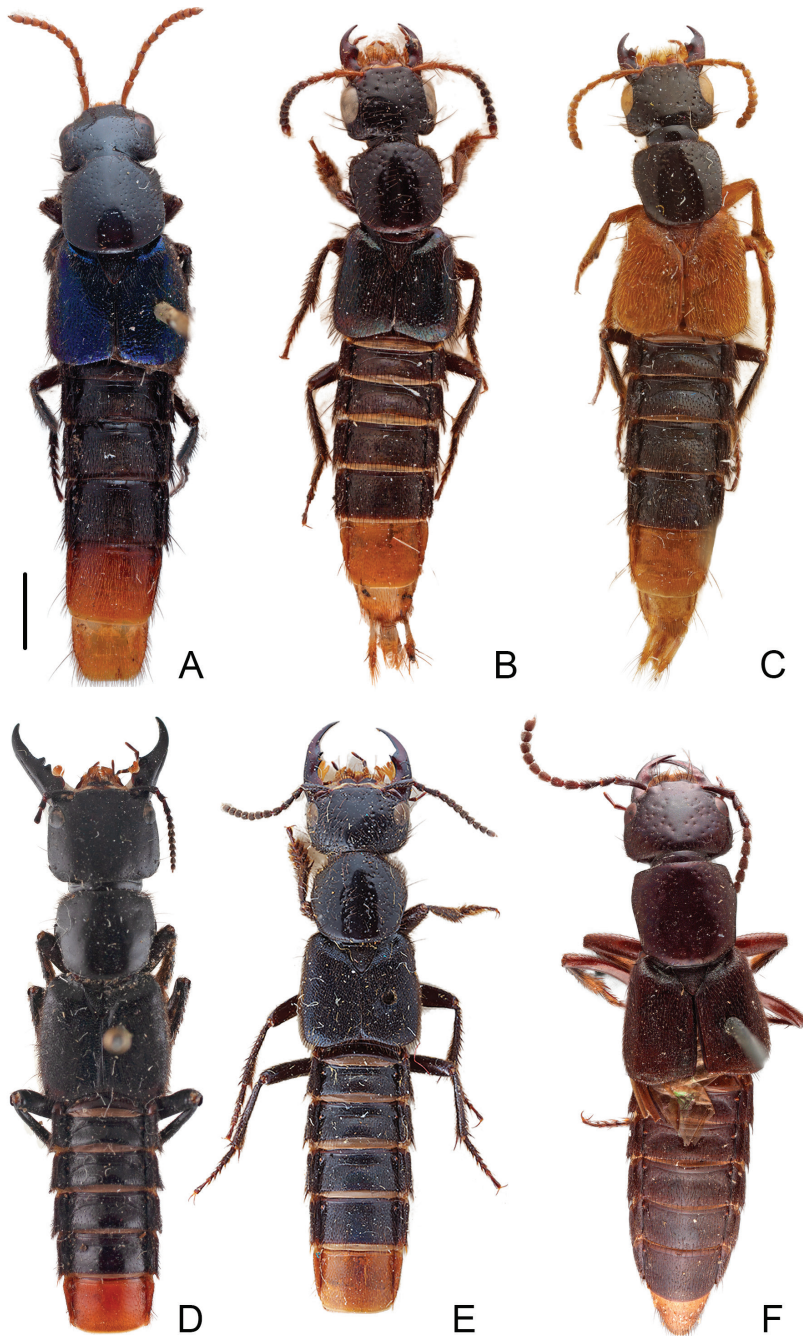
Figure 1. Habitus photographs of species of *Xanthopygus* sensu Herman 2001 **A** *Xanthopygus calidus* (Er.) **B** *Xanthopygus chapareanus* Scheerpeltz **C** *Xanthopygus dimidiatus* Bernhauer. Species **A–C** are transferred to *Photinopygus* gen. nov. **D** *Xanthopygus giganteus* (Bernhauer) **E** *Xanthopygus xanthopygus* (Nordmann) **F** *Xanthopygus skalitzkyi* (Bernhauer), transferred to *Styngetus*. Scale bars: 1.8 mm (**A**); 1.7 mm (**B**) 1.8 mm (**C**); 3.8 mm (**D**); 3.0 mm (**E**); 2.0 mm (**F**).
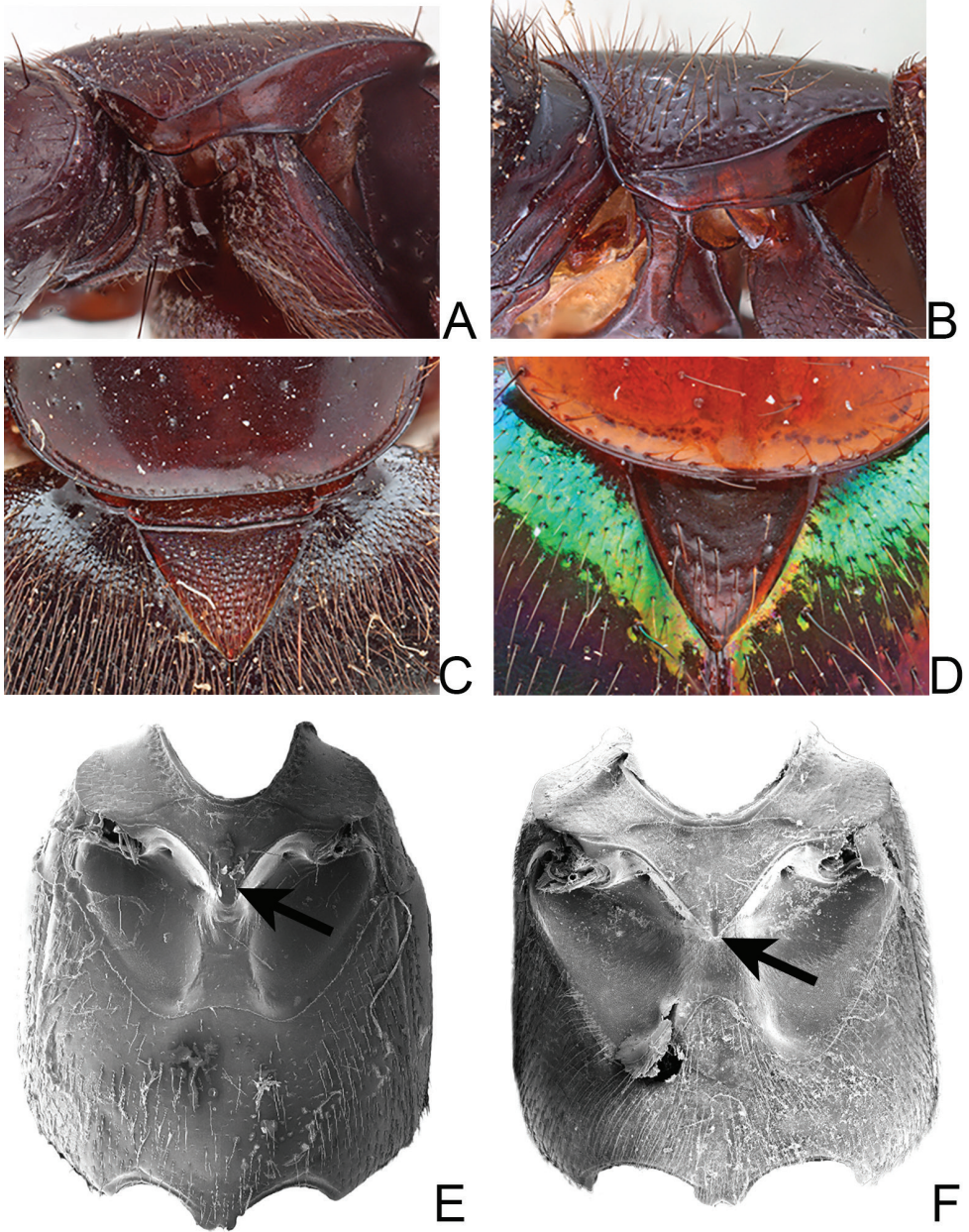
Figure 2. Diagnostic characters for *Xanthopygus* **A** pronotal hypomeron of *Xanthopygus skalitzkyi* (Bernhauer) **B** pronotal hypomeron of *Xanthopygus xanthopygus* (Nordmann) **C** mesoscutellum of *Xanthopygus cognatus* Sharp **D** mesoscutellum of *Xanthopygus mirabilis* (Erichson) **E** mesoventrite of *Xanthopygus mirabilis* (Erichson), arrow points to intercoxal process **F** mesoventrite of *Xanthopygus xanthopygus* (Nordmann), arrow points to intercoxal process. Not to scale.
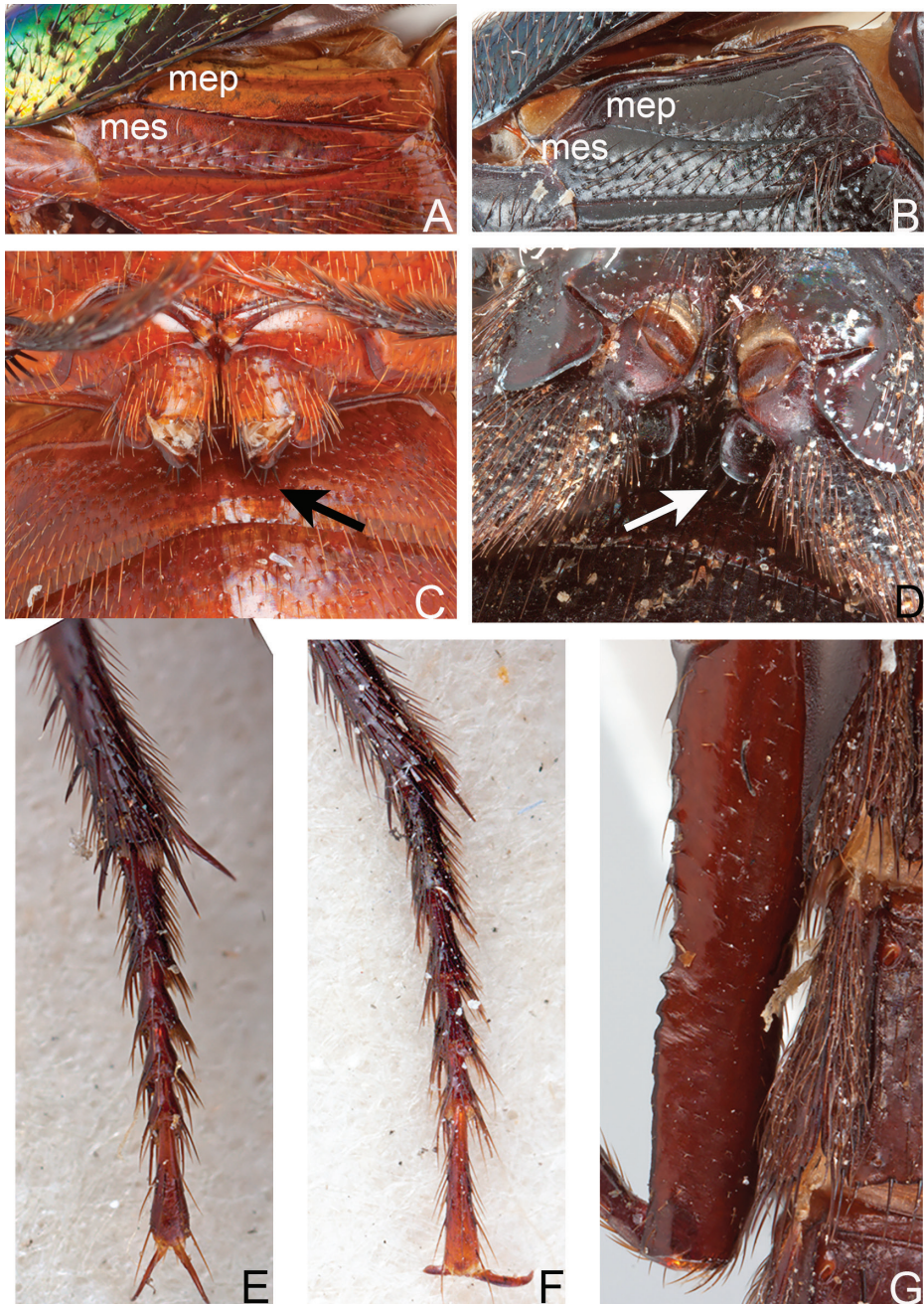
Figure 3. Diagnostic characters for *Xanthopygus* **A** metepimeron (mep) and metepisternum (mes) of *Xanthopygus mirabilis* (Erichson) **B** metepimeron (mep) and metepisternum (mes) of *Xenopygus analis* (Erichson) **C** metacoxae of *Xanthopygus mirabilis* (Erichson), arrow points to spines **D** metacoxae of *Triacrus dilatus* Nordmann, arrow points to spines **E** Metatarsus of *Xanthopygus xanthopygus* (Nordmann) **F** metatarsus of *Xanthopygus flohri* Sharp **G** metafemur of *Xanthopygus skalitzkyi* (Bernhauer), showing crenulate surface. Not to scale.

Photinopygus Chatzimanolis, gen. nov.

http://zoobank.org/ab8578bb-db63-4f34-a863-109d68a05bb9

Figs. 1A–C

Type species. *Staphylinus calidus* Erichson, here designated.

Species included. *alienus*, *apicalis*, *calidus*, *chapareanus*, *chrysopygus*, *chrysurus*, *corcovadoensis*, *cyanelytrius*, *cyanipennis*, *depressus*, *dimidiatus*, *elegans*, *faustus*, *flohri*, *haemorrhoidalis*, *hilaris*, *iopterus*, *janthinipennis*, *mirabilis*, *morosus*, *nigripes*, *punctatus*, *puncticollis*, *sapphirinus*, *tepidus*, *violaceipennis*, *violaceus* and *viridipennis* (see Table 1 for complete names).

Diagnosis. This genus can be distinguished from all other genera in Xanthopygina based on the combination of the following characteristics: head shape rectangular; posterior margin of head slightly extended posteriad on each side of the neck (apomorphy; except in *Ph. corcovadoensis* and *Ph. mirabilis*); antennomeres 1–5 elongate; labial palpomere 3 not securiform; medium size eyes; superior marginal line of pronotal hypomeron not continuing to anterior margin; postcoxal process present; pronotum with sparse micropunctures but no transverse lines visible at 70× magnification (apomorphy); mesoscutellum without dense micropunctures (apomorphy); mesoventral process narrow and rounded (apomorphy); metatarsi with setose dorsal surface (apomorphy); tergite 3 (at minimum, some species 3–4 or 3–5) with arch-like carina; and sternite 7 in males with emargination at posterior margin. For a list of characters that distinguish *Photinopygus* from *Xanthopygus*, see Table 2.

Etymology. The name is a combination of the Greek words φωτεινός (shining, bright) and πυγή (rump), and refers to the bright coloration of abdominal segments 7 and 8. The name is masculine.

Remarks. A formal revision of the genus is forthcoming (Chatzimanolis in preparation) where all species belonging to this genus will be treated and illustrated. Even though some of the species transferred to *Photinopygus* were not included in the phylogenetic analysis, they can be confidently placed in this genus since they have all the diagnostic features of *Photinopygus* (see Tables 1 and 2 for details).

Xanthopygus Kraatz, 1857 sensu novo

Figs. 1D–E

Type species. *Staphylinus xanthopygus* Nordmann, 1837, fixed by absolute tautonymy (Herman 2001).

Species included. *cognatus*, *giganteus*, *luctuosus*, *major*, *max*, *oliveirae*, *pexus* and *xanthopygus*. (see Table 1 for complete names and Herman 2001 for taxonomic history).

Diagnosis. This genus can be distinguished from all other genera in Xanthopygina based on the combination of the following characteristics: head shape rectangular; head wider than pronotum (apomorphy; however, head size can be variable among specimens of the same species but wider than pronotum); antennomeres 7–10 transverse; left mandible with two teeth separated by deep emargination (apomorphy);
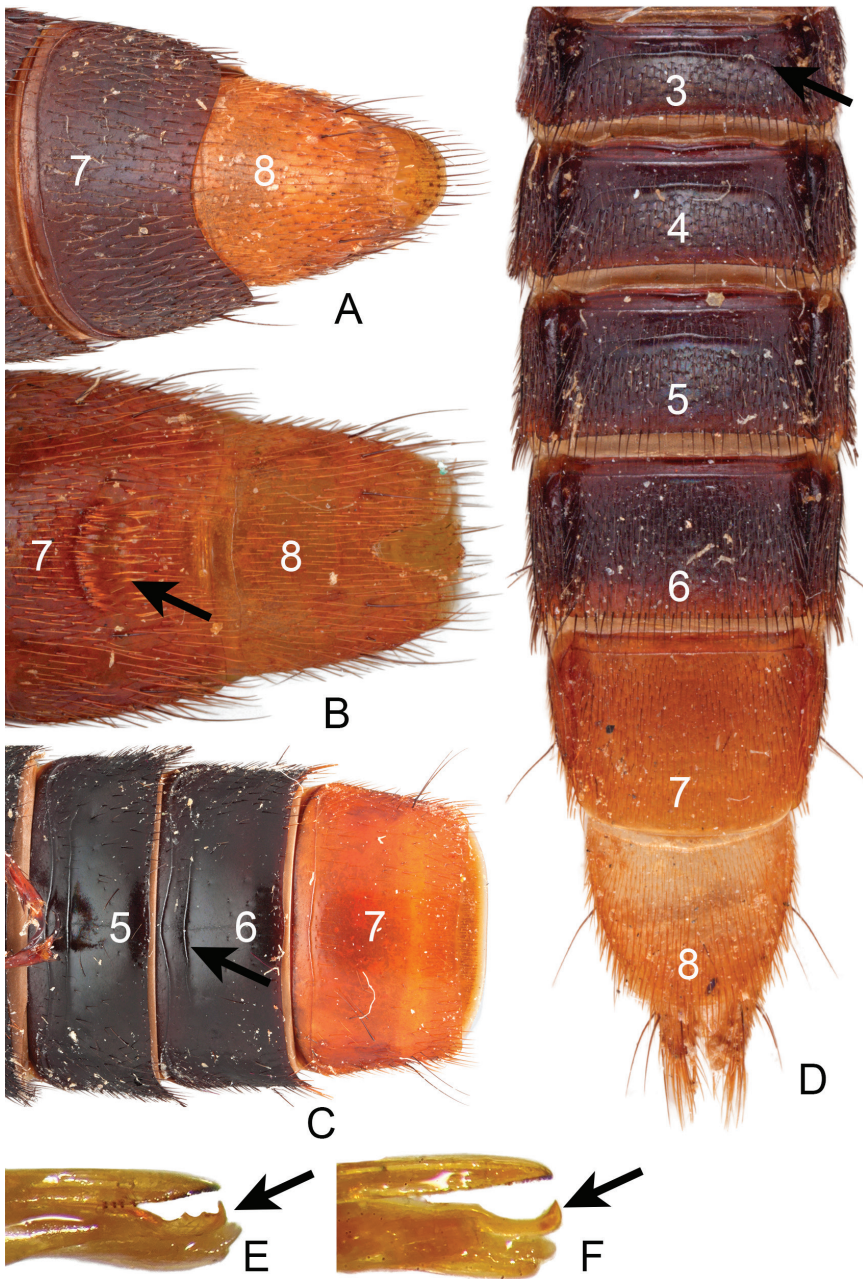
Figure 4. Diagnostic characters for *Xanthopygus* **A** abdominal sternites 7–8 of *Xanthopygus skalitzkyi* (Bernhauer) **B** abdominal sternites 7–8 of *Xanthopygus viridipennis* Sharp, arrow points to the porose structure **C** abdominal sternites 5–7 of *Xanthopygus giganeus* (Bernhauer), arrow points to the anterior transverse lines **D** abdominal tergites 3–8 of *Xanthopygus cognatus* Sharp, arrow points to arch-like carina on tergite 3 **E** lateral view of the aedeagus of *Xanthopygus faustus* (Erichson), arrow points to the serrated apical carina **F** lateral view of the aedeagus of *Xanthopygus dimidiatus* Bernhauer, arrow points to the hook-like carina. Not to scale.

labial palpomere 3 not securiform; small size eyes (apomorphy); superior marginal line of pronotal hypomeron not continuing to anterior margin; superior and inferior marginal line of hypomeron produce anterolateral angles not parallel to one other (apomorphy); postcoxal process present; elytra coloration black (except with blue metallic overtones in *Xa. xanthopygus*); dorsal 1/3 of metepisterstum without punctures (apomorphy; state also present in *Ph. mirabilis*); with more than four spines on the posterior surface of metacoxae (apomorphy; less than four in *Xa. xanthopygus*); tergites 3–5 with arch-like carina; and sternite 7 in males with emargination at posterior margin. For a list of characters that distinguish *Xanthopygus* from *Photinopygus*, see Table 2.

Remarks. A formal revision of the genus is forthcoming (Chatzimanolis in preparation) where all species belonging to this genus will be treated and illustrated.

Discussion

The phylogenetic analysis presented here strongly rejected the hypothesis that *Xanthopygus* sensu Herman is a monophyletic group. As was previously defined, *Xanthopygus* included species that belonged in four distinct (and, as far as it is known, they are not sister to each other) clades, the genera *Oligotergus*, *Photinopygus*, *Styngetus* and *Xanthopygus*. The classification changes implemented in this paper resolve this issue by defining *Xanthopygus* in a new sense that includes some species that were described in *Lampropygus* (a synonym of *Xanthopygus*), although of the four species originally included in *Lampropygus* (Sharp 1884) two are now placed in *Xenopygus* (*Xe. anali*s and *Xe. bicolor*, both included in the analysis here). However, *Lampropygus* was never clearly defined and included species (e.g., *L. skalitzkyi*) that clearly did not belong in that genus. Most of the species that belonged in *Xanthopygus* sensu Herman are placed in the new genus *Photinopygus*. Both *Xanthopygus* sensu novo and *Photinopygus* as presented in this paper are well-defined with clear diagnostic features that would hopefully prevent future misplaced species in these genera.

Styngetus skalitzkyi and *Oligotergus nigricornis* were clearly placed in *Xanthopygus* sensu Herman by mistake by Bernhauer (1906) and Scheerpeltz (1969), respectively. In both of these species, the superior marginal line of the hypomeron continues to the anterior end, which should have been a clear indication that the placement in *Xanthopygus* sensu Herman was erroneous. Granted, both of these species are atypical for either *Styngetus* or *Oligotergus* and these genera are still in dire need of revision since they contain multiple species of uncertain affinities (Chatzimanolis, unpublished data), not to mention the lack of clearly defined diagnostic features. Most species of *Styngetus* have a much narrower head than *Styngetus skalitzkyi* and some species of *Styngetus* have narrow protarsi (not seen in *Styngetus skalitzkyi*). However, the crenulate upper posterior margin of the metafemur is present in all species of *Styngetus* examined by me (and *Styngetus skalitzkyi*) and seems to be a good diagnostic character for the genus, pending its further review and phylogenetic analysis. In any case, *Styngetus* is probably more homogeneous than *Oligotergus* as currently defined. *Oligotergus* seems to include at least two distinct species groups, roughly split into species with dense small
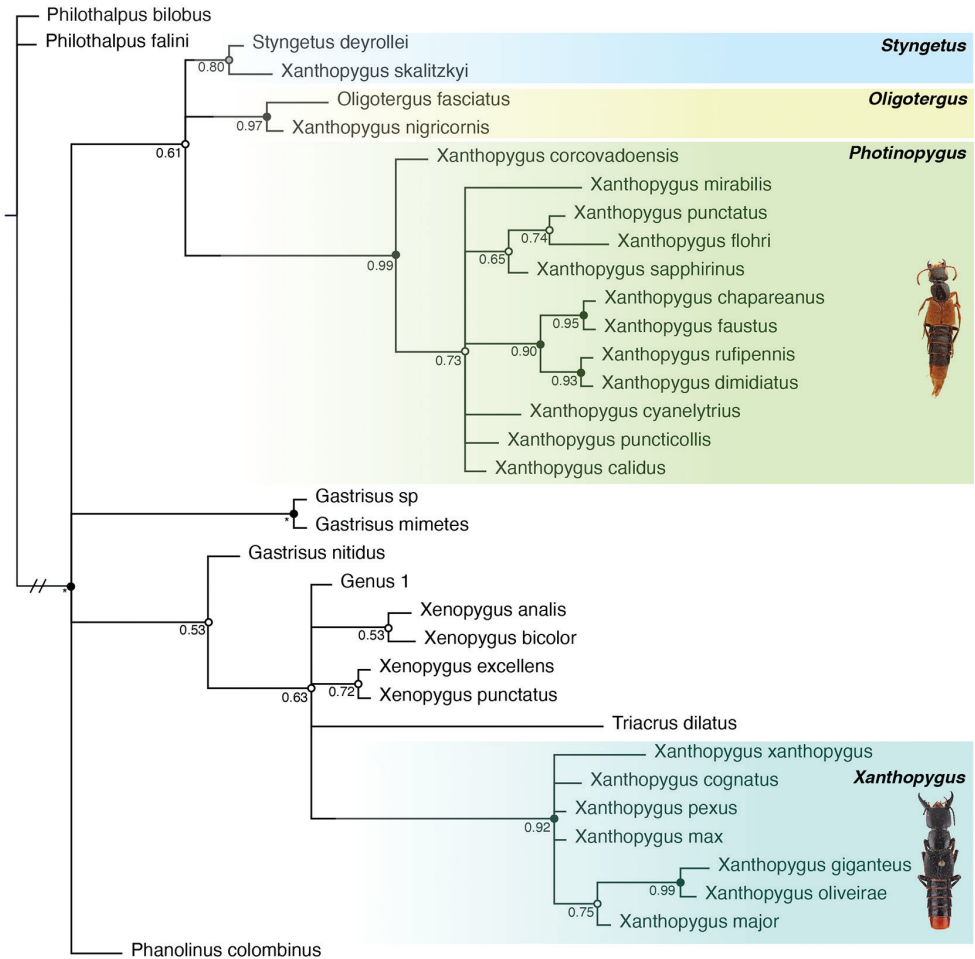
Figure 5. Fifty per cent majority rules consensus tree from a Bayesian phylogenetic analysis of 51 morphological characters. Posterior probabilities (PP) are given to the left of the corresponding node. Nodes colored based on support: PP ≥ 0.90 black; PP 0.80–0.89 grey; PP < 0.80 white.

uniform punctures on the pronotum and species with larger, less dense punctures on pronotum. *Oligotergus nigricornis* belongs in the second group and whether these two species groups both should be included in *Oligotergus* is matter of further investigation.

One of the major issues with *Xanthopygus* sensu Herman was that the characters used to define the genus (superior marginal line of pronotal hypomeron not continuing to anterior margin, postcoxal process present, and tergites 3–5 with arch-like carina) are not unique to *Xanthopygus* and the genus was not easily recognizable. Even if somebody were to argue that the phylogeny presented here is not properly resolved, meaning that perhaps *Xanthopygus* sensu novo and *Photinopygus* might be sister groups and therefore do not have to be in separate genera, the reality is that *Xanthopygus* sensu Herman was impossible to diagnose with just the characters presented above. Perhaps more impor-

tantly, *Photinopygus* and *Xanthopygus* sensu novo do not share any apomorphies that could be used to diagnose *Xanthopygus* sensu Herman 2001. The split of *Xanthopygus* sensu Herman into *Xanthopygus* sensu novo and *Photinopygus* makes both of these genera easily recognizable and identifiable, given the characters presented in Table 2.

One of the characters used to define *Xanthopygus* sensu Herman was the superior marginal line of pronotal hypomeron not continuing to anterior margin. Until recently, it was not clear how widespread this character state is among Xanthopygina. *Triacrus dilatus* has the same character state and this feature along with the position of *Triacrus* on the phylogeny of Xanthopygina (Chatzimanolis and Brunke 2019) led these authors to hypothesize that perhaps *Triacrus* belonged in *Xanthopygus* (but see below for characters that exclude *Triacrus* from *Xanthopygus*). However, the particular state of the superior marginal line of pronotal hypomeron seen in *Xanthopygus* and *Triacrus* is more common than previously thought and certain species of *Gastrisus*, Genus 1, and even some species of *Plociopterus* Kraatz exhibit this particular character state. It is likely that this character state is much more widespread in Xanthopygina than previously documented and has evolved multiple times in several different lineages. Additionally, given the parallel evolution, this character state alone should not be used as a justification for a hypothetical close relationship between *Xanthopygus* sensu novo and *Photinopygus*.

A caveat in this paper is that the backbone relationships presented are unsupported. This is certainly not uncommon in morphology-only analyses using Bayesian statistics, and previous morphology-only Bayesian analyses of Staphylinini had low support values (e.g., Chatzimanolis and Brunke 2019, 2021). Usually combining morphological with molecular data alleviates nodes with low posterior probability values. But one problem with the addition of molecular data in papers that target relationships among species within genera rather than among higher taxonomic groups is the scarcity of DNA-grade material. For example, several of the species of *Xanthopygus* sensu novo are only known from the type and/or few additional specimens. While modern techniques have enabled the use of museum specimens in molecular analyses of Staphylininae (e.g., Brunke et al. 2021), using type materials for DNA analyses is still a sensitive subject with museum curators. Also, such techniques are expensive and thus may not be feasible for smaller standalone projects like this paper. Even though molecular data would have improved the resolution of the relationships presented here, the goal of this paper was to eliminate an obvious non-monophyletic group, *Xanthopygus* sensu Herman. For this purpose, the morphology-only analysis presented here was adequate and clearly indicated that *Xanthopygus* sensu Herman was polyphyletic. Discovering the exact phylogenetic placement of every species is a pending future task. The phylogenetic analysis presented in this paper differs to the one presented by Chatzimanolis and Brunke (2019, 2021) regarding the placement of *Photinopygus* among Xanthopygina lineages. The analysis presented in this paper indicated *Photinopygus* belonging in a different lineage of Xanthopygina (the *Plociopterus* lineage) than *Xanthopygus* (that belongs in the *Xanthopygus* lineage) but that result was unsupported (in terms of posterior probabilities). However, further analyses are needed to test how closely related *Photinopygus* and *Xanthopygus* may be.

The phylogenetic position of *Xenopygus* within the *Xanthopygus* lineage of genera remains unresolved. Chatzimanolis and Caron (2016) proposed two species groups within *Xenopygus* (*punctatus*, which includes *Xe. punctatus* and *Xe. excellens*, and *analis*, which includes *Xe. analis* and *Xe. bicolor*) and cautioned that these species groups may need to be placed in different genera in the future. In Chatzimanolis and Brunke (2019) the two species of *Xenopygus* (*Xe. excellens* and *Xe. analis*) included did not form a monophyletic group. In this paper, I added two more species (*Xe. punctatus* and *Xe. bicolor*) in the analysis, hoping that the addition of these taxa may help clarify their phylogenetic position. The analysis in this paper failed to find support for a monophyletic *Xenopygus* and it is unclear if morphological data alone can resolve this puzzle. In any case, it seems unlikely (and unsupported by the current data) that the *analis* species group of *Xenopygus* and *Xanthopygus sensu novo* are closely related as had been hypothesized early on by Sharp (1884) by his placement of these taxa in *Lampropygus*.

Likewise, the position of *Triacrus* remains unresolved. In Chatzimanolis and Brunke (2019) *Tr. dilatus* was placed as the sister group of *Xa. chapareanus* (now *Photinopygus chapareanus*) and in Chatzimanolis and Brunke (2021) in a polytomy with *Xa. xanthopygus* and *Xa. chapareanus*. In this paper, *Tr. dilatus* is in a polytomy with Genus 1, *Xenopygus* and the clade that leads to *Xanthopygus* sensu novo. While the exact position of *Tr. dilatus* is unclear, it is likely that this species is not closely related to *Photinopygus*, and current data does not support its placement within *Xanthopygus* sensu novo. *Triacrus* can easily be excluded from *Photinopygus* or *Xanthopygus* sensu novo based on the shape of antennomere 5 (transverse), the shape of teeth on left mandible (one large tooth and one bicuspid tooth) and the lack of postcoxal process.

It is perhaps unfortunate that most of the species that used to belong in *Xanthopygus* sensu Herman required a new name and were transferred to *Photinopygus*. However, this action corrected existing taxonomic problems and was necessary. Unfortunately, changing the meaning of an existing genus name is not uncommon; for example, Chatzimanolis and Ashe (2005) completely changed the meaning of *Philothalpus*, and multiple other times a genus name has been drastically redefined in Xanthopygina (e.g., *Dysanellus* Bernhauer: Chatzimanolis 2012; *Trigonopselaphus* Gemminger and Harold: Chatzimanolis 2015b; *Torobus* Herman: Chatzimanolis 2018). It is very likely that further changes in the name usage might be necessary in Xanthopygina as revisionary work progresses, especially in poorly defined genera such as *Gastrisus* or *Oligotergus*.

Conclusions

The Bayesian phylogenetic analysis performed in this paper showed that *Xanthopygus* sensu Herman is polyphyletic. To solve this problem, one species was transferred to *Oligotergus*, another to *Styngetus*, a new genus *Photinopygus* was erected for many taxa previously in *Xanthopygus* and *Xanthopygus* sensu novo was restricted to the remaining species. The new diagnostic characters provided in this paper can be easily used to define *Photinopygus* or *Xanthopygus*. Even though this paper helped to untangle the

relationships within *Xanthopygus* sensu Herman, the exact relationships of the genera within the *Xanthopygus* lineage are still uncertain and would probably require comprehensive molecular phylogenetic analyses to decipher.

Acknowledgements

References

Bernhauer M (1905) Neue Staphyliniden aus Südamerika. Deutsche Entomologische Zeitschrift 1905: 177–187. https://doi.org/10.1002/mmnd.48119050305

Bernhauer M (1906) Neue Staphyliniden aus Südamerika. Deutsche Entomologische Zeitschrift 1906: 193–202. https://doi.org/10.1002/mmnd.48019060105

Bernhauer M (1917) Neue südamerikanische Staphyliniden. Wiener Entomologische Zeitung 36: 102–116. https://doi.org/10.5962/bhl.part.12925

Bernhauer M (1927) Beitrag zur Staphylindenfauna Südamerikas insbesondere Braziliens. Memorie della Società Entomologica Italiana 5(2)(1926): 152–169

Blackwelder RE (1943) Monograph of the West Indian beetles of the family Staphylinidae. United States National Museum Bulletin 182: 1–658. https://doi.org/10.5479/si.03629236.182.i

Blackwelder RE (1952) The generic names of the beetle family Staphylinidae, with an essay on genotypy. United States National Museum Bulletin 200: 1–483.

Brunke AJ, Hansen AK, Salnitska M, Kypke JL, Predeus AV, Escalona H, Chapados JT, Eyres J, Richter R, Smetana A, Ślipiński A, Zwick A, Hájek J, Leschen RA, Solodovnikov A, Dettman JR (2021) The limits of Quediini at last (Staphylinidae: Staphylininae): a rove beetle mega-radiation resolved by comprehensive sampling and anchored phylogenomics. Systematic Entomology 46: 396–421.https://doi.org/10.1111/syen.12468

Caron E, de Castro JC, Da Silva MR, Ribeiro-Costa CS (2016) Phylogeny and revision of a colorful Neotropical genus of rove beetles: *Xenopygus* Bernhauer (Coleoptera: Staphylinidae). Zootaxa 4138(1): 59–82. http://dx.doi.org/10.11646/zootaxa.4138.1.2

Chani-Posse MR, Brunke AJ, Chatzimanolis S, Schillhammer H, Solodovnikov A (2018) Phylogeny of the hyper-diverse Philonthina rove beetles with implications for classification of the tribe Staphylinini (Coleoptera: Staphylinidae). Cladistics 38: 1–40. https://doi.org/10.1111/cla.12188

Chatzimanolis S (2012) *Zackfalinus*, a new genus of Xanthopygina (Coleoptera: Staphylinidae:

Staphylinini) with description of 20 new species. Annals of the Carnegie Museum 80(4): 261–308. https://doi.org/10.2992/007.080.0401

Chatzimanolis S (2014) Phylogeny of xanthopygine rove beetles based on six molecular loci. Systematic Entomology 39(1): 141–149. https://doi.org/10.1111/syen.12040

Chatzimanolis S (2015a) New records, redescription, and notes on nomenclature for *Triacrus* Nordmann (Coleoptera: Staphylinidae: Staphylininae: Staphylinini). The Coleopterists Bulletin 69(3): 514–520. https://doi.org/10.1649/0010-065X-69.3.514

Chatzimanolis S (2015b) A revision of the genus *Trigonopselaphus* Gemminger and Harold (Coleoptera: Staphylinidae: Staphylininae). Koleopterologische Rundschau 85: 167–189.

Chatzimanolis S (2016) A revision of the myrmecophilous genus *Smilax* Laporte (Coleoptera: Staphylinidae: Staphylininae). Zootaxa 4162(2): 283–303. https://doi.org/10.11646/zootaxa.4162.2.5

Chatzimanolis S (2017) And then there were six: a revision of the genus *Phanolinopsis* Scheerpeltz (Coleoptera: Staphylinidae: Staphylininae). Zootaxa 4323(1): 49–67. https://doi.org/10.11646/zootaxa.4323.1.4

Chatzimanolis S (2018) A review of the genera *Dysanellus* Bernhauer and *Torobus* Herman (Staphylinidae: Staphylininae: Staphylinini). The Coleopterists Bulletin 72(2): 279–291. https://doi.org/10.1649/0010-065X-72.2.279

Chatzimanolis S (2019) *Lendatus*, a new genus of Xanthopygina (Coleoptera: Staphylinidae: Staphylininae) with description of three new species. PeerJ 7: e7947. https://doi.org/10.7717/peerj.7947

Chatzimanolis S, Ashe JS (2005) Revision and phylogeny of the neotropical genus *Philothalpus* (=*Eugastus* Sharp and *Allostenopsis* Bernhauer) (Coleoptera: Staphylinidae: Xanthopygina). Insect Systematics and Evolution 36: 63–119. https://doi.org/10.1163/187631205788912813

Chatzimanolis S, Brunke AJ (2019) A phylogeny of Xanthopygina (Insecta, Coleoptera) reveals major lineages and the origin of myrmecophily. Zoologica Scripta 48(4): 494–506. https://doi.org/10.1111/zsc.12358

Chatzimanolis S, Brunke AJ (2021) A new apterous rove beetle genus (Coleoptera: Staphylinidae) from the Northern Andes with an assessment of its phylogenetic position. European Journal of Taxonomy 744: 67–82. https://doi.org/10.5852/ejt.2021.744.1303

Chatzimanolis S, Caron E (2016) New species and synonymies in *Xenopygus* Bernhauer (Staphylinidae: Staphylinini). Zootaxa 4200(1): 131–142. https://doi.org/10.11646/zootaxa.4200.1.5

Chatzimanolis S, Hightower HJ (2019) *Peripus*, a new genus of Xanthopygina (Coleoptera: Staphylinidae) from South America. Zootaxa 4648(2): 371–383. https://doi.org/10.11646/zootaxa.4648.2.10

Erichson WF (1839) Genera et species Staphylinorum insectorum coleopterorum familiae. Berlin: FH. Morin, 1–400. https://doi.org/10.5962/bhl.title.59644

Erichson WF (1840) Genera et species Staphylinorum insectorum coleopterorum familiae. Berlin: FH. Morin, 401–954. https://doi.org/10.5962/bhl.title.59644

Gemminger M, von Harold E (1868) Catalogus Coleopterorum hucusque descriptorum synonymicus et systematicus. Vol. III. Monachii: Sumptu Gummi EH. https://doi.org/10.5962/bhl.title.9089

Hayashi Y (1997) Studies on the Asian Staphylininae (Coleoptera, Staphylinidae). III. The characteristics of the Xanthopygini. Elytra 25: 475–492.

Herman LH (2001) Catalog of the Staphylinidae (Insecta: Coleoptera). 1758 to the end of the second millennium. Parts I-VII. Bulletin of the American Museum of Natural History 265: 1–4218. https://doi.org/10.1206/0003-0090.265.1.1

International Commission on Zoological Nomenclature (1999) International Code of Zoological Nomenclature, 4th edn., adopted by the International Union of Biological Sciences. London: International Trust for Zoological Nomenclature.

Kraatz G (1857) Naturgeschichte der Insecten Deutschlands. Abt. 1. Coleoptera. Zweiter Band. Berlin: Nicolai, Lief. 3–4 pp. 377–768, Lief. 5–6 pp. 769–1080.

Lucas R (1920) Catalogus alphabeticus generum et subgenerum Coleopterorum orbis terrarum totius (famil., trib., subtr., sect. incl.). Archiv für Naturgeschichte (A)84(1918): 1–696.

Li L, Zhou H-Z (2011) Revision and phylogenetic assessment of the rove beetle genus *Eccoptolonthus* Hayashi, with broad reference to the subtribe Philonthina (Coleoptera: Staphylinidae: Staphylinini). Zoological Journal of the Linnean Society 163: 679–722. https://doi.org/10.1111/j.1096-3642.2011.00731.x

Maddison WP, Maddison DR (2019) Mesquite: a modular system for evolutionary analysis. Version 3.61 http://www.mesquiteproject.org

Marlowe MH, Murphy CA, Chatzimanolis S (2015) Sexual dimorphism and allometry in the sphecophilous rove beetle *Triacrus dilatus*. PeerJ 3: e1123. https://doi.org/10.7717/peerj.1123

Moore I, Legner EF (1975) A catalogue of the Staphylinidae of America North of Mexico (Coleoptera). University of California Division of Agricultural Sciences Special Publication 3015: 1–514.

Navarrete-Heredia JL (2004) Sinopsis del género *Xanthopygus* Kraatz, 1857 (Coleoptera: Staphylinidae) de México. Acta zoológica mexicana 20(3): 1–13.

Navarrete-Heredia JL, Newton AF, Thayer MK, Ashe, JS, Chandler DS (2002) Guía ilustrada para los géneros de Staphylinidae (Coleoptera) de México. Mexico: Universidad de Guadalajara and CONABIO.

Newton AF, Thayer MK, Ashe JS, Chandler DS (2000[2001]) Staphylinidae Latreille, 1802. In: Arnett Jr. RH, Thomas MC (Eds) American Beetles. Archostemata, Myxophaga, Adephaga, Polyphaga: Staphyliniformia, vol. 1. CRC Press, Boca Raton, 272–418.

Newton AF (2021) StaphBase: Staphyliniformia world catalog database (version Nov 2018). In: Catalogue of Life, et al. 2021. Species 2000 and ITIS Catalogue of Life, 2021-04-05. Digital resource at www.catalogueoflife.org. Species 2000: Naturalis, Leiden, the Netherlands. ISSN 2405–8858.

O'Reilly JE, Puttick MN, Parry L, Tanner AR., Tarver JE., Fleming J, Pisani D, Donoghue PCJ (2016) Bayesian methods outperform parsimony but at the expense of precision in the esti-

mation of phylogeny from discrete morphological data. Biology Letters 12(4): e20160081. http://doi.org/10.1098/rsbl.2016.0081

Quezada JR, Amaya CA, Herman LH (1969) *Xanthopygus cognatus* Sharp (Coleoptera: Staphylinidae), an enemy of the coconut weevil, *Rhynchophorus palmarum* L. (Coleoptera: Curculionidae) in El Salvador. Journal of the New York Entomological Society 20: 264–269.

Rodríguez DT, García GDA, Navarrete-Heredia JL (2012) Sinopsis de los géneros de Xanthopygina (Coleoptera: Staphylinidae: Staphylinini) en Colombia. Dugesiana 18(2): 217–241.

Ronquist F, Teslenko M, van der Mark P, Ayres D, Darling A, Höhna S, Larget B, Liu L., Suchard M, Huelsenbeck J (2012) MrBayes 3.2: efficient Bayesian phylogenetic inference and model choice across a large model space. Systematic Biology 61(3): 539–542. https://doi.org/10.1093/sysbio/sys029

Scheerpeltz O (1969) Die zentral- und südamerikanischen Arten der Gattung *Xanthopygus* Kraatz. (Col. Staphylinidae, Subfam. Staphylininae, Tribus Xanthopygini). Koleopterologische Rundschau 46/47: 109–118.

Sharp D (1876) Contribution to an insect fauna of the Amazon Valley (Col. Staph.). Transactions of the Entomological Society of London 1876: 27–424. https://doi.org/10.5962/bhl.title.5536

Sharp D (1884) Staphylinidae. In Godman FD, Salvin O (Eds). Biologia Centrali-Americana, insecta, coleoptera, Vol. 1(2). London: Taylor and Francis, 145–392.

Smetana A, Davies A (2000) Reclassification of the north temperate taxa associated with Staphylinus sensu lato, including comments on relevant subtribes of Staphylinini (Coleoptera: Staphylinidae). American Museum Novitates 3287: 1–88. https://doi.org/10.1206/0003-0082(2000)287<0001:ROTNTT>2.0.CO;2

Wright AM, Hillis DM (2014) Bayesian analysis using a simple likelihood model outperforms parsimony for estimation of phylogeny from discrete morphological data. PLoS ONE 9(10): e109210. https://doi.org/10.1371/journal.pone.0109210

Supplementary material 1

DarwinCore
Authors: Stylianos Chatzimanolis
Data type: Occurences.
Explanation note: DarwinCore format with all types and additional materials examined for the phylogenetic analysis.
Copyright notice: This dataset is made available under the Open Database License (http://opendatacommons.org/licenses/odbl/1.0/). The Open Database License (ODbL) is a license agreement intended to allow users to freely share, modify, and use this Dataset while maintaining this same freedom for others, provided that the original source and author(s) are credited.
Link: https://doi.org/10.3897/zookeys.1071.75947.suppl1

Supplementary material 2

Matrix
Authors: Stylianos Chatzimanolis
Data type: Data matrix.
Explanation note: The data matrix in .nex format.
Copyright notice: This dataset is made available under the Open Database License (http://opendatacommons.org/licenses/odbl/1.0/). The Open Database License (ODbL) is a license agreement intended to allow users to freely share, modify, and use this Dataset while maintaining this same freedom for others, provided that the original source and author(s) are credited.
Link: https://doi.org/10.3897/zookeys.1071.75947.suppl2

Supplementary material 3

Trace over trees
Authors: Stylianos Chatzimanolis
Data type: Analysis.
Explanation note: The analysis of "trace all characters" in Mesquite presented in .nex format.
Copyright notice: This dataset is made available under the Open Database License (http://opendatacommons.org/licenses/odbl/1.0/). The Open Database License (ODbL) is a license agreement intended to allow users to freely share, modify, and use this Dataset while maintaining this same freedom for others, provided that the original source and author(s) are credited.
Link: https://doi.org/10.3897/zookeys.1071.75947.suppl3

RESEARCH ARTICLE

ZooKeys
Launched to accelerate biodiversity research

A peer-reviewed open-access journal

Morphological and molecular identification of arrhenotokous strain of *Diglyphus wani* (Hymenoptera, Eulophidae) found in China as a control agent against agromyzid leafminers

Su-Jie Du[1], Zoya Yefremova[2], Fu-Yu Ye[1],
Chao-Dong Zhu[3], Jian-Yang Guo[1], Wan-Xue Liu[1]

1 *State Key Laboratory for Biology of Plant Diseases and Insect Pests, Institute of Plant Protection, Chinese Academy of Agricultural Sciences, Beijing, 100193, China* **2** *Steinhardt Museum of Natural History, Department of Zoology, Tel Aviv University, Ramat Aviv, 69978, Israel* **3** *State Key Laboratory of Zoological Systematics and Evolution, Institute of Zoology, Chinese Academy of Sciences, Beijing, 100101, China*

Corresponding author: Wan-Xue Liu (liuwanxue@caas.cn)

Abstract

Diglyphus species are ecologically and economically important on agromyzid leafminers. In 2018, a thelytokous species, *Diglyphus wani* Liu, Zhu & Yefremova, was firstly reported and described. Subsequently, the arrhenotokous *D. wani* were discovered in Yunnan and Guizhou Provinces of China. We compared the morphological characteristics of thelytokous and arrhenotokous strains. However, the females of two strains had a strongly similar morphology and showed subtle differences in fore- and hind-wings. The difference was that forewing of arrhenotokous female was with denser setae overall, showing that costal cell with 2 ~ 4 rows of setae on dorsal surface and the setae of basal cell with 15 ~ 21 hairs and forewing of thelytokous female was with two rows of setae on dorsal surface and basal cell with 10 ~ 15 hairs generally. The setation beneath the marginal vein of the hind-wing of arrhenotokous female is denser than the same area of thelytokous female. To explore the genetic divergence between thelytokous and arrhenotokous strains of *D. wani*, the mitochondrial and nuclear gene were applied and sequenced. The polygenic analyses revealed that two strains can be distinguished by COI, ITS1 and ITS2. The mean sequence divergence between the two strains was 0.052, 0.010 and 0.007, respectively. Nevertheless, the 28S gene was unfeasible due

to its containing a sharing haplotype between different strains. The two strains of *D. wani* are dominant parasitoids against agromyzid leafminers and such effective discernible foundation provides future in-depth studies on biological characteristics, along with insight into field application of two strains of *D. wani.*

Introduction

Agromyzidae belongs to Diptera and is a family consisting of about 2750 species (Tschirnhaus et al. 2000) and approximately 110 species of them are known to be the main pests of cultivated crops world-wide (Dempewolf 2020). In China, over 130 Agromyzidae species have been reported. Of these, at least six species, including indigenous *Chromatomyia horticola*, *Liriomyza chinensis* and invasive *L. sativae*, *L. huidobrensis*, *L. trifolii* and *L. bryoniae,* are major agricultural leaf-mining pests, especially on vegetables (Kang et al. 2009; Liu et al. 2013). For decades, the main prevention for agromyzid leafminers has been chemical control with pesticides (Kang et al. 2009). With the frequent use and abuse of chemical pesticides, agromyzid leafminers have gradually developed resistance to insecticides (Parrella and Keil 1984; Tokumaru and Yamashita 2004) and natural enemies have decreased (Trumble and Toscano 1983; Hernández et al. 2011). Therefore, it requires sustainable, effective and biocontrol strategies to regulate the damage of agromyzid leafminers. Notably, applying Hymenoptera parasitoids are considered to be primary strategies, because these species are the most effective natural enemies against agromyzid leafminers (Parrella 1987; Liu et al. 2009; Mujica and Kroschel 2011; Ridland et al. 2020).

Diglyphus (Hymenoptera: Eulophidae) are economically-important parasitoids against agromyzid leafminers (Zhu et al. 2000; Yefremova et al. 2011; Liu et al. 2013; Hansson and Navone 2017), although there are a few species (e.g. *D. begini*, *D. chabrias*, *D. isaea*) that attack other hosts, such as Lepidoptera, Lyonetiidae and Nepticulidae (Noyes 2019). Hitherto, 40 species placed within genus *Diglyphus* have been reported all over the world (Zhu et al. 2000; Hansson and Navone 2017; Ye et al. 2018) and 17 species are distributed in China (Zhu et al. 2000; Liu et al. 2013; Ye et al. 2018). Several *Diglyphus* species (e.g. *D. isaea* and *D. begini*) exhibited strong biological control capability and were released to regulate the population of agromyzid leafminers (Boot et al. 1992; Heinz et al. 1993).

In Hymenoptera parasitoids, some species have two reproduction modes: (1) arrhenotoky, where haploid males arise from unfertilised eggs and diploid females from fertilised eggs and (2) thelytoky, which is obligate parthenogenesis and produces only female progenies or occasional males (Heimpel and de Boer 2008). Amongst *Diglyphus* species, a thelytokous parasitoid named *D. wani* was firstly reported and displayed favourable biocontrol potential showing three types of host-killing behaviour (host-feeding, parasitism and host-stinging) (Ye et al. 2018).

In arthropods with haplodiploid sex determination mechanism, thelytokous strains may exist with their corresponding arrhenotokous strains (van der Kooi et al. 2017). In Eulophidae, several species with two strains (reproduction modes) have been reported, such as *Neochrysocharis formosa* (Adachi-Hagimori et al. 2011; Yang et al. 2017) and *Pnigalio soemius* (Gebiola et al. 2012). For *D. wani*, whether there is also an arrhenotokous strain is not clear. In the field investigations, we firstly discovered arrhenotokous *D. wani* in Yunnan Province of China, which was a dominant parasitoid on agromyzid leafminers and established a stable colony in the laboratory. We preliminarily attempted to make a morphological distinction, but two strains of *D. wani* were likely to be so similar that it would be difficult to discriminate each other accurately. However, accurate identification was essential for potential application of *D. wani*. Thus, in addition to traditional morphological classification, molecular methods were also adopted, because multiple gene markers, such as the cytochrome *c* oxidase subunit I gene (COI) and nuclear internal transcribed spacers (ITS1 and ITS2), have been also applied widely for species identification (Campbell et al. 1993; Chen et al. 2004; Sha et al. 2006; Munro et al. 2011; Om et al. 2017; Ye et al. 2018).

In this paper, the combination of morphological and molecular tools (COI, ITS1, ITS2 and 28S) was applied to characterise and compare differences between arrhenotokous and thelytokous strains of *D. wani*. The results will promote the future biocontrol application of two strains of *D. wani*.

Materials and methods

Sampling

Sampling of the parasitoids on agromyzid leafminers was conducted in the different geographical regions of China as described in Table 1. The collected individuals of *D. wani* were 40 thelytokous individuals (Qinghai: 15♀; Hebei: 16♀; Tibet: 9♀) and 54 arrhenotokous individuals (Yunnan: 20♀+9♂; Guizhou: 19♀+6♂). *D. isaea* (Beijing: 3♀) and *D. crassinervis* (Jilin: 5♀) were also collected for phylogenetic data (Table 1). The collected samples were carefully labelled and kept individually according to the different locations. All specimens from plant leaves infested with parasitised leafminer larvae were maintained in climate chambers set to 25 ± 1°C, relative humidity of 30 w～50% and a photoperiod of 14 h: 10 h (light: dark) until parasitoids emerged.

Morphological Identification

The collected parasitoid samples were transferred to plastic tubes filled with 99.7% ethanol and then stored at -20°C for subsequent classification. These samples were examined with a stereomicroscope (Olympus Corporation, SZX-16, Tokyo, Japan). Terminology and measurement methods referred to Gibson (2003). The abbreviations used are: F1-F2, first to second flagellomeres; SMV, MV, PMV and STV, which are

Table 1. Specimens collected from leaves damaged by *Chromatomyia horticola* in China, 2018.

Species	Sex	Plants	Locality	Coordinates
Arrhenotokous *D. wani*	5♀+ 2♂	*Pisum sativum*	Guiyang, Guizhou	26°37'N, 106°36'E
	9♀+ 4♂	*Pisum sativum*	Guiyang, Guizhou	26°34'N, 106°43'E
	5♀	*Brassica napus*	Guiyang, Guizhou	26°34'N, 106°43'E
	8♀+ 3♂	*Brassica napus*	Kunming, Yunnan	24°53'N, 102°47'E
	8♀+ 6♂	*Brassica napus*	Kunming, Yunnan	25°00'N, 102°45'E
	4♀	*Gypsophila paniculata*	Kunming, Yunnan	25°00'N, 102°45'E
Thelytokous *D. wani*	9♀	*Pisum sativum*	Lhasa, Tibet	29°38'N, 91°02'E
	8♀	*Raphanus sativus*	Xining, Qinghai	36°39'N, 101°36'E
	2♀	*Brassica napus*	Xining, Qinghai	36°39'N, 101°36'E
	5♀	*Brassica napus*	Xining, Qinghai	36°43'N, 102°45'E
	6♀	*Orychophragmus violaceus*	Zhangjiakou, Hebei	40°46'N, 114°52'E
	5♀	*Pisum sativum*	Zhangjiakou, Hebei	40°46'N, 114°52'E
	5♀	*Pisum sativum*	Zhangjiakou, Hebei	40°58'N, 115°17'E
D. isaea	3♀	*Pisum sativum*	Beijing	39°56'N, 116°20' E
D. crassinervis	5♀	*Allium fistulosum*	Gongzhuling, Jilin	43°50'N, 124°82'E

submarginal, marginal, post-marginal and stigmal veins; OOL, the minimum distance between an eye margin and the adjacent posterior ocellus; and POL, the minimum distance between the posterior ocelli. Measurements of body, gaster and ovipositor lengths were taken using an optical microscope (Keyence Corporation, VHX-2000, Tokyo, Japan). Relative measurements were used for the other parts. The ratio of gaster to ovipositor was calculated in Microsoft Excel 2016 using Mean ± SD (standard deviation). Photographs of arrhenotokous and thelytokous *D. wani* were taken by an Olympus CX31 microscope and an Olympus BX43 microscope with a Helicon Focus system, respectively. Of *Diglyphus* parasitoids that we surveyed, *D. crassinervis* was close to *D. wani* relatively in terms of morphology. Additionally, *D. isaea* was a common parasitoid on agromyzid leafminers. We selected the two species to discover further phylogenetic relationships between them and *D. wani*.

Molecular diagnosis

Parasitoid DNA extraction

Using the QIAGEN blood or tissue genome kit (Germany) we followed the steps according to the manufacturer's standard protocol of kit to extract DNA of a single parasitoid. The DNA was stored at -20°C for molecular research.

Amplification and sequencing of gene fragments

This study used primers COISF (5'-TAAGATTTTGATTATT(AG)CC(TA)CC-3') (Sha et al. 2006) and COI2613 (5'-ATTGCAAATACTGCACCTAT-3') (Chen et al. 2004) to amplify the parasitoid COI gene fragment. ITS1 primers were 18sf1 (5'-TA-CACACCGCCCGTCGCTACTA-3') and 5p8sB1d (5'-ATGTGCGTTCRAAAT-GTCGATGTTCA-3') (Ji et al. 2003). Primers ITS2F (5'-TGTGAACTGCAG-

GACACATG-3') and ITS2R (5'-AATGCTTAAATTTAGGGGGTA-3') (Campbell et al. 1993) were used to amplify the parasitoid ITS2 gene fragment. Primers D2F (5'-AGTCGTGTTGCTTGATAGTGCAG-3') and D2R (5'-TTGGTCCGT-GTTTCAAGACGGG-3') (Campbell et al. 1993) were used to amplify the D2 region of the 28S gene fragment of parasitoids.

The PCR reaction systems were that, 0.4 µl *Taq* enzyme (2.5 Uµl⁻¹), 0.4 µl dNTP (2.5 mM), 2.5 µl 10× buffer (containing Mg²⁺), 0.4 µl forward primer, 0.4 µl reverse primer, 50 ng DNA template and adding ddH$_2$O to 25 µl finally. The primer annealing temperatures of COI, ITS1, ITS2 and 28S were 48°C, 58°C, 52°C and 58°C, respectively. The rest of the programmes were set uniformly and they were initial denaturation at 95°C for 3 min followed by 35 cycles of denaturation at 95°C for 15 s, annealing for 15 s, extension at 72°C for 60 s and a single cycle of final extension at 72°C for 5 min. The PCR instrument was an ABI thermal cycler (Veriti Applied Biosystems 9902, Singapore). At the same time, a negative control made sure the PCR amplification system was not contaminated.

After the PCR reaction, taking 4 µl of the PCR product, mixing it with 0.3 µl of 10× Loading buffer, then electrophoresing products in 1% agarose solution containing Gold View II (Solarbio, Beijing, China), setting voltage 100 V, current 400 mA and 30 minutes. After the electrophoresis, we observed the results in the gel imaging system and saved the photos. The PCR unpurified products containing the target bands were sent to Tsing Ke Biological Technology, Beijing of China, for Bi-directional sequencing.

When the gene sequence peak map showed double peaks in Bi-direction, the sequences needed to be cloned. After the PCR products were purified, the target fragments were ligated into the pEASY-T3 cloning vector (Transgen Biotech, Beijing, China) and transferred into *E. coli* competent cells Trans-T1 (Transgen Biotech, Beijing, China) according to the manufacturer's instructions. Finally, using the universal M13 vector primer to detect whether the target fragments were successfully connected, each sample tested five positive clones to evaluate the difference between clones. In this study, the sequence divergence of clones of every sample was small about 0 ~ 0.003, usually about 0.001. Thus, we randomly selected a sequence for phylogenetic analysis.

Sequence analysis

All sequences were analysed by BLAST (Basic Local Alignment Search Tool) in the NCBI database to determine whether the amplified sequences belonged to mitochondria and nuclear genes. The sequences were aligned by using the CLUSTAL W tool of MEGA 7.0 (Kumar et al. 2016) and using the default options. Pairwise and mean sequence divergence, variation sites and parsimony informative sites were estimated, based on the Kimura-2 parameter (K2-P) (Kimura 1980). For COI, the sequences were translated into the amino acid sequence, based on the invertebrate mitochondrial genetic code so as to examine no stop codes. Then, version 5 of the DNASP(Librado and Rozas 2009)was used to calculate gene haplotypes.

Phylogenetic analysis

The phylogenic tree was constructed with UPGMA (the unweighted pair group method, based on arithmetic averages) methods, based on the K2-P model and were performed with MEGA 7.0 (Kumar et al. 2016). Bootstrap values were obtained after conducting 1000 replications for sequence divergence and phylogenetic relationships. Bootstrap support > 70% and taxonomically relevant splits, were indicated above branches of the phylogenic tree.

Results

Morphological description

Diglyphus wani Liu, Zhu & Yefremova, 2018

Type material. The type specimens of arrhenotokous *D. wani* were deposited in the Institute of Plant Protection, Chinese Academy of Agricultural Sciences, Beijing, China.

Arrhenotokous male (Figs 1A, B). Body length 1.0–1.9 mm, forewing length 0.9–1.2 mm. Body light green with a metallic tint; tegulae dark brown, antenna and mandibles brownish, labial and maxillar palpae pale yellow, compound eyes dark red. Legs with dark green and metallic coxae, brownish and metallic trochanters, anterior 3/4 to the middle of all femora dark brown and metallic, posterior pale yellow, all tibiae dark brown with metallic shine, except base and apical 1/5–2/5 part white or pale yellow, hind tibia with anterior surface dark to white-yellow and posterior surface dark, tarsi yellow, except last 4th tarsomere (dark brown) and 3rd tarsomere (brownish), wings hyaline.

Antenna (Fig. 1C). Antenna with scape 3.8× as long as broad, pedicel 2.1× as long as broad, 2 anelli, F1 1.9× as long as broad, F2 1.7× as long as broad, clava 3-segmented 3.4× as long as broad. F1 1.2× as long as F2, clava 1.7× as long as scape and 2.6× as long as F2.

Head (Figs 1C, F). Head wider than height. Toruli inserted a little above the level with the lower margin of eyes. Malar sulcus present, straight, mouth width 1.6× of malar space.

Thorax (Figs 1C, E). Pronotum, mesonotum and scutellum metallic green. Mesoscutum as long as scutellum. Scutellum 1.09 × as long as broad. Propodeum 2.8× as broad as long, smooth, without median carina.

Wing (Fig. 1D). Forewings 2.2× as long as broad. SMV tapering to apex, with six setae dorsally. Costal cell with three rows of setae, ~ 10 dorsal setae on anterior margin apically. Speculum is very small with sparse setations. Relative measurements: SMV: MV: PMV: STV = 10.6: 14.7: 4.7: 4.1.

Metasoma (Figs. 1G and 1H). Petiole short. Gaster 1.8–1.9× as long as broad. Genitalia: digitus with two developed and two reduced spines.
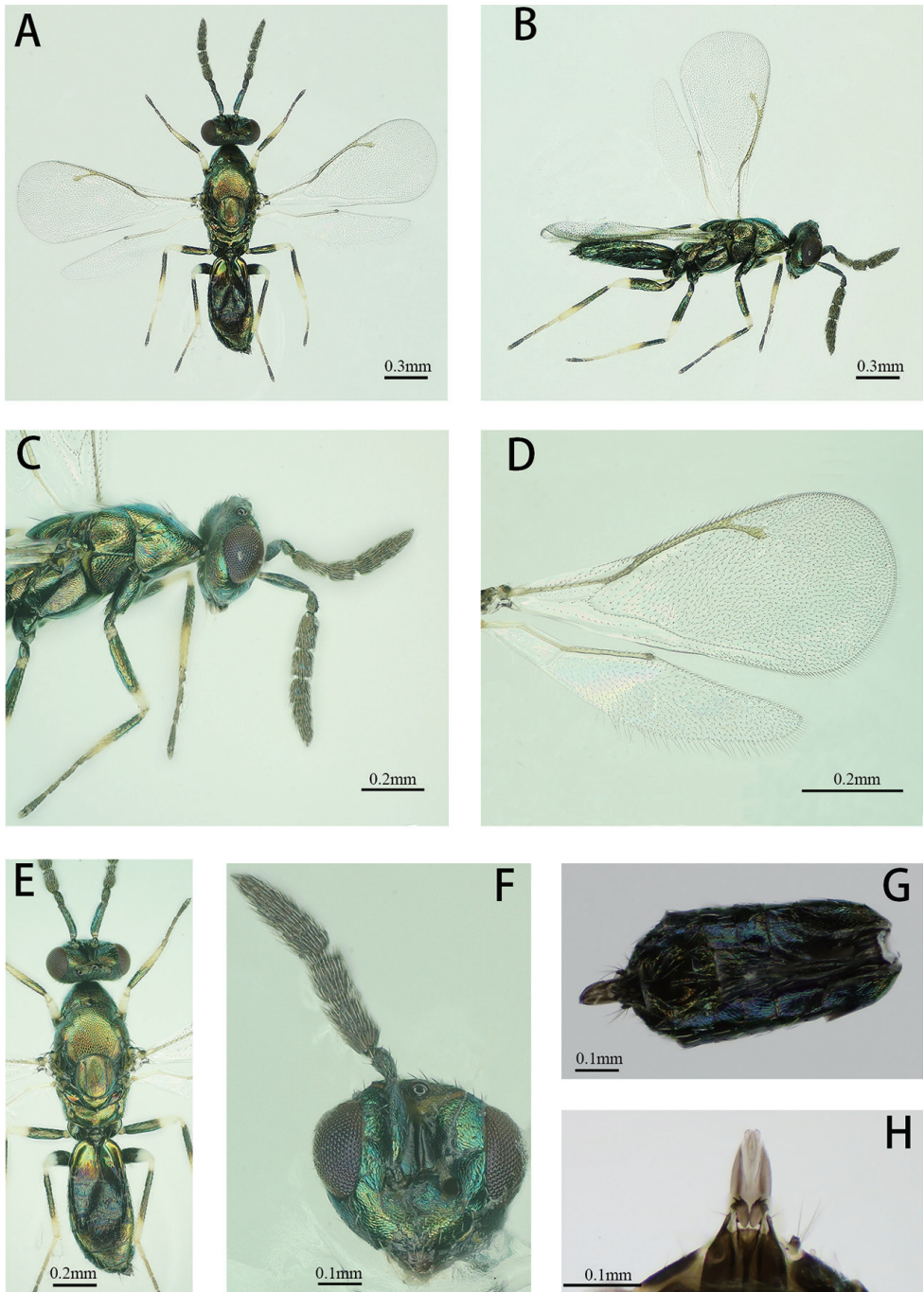
Figure 1. *Diglyphus wani*, arrhenotokous male **A** Body, dorsal view **B** Body, lateral view **C** Head and mesosoma, lateral view **D** Right fore and hind wing **E** Head, tergum and gaster, dorsal view **F** Head, front view **G** Metasoma, ventral view **H** Genitalia, ventral view.
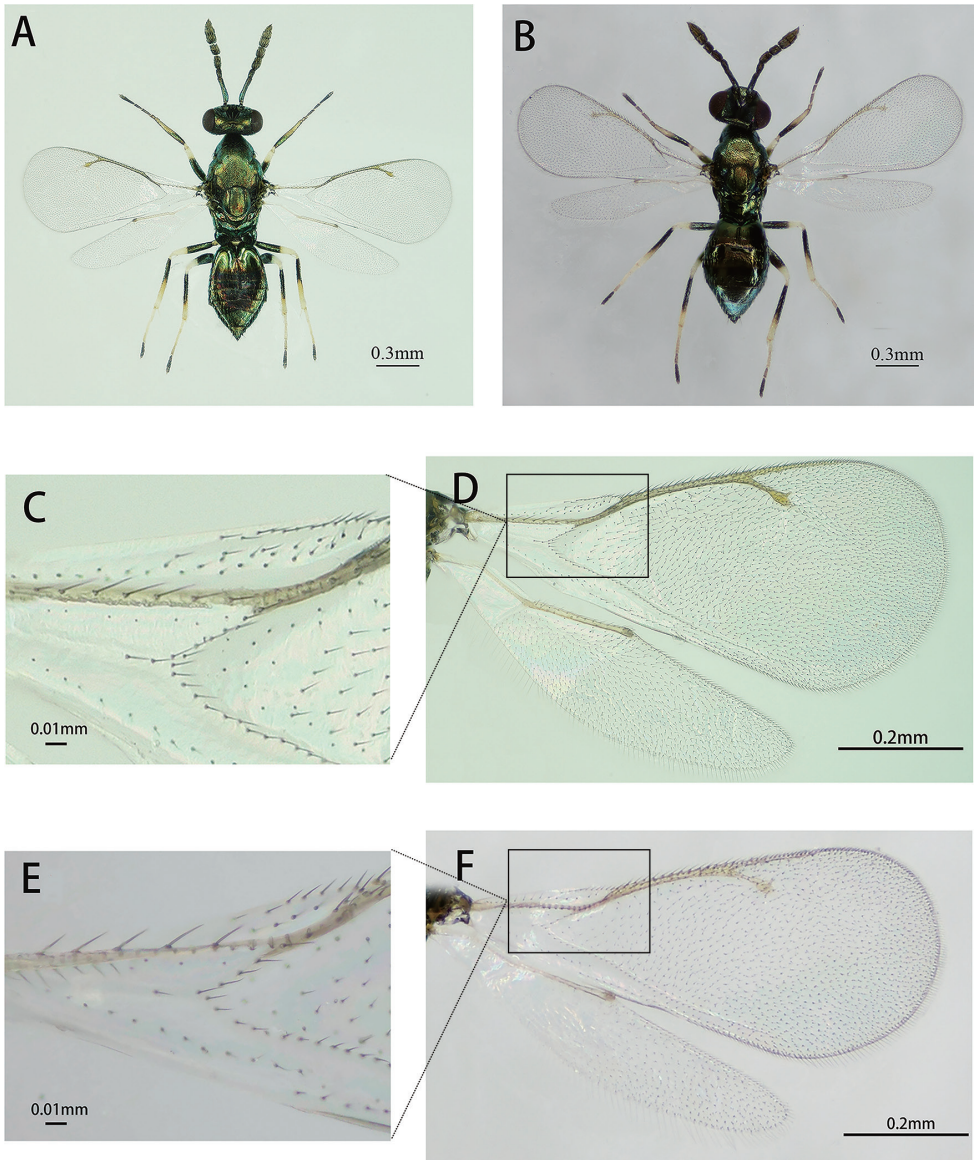
Figure 2. A Arrhenotokous female, body, dorsal view **B** Thelytokous female, body, dorsal view **C** Arrhenotokous female, right forewing **D** Arrhenotokous female, right fore and hind-wings **E** Thelytokous female, right forewing **F** Thelytokous female, right fore and hind-wings.

Arrhenotokous female. (Fig. 2A). The arrhenotokous female was similar to the thelytokous female in morphological characteristics (Table 2). We only found a little difference on fore- and hind-wings between arrhenotokous and thelytokous *D. wani* (Figs. 2A, B). For the arrhenotokous and thelytokous females, the forewing with denser setae overall, the costal cell with 2 ~ 4 rows and 2 rows of setae on dorsal surface,

Table 2. Comparison of morphological of thelytokous and arrhenotokous females.

Portion	Thelytokous female	Arrhenotokous female
Antenna	Scape 3.3× as long as broad	Scape 3.9× as long as broad
	Pedicel 1.8× as long as broad	Pedicel 2.1× as long as broad
	F1 1.5× as long as broad	F1 1.7× as long as broad
	F2 1.3× as long as broad	F2 1.4× as long as broad
	Clava 2.3× as long as broad	Clava 2.2× as long as broad
	F1 1.1× as long as F2	F1 1.1× as long as F2
	Clava 1.2× as long as scape	Clava 1.2× as long as scape
	and 2.2× as long as F2	and 1.9× as long as F2
Forewing	SMV:MV:PMV:STV =26:42:22:20.	SMV:MV:PMV:STV=44:64:24:21.
Head	POL 2.7× as long as OOL.	POL 2.6× as long as OOL.
Metasoma	Gaster 1.5× as long as broad.	Gaster 1.6× as long as broad.
Ratio of gaster to ovipositor	2.7 ± 0.2	2.6 ± 0.3
Body length	1.0–1.9 mm	0.9–1.8 mm

respectively and basal cell with 15 ~ 21 hairs and 10 ~ 15 hairs, respectively (Figs 2C-2F, indicated by squares). The setation beneath the marginal vein of the hind-wing of the arrhenotokous female (Fig. 2D) is denser than the same area of the thelytokous female (Fig. 2F).

Molecular recognition

COI gene

There were 23 variable sites with 21 parsimony informative sites of thelytokous strain and seven variable sites with four parsimony informative sites of arrhenotokous strain in 744 bp. Base insertion, deletion and stop codons were not found in all sequences. The identities of the COI gene sequence of arrhenotokous *D. wani* with seven haplotypes were 95 ~ 96% with *D. wani* (MF590062), 90% with *D. pulchripes* (DQ390435), *D. isaea* (DQ149173) and *D. pachyneurus* (DQ149193) and 87% with *D. bimaculatus* (DQ149161) in GenBank.

A total of 15 haplotypes (COI-1 ~ COI-15) was found, seven (COI-1 ~ COI-7) of the arrhenotokous strain and eight (COI-8 ~ COI-15) of the thelytokous strain. The haplotype sequences of *D. wani* and *D. isaea* and *D. crassinervis* were uploaded to GenBank (accession numbers: MW403074, MW403090). *Diglyphus wani* individuals showed intraspecific genetic variation (Table 3). The mean sequence divergence was 0.052 between two strains and 0.112 ~ 0.134 between related *Diglyphus* species. Phylogenetic analysis showed *D. wani* species formed two major branches, which were thelytokous and arrhenotokous strains, respectively (Fig. 3).

ITS1 gene

The ITS1 gene sequences of arrhenotokous and thelytokous strains were 617 bp and 636 ~ 680 bp, respectively. A total of eight variation sites were detected in the thely-
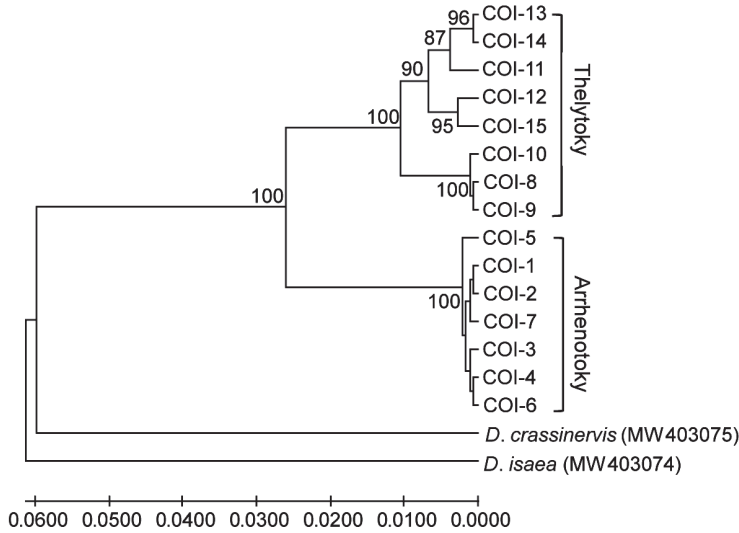
Figure 3. Phylogenetic tree of *Diglyphus wani* and related *Diglyphus* species, based on COI gene of the primers COISF/COI2613 amplification. COI-1 ~ COI-15 were indicated as the COI gene haplotypes of *D. wani*.

Table 3. The mean genetic divergence between two strains of *D. wani* and related *Diglyphus* species.

Number	Species	COI				ITS1				ITS2			
		1	2	3	4	1	2	3	4	1	2	3	4
1	Arrhenotokous *D. wani*												
2	Thelytokous *D. wani*	0.052				0.010				0.007			
3	*D. crassinervis*	0.128	0.112			0.265	0.265			0.082	0.076		
4	*D. isaea*	0.134	0.113	0.123	—	0.241	0.238	0.265	—	0.072	0.064	0.107	—

tokous strain and two parsimony informative sites (excluding gaps) were found. The sequences exhibited characters of internal repeat sequences. Then the ITS1 gene sequences of arrhenotokous *D. wani* were identified after BLAST in GenBank. The identities of the ITS1 gene sequences of arrhenotokous *D. wani* were 93.96% with *D. isaea* (AY948091.1), 87.19% with *D. crassinervis* (AY948110.1), 88.93% with *D. begini* (AY948107.1) and 82.56% with *D. bimaculatus* (AY948109.1).

In comparison with the COI gene, the ITS1 gene showed lower haplotype diversity, showing six haplotypes (ITS1–1 ~ ITS1–6) when gaps were not considered. Of ITS1 gene haplotypes, only one haplotype (ITS1–1) was found in the arrhenotokous strain; however, the thelytokous strain had five haplotypes (ITS1–2 ~ ITS1–6). The haplotype sequence of *D. wani*, *D. isaea* and *D. crassinervis* were uploaded to GenBank (accession number: MW393894, MW393901). The mean sequence divergence was 0.010 between two strains and 0.241 ~ 0.265 between related *Diglyphus* species (Table 3). Similar to the COI analysis, *D. wani* species formed two major branches, which were thelytokous and arrhenotokous strains, respectively, separated from *D. isaea* and *D. crassinervis* (Fig. 4).
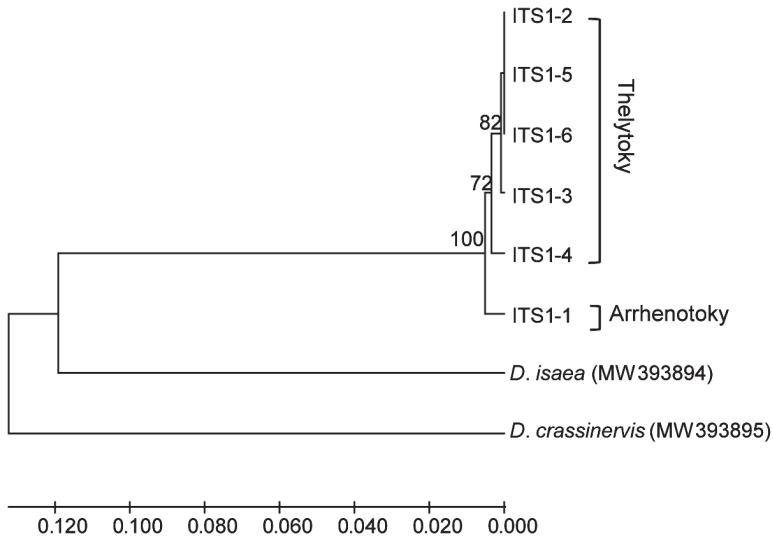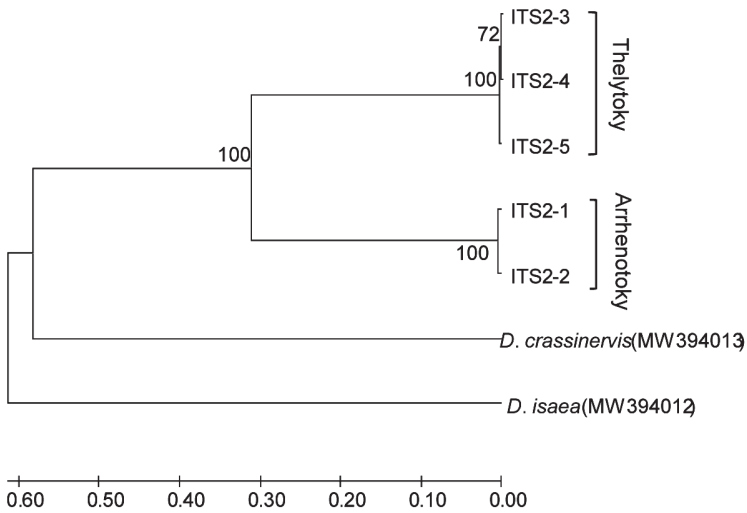
Figure 4 Phylogenetic tree of *Diglyphus wani* and related *Diglyphus* species, based on ITS1 gene of the primers 18sf1/5p8sB1d amplification. ITS1–1 ~ ITS1–6 were indicated as the ITS1 gene haplotypes of *D. wani*.

ITS2 gene

The ITS2 sequence length of arrhenotokous and thelytokous strains was 389 bp and 388 bp, respectively. Sequence analysis showed three variation sites and no parsimony informative sites when analysing sequences of two strains integrally. The identities of the ITS2 sequences of arrhenotokous species were 87% with *D. begini* (MH818358.1) and 77% with *D. isaea* (MH818359.1) in GenBank.

A total of five haplotypes (ITS2–1 ~ ITS2–5) was found when gaps were not considered. Amongst them, there were two haplotypes (ITS2–1 ~ ITS2–2) of the arrhenotokous strain and three haplotypes (ITS2–3 ~ ITS2–5) of the thelytokous strain. The haplotype sequence of *D. wani*, *D. isaea* and *D. crassinervis* were uploaded to GenBank (accession numbers: MW394012, MW394018). The mean sequence divergence was 0.007 between two strains and 0.064 ~ 0.107 between interspecies variation (Table 3). The phylogenetic relationship of the ITS2 region is shown in Fig. 5. The two strains of *D. wani* form two branches including arrhenotokous and thelytokous strains, respectively, which grouped with *D. crassinervis*.

28S gene

The length of the 28S sequences from two strains of *D. wani* was 529–530 bp in all individuals and only one site had undergone C and T transition mutually. The identities

of arrhenotokous species were 100% with *D. isaea* (MH169044.1), 99% with *D. begini* (MH814438.1) and *D. minoeus* (DQ390423.1) and 98% with *D. pachyneurus* (DQ390424.1) in GenBank.

Two haplotypes were found within two strains. The haplotypes sequences of *D. wani*, *D. isaea* and *D. crassinervis* were uploaded to GenBank (accession numbers: MW393685, MW393688). Nevertheless, two strains shared a common haplotype. Haplotype 28S-1 was across all arrhenotokous and partial thelytokous individuals and haplotype 28S-2 was included in the other thelytokous individuals. The phylogenetic analysis showed haplotype 28S-1 and *D. crassinervis* formed one branch due to the same sequences, then clustered with 28S-2 and *D. isaea* (Fig. 6).

Figure 5. Phylogenetic tree of *Diglyphus wani* and related *Diglyphus* species, based on ITS2 gene of the primers ITS2F/ITS2R amplification. ITS2–1 ~ ITS2–5 were indicated as the ITS2 gene haplotypes of *D. wani*.
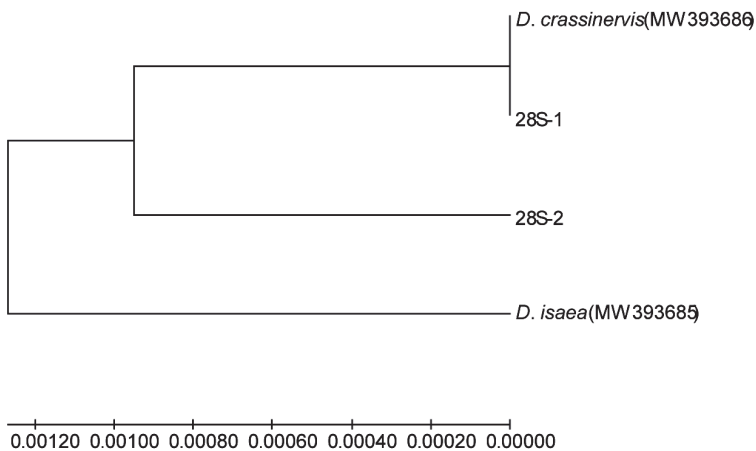

Figure 6. Phylogenetic tree of *Diglyphus wani* and related *Diglyphus* species, based on 28S gene of the primers D2F/D2R amplification. 28S-1 and 28S-2 were indicated as the 28S gene haplotypes of *D. wani*.

Discussion

In many insect orders, both arrhenotokous and thelytokous strains can be commonly found, such as Hemiptera and Psocodea (Bøcher and Nachman 2011; Yang et al. 2015; van der Kooi et al. 2017). In Hymenopteran parasitoids, species with arrhenotoky and thelytoky are not rare (Schneider et al. 2002; Adahi-Hagimori et al. 2011; Gebiola et al. 2012). However, systematic taxonomical studies on different strains of the conspecific parasitoids are relatively few. Our results indicated that *D. wani* confirmed both arrhenotokous and thelytokous reproduction modes existed in this species. Besides, the current study is the first directly targeting the morphological and molecular identification of arrhenotokous and thelytokous strains of *D. wani*.

In general, arrhenotokous and thelytokous strains of Hymenopteran parasitoids are similar in morphology. They may differ in body colour, body length, eyes, wing size and shape, spermathecae and ovaries occasionally (Reineke et al. 2004; Reumer et al. 2013; Petrović et al. 2015; Gebiola et al. 2017). The important distinguishing features we found in the fore- and hind-wings provided an enormous convenience for quickly distinguishing two strains of *D. wani*. These features were mainly on the density of setae in the costal cell and basal cell. At the same time, based on COI gene, ITS1 gene and ITS2 gene, the sequences divergence between *D. wani* and related *Diglyphus* species was far greater than inter-strains divergence. Phylogenetic analysis results showed that the COI gene, ITS1 gene and ITS2 gene can distinguish two strains of *D. wani* according to the cluster of phylogenetic trees. The COI gene was the best maker to distinguish the two strains of *D. wani* due to a greater sequence divergence, followed by the ITS gene and the 28S gene cannot distinguish them, because the sequence conservation of the ITS gene and 28S gene was significantly higher than that of the COI gene. Thus, the COI gene can be used as a more effective marker to judge different strains of *D. wani*, as well as strains of *Tetrastichus coeruleus* (Hymenoptera: Eulophidae) (Reumer et al. 2013).

Although Hebert et al. (2003) analysed that COI-based sequences divergences amongst the 13320 species and argued 2% gene divergence possessing at least 400 bp of COI sequence was employed as a threshold for species diagnosis, it is controversial (Mallet and Willmot 2003), especially for different strains of a species. Besides, the length of the sequence will affect the delimitation of this threshold (Yang et al. 2017). Yang et al. (2017) reported the COI gene divergence of two strains of *N. formosa* were 2.3% and 3.9% when using a primer combination (COI1 and COI2) to amply the 520 bp region and another primer combination (LCO1490 and HCO2198) to amply the 710 bp region, respectively. The COI gene sequence divergence between two strains of *T. coeruleus* was 3.3% ~ 3.7% according to 991 bp of the sequence (Reumer et al. 2013). In this study, the gene divergence between two strains of *D. wani* was more than 2%, based on the 744 bp of COI sequence. Therefore, the threshold of 2% COI gene divergence is not available for species delimitation in some situations (Murata et al. 2009; Reumer et al. 2013; Yang et al. 2017; Fujie et al. 2019). Furthermore, some species obtaining two strains may have become a genetically-distinct complex or cryptic species on account of a high level of genetic divergence. Cryptic

species are at least superficially morphologically indistinguishable, but have distinct genetic structures (Bickford et al. 2007). Based on the COI gene, the sequence divergence between two strains of *N. formosa* from China was 2.3%, amongst which the thelytokous strain had a closer genetic relationship with thelytokous *N. formosa* from Japan (Yang et al. 2017). However, the sequence divergence between thelytokous and arrhenotokous strains of *N. formosa* in Japan is 8.6% (Adachi-Hagimori et al. 2011). Molecular analyses suggested that *N. formosa* could be a complex of at least two cryptic species, the first one including the thelytokous strain from Japan and two strains of *N. formosa* from China, the second one from Japan which was arrhenotoky (Yang et al. 2017, unpublished data).

In general, a crossing experiment was carried out to verify whether there were reproductive barriers between the two strains of a parasitoids (Arakaki et al. 2000; Kraaijeveld et al. 2009; Reumer et al. 2013). Thelytokous *Leptopilina clavipes* (Hymenoptera: Figitidae) was infected with *Wolbachia* and males were produced by antibiotic treatments (Kraaijeveld et al. 2009). The discoveries were that arrhenotokous males and males derived from thelytokous strains can mate with thelytokous and arrhenotokous females (Kraaijeveld et al. 2009). In contrast, in the parasitoid *T. coeruleus* whose thelytoky is the result of infection with *Wolbachia*, although thelytokous females were attractive to arrhenotokous males, thelytokous females were unreceptive to males (Reumer et al. 2014). For thelytokous *D. wani*, we did not detect thelytoky-inducing endosymbionts reported previously; moreover, high temperature or antibiotic treatment for five generations did not reverse the thelytokous reproductive pattern to produce males (unpublished data). We also conducted laboratory crossing between strictly thelytokous females and arrhenotokous males of *D. wani*; however, no male progeny was produced (unpublished data).

Previous studies demonstrated thelytokous *D. wani* had high fecundity and three types of host-killing behaviour (Ye et al. 2018). The arrhenotokous strains of *D. wani* also exhibited strong biocontrol potential and the two strains of *D. wani* most notably attacked agromyzid leafminers, especially against *C. horticola*, *L. sativae* and *L. huidobrensis* in the field. In the follow-up studies, it is particularly important to compare and evaluate the biological characteristics of the two strains and to clarify control efficiency when releasing one strain alone, releasing two strains together or releasing them with other parasitoids jointly.

Acknowledgements

References

Adachi-Hagimori T, Miura K, Abe Y (2011) Gene flow between sexual and asexual strains of parasitic wasps: a possible case of sympatric speciation caused by a parthenogenesis-inducing bacterium. Journal of Evolutionary Biology 24(6): 1254–1262. https://doi.org/10.1111/j.1420-9101.2011.02257.x

Arakaki N, Noda H, Yamagishi K (2000) *Wolbachia*-induced parthenogenesis in the egg parasitoid *Telenomus nawai*. Entomologia Experimentalis et Applicata 96(2): 177–184. https://doi.org/10.1046/j.1570-7458.2000.00693.x

Bickford D, Lohman DJ, Sodhi NS, Ng PK, Meier R, Winker K, Ingram KK, Das I (2007) Cryptic species as a window on diversity and conservation. Trends in Ecology and Evolution 22(3): 148–155. https://doi.org/10.1016/j.tree.2006.11.004

Bøcher J, Nachman G (2011) Coexistence of bisexual and unisexual populations of *Nysius groenlandicus* in the Zackenberg Valley, Northeast Greenland. Entomologia Experimentalis et Applicata 140(3): 196–206. https://doi.org/10.1111/j.1570-7458.2011.01153.x

Boot WJ, Minkenberg OPJM, Rabbinge R, Moed GHd (1992) Biological control of the leafminer *Liriomyza bryoniae* by seasonal inoculative releases of *Diglyphus isaea*: simulation of a parasitoid- host system. Netherlands Journal of Plant Pathology 98(3): 203–212. https://doi.org/10.1007/BF01974383

Campbell BC, Steffen-Campbell JD, Werren JH (1993) Phylogeny of the *Nasonia* species complex (Hymenoptera: Pteromalidae) inferred from an internal transcribed spacer (ITS2) and 28S rDNA sequences. Insect Molecular Biology 2(4): 225–237. https://doi.org/10.1111/j.1365-2583.1994.tb00142.x

Chen Y, Hui XA, Fu JZ, Huang DW (2004) A molecular phylogeny of eurytomid wasps inferred from DNA sequence data of 28S, 18S, 16S, and COI genes. Molecular Phylogenetics and Evolution 31(1): 300–307. https://doi.org/10.1016/S1055-7903(03)00282-3

Dempewolf, M. 2020. Arthropods of economic importance. Agromyzidae of the world (CD-ROM) ETI. University of Amsterdam, Amsterdam http://nlbif.eti.uva.nl/bis/agromyzidae.php [accessed 27 July 2021]

Fujie S, Wachi N, Umemoto H, Maeto K (2019) Mitochondrial DNA diversity and geographical distribution of sexual and asexual strains of the braconid parasitoid *Meteorus pulchricornis*. Entomologia Experimentalis et Applicata 167(12): 977–985. https://doi.org/10.1111/eea.12853

Gebiola M, Gomez-Zurita J, Monti MM, Navone P, Bernardo U (2012) Integration of molecular, ecological, morphological and endosymbiont data for species delimitation within the *Pnigalio soemius* complex (Hymenoptera: Eulophidae). Molecular Ecology 21(5): 1190–1208. https://doi.org/10.1111/j.1365-294X.2011.05428.x

Gebiola M, Monti MM, Johnson RC, Woolley JB, Hunter MS, Giorgini M, Pedata PA (2017) A revision of the *Encarsia pergandiella* species complex (Hymenoptera: Aphelinidae) shows cryptic diversity in parasitoids of whitefly pests. Systematic Entomology 42(1): 31–59. https://doi.org/10.1111/syen.12187

Gibson GAP (2003) Phylogenetics and classification of Cleonyminae (Hymenoptera: Chalcidoidea: Pteromalidae). Phylogenetics and classification of Cleonyminae, 339 pp.

Hansson C, Navone P (2017) Review of the European species of *Diglyphus* Walker (Hymenoptera: Eulophidae) including the description of a new species. Zootaxa 4269 (2): 197–229. https://doi.org/10.11646/zootaxa.4269.2.2

Hebert PDN, Ratnasingham S, deWaard JR (2003) Barcoding animal life: cytochrome *c* oxidase subunit 1 divergences among closely related species. Proceedings of the Royal Society B-Biological Sciences 270 (Suppl 1): S96-S99. https://doi.org/10.1098/rsbl.2003.0025

Heimpel GE, de Boer JG (2008) Sex determination in the Hymenoptera. Annual Review of Entomology 53: 209–230. https://doi.org/10.1146/annurev.ento.53.103106.093441

Heinz KM, Nunney L, Parrella MP (1993) Toward predictable biological control of *Liriomyza trifolii* (Diptera: Agromyzidae) infesting greenhouse cut chrysanthemums. Environmental Entomology 22(6): 1217–1233. https://doi.org/10.1093/ee/22.6.1217

Hernandez R, Harris M, Liu TX (2011) Impact of insecticides on parasitoids of the leafminer, *Liriomyza trifolii*, in pepper in south Texas. Journal of Insect Science (Madison) 11(61): e61. https://doi.org/10.1673/031.011.6101

Ji YJ, Zhang DX, He LJ (2003) Evolutionary conservation and versatility of a new set of primers for amplifying the ribosomal internal transcribed spacer regions in insects and other invertebrates. Molecular Ecology Notes 3(4): 581–585. https://doi.org/10.1046/j.1471-8286.2003.00519.x

Kang L, Chen B, Wei J-N, Liu T-X (2009) Roles of thermal adaptation and chemical ecology in *Liriomyza* distribution and control. Annual Review of Entomology 54(1): 127–145. https://doi.org/10.1146/annurev.ento.54.110807.090507

Kimura, M (1980) A simple method for estimating evolutionary rates of base substitutions through comparative studies of nucleotide sequences. Journal of Molecular Evolution 16(2): 111–120. https://doi.org/10.1007/BF01731581

Kraaijeveld K, Franco P, Reumer BM, van Alphen JJM (2009) Effects of parthenogenesis and geographic isolation on female sexual traits in a parasitoid wasp. Evolution 63(12): 3085–3096. https://doi.org/10.1111/j.1558-5646.2009.00798.x

Kumar S, Stecher G, Tamura K (2016) MEGA7: molecular evolutionary genetics analysis version 7.0 for bigger datasets. Molecular Biology and Evolution 33(7): 1870–1874. https://doi.org/10.1093/molbev/msw054

Librado P, Rozas J (2009) DnaSP v.5: a software for comprehensive analysis of DNA polymorphism data. Bioinformatics 25(11): 1451–1452. https://doi.org/10.1093/bioinformatics/btp187

Liu TX, Kang L, Heinz KM, Trumble J (2009) Biological control of *Liriomyza* leafminers: progress and perspective. CAB Reviews: Perspectives in Agriculture, Veterinary Science, Nutrition and Natural Resources 4(4): 1–16. https://doi.org/10.1079/PAVSNNR20094004

Liu WX, Wang WX, Wang W, Zhang YB, Wan FH (2013) Characteristics and application of *Diglyphus* parasitoids (Hymenoptera: Eulophidae: Eulophinae) in controlling the agromyzid leafminers. Acta Entomologica Sinica 56(4): 427–437. [In Chinese]

Mallet J, Willmott K (2003) Taxonomy: renaissance or Tower of Babel? Trends in Ecology & Evolution 18(2): 57–59. https://doi.org/10.1016/S0169-5347(02)00061-7

Mujica N, Kroschel J (2011) Leafminer fly (Diptera: Agromyzidae) occurrence, distribution, and parasitoid associations in field and vegetable crops along the Peruvian coast. Environmental Entomology 40(2): 217–230. https://doi.org/10.1603/EN10170

Munro JB, Heraty JM, Burks RA, Hawks D, Mottern J, Cruaud A, Rasplus JY, Jansta P (2011) A molecular phylogeny of the Chalcidoidea (Hymenoptera). PLOS ONE 6(11): e27023. https://doi.org/10.1371/journal.pone.0027023

Murata Y, Ideo S, Watada M, Mitsui H, Kimura MT (2009) Genetic and physiological variation among sexual and parthenogenetic populations of *Asobara japonica* (Hymenoptera: Braconidae), a larval parasitoid of drosophilid flies. European Journal of Entomology 106(2): 171–178. https://doi.org/10.14411/eje.2009.020

Noyes JS (2019) Universal Chalcidoidea Database. http://www.nhm.ac.uk/chalcidoids [accessed 27 July 2021]

Om N, Yefremova ZA, Yegorenkova EN, Beattie GAC, Donovan N, Holford P (2017) A new species of *Tamarixia* Mercet (Hymenoptera, Eulophidae), a parasitoid of *Diaphorina communis* Mathur (Hemiptera, Liviidae) in Bhutan. Journal of Asia-Pacific Entomology 20(2):728-738. https://doi.org/10.1016/j.aspen.2017.08.017

Parrella MP (1987) Biology of *Liriomyza*. Annual Review of Entomology 32(1): 201–224. https://doi.org/10.1146/annurev.en.32.010187.001221

Parrella MP, Keil CB (1984) Insect pest management: the lesson of *Liriomyza*. Bulletin of the Entomological Society of America 30(2):22-25. https://doi.org/10.1093/besa/30.2.22

Petrović A, Mitrović M, Ivanović A, Žikić V, Kavallieratos NG, Starý P, Bogdanović AM, Tomanović Ž, Vorburger C (2015) Genetic and morphological variation in sexual and asexual parasitoids of the genus *Lysiphlebus* – an apparent link between wing shape and reproductive mode. BMC Evolutionary Biology 15(1): 5. https://doi.org/10.1186/s12862-015-0293-5

Reineke A, Roberts HLS, Schmidt O (2004) Two coexisting lines of the endoparasitoid *Venturia canescens* show differences in reproductive success under conspecific superparasitism. Journal of Insect Physiology 50(2-3): 167–173. https://doi.org/10.1016/j.jinsphys.2003.11.003

Reumer BM, van Alphen JJM, Kraaijeveld K (2013) Population genetics of *Wolbachia*-infected, parthenogenetic and uninfected, sexual populations of *Tetrastichus coeruleus* (Hymenoptera: Eulophidae). Molecular Ecology 22(17): 4433–4444. https://doi.org/10.1111/mec.12397

Reumer BM, van Alphen JJM, Kraaijeveld K (2014) Reduced sexual functionality of PI-Wolbachia-infected females of *Tetrastichus coeruleus*. Entomologia Experimentalis et Applicata 153(1): 47–54. https://doi.org/10.1111/eea.12227

Ridland PM, Umina PA, Pirtle EI, Hoffmann AA (2020) Potential for biological control of the vegetable leafminer, *Liriomyza sativae* (Diptera: Agromyzidae), in Australia with parasitoid wasps. Austral Entomology 59(1): 16–36. https://doi.org/10.1111/aen.12444

Schneider MV, Beukeboom LW, Driessen G, Lapchin L, Bernstein C, Van Alphen JJM (2002) Geographical distribution and genetic relatedness of sympatrical thelytokous and arrhenotokous populations of the parasitoid *Venturia canescens* (Hymenoptera). Journal of Evolutionary Biology 15(2): 191–200. https://doi.org/10.1046/j.1420-9101.2002.00394.x

Sha ZL, Zhu CD, Murphy RW, La Salle J, Huang DW (2006) Mitochondrial phylogeography of a leafminer parasitoid, *Diglyphus isaea* (Hymenoptera: Eulophidae) in China. Biological Control 38(3): 380–389. https://doi.org/10.1016/j.biocontrol.2006.04.008

Tokumaru S, Yamashita K (2004) Insecticide susceptibility of the garden pea leafminer, *Chromatomyia horticola* (Goureau) (Diptera: Agromyzidae). Annual Report of the Kansai Plant Protection Society 46: 91–94. https://doi.org/10.4165/kapps.46.91

Trumble JT, Toscano NC (1983) Impact of methamidophos and methomyl on populations of *Liriomyza* species (Diptera: Agromyzidae) and associated parasites in celery. Canadian Entomologist 115(10): 1415–1420. https://doi.org/10.4039/Ent1151415-10

Tschirnhaus MV, Irwin M, Hauser M, Evenhuis N, Pape T (2000) Provisional checklist of the Agromyzidae, Therevidae, Mythicomyiidae, Sarcophagidae and Stratiomyidae (Diptera) of the Brandberg Massif, Namibia. Cimbebasia Memoir 9: 383–384.

van der Kooi CJ, Matthey-Doret C, Schwander T (2017) Evolution and comparative ecology of parthenogenesis in haplodiploid arthropods. Evolution Letters 1(6): 304–316. https://doi.org/10.1002/evl3.30

Yang QQ, Kucerova Z, Perlman SJ, Opit GP, Mockford EL, Behar A, Robinson WE, Stejskal V, Li ZH, Shao RF (2015) Morphological and molecular characterization of a sexually reproducing colony of the booklouse *Liposcelis bostrychophila* (Psocodea: Liposcelididae) found in Arizona. Scientific Reports 5(1): e10429. https://doi.org/10.1038/srep10429

Yang YM, Xuan JL, Ye FY, Guo JY, Yang LP, Liu WX (2017) Molecular identification of the thelytokous strain of *Neochrysocharis formosa* (Hymenoptera: Eulophidae) newly found in China and detection of its endosymbiont *Rickettsia*. Acta Entomologica Sinica 60(5): 582–593. [In Chinese]

Ye FY, Zhu CD, Yefremova Z, Liu WX, Guo JY, Wan FH (2018) Life history and biocontrol potential of the first female-producing parthenogenetic species of *Diglyphus* (Hymenoptera: Eulophidae) against agromyzid leafminers. Scientific Reports 8: e3222. https://doi.org/10.1038/s41598-018-20972-3

Yefremova Z, Civelek HS, Boyadzhiyev P, Dursun O, Eskin A (2011) A review of Turkish *Diglyphus* Walker (Hymenoptera: Eulophidae), with description of a new species. Annales de la Societe Entomologique de France 47 (3-4): 273–279. https://doi.org/10.1080/00379271.2011.10697720

Zhu CD, LaSalle J, Huang DW (2000) A review of the Chinese *Diglyphus* Walker (Hymenoptera: Eulophidae). Oriental Insects 34(1): 263–288. https://doi.org/10.1080/00305316.2000.10417266

RESEARCH ARTICLE

Contribution to the knowledge of the genus *Takobia* Novikova & Kluge, 1987 (Ephemeroptera, Baetidae) in Central Asia

Pavel Sroka[1], Zohar Yanai[2], Dmitry Palatov[3], Jean-Luc Gattolliat[4,5]

1 *Biology Centre of the Czech Academy of Sciences, Institute of Entomology, Branišovská 31, 37005 České Budějovice, Czech Republic* **2** *The Steinhardt Museum of Natural History, Tel Aviv University, Tel Aviv 6997801, Israel* **3** *A. N. Severtsov Institute of Ecology and Evolution of RAS, 119071, Moscow, Russia* **4** *Musée cantonal de zoologie, Palais de Rumine, Place de la Riponne 6, 1014 Lausanne, Switzerland* **5** *University of Lausanne (UNIL), Department of Ecology and Evolution, 1015 Lausanne, Switzerland*

Corresponding author: Pavel Sroka (pavel.sroka@centrum.cz)

Citation: Sroka P, Yanai Z, Palatov D, Gattolliat J-L (2021) Contribution to the knowledge of the genus *Takobia* Novikova & Kluge, 1987 (Ephemeroptera, Baetidae) in Central Asia. ZooKeys 1071: 127–154. https://doi.org/10.3897/zookeys.1071.71582

Abstract

Based on the original type material, the nymphal stage of the mayfly *Takobia maxillare* is redescribed; in parallel, a lectotype is designated. *Takobia maxillare* is the type species of the genus *Takobia*, and an accurate and complete knowledge of its morphology is crucial to the delimitation of this problematic genus and clarification of its phylogenetic affinities. Ambiguous characters, previously reported for this species in the literature are clarified. Furthermore, two new species in the same genus are described, namely *Takobia sinusopalpata* **sp. nov.** and *Takobia shughnonica* **sp. nov.** based on the morphology of nymphs from Central Asia, supplemented with *COI* sequences. Implications for the systematics of *Takobia* and related taxa are discussed and the need for an extensive phylogenetic study of this group is stressed.

Keywords

Alainites, mayflies, new species, *Nigrobaetis*, redescription, systematics, taxonomy

Introduction

Baetidae encompass more than 1150 species nested in 115 genera, making it the most speciose family of all mayflies. Its systematics is accordingly complicated, and subject to frequent changes mainly related to generic concepts and species delimitation. Some taxa within Baetidae have particularly complex histories, such as *Nigrobaetis* Novikova & Kluge, 1987, *Alainites* Waltz & McCafferty, 1994, and *Takobia* Novikova & Kluge, 1987, which have all been subject to several synonymies and changes in rank between species groups, subgenera, and genera (Müller-Liebenau 1969; Novikova and Kluge 1987, 1994; Waltz et al. 1994; Waltz & McCafferty 1997; Jacob 2003; Kluge and Novikova 2014).

In this study, we focus on *Takobia maxillare* (Braasch & Soldán, 1983), the type species of the problematic taxon *Takobia*. For any future extensive analysis aimed at assessing the relevance and extent of *Takobia*, detailed knowledge of its type species is of crucial importance. The species was originally described by Braasch and Soldán (1983) under the binomial combination "*Centroptilum maxillare*". The description was based on 69 nymphs collected in Uzbekistan in 1980. Novikova and Kluge (1987) published a redescription of this species using material from Tajikistan and Kazakhstan, without studying the original type material from Braasch and Soldán. A description of the female imago was also provided for the first time by Novikova and Kluge (1987), associated with a nymph by rearing. These authors placed *C. maxillare* as a type species of the newly created subgenus *Takobia* Novikova & Kluge, 1987 within the genus *Baetis* Leach, 1815.

Subsequently, Novikova and Kluge (1994) redefined the delimitation of the genus *Baetis* in a wider sense to encompass three subgenera: *Baetis* s. s., *Labiobaetis* Novikova & Kluge, 1987, and *Nigrobaetis*. They claimed the latter was a senior synonym of *Takobia*, hence introducing a new combination entitled *Baetis* (*Nigrobaetis*) *maxillaris* (Braasch & Soldán, 1983). Some characters of the male imago were also reported for the first time in Novikova and Kluge (1994), based on reared material from Tajikistan. The authors also provided important details on nymphal habitats. The species was included in the key to freshwater invertebrates of Russia (Kluge 1997) as *Baetis* (*Nigrobaetis*) *maxillaris*. It is worth mentioning that the subgeneric delimitations suggested by Novikova and Kluge (1994) are no longer accepted, not even by their original proponents (Kluge and Novikova 2014, 2016).

Waltz et al. (1994) revalidated *Takobia* and raised it, together with *Nigrobaetis*, to the generic level. *Takobia* was still considered monospecific. In the same paper, Waltz et al. (1994) established the new genus *Alainites* for *Baetis muticus* (Linnaeus, 1758) and related species.

Kluge and Novikova (2014) synonymized the widely distributed and diversified genus *Alainites* with *Takobia*, thus considerably increasing the number of species in *Takobia*. Some subsequent authors used *Takobia* sensu Kluge and Novikova (2014) as a subgenus of *Nigrobaetis* (e.g., Martynov and Godunko 2017; Bojková et al. 2018). However, the synonymy of *Alainites* with *Takobia* was not generally followed and accepted, therefore many authors continued to use the genus *Alainites* (e.g., Gattolliat et al. 2015; Fujitani et al. 2017; Cruz et al. 2020). It is important to note that none of the proposals for the systematic treatment of the taxa mentioned above were based on cladistic analyses.

Since *T. maxillare* represents the type species of *Takobia*, an accurate knowledge of its morphology is a key prerequisite for the precise delimitation of the genus and is of significant importance for the generic attribution of all species of *Alainites* (also including species previously described in *Acerbaetis* Kang & Yang, 1994, in Kang et al. 1994, which was synonymized with *Alainites* by Waltz and McCafferty 1997). The original description and illustrations of *T. maxillare* are of reasonably good quality, however several characters important for assessing its relationship to other taxa within the *Alainites/Nigrobaetis/Takobia* complex have only been introduced in subsequent studies. Increasing uncertainty and confusion about *T. maxillare* morphology, inconsistencies on important morphological characters persist between the original description of Braasch and Soldán (1983) and the redescription of Novikova and Kluge (1987).

Therefore, the present study aims to provide an updated redescription of *T. maxillare* and analyze discrepancies between the descriptions of Braasch and Soldán (1983) and Novikova and Kluge (1987), based on the direct observation of the original type material. While searching for the fresh material of *T. maxillare* from Central Asia, we have discovered two new species closely related to *T. maxillare* and describe them herein. We also discuss the character distribution of these two species and compare them with *T. maxillare* and other members of the *Alainites/Nigrobaetis/Takobia* complex.

Materials and methods

Material examined

The original type material of *T. maxillare* was obtained from the collection of the Biology Centre of the Czech Academy of Sciences, Institute of Entomology, České Budějovice, Czech Republic (**IECA**), where it has been stored in ca. 70% ethanol in room temperature. It counts 164 nymphs (including lectotype) still deposited in IECA (159 in EtOH, 3 on slides, and 2 on SEM stubs) and 10 nymphs newly deposited in Museum of Zoology, Lausanne, Switzerland (**MZL**) (8 in alcohol, code GBIFCH 00829873; 2 used for DNA extraction (failed), codes GBIFCH00895419 and GBIFCH00895420). A comparative material of *Alainites* and *Nigrobaetis* species was obtained from IECA and MZL. The material of two new species described in this study was obtained by D. Palatov during several field trips to Central Asia between years 2012 and 2017, always in the period May-July. The nymphs were collected by kick sampling and after sorting subsequently stored in 96% ethanol in -20 °C. This material is deposited in IECA, MZL, and Zoological Museum of Moscow State University, Moscow (**ZMMU**) (for the number of specimens see the descriptions of individual species).

Morphological study

Some specimens were mounted on slides with HydroMatrix (MicroTech Lab, Graz, Austria). Drawings were made using a stereomicroscope Leica M205 C and a microscope Olympus BX41, both equipped with a drawing attachment. Photographs were made

using a Canon EOS 6D camera and the Visionary Digital Passport imaging system and processed with Adobe Photoshop Lightroom (http://www.adobe.com) and Helicon Focus version 5.3 (http://www.heliconsoft.com). Photographs were subsequently enhanced with Adobe Photoshop CS6. For scanning electron microscopy, samples were gradually transferred to acetone, critical point dried, and coated with gold by sputtering using a Baltec SCD050 Sputter Coater. Observations were made on the Jeol JSM 7401F at 4 kV scanning microscope at the Biology Centre CAS, České Budějovice, Czech Republic.

Molecular study

DNA was extracted from two individuals per species of *Takobia maxillare* (failed) and of the two newly described species. In addition, we extracted DNA for the first time from two additional species from central Asia: *Alainites talasi* (Novikova & Kluge, 1994) and *A. kars* (Thomas & Kazancı, in Kazancı and Thomas 1989) (Table 1). Total genomic DNA was extracted using the BioSprint 96 extraction robot (Qiagen Inc., Hilden, Germany), following the supplier's instructions. The non-destructive protocol described in Vuataz et al. (2011), which enables post-extraction morphological study of specimens, was implemented. We then amplified a 658-bp fragment at the 5' end of the mitochondrial cytochrome c oxidase subunit I gene (COI), corresponding to the standard animal barcode region, using the HCO2198 and LCO1490 primers (Folmer et al. 1994). Polymerase Chain Reaction (PCR) was conducted in a volume of 33 µl, consisting of 5 µl of template DNA, 1.65 µl (10 µM) of each primer, 0.26 µl (25 mM) of dNTP solution (Promega), 6.6 µl of 10X buffer (Promega) containing 7.5 mM of $MgCl_2$, 3.3 µl (25 mM) of $MgCl_2$, 1 U of Taq polymerase (Promega), and 14.34 µl of sterile ddH_2O. Optimized PCR conditions included initial denaturation at 95 °C for 5 min, 38 cycles of denaturation at 95 °C for 40 s, annealing at 50 °C for 40 s, and extension at 72 °C for 40 s, with final extension at 72 °C for 7 min. Purification and automated sequencing was carried out in Microsynth (Balgach, Switzerland).

Table 1. Taxa used for genetic distance analysis (mitochondrial COI sequences) with GenBank accession numbers (novel sequences are highlighted in bold font).

Species	GenBank accession numbers
Takobia shughnonica sp. nov. (paratype)	**MZ983793, MZ983794**
Takobia sinusopalpata sp. nov. (paratype)	**MZ983795, MZ983796**
Alainites albinatii	HG934994, HG934995
Alainites kars	**MZ983797, MZ983798**
Alainites muticus	HG934999, JN299112
Alainites talasi	**MZ983799, MZ983800**
Alainites yixianii	GU479735
Nigrobaetis bacillus	MH823363, MH823364
Nigrobaetis digitatus	JN164308, JN164309, LT626141
Nigrobaetis gracilis	JN164320
Nigrobaetis minutus	HM417038
Nigrobaetis niger	JN164310, JN164311, KC158570, KC158571
Nigrobaetis paramakalyani	LC056973
Nigrobaetis vuatazi	HE651544

Related taxa were added to the analysis, based on published sequences in GenBank database (https://www.ncbi.nlm.nih.gov/; see Table 1). Sequences were inspected and edited using Geneious Prime v. 2019.0.4 (Biomatters Ltd.) and pairwise distances calculated with MEGA-X v. 10.0.5 (Kumar et al. 2018) using a K2P model.

Results

Redescription of *Takobia maxillare*

Takobia maxillare (Braasch & Soldán, 1983)
Figs 1A, D; 3, 4

Differential diagnosis. *Takobia maxillare* can be easily separated from other related species by the combination of the following characters: 1) maxillary palp highly developed with the segment I widened apically and segment II straight; 2) labrum dorsally covered with numerous setae, none of them arranged in a row; 3) right prostheca reduced, apically bifid; 4) labial palp segment III quadrangular, asymmetrical, with a short projection lateroapically; 5) claw edentate, subequal to 1/2 of corresponding tarsus; 6) paraproct with a short prolongation bent ventrally.

Description of nymph. Length. Female body 6.8–9.1 mm; cerci 4.6–5.4 mm; median caudal filament 3.4–4.5 mm; male body 5.0–7.2 mm; cerci 4.2–5.8 mm; median caudal filament 2.5–3.5 mm.

Coloration and texture. General coloration brown (Fig. 1A, D). Head uniformly brown with vermiform marks visible on vertex and frons in some specimens. Turbinate eyes in male nymphs purple-brown. Legs ecru. Thorax brown with some areas of darker coloration. Abdominal tergites medium brown without any pattern. Abdominal sternites light brown. Cerci ecru to light brown without bands or pattern. Original coloration probably faded after more than 40 years of storage in alcohol. Surface of body shagreened, most pronounced on head capsule and thorax (Fig. 4C).

Head. Antennae close to each other, with a narrow interantennal carina; scape and pedicel with V-shaped scale insertions and sparse setae. Dorsal surface of labrum (Fig. 3A) evenly covered with numerous long setae and scattered small fine setae, distolateral arc of more prominent setae not distinguishable, almost no setae present along midline; ventral surface with row of ca. ten submarginal small, pointed setae laterally; distal margin fringed with ca. 12–17 short, followed by 8–12 long, feathered setae. Right mandible (Figs 3C, D; 4A) with sparse fine setae; incisors composed of eight pointed denticles (in nymphs long after molting, denticles become worn out and rounded), outer and inner incisor group with four denticles each; row of short fine setae along inner margin of incisors present; prostheca reduced and apically asymmetrically bifid (this bifurcation very inconspicuous, see Fig. 4A), slightly feathered; margin between prostheca and mola with tuft of fringed setae. Left mandible (Fig. 3B, E) with sparse fine setae; incisors composed of seven apically pointed denticles, outer and inner incisor groups not distinctly separated; prostheca

Figure 1. *Takobia* nymphs, habitus photographs **A** *T. maxillare*, habitus in dorsal view **B** *T. sinusopalpata* sp. nov., habitus in dorsal view **C** *T. shughnonica* sp. nov., habitus in dorsal view **D** *T. maxillare*, habitus in lateral view **E** *T. sinusopalpata* sp. nov., habitus in lateral view **F** *T. shughnonica* sp. nov., habitus in lateral view. Scale bar: 1 mm.
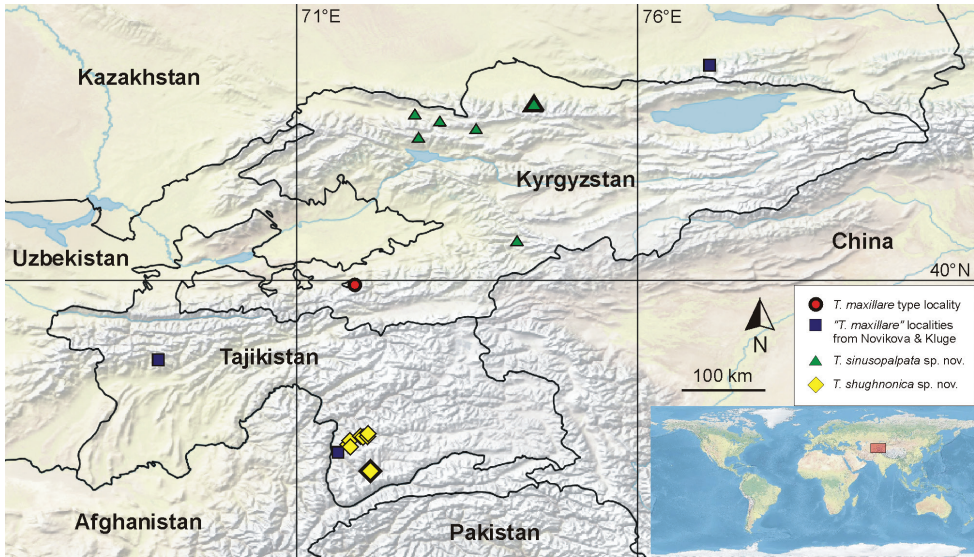
Figure 2. Map with known occurrences of individual *Takobia* species. Explanation of symbols directly in the figure. The larger symbol with thickened border indicates a type locality.

with denticles and comb-shaped structure; margin between prostheca and mola with short, fringed setae. Hypopharynx apically covered with thin setae; lingua with central small protuberance; superlingua slightly longer than lingua. Maxilla (Fig. 3F) with incisors composed of three elongated and curved teeth; crown with two rows of setae, ventral one with small setae, dorsal row with three long stout dentisetae (apical dentiseta similar to maxillary teeth, relatively narrow); maxillary palp very long, nearly 3 × longer than galeolacinia, two-segmented, length of segment I nearly double length of galeolacinia, length of segment II subequal to segment I; segment I widened apically and slightly curved outward; segment II apically rounded; both segments with numerous thin setae, most dense along inner margin. Labium (Fig. 3G) with glossae subequal to paraglossae; both inner and outer margins of glossae with row of pointed setae, dorsal surface of glossae with well-defined group of fine setae subapically; ventral surface of glossae with group of long setae extending from basal part of glossa along its inner margin to apex; paraglossae with two rows of long, stout setae apically; labial palp three-segmented; segment I slightly shorter than segments II and III combined; segment II with very small medioapical protuberance and dorsal oblique row generally of six long setae; segment III asymmetrical, with medioapical part widely rounded and short projection lateroapically; all segments of labial palp with hair-like setae, present only occasionally on segments I and II, most dense on ventral surface of segment III; several distinct stout pointed setae present along apical part of segment III.

Thorax. Forelegs (Fig. 3H). Trochanter with ca. five marginal spine-like setae. Femur dorsally with one row of 16–18 medium, stout setae; additional dorsoapical setal patch formed by another 6–9 stout, medium setae; ventral margin with numerous stout, pointed short setae, some of these setae on lateral margin subparallel to ventral margin,
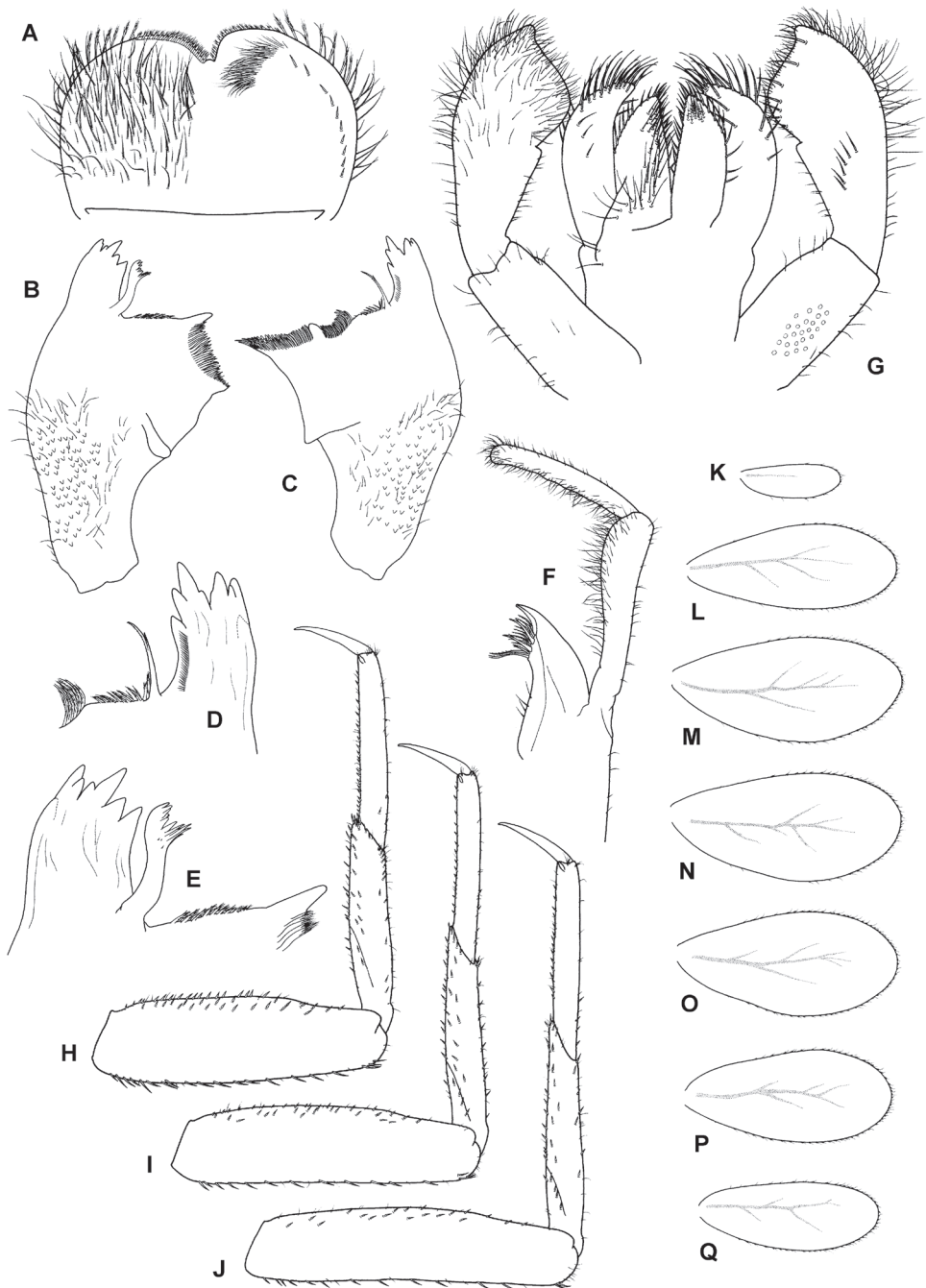
Figure 3. *T. maxillare*, nymph **A** labrum (left side dorsal view, right side ventral view) **B** left mandible (dorsal view) **C** right mandible (dorsal view) **D** right mandible, detail of incisors and prostheca (dorsal view) **E** left mandible (dorsal view), detail of incisors and prostheca (dorsal view) **F** maxilla (dorsal view) **G** labium (left side ventral view, right side dorsal view) **H** foreleg (dorsal view) **I** middle leg (dorsal view) **J** hind leg (dorsal view) **K–Q** gills.
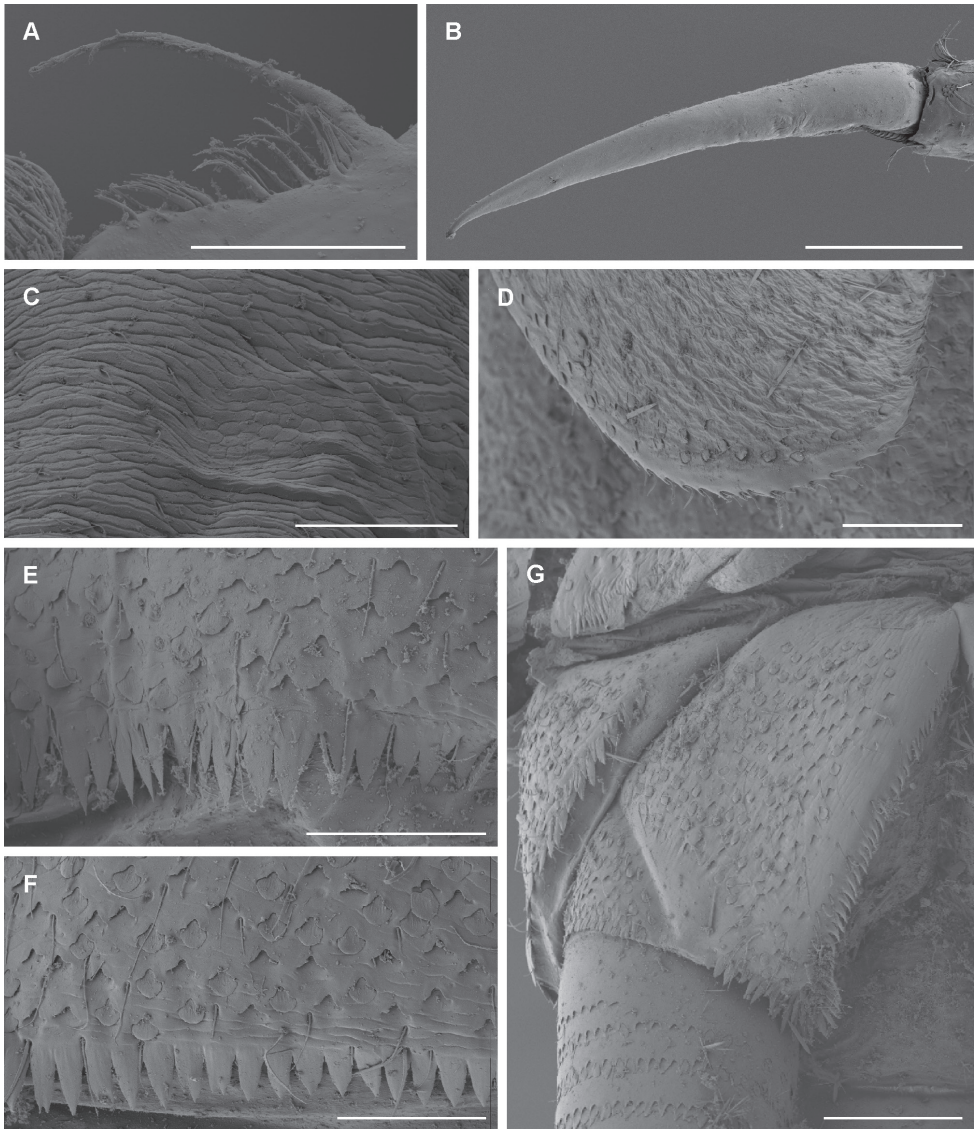
Figure 4. *T. maxillare*, nymph **A** detail of right prostheca **B** tarsal claw **C** pronotum texture **D** margin of gill plate V (dorsal view) **E** posterior margin of abdominal tergite V **F** posterior margin of abdominal sternite V **G** paraproct. Scale bars: 50 μm (**A, C–F**); 100 μm (**B, G**).

villopore absent; lateral margin with occasional short hair-like setae and V-shaped scale bases with scales (not figured in Fig. 3H). Tibia with many setae along ventral margin and group of setae apically; scarce setae also elsewhere on surface of tibia and along dorsal margin; tibiopatellar suture present; lateral margins with scales and numerous scale bases. Tarsus with row of ca. 20 small, pointed setae on ventral margin; lateral margins with numerous scale bases. Tarsal claw (Fig. 4B) very slightly hooked, without any teeth,

apical setae present, minute; length of tarsal claw subequal to 1/2 of tarsus; Mid and hindleg (Fig. 3I, J) similar to foreleg, except setae along ventral margin of femora less robust and more scarce in mid and hindlegs compared to forelegs. Hindwing pads present.

Abdomen. Tergites (Fig. 4E) not shagreened, with numerous V-shaped scale bases, scales (rounded apically), and thin hair-like setae; distal margin of tergite I with few occasional small triangular spines, tergites II–X with well-developed row of triangular spines (length:width ratio of spines in middle part of segment IV ca. 3:1–3:2); row of triangular spines on tergite X not interrupted in middle. Sternites (Fig. 4F) with scales, scale bases and setae similar to tergites; distal margin of sternites III–IX with row of triangular spines, this row interrupted in middle in sternite III and also interrupted in places of emerging gonostyli in male nymphs; triangular spines in lateral parts of sternite generally narrower than in central part of same sternite. Gills (Fig. 3K–Q) on segments I–VII, slightly asymmetrical, widened in distal portion, widely rounded apically; dorsal surface with scales and scale bases submarginally (Fig. 4D); tracheation faintly visible; margins serrated in distal 1/2, with row of fine setae; gill VII similar to gills II to VI. Paraproct (Fig. 4G) with abundant scales and scale bases (of same shape as on tergites and sternites); distinct prolongation bent dorsally; paraproct margin with ca. six or seven triangular spines laterally from prolongation and numerous slightly smaller spines medially from prolongation; prolongation margined with ca. ten elongated medium spines, with spines also on ventral surface; cercotractor with scales and scale bases, margin with triangular spines.

Description of two new species of *Takobia*

Takobia sinusopalpata Sroka & Gattolliat, sp. nov.
http://zoobank.org/a0e1990c-fdaa-4a11-ac04-3c90d03ae1a2
Figs 1B, E; 5, 6

Material examined. *Holotype*. mature male nymph (in EtOH): Kyrgyzstan, Chuy Region. Spring – left tributary of the Adygene Riv., 144 m a.s.l., 42°34.19'N, 74°28.57'E, 29.4.2016, Palatov leg., locality code: 17Kyrg. *Paratypes*. 39 nymphs: same data as holotype (33 in EtOH, 2 on slides with HydroMatrix mounting medium, 2 on SEM stubs, 2 DNA voucher specimens). 1 nymph (in EtOH): Kyrgyzstan, Chuy Region, Korumdy Riv., 300 m upstream its mouth to Suusamyr Riv., 2214 m a.s.l., 42°12.40'N, 73°41.48'E, 1.5.2016, Palatov leg., locality code: 19Kyrg. 3 nymphs (in EtOH): Kyrgyzstan, Talas Region, Oshibulag Riv. – right tributary of Chychkan Riv., 1629 m a.s.l., 42°05.77'N, 72°48.19'E, 2.5.2016, Palatov leg., locality code: 25Kyrg. 1 nymph (in EtOH): Kyrgyzstan, Talas Region, Chon-chychkan Riv., ca. 1.5 km upstream Talas-Bishkek highway bridge, 1924 m a.s.l., 42°25.76'N, 72°44.03'E, 11.5.2016, Palatov leg., locality code: 60Kyrg. 12 nymphs (11 in EtOH, 1 on slide with HydroMatrix mounting medium): Kyrgyzstan, Talas Region. Otmek Riv. 2801 m a.s.l., 42°19.08'N, 73°05.77'E, 12.6.2016, Palatov leg., locality code: 65Kyrg. 6 nymphs (in EtOH): Kyrgyzstan, Osh Region, Kulun

Riv., upstream from confluence of Kulaimende and Dungar Riv., 2229 m a.s.l., 40°30.46'N, 74°14.37'E, 1.5.2017, Palatov leg., locality code: 74 Kyrg.

Holotype and 30 paratypes are deposited in IECA, 5 paratypes including DNA voucher specimens are deposited in MZL, 27 paratypes are deposited in ZMMU. The inventory numbers for the MZL specimens are GBIFCH 00829874 for the specimens in alcohol, GBIFCH00895421 and GBIFCH00895422 for the specimens used for DNA extraction. GenBank accession numbers in Table 1.

Differential diagnosis. *Takobia sinusopalpata* sp. nov. can be separated from other related species by the combination of the following characters: 1) maxillary palp highly developed with the segment I straight and segment II sinusoidal; 2) labrum dorsally covered with numerous setae, one central and two lateral forming the traditional distolateral arc of setae; 3) right prostheca reduced, basally bifid; 4) labial palp segment III quadrangular, slightly asymmetrical; 5) claw with one row of small teeth, subequal to 1/3 of corresponding tarsus; 6) paraproct with a short bent prolongation.

Description of nymph. Length. Female body 6.8–7.4 mm; cerci and median caudal filament partially broken off, cerci assumed ca. 5 mm, medial caudal filament ca. 3.5 mm; male body 6.0–6.7 mm; cerci 4–5.2 mm; median caudal filament 2.6–3.4 mm.

Coloration and texture. General coloration brown (Fig. 1B, E). Head uniformly brown, darker between ocelli. Turbinate eyes in male nymphs brown. Legs ecru. Thorax dorsally brown without markings or pattern, thin pale longitudinal line medially. Abdominal tergites medium brown without any pattern. Abdominal sternites light brown. Gill plates whitish with dark margins. Cerci ecru to pale brown without bands or pattern. Surface of body indistinctly shagreened, most pronounced on head capsule and thorax (Fig. 6C).

Head. Antennae close to each other, with a narrow interantennal carina; scape and pedicel with V-shaped scale insertions and sparse setae. Dorsal surface of labrum (Fig. 5A) covered with long setae and scattered small fine setae, in place of distolateral arc of prominent setae only one or two long setae, one prominent long seta submedially, almost no setae present along midline; ventral surface with short row of submarginal small, pointed setae laterally; distal margin fringed with ca. 17–21 short, followed by 8–12 long, feathered setae. Right mandible (Figs 5C, D; 6A) with sparse fine setae and scales dorsally in basal 1/2; incisors composed of eight apically pointed denticles (in nymphs long after molting, denticles become worn out and rounded), outer and inner incisor group with four denticles each; row of short fine setae along inner margin of incisors present; prostheca reduced and bifid, inserted on elevated projection, conspicuously feathered; margin between prostheca and mola with tuft of fringed setae. Left mandible (Fig. 5B, E) with sparse fine setae dorsally in basal 1/2; incisors composed of seven apically pointed denticles, outer and inner incisor group not distinctly separated; prostheca with denticles and comb-shaped structure; margin between prostheca and mola with short, fringed setae. Hypopharynx apically covered with thin setae; lingua with central small protuberance; superlingua of approximately same length as lingua. Maxilla (Fig. 5F) with incisors composed of three elongated and curved teeth; crown with two rows of setae, ventral one with only small setae, dorsal row with three long
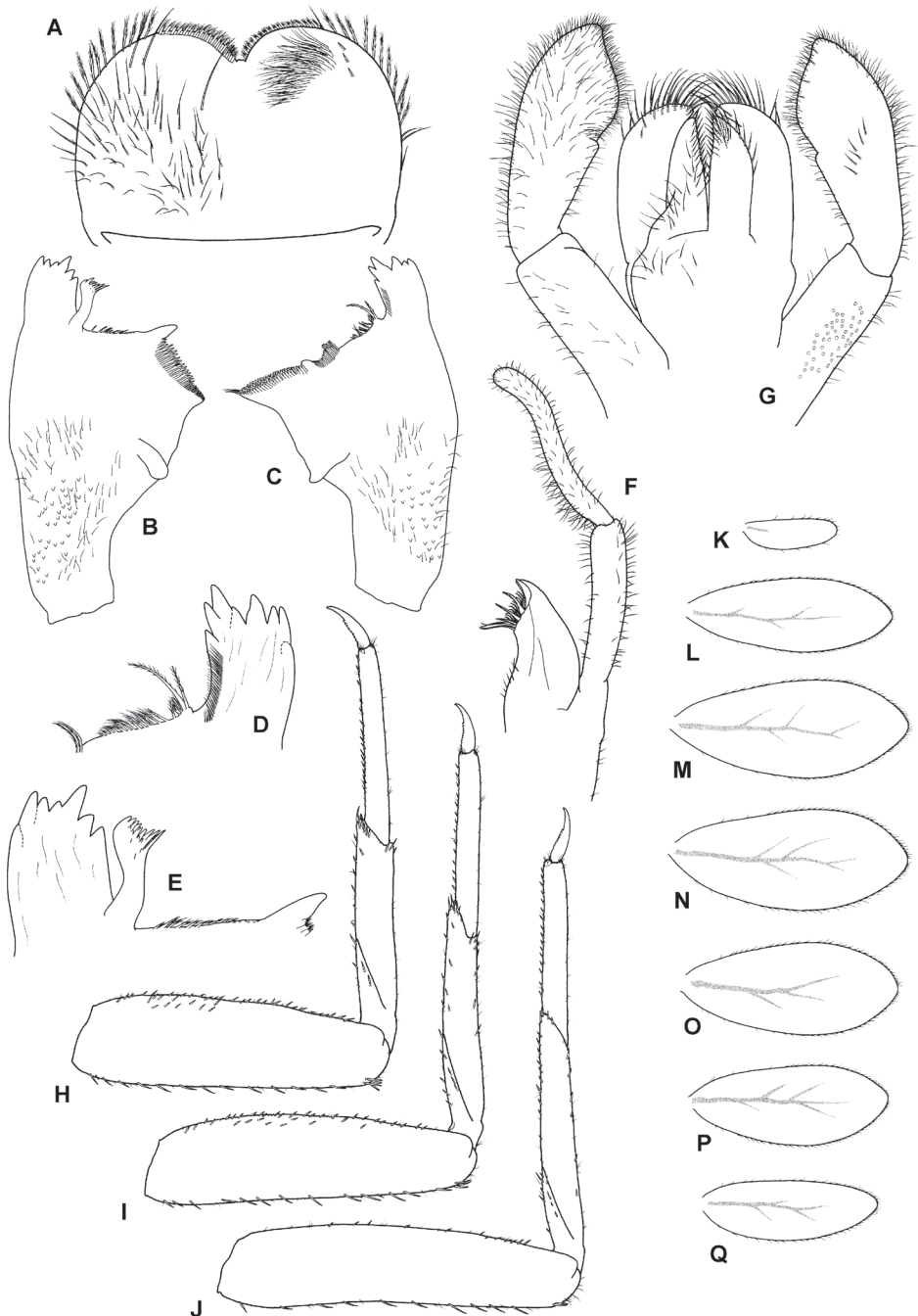
Figure 5. *Takobia sinusopalpata* sp. nov., nymph **A** labrum (left side dorsal view, right side ventral view) **B** left mandible (dorsal view) **C** right mandible (dorsal view) **D** right mandible, detail of incisors and prostheca (dorsal view) **E** left mandible (dorsal view), detail of incisors and prostheca (dorsal view) **F** maxilla (dorsal view) **G** labium (left side ventral view, right side dorsal view) **H** foreleg (dorsal view) **I** middle leg (dorsal view) **J** hind leg (dorsal view) **K–Q** gill plates.
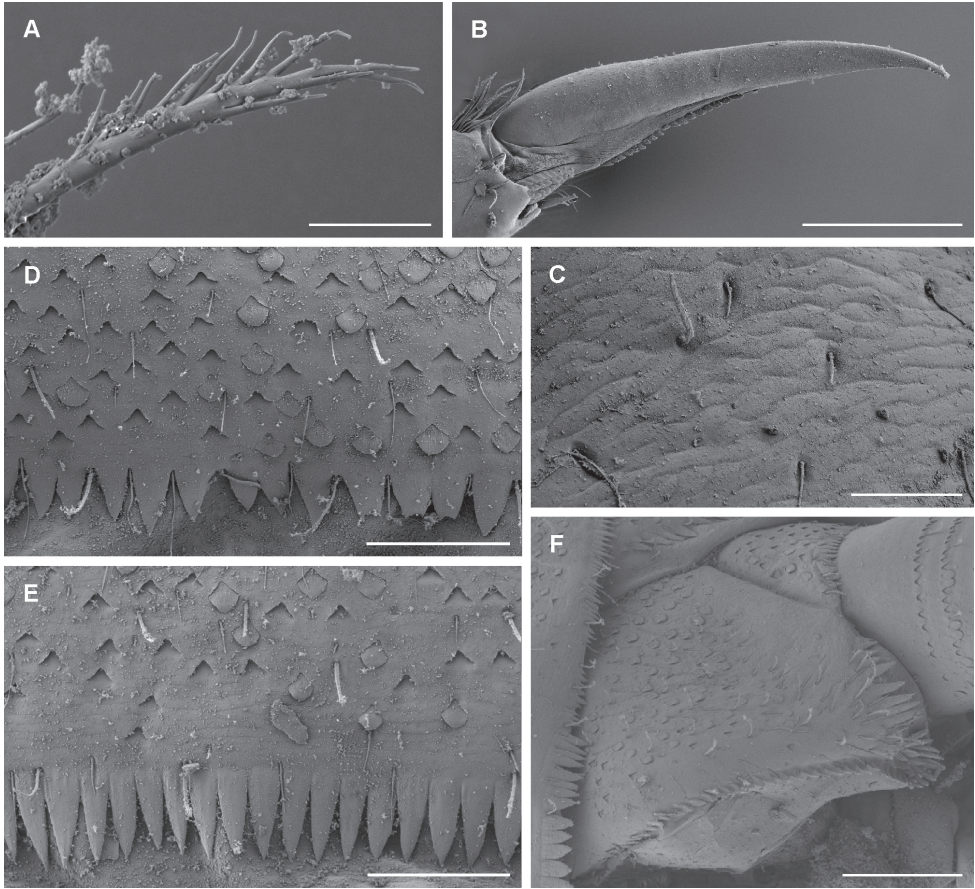
Figure 6. *Takobia sinusopalpata* sp. nov., nymph **A** detail of right prostheca **B** tarsal claw **C** pronotum texture **D** posterior margin of abdominal tergite V **E** posterior margin of abdominal sternite V **F** paraproct. Scale bars: 10 μm (**A**); 100 μm (**B, G**); 20 μm (**C**); 50 μm (**D, E**).

stout dentisetae (apical dentiseta similar to maxillary teeth, relatively broad); maxillary palp very long, ca. 2.7 × longer than galeolacinia, two-segmented, length of segment II approximately equal to segment I; segment I slightly curved inward, not distinctly widened apically; segment II sinusoidal, apically rounded; both segments with numerous thin setae, longest and most dense along inner margin of segment II in its basal 1/2. Labium (Fig. 5G) with glossae subequal to paraglossae; both inner and outer margins of glossae with row of pointed setae, dorsal surface of glossae with well-defined group of fine setae subapically; ventral surface of glossae with group of long setae extending from basal part of glossa along its inner margin to apex; paraglossae with two rows of long, stout setae apically; labial palp three-segmented; segment I slightly shorter than segments II and III combined; segment II with very small medioapical protuberance and dorsal oblique row of ca. 5–7 long setae; segment III elongated, asymmetrical, with medioapical part widely rounded and lateroapical part extended, with short indis-

tinct projection; all segments of labial palp with hair-like setae, present only occasionally on segments I and II, most dense on ventral surface of segment III; several distinct stout pointed setae present along apical part of segment III.

Thorax. Forelegs (Fig. 5H). Trochanter with ca. six marginal spine-like setae. Femur dorsally with one row of ca. 13–16 medium, stout setae; additionally, dorsoapical setal patch formed by another 7–9 stout, medium setae; ventral margin with numerous stout, pointed short setae, some of these setae on lateral margin subparallel to ventral margin, villopore absent; lateral margin with occasional short hair-like setae and V-shaped scale bases with scales (not figured in Fig. 5H). Tibia with many setae along ventral margin and group of setae apically; scarce setae also elsewhere on surface of tibia and along dorsal margin; tibiopatellar suture present; lateral margins with scales and numerous scale bases. Tarsus with row of ca. 15–20 small, pointed setae on ventral margin; lateral margins with numerous scale bases. Tarsal claw (Fig. 6B) slightly hooked, with one row of ca. 10–16 small teeth, slightly increasing in size distally, apical setae present, very minute; length of tarsal claw ca. 1/3 of tarsus length; Mid and hindleg (Fig. 5I, J) similar to foreleg, except setae along ventral margin of femora, less robust and more scarce in mid and particularly hindlegs compared to forelegs. Hindwing pads present.

Abdomen. Tergites (Fig. 6D) not shagreened, with numerous V-shaped scale bases, scales (rounded apically), and thin hair-like setae; distal margin of tergite I without triangular spines, tergites II–X with well-developed row of triangular spines, slightly longer than wide; row of triangular spines on tergite X not interrupted in middle. Sternites with scales, scale bases and setae similar to tergites; distal margin of sternites IV–IX with row of long triangular spines, this row interrupted in middle in sternite IV and also interrupted in places of emerging gonostyli in male nymphs. Gills (Fig. 5K–Q) on segments I–VII, slightly asymmetrical, margins serrated mainly in distal 1/2, dorsal surface with scales and scale bases submarginally, tracheation faintly visible; gill I oval-shaped, rounded apically, ca. 3 × wider than long; gills II–VI widened in distal portion, narrowing and rounded apically, ca. 2.3–2.7 × wider than long; gill VII narrow, widened in middle portion, ca. 3 × wider than long. Paraproct (Fig. 6F) with abundant scales and scale bases (of same shape as on tergites and sternites); distinct prolongation bent dorsally; paraproct margin with ca. 5–10 triangular spines laterally from prolongation and numerous slightly smaller spines medially from prolongation; prolongation margined with ca. 10–20 elongated medium spines, with spines also on ventral surface; cercotractor with scales and scale bases, margin with triangular spines.

Etymology. The name of the new species, *sinusopalpata*, refers to the sinusoidal shape of the second segment of the maxillary palps, very pronounced and characteristic for this species.

Distribution and ecology. So far known from several localities in the Tien Shan Mountains (Kyrgyzstan). Nymphs were collected from stones and boulders sometimes covered with algae and moss in mountain springs, streams, and small rivers located at altitudes of 1600–2800 m a.s.l., at flow rates of 0.5–1.0 m/s, with water temperatures ca. 10–12°C (Fig. 9A, B).

Takobia shughnonica **Sroka & Gattolliat, sp. nov.**
http://zoobank.org/2548add0-5f15-41f9-973f-8428e59e37f0
Figs 1C, F; 7, 8

Material examined. *Holotype*. mature female nymph (in EtOH): Tajikistan, Roshtqal'a District. Spring near Sezhd village, 2966 m a.s.l., 37°12.65'N, 72°04.44'E, 2.7.2016, Palatov leg., locality code: 243Tj. *Paratypes*. 39 nymphs (33 in EtOH, 2 on slides with HydroMatrix mounting medium, 2 on SEM stubs, 2 DNA voucher specimens): same data as holotype. 13 nymphs (in EtOH): Tajikistan, Shughnon District, unnamed river, right tributary of Gunt Riv., ca. 500 m S from Dehmiyona village, 2700 m a.s.l., 37°42.88'N, 71°53.61'E, 23.5.2012, Palatov leg., locality code: 15Tj. 28 nymphs (in EtOH): Tajikistan, Shughnon District. Vuzh-dara Riv., 3 km upstream Dehmiyona village, 2500 m a.s.l., 37°42.47'N, 71°57.29'E, 24.5.2012, Palatov leg., locality code: 31Tj. 2 nymphs (in EtOH): Tajikistan, Shughnon District, unnamed river, tributary of Gunt Riv. near Shitam village, 2500 m a.s.l., 37°44.30'N, 72°2.19'E, 31.5.2012, Palatov leg., locality code: 76Tj. 54 nymphs (in EtOH): Tajikistan, Shughnon District, stream on the slope of Gunt Riv. valley, ca. 3 km downstream from Ver village, 2875 m a.s.l., 37°43.27'N, 72°1.85'E, 5.6.2012, Palatov leg., locality code: 93Tj. 1 nymph (in EtOH): Tajikistan, Shughnon District, unnamed river near Tong village, 2480 m a.s.l., 37°35.78'N, 71°43.79'E, 8.6.2012, Palatov leg., locality code: 113Tj. 1 nymph (in EtOH): Tajikistan, Shughnon District, spring on slope of the Bogev-dara gorge. 2578 m a.s.l., 37°31.13'N, 71°41.98'E, 9.6.2012, Palatov leg., locality code: 120Tj. 17 nymphs (in EtOH): Tajikistan, Shughnon District, right source of the Bogev-dara Riv., 2928 m a.s.l., 37°29.89'N, 71°44.36'E, 10.6.2012, Palatov leg., locality code: 123Tj.

Holotype and 34 paratypes are deposited in IECA, 5 paratypes including DNA voucher specimens are deposited in MZL, 118 paratypes are deposited in ZMMU. The inventory numbers for the MZL specimens are GBIFCH 00829875 for the specimens in alcohol, GBIFCH00895421 and GBIFCH00895422 for the specimens used for DNA extraction. GenBank accession numbers in Table 1.

Differential diagnosis. *Takobia shughnonica* sp. nov. can be separated from other related species by the combination of the following characters: 1) maxillary palp highly developed with the segment I straight and segment II slightly sinusoidal; 2) labrum dorsally covered with numerous setae, one central and two lateral forming the traditional disto-lateral arc of setae; 3) right prostheca reduced, basally bifid; 4) labial palp segment III symmetrical and almost conical; 5) claw with one row of teeth increasing in size toward the apex, subequal to 1/3 of corresponding tarsus; 6) paraproct with a short bent prolongation.

Description of nymph. Length. Female body 6.4–7.4 mm; cerci 4.2–5.1 mm; median caudal filament 3.4–4.2 mm; male body 5.6–6.6 mm; cerci 3.5–3.6 mm; median caudal filament 2.7–3.0 mm.

Coloration and texture. General coloration brown (Fig. 1C, F). Head uniformly brown, darker in areas between compound eyes and between ocelli. Turbinate eyes in
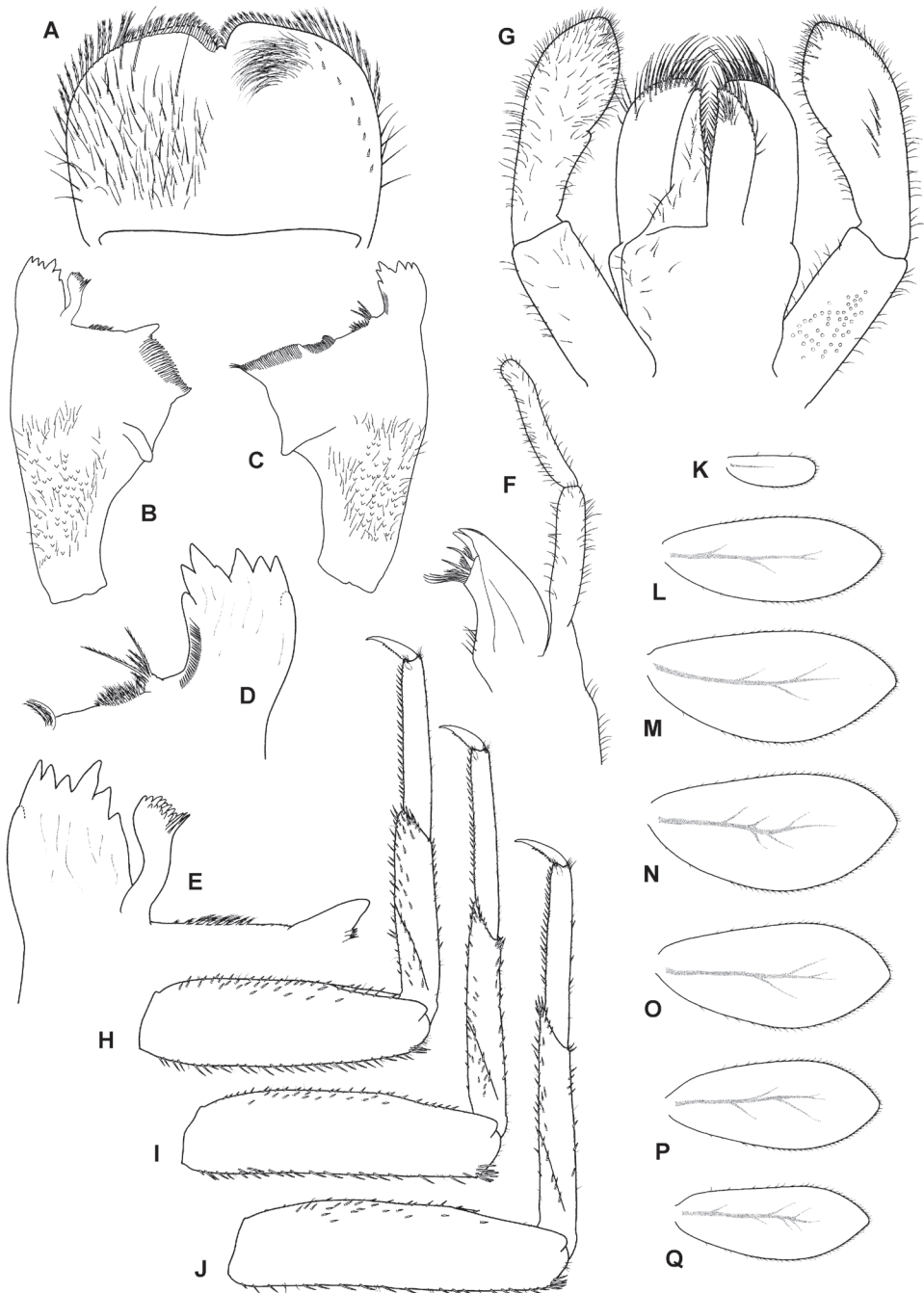
Figure 7. *Takobia shughnonica* sp. nov., nymph **A** labrum (left side dorsal view, right side ventral view) **B** left mandible (dorsal view) **C** right mandible (dorsal view) **D** right mandible, detail of incisors and prostheca (dorsal view) **E** left mandible, detail of incisors and prostheca (dorsal view) **F** maxilla (dorsal view) **G** labium (left side ventral view, right side dorsal view) **H** foreleg (dorsal view) **I** middle leg (dorsal view) **J** hind leg (dorsal view) **K–Q** gill plates.
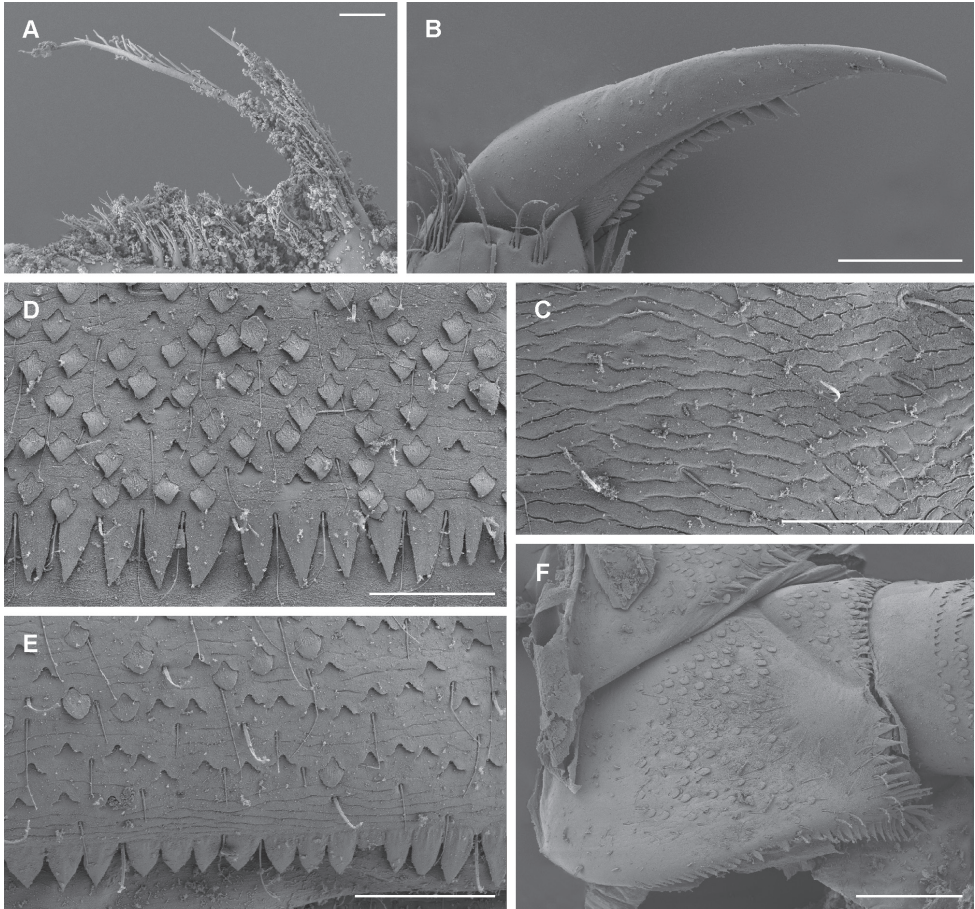
Figure 8. *Takobia shughnonica* sp. nov., nymph **A** detail of right prostheca **B** tarsal claw **C** pronotum texture **D** posterior margin of abdominal tergite VI **E** posterior margin of abdominal sternite VI **F** paraproct. Scale bars: 10 μm (**A**); 100 μm (**B, F**); 50 μm (**C–E**).

male nymphs dark brown. Legs light brown with patches of pale whitish color on lateral margin of femora. Thorax dorsally brown without markings or pattern, thin pale longitudinal line medially. Abdominal tergites I–VIII medium brown, lateral portions slightly paler. Tergites IX and X pale brown. In some specimens, two pale dots observable submedially on tergites VII and VIII. Abdominal sternites II–XIII light brown, sternite IX slightly paler, sternite I whitish. Gill plates whitish with dark margins. Cerci ecru to light brown without bands or pattern. Surface of body shagreened, most pronounced on head capsule and thorax (Fig. 8C).

Head. Antennae close to each other, with a narrow interantennal carina; scape and pedicel with V-shaped scale insertions and sparse setae. Dorsal surface of labrum (Fig. 7A) evenly covered with numerous long setae and scattered small fine setae, in place of distolateral arc of prominent setae only two long setae, one promiment long seta submedially,

almost no setae present along midline; ventral surface with row of submarginal small, pointed setae laterally; distal margin fringed with ca. 20–23 short, followed by 13–15 long, feathered setae. Right mandible (Figs 7C, D; 8A) with sparse fine setae; incisors composed of eight apically pointed denticles (in nymphs long after molting, denticles become worn out and rounded), outer and inner incisor group with four denticles each (outermost denticle of inner incisor group often worn out and indistinct); row of short fine setae along inner margin of incisors present; prostheca inserted on elevated projection, reduced, consisting of two prominent setae, accompanied by several shorter ones, all conspicuously feathered; margin between prostheca and mola with tuft of fringed setae. Left mandible (Fig. 7B, E) with sparse fine setae; incisors composed of seven apically rounded denticles, outer and inner incisor group not distinctly separated; prostheca with denticles and comb-shaped structure; margin between prostheca and mola with short, fringed setae. Hypopharynx apically covered with thin setae; lingua with central small protuberance; superlingua of approximately same length as lingua. Maxilla (Fig. 7F) with incisors composed of three elongated and curved teeth; crown with two rows of setae, ventral one with only small setae, dorsal row with three long stout dentisetae (apical dentiseta similar to maxillary teeth, relatively broad); maxillary palp very long, nearly 2 × longer than galeolacinia, two-segmented, length of segment II approximately equal to segment I; segment I straight, not distinctly widened apically; segment II slightly sinusoidal, apically rounded; both segments with numerous thin setae. Labium (Fig. 7G) with glossae subequal to paraglossae; both inner and outer margins of glossae with row of pointed setae, dorsal surface of glossae with well-defined group of fine setae subapically; ventral surface of glossae with group of long setae extending from basal part of glossa along its inner margin to apex; paraglossae with two rows of long, stout setae apically; labial palp three-segmented; segment I slightly shorter than segments II and III combined; segment II with very small medioapical protuberance and irregular dorsal oblique row of ca. seven or eight long setae; segment III symmetrical, elongated, narrowing towards apex, without any projection; all segments of labial palp with hair-like setae, present only sparsely on segments I and II, most dense on ventral surface of segment III; several distinct stout pointed setae present along inner margin of segment III.

Thorax. Forelegs (Fig. 7H). Trochanter with ca. six marginal spine-like setae. Femur dorsally with one row of 18–23 medium, stout setae; additionally, dorsoapical setal patch formed by another 7–9 stout, medium setae; ventral margin with numerous stout, pointed short setae, some of these setae on lateral margin subparallel to ventral margin, villopore absent; lateral margin with occasional short hair-like setae and V-shaped scale bases with scales (not figured in Fig. 7H). Tibia with many setae along ventral margin and group of setae apically; fewer setae also elsewhere on surface of tibiae and along dorsal margin; tibiopatellar suture present; lateral margins with scales and numerous scale bases. Tarsus with row of ca. 25–30 small, pointed setae on ventral margin; lateral margins with numerous scale bases. Tarsal claw (Fig. 8B) hooked, with single row of 12–15 well developed teeth, increasing in size distally; apical setae present, very minute; length of tarsal claw ca. 1/3 of tarsus length; Mid and hindleg
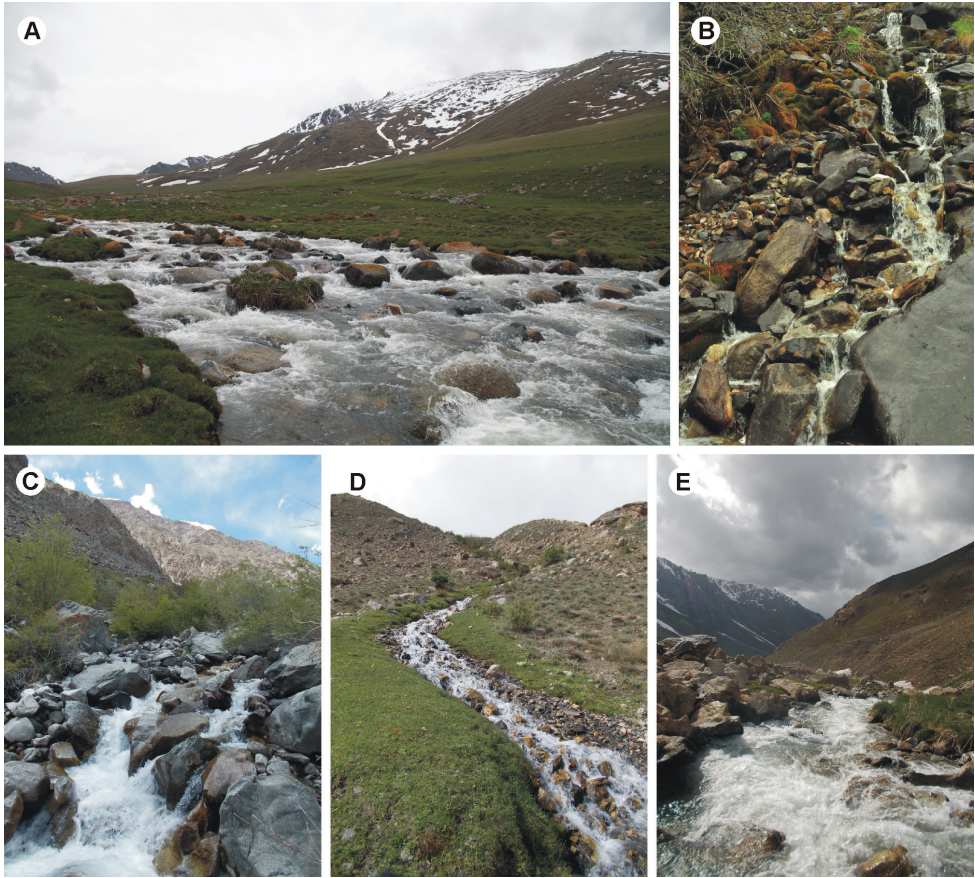
Figure 9. *Takobia* spp., examples of habitats **A** locality of *T. sinusopalpata* sp. nov. (Otmek Riv., locality code: 65Kyrg) **B** type locality of *T. sinusopalpata* sp. nov. (left tributary of the Adygene Riv., code: 17Kyrg) **C** locality of *T. shughnonica* sp. nov. (right tributary of Gunt Riv., code: 15Tj) **D** locality of *T. shughnonica* sp. nov. (stream on the slope of Gunt Riv. valley, code: 93Tj) **E** locality of *T. shughnonica* sp. nov. (right source of the Bogev-dara Riv., code: 123Tj).

(Fig. 7I, J) similar to foreleg, except setae along ventral margin of femora, less robust and more scarce in mid and hindlegs compared to forelegs. Hindwing pads present.

Abdomen. Tergites (Fig. 8D) slightly shagreened, with numerous V-shaped scale bases, scales (rounded apically), and thin hair-like setae; distal margin of tergite I without triangular spines, tergites II–X with well-developed row of triangular spines, slightly longer than wide; row of triangular spines on tergite X not interrupted in middle. Sternites with scales, scale bases and setae similar to tergites; distal margin of sternites IV–IX with row of triangular spines, this row interrupted in middle in sternite IV and also interrupted in places of emerging gonostyli in male nymphs; triangular spines in lateral parts of sternite generally narrower than in central part of same sternite. Gills (Fig. 7K–Q) on segments I–VII, slightly asymmetrical, margins serrated mainly in

distal 1/2, dorsal surface with scales and scale bases submarginally, tracheation faintly visible; gill I oval-shaped, rounded apically, ca. 3 × wider than long; gills II to VII widened in distal portion, pointed apically, ca. 2.1–2.6 × wider than long. Paraproct (Fig. 8F) with abundant scales and scale bases (of same shape as on tergites and sternites); distinct prolongation bent dorsally; paraproct margin with ca. 3–5 triangular spines laterally from prolongation and numerous slightly smaller spines medially from prolongation; prolongation margined with ca. 15 elongated medium spines, with only minor spines on ventral surface; cercotractor with scales and scale bases, margin with triangular spines.

Etymology. The species is named *shughnonica* after the local ethnicity and the historical region of Shughnon, where the species was discovered.

Distribution and ecology. So far known from several localities in the Pamir Mountains (Tajikistan). Nymphs were collected from stones and boulders sometimes covered with algae and moss in mountain springs and streams located at altitudes of 2480–2928 m a.s.l., at flow rates of 0.5–1.0 m/s, with water temperatures ca. 10–12°C (Fig. 9C–E).

Molecular results

The monophyly of the two new *Takobia* species, as well as that of *A. talasi* and *A. kars*, were confirmed (Table 2): each of these species exhibited intra-specific similarities of 0–0.1%. The COI sequences of the two *Takobia* species are 13.5% different, confirming a close sibling relationship, yet far enough to be considered independent species. Between species in other genera, our analysis yielded a minimum distance of 7.5%, and usually much higher (> 20%). Our table contains a few problematic results. On the one hand, a few inter-specific distances lower than expected may be due to misidentification of the GenBank samples, which are not available to us for morphological re-examination. On the other hand, intra-specific distances higher than expected may be explained by taxa representing complexes of cryptic species, as shown by Sroka (2012) for *A. muticus*. These species belong to *Alainites* and *Nigrobaetis*, and are out of the scope of the present study.

Discussion

Remarks on the *T. maxillare* type material

The original type series consisted of nymphal material collected on a single locality ("Uzbekische SSR, Kuk-kul-See, S von Fergana, 20.5.1980, leg. T. SOLDÁN et M. TONNER", as given in Braasch and Soldán 1983). The authors specified the existence of the holotype and 68 paratypes, split between the collections of T. Soldán in Prague (Czechia) and D. Braasch in Potsdam (Germany). The exact number of paratypes deposited in each collection was not specified in the original description, it is supposed

Table 2. Kimura 2 parameter distance among sequences of the mitochondrial COI gene of selected *Takobia*, *Alainites*, and *Nigrobaetis* species (presenting mean and min–max distance for each group with >1 individual; for number of samples per each taxon see Table 1).

	1	2	3	4	5	6	7	8	9	10	11	12	13	14
1 T. shughnonica	0.0													
2 T. sinuspalpata	13.5 (13.5–13.5)	0.0												
3 A. albinatii	22.5 (22.2–22.8)	22.0 (21.9–22.1)	1.5											
4 A. kars	22.8 (22.7–22.9)	23.2 (23.1–23.3)	20.1 (19.9–20.3)	0.1										
5 A. muticus	25.0 (24.2–25.7)	24.8 (24.7–24.9)	17.0 (16.6–17.5)	22.3 (22.1–22.5)	17.4									
6 A. talasi	25.4 (25.4–25.4)	23.1 (23.1–23.1)	27.3 (27.1–27.6)	24.9 (24.8–25.0)	26.0 (24.3–27.8)	0.0								
7 A. yixianii	25.9 (25.9–25.9)	24.7 (24.7–24.7)	20.8 (20.5–21.1)	20.3 (20.2–20.4)	23.7 (23.1–24.3)	24.2 (24.2–24.2)	NA							
8 N. bacillus	26.6 (26.3–26.8)	26.1 (25.9–26.3)	22.3 (21.8–22.8)	22.1 (21.7–22.5)	25.4 (24.1–26.8)	24.9 (24.6–25.3)	0.8 (0.5–1.1)	0.6						
9 N. digitatus	22.5 (21.4–24.4)	22.8 (22.1–24.2)	23.3 (22.6–24.0)	24.2 (23.9–24.6)	25.3 (23.4–27.6)	24.6 (24.3–25.1)	23.5 (21.8–24.5)	24.4 (21.9–26.1)	9.9 (0.6–14.6)					
10 N. gracilis	28.3 (28.3–28.3)	27.7 (27.7–27.7)	23.6 (23.6–23.6)	25.1 (25.0–25.3)	25.1 (24.7–25.4)	24.8 (24.8–24.8)	25.4	26.5 (26.0–27.0)	24.5 (24.2–25.2)	NA				
11 N. minutus	25.1 (25.1–25.1)	25.5 (22.5–22.5)	25.5 (25.0–26.1)	24.5 (24.4–24.6)	27.1 (26.7–27.5)	25.4 (25.4–25.4)	24.3	25.7 (25.4–26.1)	23.9 (23.6–24.6)	21.8	NA			
12 N. niger	26.7 (25.8–27.6)	25.5 (24.8–26.4)	23.1 (22.0–24.2)	22.0 (21.6–22.4)	24.6 (23.4–25.8)	24.9 (24.3–25.7)	22.8 (22.0–23.0)	24.6 (23.2–25.8)	20.2 (19.4–21.3)	23.2 (22.4–24.8)	24.1 (22.9–25.3)	1.0 (0.5–1.9)		
13 N. paramakabyani	25.5 (25.5–25.5)	24.1 (24.1–24.1)	26.5 (25.9–27.1)	25.0 (24.9–25.1)	27.3 (27.2–27.5)	28.0 (28.0–28.0)	26.8	28.0 (27.7–28.4)	24.5 (22.8–25.3)	18.7	20.2	24.7 (24.3–25.5)	NA	
14 N. vuatazi	24.8 (24.8–24.8)	23.6 (23.6–23.6)	24.4 (24.1–24.6)	22.7 (22.6–22.9)	28.0 (27.7–28.4)	24.0 (24.0–24.0)	23.7	25.4 (25.1–25.0)	21.9 (21.4–22.3)	7.5	18.1	23.8 (22.9–24.4)	17.8	NA

that the holotype was most likely in Prague ("Typen in der Coll. SOLDÁN, Prag, Paratypen in der Coll. BRAASCH, Potsdam." in Braasch and Soldán 1983).

The collection of Dietrich Braasch is now housed mostly in the Stuttgart State Museum of Natural History, Germany, and partially in the Natural History Museum Potsdam and Senckenberg German Entomological Institute, Müncheberg, Germany. According to our inquiry to the curators of all these collections, there is no material of *T. maxillare* in any of them. Thus, either the types from D. Braasch should be considered lost or the type material was never split and all the types remained in T. Soldán's collection.

The collection of Tomáš Soldán is now housed in the Biology Centre CAS, Institute of Entomology (IECA). There is material identified as *T. maxillare*, morphologically identical to the original description and labeled with the corresponding locality and the date of collection. However, there is no unambiguous label designating holotype and/or paratypes. Furthermore, the number of nymphs does not correspond to Braasch and Soldán (1983), since the vial contains 174 individuals instead of 69, as specified in the original description. There are no microscopic slides preserved.

Type locality

The exact location of the *T. maxillare* type locality is unclear. The original publication specifies a lake in Uzbekistan, south of the town Fergana. However, the border with Kyrgyzstan is ca. 20 km south of Fergana (Farg'ona), and there is no substantial water body south of Fergana within the main territory of Uzbekistan. Nevertheless, there is a small exclave of Uzbekistan within Kyrgyzstan further south. Two lakes are situated nearby, although not directly within the exclave, but a few hundred meters past the border in Kyrgyzstan. The borders have however shifted compared to where they were in the 1980s when the lakes were administratively located in Uzbekistan. Soldán and Tonner, the collectors of the original material, probably would not have realized that they had crossed the administrative border anyway, being technically still within the USSR in 1980.

The above-mentioned lakes are named Qurbonko'l and Ko'kko'l in Kyrgyzian sources, Курбан-Кёль (Kurban-Kiol') and Кок- Кёль (Kok-Kiol') in Russian, although exact transliteration varies. We are convinced that "Kuk-Kul" in the original publication is a version of Ko'kko'l and the present location in Kyrgyzstan instead of Uzbekistan is caused by the close proximity to the Uzbekistan exclave and the recent changes in the administrative borders in the area. Thus, we define the type locality of *Takobia maxillare* as follows: Kyrgyzstan, Ko'kko'l Lake, near border with Uzbekistan, Shakhimardan (Shohimardon) town, S of Fergana (Farg'ona), 39°56.10'N, 71°51.00'E.

Lectotype designation

Based on the identical locality, morphology, and deposition of the material and despite the lack of proper labeling, we consider the material located in T. Soldán's former collection as the type material of *T. maxillare*; all the specimens constitute syntypes according to ICZN Arti-

cle 73.2. To ensure the stability of the species, we thus designate a lectotype (female mature nymph) and paralectotypes (173 nymphs, same data as lectotype) according to the ICZN Article 74. The material was collected by T. Soldán and M. Tonner on 20.5.1980 in the type locality specified above. For the deposition of the material, see the chapter "Material examined".

Amendment to the morphology of *T. maxillare*

When comparing the original description of *T. maxillare* by Braasch and Soldán (1983) with the type material, all morphological characters are congruent. However, the re-description published four years later (Novikova and Kluge 1987), exhibited multiple inconsistencies with both the original description, and the type material itself.

A very distinctive feature of *T. maxillare* is the elongated maxillary palps with the first segment widened apically and the second segment distinctly narrow in diameter (Fig. 3F; Braasch and Soldán 1983: fig. 15). This unique feature is visible even without the need to prepare a slide. In Novikova and Kluge (1987), the first segment of maxillary palp is not distinctly widened apically, and the second segment is even wider in diameter than the first (Novikova and Kluge 1987: fig. 2). The shape of the prostheca also slightly differs, although in this case it might be the result of variability or the limited visibility of some structures. The left prostheca is slightly wider apically in Novikova and Kluge (1987) than in Braasch and Soldán (1983). In the right prostheca, apical bifurcation is present in Braasch and Soldán (1983: fig. 14) and absent in Novikova and Kluge (1987: fig. 2). Our observations confirm the characters as depicted in Braasch and Soldán 1983 (Figs 3C, D, 4A). However, the right prostheca is bifurcated only in the apical part, which is sometimes hardly recognizable, only seen with certainty by using SEM (Fig. 4A). One more discrepancy occurs in the mouthparts in the shape of the labial palp, with the apical projection of the third segment being much broader in Novikova and Kluge (1987: fig. 2) than in Braasch and Soldán (1983: fig. 16) and the type material we have investigated (Fig. 3G).

In the type material of *T. maxillare*, the claws are apparently longer compared to the claws depicted in Novikova and Kluge (1987: fig. 2); in the types the tarsus is 2.3–2.5 × longer than the claw, whereas this ratio is 2.9 according to the illustration in Novikova and Kluge (1987: fig. 2). Scales feathered apically, documented on various body parts by Novikova and Kluge (1987: fig. 2), are actually not present on the type material of *T. maxillare* at all; these scales are instead smoothly rounded apically (Fig. 4D–G). The rectangular shape of scale sockets presented by Novikova and Kluge (1987: fig. 2) probably does not represent the true shape of the sockets, but rather the shape of scales themselves, since the shape of the scale base inserted inside a socket is often prominent to the eye when observed under a light microscope. This is identical in the *T. maxillare* type material.

The shape of the gills is also different between Novikova and Kluge (1987: fig. 2) and Braasch and Soldán (1983: fig. 16). In Novikova and Kluge (1987), gills II–VII are bluntly pointed apically, with the widest part at ca. 1/2 of the respective plate length. In the *T. maxillare* type material, these plates are more widely rounded apically, with

the widest part at ca. 2/3 of the plate length (Fig. 3L–Q). This is consistent with the drawing of Braasch and Soldán (1983: fig. 22). Gill I in Novikova and Kluge (1987) is widened basally, which also does not correspond with the original description and the type material (Fig. 3K). The shape of paraproct is mostly similar in Novikova and Kluge (1987: fig. 2) and Braasch and Soldán (1983: fig. 20). The posteromedial extension is bent dorsally, thus not immediately visible from the ventral view.

Based on the characters compared above, we are rather confident that Novikova and Kluge (1987) actually depicted a different species than *T. maxillare*. It probably represents an additional undescribed species occurring in Central Asia, sharing some diagnostic characters with *T. maxillare*, although distinguishable on a specific level. This misidentification may have been derived from the uniquely long maxillary palp, which caused Novikova and Kluge (1987) to confuse their material with the only locally described species to share such a character. Consequently, the male and female imagines assigned to *T. maxillare* possibly do not actually belong to *T. maxillare*. The adult females were described by Novikova and Kluge (1987), reared from nymphs with morphology presumably specified in the species' redescription, presented in the same paper (and as demonstrated above, different from *T. maxillare* types). The adult males were described later in Novikova and Kluge (1994), also based on reared material, and possibly from the same nymphal morphotype. The conspecificity of the adult stage of "*T. maxillare*" and a possible undescribed related nymph from the area remain to be tested in the future either by new rearing or DNA comparison.

Distinctive morphological characters of *T. maxillare*, *T. sinusopalpata* sp. nov., and *T. shughnonica* sp. nov.

These three species possess a distinctive paraproct with a short bent prolongation. The paraproct presents similar but more pronounced prolongation in various species historically assigned to *Alainites* (Gattolliat 2011; Zrelli et al. 2012). A similar projection is exceptional in other lineages; it also occurs in *Indobaetis* Müller-Liebenau & Morihara, 1982 and *Papuanatula* Lugo-Ortiz & McCafferty, 1999, although its structure is different in these two taxa, and varies among species (Kluge and Novikova 2014).

The elongated maxillary palp is a character shared by *T. maxillare*, *T. sinusopalpata* sp. nov., and *T. shughnonica* sp. nov., and is much less developed in the various species assigned to *Alainites*. The shape of the palp significantly differs between these three species: in *T. maxillare*, the first segment is widened apically and curved outwards, while it is almost straight in *T. sinusopalpata* sp. nov. and *T. shughnonica* sp. nov.; the second segment is sinusoidal in *T. sinusopalpata* sp. nov., slightly sinusoidal in *T. shughnonica* sp. nov., and straight in *T. maxillare*.

It seems that the nymphal morphology of *T. sinusopalpata* sp. nov. and *T. shughnonica* sp. nov. is somewhat intermediary between *Alainites* sensu Waltz et al. (1994) (with type species *A. muticus*) and *Takobia* (with type species *T. maxillare*). Both new species exhibit a combination of characters partially similar to *T. maxillare*, notably sharing the elongated maxillary palps. On the other hand, both species possess denticles

on the tarsal claws, contrary to *T. maxillare* and the undescribed *Takobia* species illustrated by Novikova and Kluge (1987), which exhibit tarsal claws devoid of even minute denticles. It is worth mentioning that in *T. sinusopalpata* sp. nov., the claw is only slightly curved, more distinctly elongated and the denticles are very small, more closely resembling the situation in *T. maxillare* than in the case of *T. shughnonica* sp. nov.

The presence of claw denticles is considered as a plesiomorphic condition in Baetidae, being subject to reduction in several non-related lineages. On the other hand, the elongated maxillary palp is almost unique within Baetidae and probably represents a synapomorphy of *T. maxillare*, *T. sinusopalpata* sp. nov., and *T. shughnonica* sp. nov. Therefore, we assign both new species described herein to the genus *Takobia*, primarily based on this character. The three species are also closely distributed geographically, therefore they may form a single lineage restricted to Central Asia.

Synonymy of *Alainites* with *Takobia*

In the recent Baetidae phylogeny by Cruz et al. (2020), *Alainites* and *Takobia* were recovered as sister lineages, nesting within the same clade as *Nigrobaetis*, *Fallceon*, and *Caribaetis*. Kluge and Novikova (2014) suggested the synonymy of *Alainites* with *Takobia*. These authors argued that *T. maxillare* is a species with a unique morphology, phylogenetically clustering within *Alainites*, but exhibiting several apomorphies within the lineage, such as elongated maxillary palps and secondarily reduced claw denticles. The remaining representatives of *Alainites* are defined only by plesiomorphies with regard to *T. maxillare*. Since *T. maxillare* is only a single aberrant species within the lineage, using a generic name is redundant to distinguish a single apomorphic species; it should be classified in the same taxon with its plesiomorphic relatives instead. And since the genus *Takobia* is senior to *Alainites*, all *Alainites* species should be reclassified into *Takobia*.

However, the inconsistencies in the description of *T. maxillare* and later redescription by Novikova and Kluge (1987) point to the existence of more species in Central Asia with the same apomorphies as *T. maxillare*, as demonstrated above. This implication is further corroborated by our description of two more species exhibiting elongated maxillary palp closely resembling *T. maxillare*. More undescribed species similar to *T. maxillare* possibly occur in the Himalayas (unpublished data). There is likely a monophyletic lineage comprised of *T. maxillare* and all these species. The relationship of this lineage to *Alainites* is not clear at present. It might represent a lineage inside *Alainites*, rendering this genus paraphyletic and justifying the synonymy of *Alainites* with *Takobia* as suggested by Kluge and Novikova (2014). However, *Takobia* might also well constitute a sister lineage to *Alainites*. Thus, we prefer to consider *Takobia* and *Alainites* as separate genera, since *Takobia* comprises several derived species defined by a common apomorphic characters.

In conclusion, our results prove the existence of several Central Asian mayfly species closely related to *T. maxillare*. Two of them are newly described herein and another one erroneously assigned to *T. maxillare* in the literature. This was tested by the study of the original type material. The fact that *Takobia* hitherto consisted of a single species

was only a consequence of our poor knowledge of the Central Asian mayfly fauna rather than *T. maxillare* really being something unique. The reclassification of all *Alainites* species based on such a premise is undesirable. Therefore, we refrain for the moment to follow the nomenclatural changes proposed by Kluge and Novikova (2014). We are convinced that any newly proposed classification of the *Alainites*/*Nigrobaetis*/*Takobia* complex must be based on a global phylogenetic analysis. Our study highlights the need for such an analysis and forms one of the necessary preliminary steps for the accomplishment of such a task.

Acknowledgements

References

Bojková J, Sroka P, Soldán T, Namin JI, Staniczek AH, Polášek M, Hrivniak Ľ, Abdoli A, Godunko RJ (2018) Initial commented checklist of Iranian mayflies, with new area records and description of *Procloeon caspicum* sp. n. (Insecta, Ephemeroptera, Baetidae). ZooKeys 749: 87–123. https://doi.org/10.3897/zookeys.749.24104

Braasch D, Soldán T (1983) Baetidae in Mittelasien III (Ephemeroptera). Entomologische Nachrichten und Berichte 27: 266–271.

Cruz PV, Nieto C, Gattolliat J-L, Salles FF, Hamada N (2020) A cladistic insight into the higher level classification of Baetidae (Insecta: Ephemeroptera). Systematic Entomology 46(1): 44–55. https://doi.org/10.1111/syen.12446

Folmer O, Black M, Hoeh W, Lutz R, Vrijenhoek R (1994) DNA primers for amplification of mitochondrial cytochrome c oxidase subunit I from diverse metazoan invertebrates. Molecular Marine Biology and Biotechnology 3: 294–299.

Fujitani T, Kobayashi N, Hirowatari T, Tanida K (2017) Morphological description of four species belonging to the genus *Nigrobaetis* (Ephemeroptera: Baetidae) from Japan. Limnology 18: 315–331. https://doi.org/10.1007/s10201-016-0509-4

Gattolliat J-L (2011) A new species of *Alainites* (Ephemeroptera: Baetidae) from Borneo (East Kalimantan, Indonesia). Mitteilungen der Schweizerischen entomologischen Gesellschaft, 84(3–4): 185–192. http://doi.org/10.5169/seals-403033

Gattolliat J-L, Cavallo E, Vuataz L, Sartori M (2015) DNA barcoding of Corsican mayflies (Ephemeroptera) with implications on biogeography, systematics and biodiversity. Arthropod Systematics and Phylogeny 73(1): 3–18.

Jacob U (2003) *Baetis* Leach, 1815, sensu stricto oder sensu lato. Ein Beitrag zum Gattungskonzept auf der Grundlage von Artengruppen mit Bestimmungsschlüsseln. Lauterbornia 47: 59–129. [in German]

Kang SC, Chang HC, Yang CT (1994) A revision of the genus *Baetis* in Taiwan (Ephemeroptera, Baetidae). Journal of Taiwan Museum 47: 9–44.

Kazancı N, Thomas A (1989) Compléments et corrections à la faune des Éphéméroptères du Proche-Orient: 2. *Baetis kars* n. sp. de Turquie (Ephemeroptera: Baetidae). Mitteilungen der Schweizerischen Entomologischen Gesellschaft 62: 323–327.

Kluge NJ (1997) Order mayflies – Ephemeroptera. In: Tsalolikhin SJ (Ed.) Key to freshwater invertebrates of Russia and adjacent lands, vol. 3., Zoological Institute RAS, St. Petersburg, 176–220. [in Russian]

Kluge NJ, Novikova EA (2014) Systematics of *Indobaetis* Müller-Liebenau & Morihara, 1982, and related implications for some other Baetidae genera (Ephemeroptera). Zootaxa 3835(2): 209–236. https://doi.org/10.11646/zootaxa.3835.2.3

Kluge NJ, Novikova EA (2016) New tribe Labiobaetini tribus n., redefinition of *Pseudopannota* Waltz & McCafferty, 1987 and descriptions of new and little known species from Zambia and Uganda. Zootaxa 4169: 1–43. https://doi.org/10.11646/zootaxa.4169.1.1

Kumar S, Stecher G, Li M, Knyaz C, Tamura K (2018) MEGA X: Molecular Evolutionary Genetics Analysis across computing platforms (Version 10.0.2). Molecular Biology and Evolution 35: 1547–1549. https://doi.org/10.1093/molbev/msy096

Lugo-Ortiz CR, McCafferty WR (1999) A new genus of small Minnow Mayflies (Insecta: Ephemeroptera: Baetidae) with six new species from New Guinea and New Britain. Annales de Limnologie - International Journal of Limnology 35: 57–70. https://doi.org/10.1051/limn/1999013

Martynov AV, Godunko RJ (2017) Mayflies of the Caucasus Mountains IV. New species of the genus *Nigrobaetis* Novikova & Kluge, 1987 (Ephemeroptera, Baetidae) from Georgia. Zootaxa 4231(1): 70–84. https://doi.org/10.11646/zootaxa.4231.1.4

Müller-Libenau I (1969) Revision der europäischen Arten der Gattung *Baetis* Leach, 1815. (Insecta, Ephemeroptera). Gewässer und Abwässer 48/49: 1–214.

Müller-Liebenau I, Morihara DK (1982) *Indobaetis*: A New Genus of Baetidae from Sri Lanka (Insecta: Ephemeroptera) with Two New Species. Gewässer und Abwässer 68/69: 26–34.

Novikova EA, Kluge NJ (1987) Systematics of the genus *Baetis* (Ephemeroptera, Baetidae), with description of new species from Middle Asia. Vestnik Zoologii 1987(4): 8–19. [in Russian]

Novikova EA, Kluge NJ (1994) Mayflies of the subgenus *Nigrobaetis* (Ephemeroptera, Baetidae, Baetis). Entomologicheskoe Obozrenie 73(3): 623–644. [in Russian]

Sroka P (2012) Systematics and phylogeny of the West Palaearctic representatives of subfamily Baetinae (Insecta: Ephemeroptera): combined analysis of mitochondrial DNA sequences and morphology. Aquatic Insects 34(1): 23–53. https://doi.org/10.1080/01650424.2012.718081

Vuataz L, Sartori M, Wagner A, Monaghan MT (2011) Toward a DNA taxonomy of alpine *Rhithrogena* (Ephemeroptera: Heptageniidae) using a mixed yule-coalescent analysis of mitochondrial and nuclear DNA. PLoS ONE 6: e19728. https://doi.org/10.1371/journal.pone.0019728

Waltz RD, McCafferty WP, Thomas A (1994) Systematics of *Alainites* n. gen., *Diphetor*, *Indobaetis*, *Nigrobaetis* n. stat., and *Takobia* n. stat. (Ephemeroptera, Baetidae). Bulletin de la Société d'histoire Naturelle de Toulouse 130: 33–36.

Waltz RD, McCafferty WP (1997) New generic synonymies in Baetidae (Ephemeroptera). Entomological News 108(2): 134–140.

Zrelli S, Gattolliat J-L, Boumaiza M, Thomas A (2012) First record of *Alainites sadati* Thomas, 1994 (Ephemeroptera: Baetidae) in Tunisia, description of the larval stage and ecology. Zootaxa 3497: 60–68. https://doi.org/10.11646/zootaxa.3497.1.6.

RESEARCH ARTICLE

A peer-reviewed open-access journal
ZooKeys
Launched to accelerate biodiversity research

Hexatoma (*Eriocera*) Macquart (Diptera, Limoniidae) from Xizang, China

Bing Zhang¹, Qicheng Yang², Yan Li³, Ding Yang¹

1 *Department of Entomology, College of Plant Protection, China Agricultural University, Beijing 100193, China* **2** *Hubei Insect Resources Utilization and Sustainable Pest Management Key Laboratory, College of Plant Science & Technology of Huazhong Agriculture University, Wuhan, 430070, China* **3** *College of Plant Protection, Shenyang Agricultural University, Shenyang, 110866, China*

Corresponding author: *Ding Yang* (dyangcau@126.com)

Citation: Zhang B, Yang Q, Li Y, Yang D (2021) *Hexatoma* (*Eriocera*) Macquart (Diptera, Limoniidae) from Xizang, China. ZooKeys 1071: 155–173. https://doi.org/10.3897/zookeys.1071.66750

Abstract

One new species of the subgenus *Eriocera* Macquart,1838, *Hexatoma (Eriocera) xizangensis* **sp. nov.** is described and illustrated from Xizang, China. The following four species are re-described and reported from Xizang for the first time: *H. (E.) latigrisea* Alexander, 1971, *H. (E.) nepalensis* (Westwood, 1836), *H. (E.) paragnava* Alexander, 1973 and *H. (E.) perhirsuta* Alexander, 1973. A key to the species of *Eriocera* from Xizang is presented.

Keywords

Biodiversity, craneflies, Limnophilinae, systematics, taxonomy, Tibet

Introduction

Eriocera Macquart, 1838 is a subgenus of the genus *Hexatoma* Latreille, 1809 in the family Limoniidae. It is distributed worldwide with 563 known species and subspecies, of which 69 taxa are from the Palaearctic Realm, 34 taxa from the Nearctic Realm, 143 taxa from the Neotropical Realm, 30 taxa from the Afrotropical Realm, 290 taxa from the Oriental region, and five taxa from the Australasian/Oceania realms (Oosterbroek 2021). The subgenus is thus large and morphologically diverse, and was confirmed to be non-monophyletic by Ribeiro (2008). It is characterized by the following characters: body medium to large sized; antenna with four to ten flagellomeres; wings often unpatterned through variously darkened, or with a conspicuous hyaline and yellow cross banded pattern, or abundantly spotted and dotted with brown; cell *dm* present; two or three branches of M reaching margin; clasper of gonostylus narrowed apically into a long curved spine; lobe of gonostylus short and stout with setae; gonocoxite moderately stubby or elongate cylindrical; interbase usually cylindrical, or triangular with a sharp spine at base, or two-layered membranous structure with spine at apex; aedeagus usually short and relatively inconspicuous, or directed ventrally (Alexander and Lloyd 1914; Edwards 1921; Alexander 1948; Alexander and Byers 1981; Savchenko 1986; Podenas et al. 2006; Ribeiro 2008; Podeniene and Gelhaus 2015).

So far, only the following four species of the subgenus *Eriocera* were known to occur in Xizang (Men and Yu 2015; Oosterbroek 2021): *H.* (*E.*) *lanigera* Alexander, 1933, *H.* (*E.*) *mediofila* Alexander, 1933, *H.* (*E.*) *nudivena* Alexander, 1933 and *H.* (*E.*) *tibetana* Alexander, 1933. To enrich the knowledge of the species composition of craneflies in Xizang, we conducted a scientific survey of craneflies in Xizang from 1978 to 2019. Presently, five species including one new species of the subgenus *Eriocera* are added to the fauna of Xizang. The following three species are reported from China for the first time: *H.* (*E.*) *latigrisea* Alexander, 1971, *H.* (*E.*) *paragnava* Alexander, 1973 and *H.* (*E.*) *perhirsuta* Alexander, 1973. *Hexatoma* (*E.*) *nepalensis* (Westwood, 1836) is for the first time reported from Xizang. *Hexatoma* (*Eriocera*) *xizangensis* sp. nov. is described and illustrated from Xizang. A key to the species of *Eriocera* from Xizang is presented.

Materials and methods

The specimens were studied and illustrated with a ZEISS Stemi 2000-c stereo microscope. Details of coloration were checked in specimens immersed in 75% ethyl alcohol. Male genitalia were prepared by macerating the apical portion of the abdomen in cold 10% NaOH for 12–15 hours. After examination, it was transferred to fresh glycerine ($C_3H_8O_3$) and stored in a microvial pinned below the specimen. The specimens studied, which were collected in Xizang are deposited in the Entomological Museum of China Agricultural University (CAU), Beijing, China.

Holotype material of *Hexatoma* (*Eriocera*) *latigrisea* Alexander, 1971 used in this paper was borrowed from the National Museum of Natural History, Smithsonian In-

stitution, Washington, DC, USA (USNM) and holotype material of *Hexatoma* (*Eriocera*) *nepalensis* (Westwood, 1836) was borrowed from the Natural History Museum, London, UK (BMNH). The terminology applied to the wing veins follows the interpretation of de Jong (2017). Terminology of the male terminalia follows Ribeiro (2006, 2008). The following abbreviations in figures are used: 9s = ninth sternite, 9t = ninth tergite, goncx = gonocoxite, cgonst = clasper of gonostylus, lgonst = lobe of gonostylus, aed = aedeagus, ce = cercus, hy = hypogynial valve.

Taxonomy

Key to species of subgenus *Eriocera* from Xizang, China (adult)

1   Wing with cell M_1 (Figs 34, 40) **2**
–   Wing without cell M_1 (Figs 1, 3, 9, 10, 12, 16, 22, 24, 28, 46, 48) **4**
2   Antenna of male approximately as long as body (Alexander, 1933: 150) ....
    ....***H. (E.) tibetana* Alexander, 1933**
–   Antenna of male approximately three times as long as body (Figs 34; Alexander, 1973: 8; Alexander, 1933: 149)..**3**
3   Femora yellow (Figs 34; Alexander, 1973: 9); R_{2+3} two times longer than R_{2+3+4} (Figs 34, 40; Alexander, 1973: 4, fig. 6) ..... ***H. (E.) perhirsuta* Alexander, 1973**
–   Basal 1/3 of femora yellow, outer 2/3 black (Alexander, 1933: 149); R_{2+3} as long as R_{2+3+4} (Alexander, 1933: plate I; Fig. 11) ....***H. (E.) lanigera Alexander*, 1933**
4   Wing without markings (Figs 22, 24, 28) **5**
–   Wing bicolorous, with markings (Figs 1, 3, 9, 10, 12, 16, 46, 48) **7**
5   Wing without stigma (Alexander, 1933: 158); R_2 longer than R_{2+3} (Alexander, 1933: plate I. Fig. 19) ....***H. (E.) nudivena* Alexander, 1933**
–   Wing with stigma; R_2 shorter than R_{2+3} (Figs 22, 24, 28) **6**
6   Antenna of male approximately as long as body (Alexander, 1933: 151); R_{2+3} longer than R_{2+3+4} (Alexander, 1933: plate I; Fig. 13) ....
    ....***H. (E.) mediofila* Alexander, 1933**
–   Antenna of male approximately three times longer than body (Figs 22; Alexander, 1973: 8); R_{2+3} shorter than R_{2+3+4} (Figs 22, 24, 28; Alexander, 1973: 4, fig. 5) .....
    ....***H. (E.) paragnava Alexander*, 1973**
7   Male terminalia yellow (Fig. 46); wing with many hyaline markings; R_2 contacts vein R_{2+3+4} (Figs 46, 48) ....***H. (E.) xizangensis* sp. nov.**
–   Male terminalia black or dark brown (Figs 1, 9, 10); wing with a whitened or hyaline marking before discal area; R_2 contacts vein R_{2+3} (Figs 1, 3, 9, 12, 16) **8**
8   Antenna blackish brown; femora blackish brown; abdomen of male with four pale white gray markings (Figs 9, 10) ...... ***H. (E.) nepalensis* (Westwood, 1836)**
–   Scape and pedicel blackish brown, flagellum reddish yellow except outer two segments dark brown; basal 5/6 of femora yellow, outer 1/6 dull black; abdomen glossy black or dull black (Fig. 1; Alexander, 1971: 116) ....
    ....***H. (E.) latigrisea* Alexander, 1971**

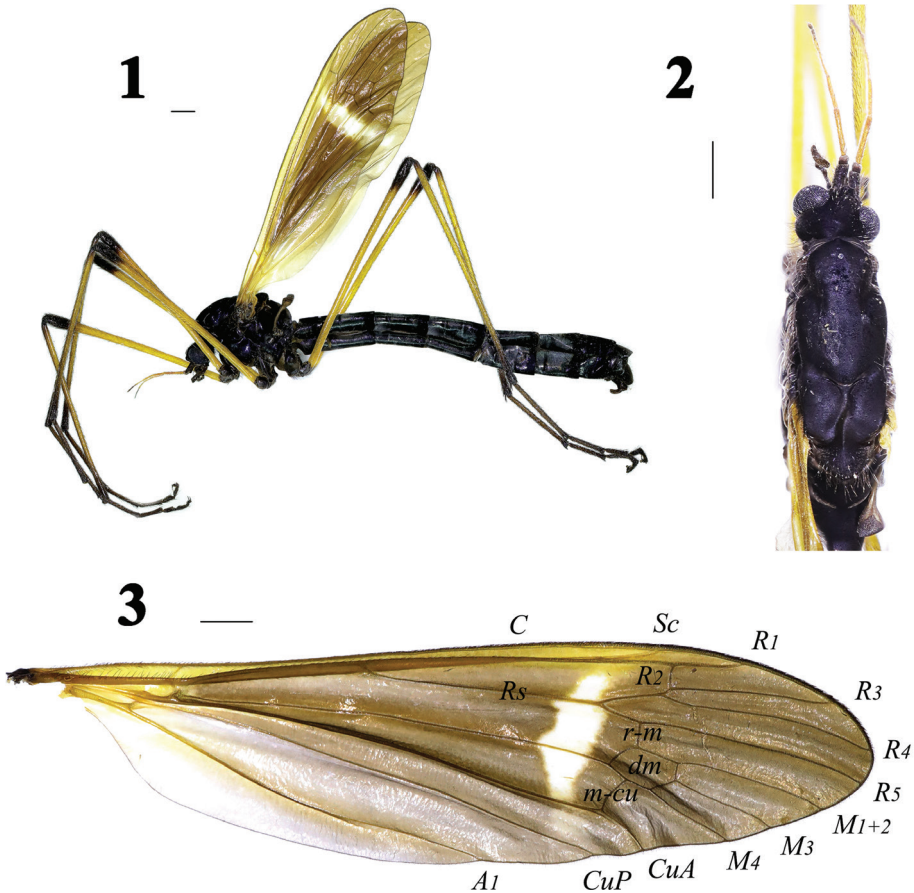### *Hexatoma* (*Eriocera*) *latigrisea* Alexander, 1971
Figs 1–8

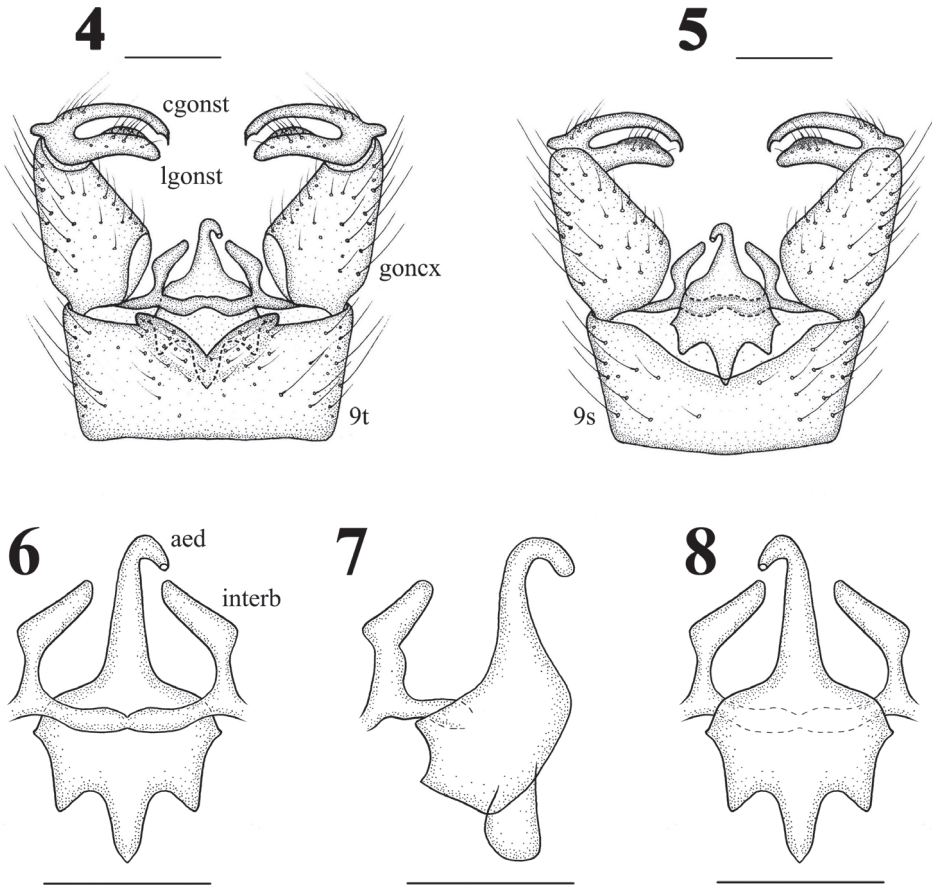*Hexatoma* (*Eriocera*) *latigrisea* Alexander, 1971: 116. Type locality: India, Assam

Specimens examined. 2 males (CAU), China: Xizang, Motuo, 80K, 2014.VII.31, Yan Li (light trap). ***Holotype***: male, Kujjalong, Kameng, North East Frontier Agency, Assam, 4500 feet, June 28–30, 1961 (Schmid).

Diagnosis. Antenna has 8 segments. Wing is brown, but narrowly yellow at base; anal cells are much paler; cells *C* and *Sc* are dark yellow; a narrow white discal area is before cord, including cell R_1 to cell *M*; *m-cu* is nearly at middle of cell *dm.* Posterior margin of male ninth tergite has a V-shaped notch, both sides of notch have a process; interbase is triangular, swollen at base.

Redescription. Male (*N* = 2): Body length 18.0–19.8 mm, wing length 14.0–16.7 mm, antenna length 3.6–4.1 mm.

Figures 1–3. *Hexatoma* (*Eriocera*) *latigrisea* Alexander, male **1** habitus, lateral view **2** male head and thorax, dorsal view **3** right wing. Scale bars: 1.0 mm (1–3).

Figures 4–8. *Hexatoma* (*Eriocera*) *latigrisea* Alexander, male **4** terminalia, dorsal view **5** terminalia, ventral view **6** aedeagal complex, dorsal view **7** aedeagal complex, lateral view **8** aedeagal complex, ventral view. Scale bars: 0.5 mm (4–8).

Thorax (Figs 1, 2) dull black with blackish brown setae. Legs with blackish brown setae; coxae and trochanters blackish brown; basal 5/6 of femora yellow, outer 1/6 dull black; tibiae obscure yellow, black apically; tarsi dark brown. Wing (Figs 1, 3) brown, narrowly yellowed at base; anal cells much paler; cells *C* and *Sc* dark yellow; a narrow white discal area before cord, including cell R_1 to cell *M*; veins brown, more yellow in brightened areas. Venation: R_2 moderately oblique, R_{2+3} relatively short, shorter than R_2; cell M_1 lacking; *m-cu* nearly at middle of cell *dm*. Halter (Figs 1, 2) length approximately 2.2 mm, halter stem pale brown with brown setae; knob brown with blackish brown setae.

Abdomen (Fig. 1) with short black setae. Segments 1–6 extensively glossy black, segments 7–8 dull black.

Male terminalia (Figs 1, 4–8) with 180° rotation, dull black with black setae. Posterior margin of ninth tergite with a V-shaped notch, both sides of notch with a lateral projection; posterior margin of ninth sternite with a deep V-shaped shallow; gonocoxite moderately stubby; clasper of gonostylus with long setae at base, slender, terminal

spine decurved; lobe of gonostylus short and stout, terminal margin swollen with long setae; interbase triangular; aedeagus longer, apically directed ventrally.

Female. Unknown.

Distribution. India (Assam), China (Xizang).

Remarks. This species was known previously only from India. With the present contribution it is recorded from China for the first time.

Hexatoma (*Eriocera*) *nepalensis* (Westwood, 1836)
Figs 9–21

Caloptera nepalensis Westwood, 1836: 681. Type locality: Nepal.
Pterocosmus velutinus Walker, 1848: 79. Type locality: Nepal.
Lechria nepalensis Brunetti, 1918: 317. Type locality: Nepal (Katmandu).
Eriocera nepalensis Westw. (= *velutina*, Walk.): Edwards 1921: 76.
Pterocosmus velutinus (*Eriocera nepalensis*): Edwards 1921: 99.
Lechria nepalensis: Edwards 1924: 301.
Trichoneura (*Xipholimnobia*) *nepalensis*: Alexander 1963: 24; Alexander 1968: 95.
Hexatoma (*Eriocera*) *nepalensis*: Mitra et al. 2006: 234; Men and Yu 2015: 165.

Specimens examined. 1 male (CAU), China: Xizang, Chayu, 1570 m, 1978.VI.25, Fasheng Li. 1 male (CAU), China: Xizang, Chayu, 1700 m, 1978.VI.26, Fasheng Li.

Figure 9. *Hexatoma* (*Eriocera*) *nepalensis* (Westwood, 1836), male. Photo by Qicheng Yang.
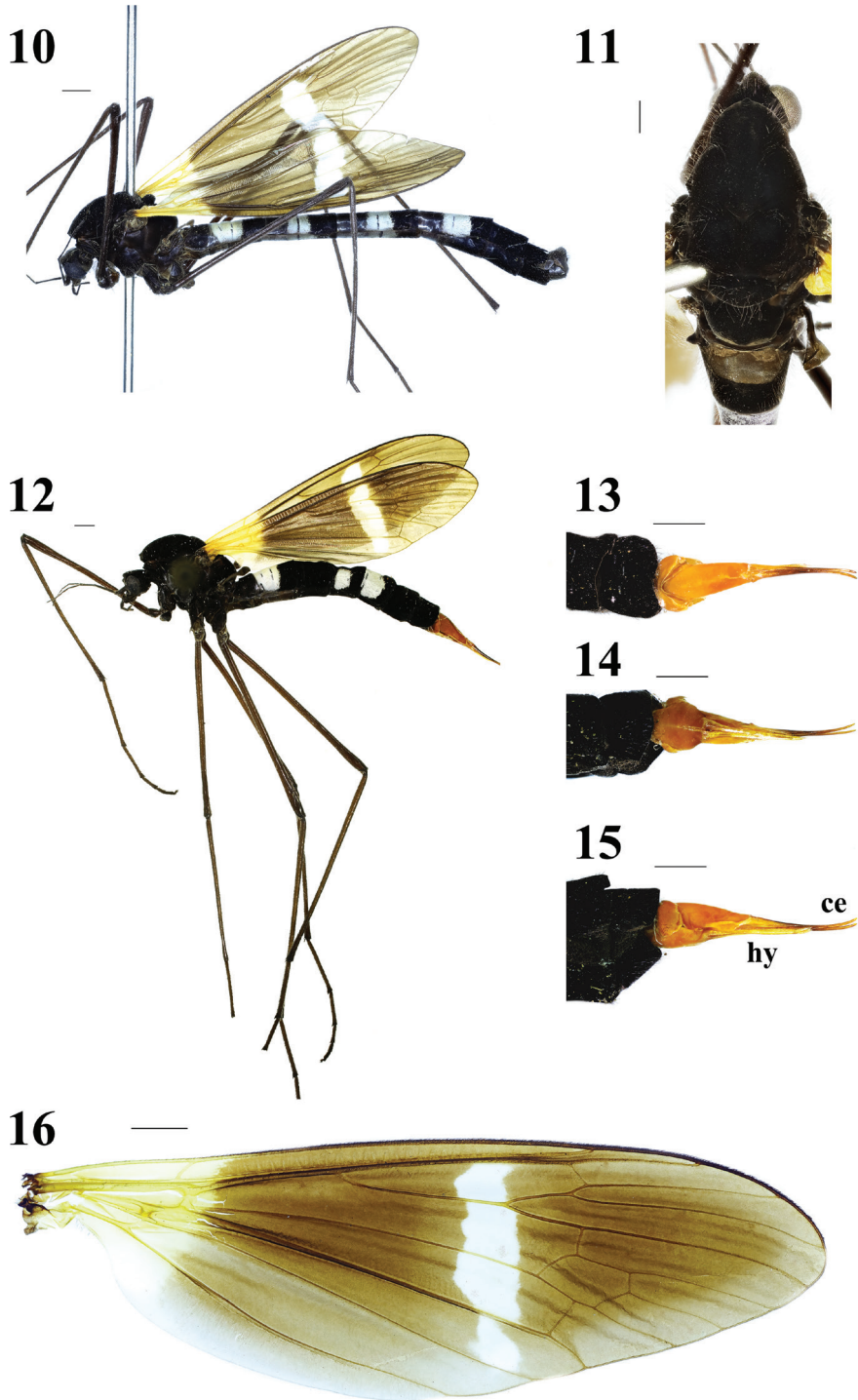
Figures 10–16. *Hexatoma (Eriocera) nepalensis* (Westwood, 1836) **10** male habitus, lateral view **11** male head and thorax, dorsal view **12** female habitus, lateral view **13** ovipositor, dorsal view **14** ovipositor, ventral view **15** ovipositor, lateral view **16** male right wing. Scale bars: 1 mm (10–16).

17 ____   **18** ____

19   **20**   **21**
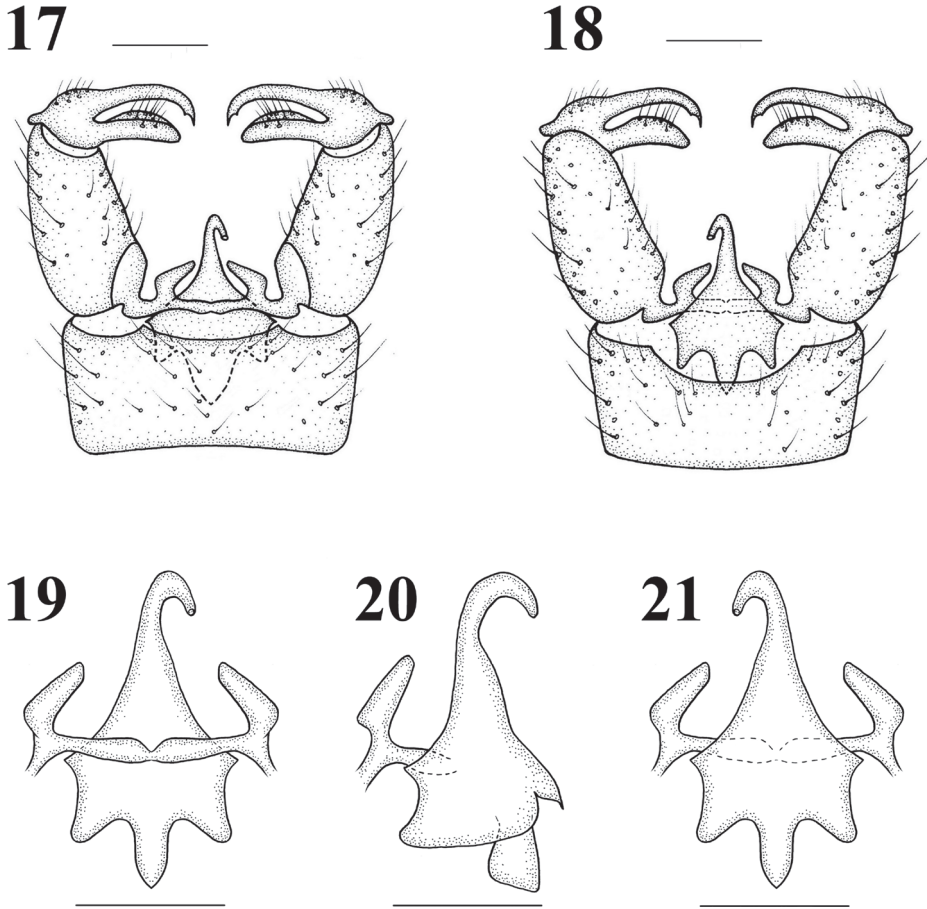
Figures 17–21. *Hexatoma* (*Eriocera*) *nepalensis* (Westwood, 1836), male **17** terminalia, dorsal view **18** terminalia, ventral view **19** aedeagal complex, dorsal view **20** aedeagal complex, lateral view **21** aedeagal complex, ventral view. Scale bars: 0.5 mm (17–21).

1 male (CAU), China: Xizang, Beibeng, 2014.VII.27, Yan Li. 1 female (CAU), China: Xizang, Chayu, 2014.VIII.3, Yan Li. 1 male, 2 females (CAU), China: Xizang, Linzhi, Gongbujiangda, Ganglangcun. *Holotype*: male, Nepal, Hardwicke Bequest; accession no. NHMUK010397658, BMNH(E)247599 (BMNH).

Diagnosis. Antenna has 8 segments. Wing is brown, but yellowed at basal 1/5; anal cells are much paler; a white discal area is before cord, including cell R_1 to cell CuA_1; *m-cu* is near 2/3 of cell *dm*. Posterior margin of tergite 9 is produced; interbase is triangular, stubby at base.

Redescription. Male ($N = 4$): Body length 12.5–22.5 mm, wing length 12.4–15.5 mm, antenna length 3.3–3.8 mm.

Head (Figs 9–11) velvet black with black setae. Rostrum and palpus blackish brown. Antenna 8 segmented, blackish brown with brown setae.

Thorax (Figs 9–11) velvet black with blackish brown setae. Legs with blackish brown setae; coxae and trochanters velvet black with long setae; femora, tibiae and tarsi blackish brown. Wing (Figs 9–10, 16) brown, basal 1/5 yellowed, anal cells much paler; a white discal area before cord, including cell R_1 to cell CuA_1; veins brown, more yellowed in brightened areas. Venation: R_2 oblique, R_{2+3} relatively short, shorter than R_2; cell M_1 lacking; *m-cu* near 2/3 of cell *dm*. Halter (Figs 9–11) length approximately 2.1 mm, grayish brown with blackish brown setae.

Abdomen (Figs 9–10) with short black setae. Segments 2–5 elongate, shining black at base, pale white gray in middle, velvet black at tip; segments 1 and 6–7 velvet black; segment 8 shining black.

Male terminalia (Figs 9–10, 17–21) shining black with blackish brown setae. Posterior margin of ninth tergite produced, its margin concave; posterior margin of ninth sternite with a deep U-shaped shallow; gonocoxite moderately stubby; clasper of gonostylus with long setae at base, slender, terminal spine decurved; lobe of gonostylus short and stout, terminal margin swollen with long setae; interbase triangular, stubby at base; aedeagus longer, apically directed ventrally.

Female (*N*=3): Body length 17.3–19.4 mm, wing length 13.3–15.4 mm, antenna length 3.6–4.4 mm.

Female (Figs 12–15) resembles male. Abdomen shorter; tergites 2, 4–5 pale white gray at base, velvet black at tip; tergites 1, 3, 6–7 velvet black; sternites 1–7 velvet black; segment 8 velvet orange.

Ovipositor (Figs 12–15) elongate, velvet orange. Cercus narrowed toward tip. Hypogynial valve shorter, narrowed toward tip.

Distribution. Afghanistan; China (Sichuan, Guangdong, Xizang), India (Assam and/or Arunachal Pradesh), Malaysia (Peninsula), Nepal.

Remarks. This species is here recorded from Xizang, China for the first time.

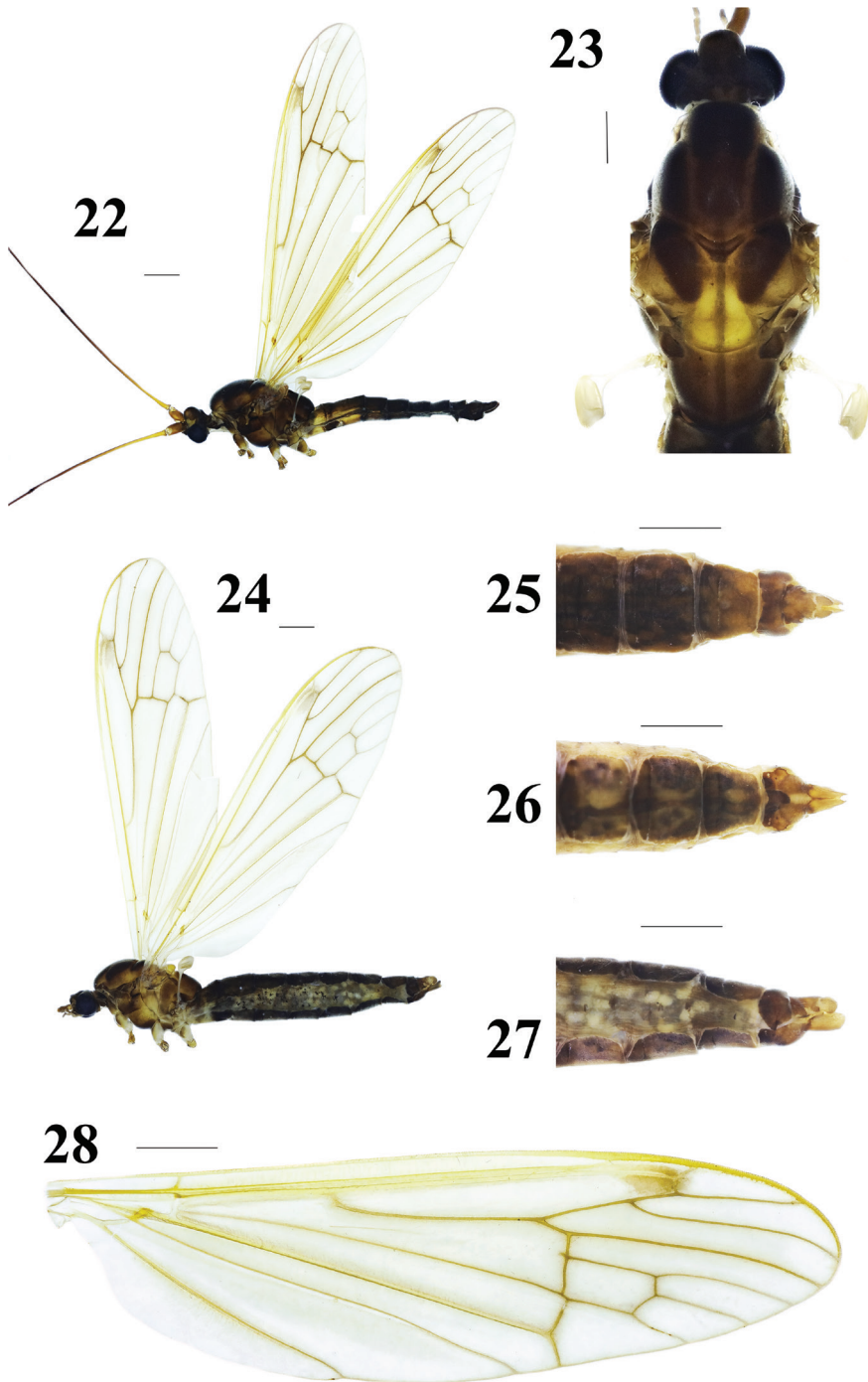## *Hexatoma* (*Eriocera*) *paragnava* Alexander, 1973
Figs 22–33

Hexatoma (*Eriocera*) *paragnava* Alexander, 1973: 7. Type locality: India, Assam.

Specimens examined. 19 males, 2 females (CAU), China: Xizang, Motuo, Beibeng, Jiangxincun, 800 m, 2019.V.29, Qicheng Yang (light trap). 1 female (CAU), China: Xizang, Motuo, Beibeng, Jiangxincun, 800 m, 2019.V.30, Qicheng Yang (light trap). 4 males, 3 females (CAU), China: Xizang, Motuo, 2019.V.31, Qicheng Yang (light trap).

Diagnosis. Front and mouth parts are very reduced; antenna is very long and 6-segmented; vertical tubercle is very large. Wing is pale yellow; *m-cu* is near 1/6 of cell *dm*. Posterior margin of ninth tergite has a U-shaped notch; interbase is two-layered membranous structure with spine-like apex.

Redescription. Male (*N*=23): Body length 8.6–11.0 mm, wing length 10.2–15.0 mm, antenna length 35.5–47.0 mm.
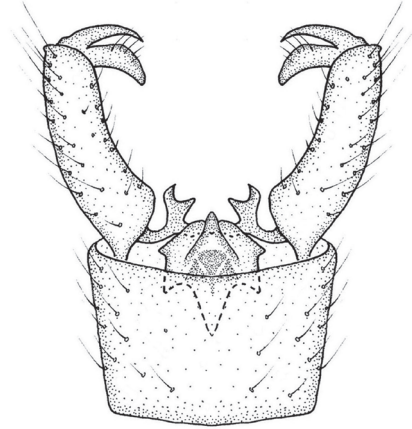
Figures 22–28. *Hexatoma* (*Eriocera*) *paragnava* Alexander, 1973. **22** male habitus, lateral view **23** male head and thorax, dorsal view **24** female habitus, lateral view **25** ovipositor, dorsal view **26** ovipositor, ventral view **27** ovipositor, lateral view **28** right wing. Scale bars: 1 mm (22–28).
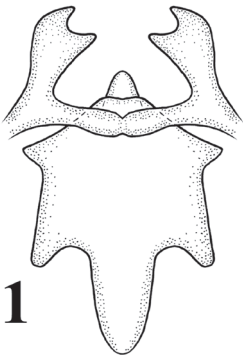
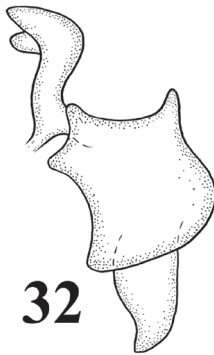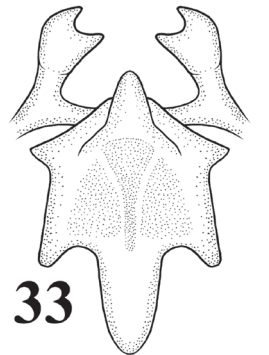**29**
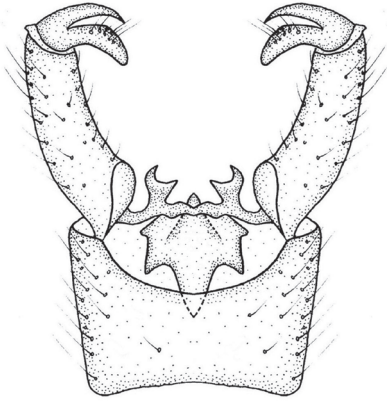
30

31

32

33

Figures 29–33. *Hexatoma* (*Eriocera*) *paragnava* Alexander, 1973, male **29** terminalia, dorsal view **30** terminalia, ventral view **31** aedeagal complex, dorsal view **32** aedeagal complex, lateral view **33** aedeagal complex, ventral view. Scale bars: 0.5 mm (29–33).

Head (Figs 22–23) brown. Front and mouth parts very reduced, brownish yellow, palpus brown. Antenna 6-segmented, very long approximately three or four times as long as wing; scape and pedicel shorter, brownish yellow; flagellum very long, first flagellomere brownish yellow at base, brown at tip; remainder of flagellum brown with short blackish brown setae. Vertical tubercle more brown, very large, bulbous with setae on posterior aspect.

Thorax (Figs 22–23) brownish yellow to brown with gray setae. Pronotum brownish yellow; propleuron brown; prescutum dark brown with a broad brown stripe at middle; prescutal suture brown; scutum brownish yellow to brown; scutellum yellow with a slender brownish yellow stripe at middle; mediotergite brownish yellow to brown. Thoracic pleuron mostly brown throughout, except prescutum, anepimeron, katepisternum and metakatepisternum partly brownish yellow. Legs: coxae and trochanters brownish yellow with gray setae; femora and tibiae brownish yellow with short

brown setae; tarsi brown with brown setae. Wing (Figs 22, 28) pale yellow; stigma and veins brownish yellow. Venation: R_2 moderately straight; R_{2+3} near half of R_{2+3+4}; cell M_1 lacking; *m-cu* near 1/6 of cell *dm*. Halter (Figs 22, 23) length approximately 1.9 mm, whitened gray.

Abdomen (Fig. 22) with brownish yellow setae. First two segments more yellowed at lateral margin; segments 3–8 dark brown.

Male terminalia (Figs 22, 29–33) brown with brownish yellow setae. Posterior margin of ninth tergite with a U-shaped notch; gonocoxite large, elongate cylindrical, gently curved; clasper of gonostylus slender, terminal spine decurved; lobe of gonostylus short and stout, swollen with setae at middle; interbase two-layered membranous structure with spine-like apex; aedeagus smaller.

Female (*N*=6): Body length 9.3–13.2 mm, wing length 10.8–12.3 mm, antenna length 1.2–1.4 mm.

Female (Figs 24–27) resembles male. Thoracic pleuron more brownish yellow. Abdomen plump, dark brown.

Ovipositor (Figs 24–27) short and fleshy, brownish yellow; cercus oval; Hypogynial valve longer.

Distribution. India (Assam); China (Xizang).

Remarks. This species was known previously only from India. With the present contribution it is recorded from China for the first time.

Hexatoma (*Eriocera*) *perhirsuta* Alexander, 1973
Figs 34–45

Hexatoma (*Eriocera*) *perhirsuta* Alexander, 1973: 8. Type locality: India, Assam.

Specimens examined. 1 male (CAU), China: Xizang, Sejilashan, 3200 m, 2013. VIII.2. 2 females (CAU), China: Xizang, Lulang, 2013.VII.28. 1 male (CAU), China: Xizang, Motuo, 80K, 2014.VII.23, Yan Li (light trap). 1 male (CAU), China: Xizang, Motuo, 80K, 2014.VII.31, Yan Li (light trap). 1 male (CAU), China: Xizang, Yigong, 2017.VIII.8, Qicheng Yang.

Diagnosis. Rostrum is very short; antenna has 6 segments, very long; vertical tubercle is large bulbous. Wing is brownish yellow; R_{2+3} is nearly three times length of R_{2+3+4}; cell M_1 is present; *m-cu* is near 1/6 of cell *dm*. Posterior margin of ninth tergite has a deep U-shaped notch; interbase is well-developed, a two-layered membranous structure with spine apex.

Redescription. Male (*N* = 4): Body length 16.0–18.3 mm, wing length 18.2–21.3 mm, antenna length 46.0–61.2 mm.

Head (Figs 34–35) dark brown with very long abundant brown setae. Rostrum very short, dark brown; palpi brown. Antenna 6-segmented, very long, more than three times as long as wing; scape and pedicel blackish brown with long brown setae; flagellum dark brown with short brown setae. Vertical tubercle large bulbous, dark brown with abundant very long brown setae.
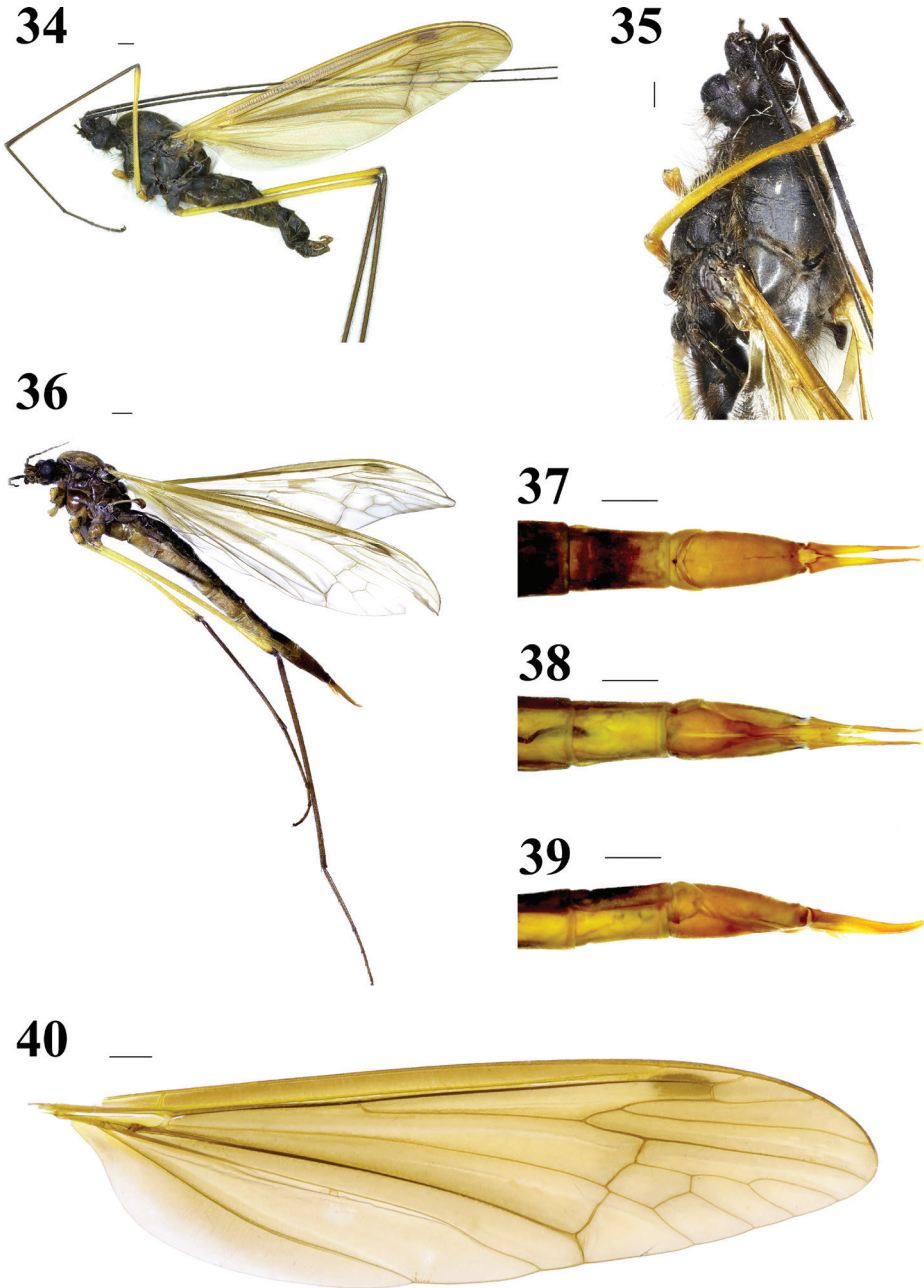
Figures 34–40. *Hexatoma* (*Eriocera*) *perhirsuta* Alexander, 1973 **34** male habitus, lateral view **35** male head and thorax, dorsal view **36** female habitus, lateral view **37** ovipositor, dorsal view **38** ovipositor, ventral view **39** ovipositor, lateral view **40** right wing. Scale bars: 1 mm (34–40).

Thorax (Figs 34–35) dark brown with abundant very long brownish yellow setae. Legs: coxae dark brown with abundant very long brownish yellow setae; trochanters brownish yellow with long brownish yellow setae; femora yellow with short brownish

41 ——   **42** ——

43   **44**   **45**
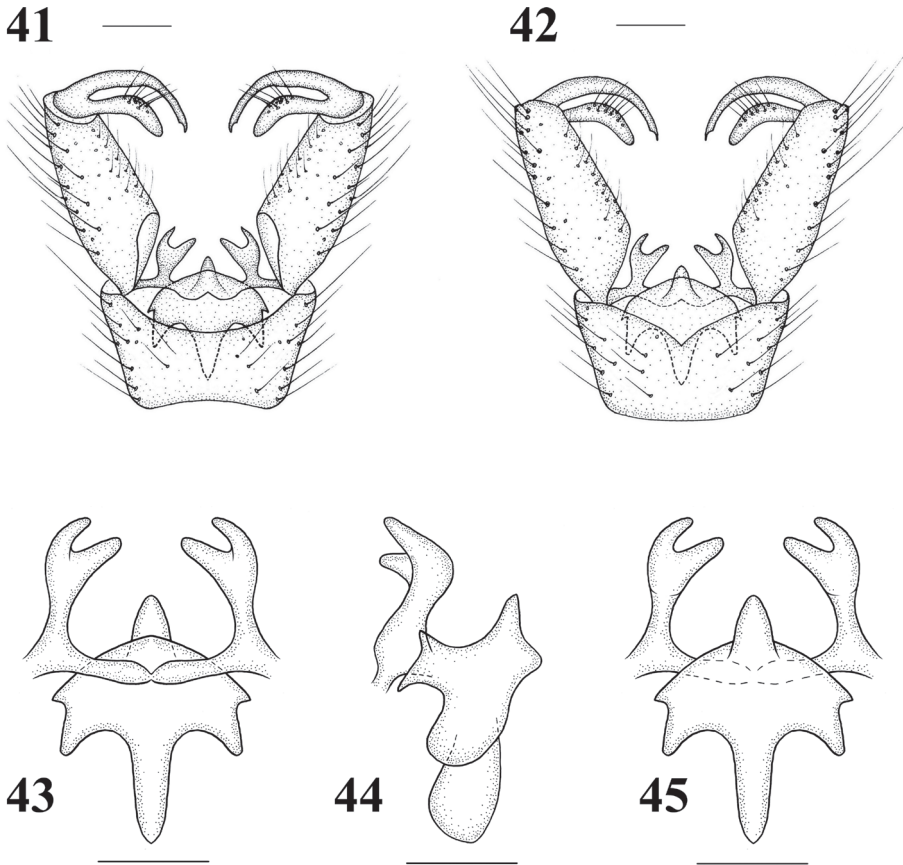
Figures 41–45. *Hexatoma* (*Eriocera*) *perhirsuta* Alexander, 1973, male **41** terminalia, dorsal view **42** terminalia, ventral view **43** aedeagal complex, dorsal view **44** aedeagal complex, lateral view **45** aedeagal complex, ventral view. Scale bars: 0.5 mm (41–45).

yellow setae; tibiae and tarsi brown with short brown setae. Wing (Figs 34, 40) brownish yellow, stigma slightly brown; veins slightly brown, very inconspicuous against the ground. Venation: R_2 moderately straight; R_{2+3} nearly three times as long as R_{2+3+4}; cell M_1 slightly longer than its petiole; *m-cu* near 1/6 of cell *dm*. Halter (Figs 34–35) length approximately 3.2 mm, halter stem grayish brown with brown setae; knob brown.

Abdomen (Fig. 34) with abundant very long brownish yellow setae. First three segments brown; segments 4–8 dark brown.

Male terminalia (Figs 34, 41–45) brown with long brownish yellow setae. Posterior margin of ninth tergite with a deep U-shaped notch; posterior margin of ninth sternite with a deep V-shaped shallow; gonocoxite large, elongate cylindrical; clasper of gonostylus long and slender, terminal spine decurved; lobe of gonostylus short and stout, swollen with setae at middle; interbase well-developed, a two-layered membranous structure with spine-like apex; aedeagus smaller.

Female (*N*=2): Body length 21.3–24.7 mm, wing length 19.6–22.5 mm, antenna length 3.1–3.5 mm.

Female (Figs 36–39) resembles male. Thorax more brownish yellow. Abdomen longer, venter more brownish yellow.

Ovipositor (Figs 36–39) elongate, reddish yellow. Cercus narrowed toward tip. Hypogynial valve shorter, narrowed toward tip.

Distribution. India (Assam); China (Xizang).

Remarks. This species was known previously only from India. This is the first record from China.

Hexatoma (*Eriocera*) *xizangensis* sp. nov.

http://zoobank.org/72D7BB50-F2AB-40AC-AA95-C86E200960B1

Figs 46–48; 50–54

Type material. *Holotype*: male (CAU), China: Xizang, Beibeng, Jiangxincun, 2019.V.30, Qicheng Yang (light trap).

Diagnosis. Femora are yellow. Wing is brownish yellow with the following markings: an oblique transverse hyaline marking from R extended up to CuA in base of wing; origin of Rs with a small hyaline marking; a longer oblique transverse hyaline marking from R extended to wing margin before cord; both sides of R_2 with a hyaline marking; tip of R_1 from Sc to R_3 with an oblique transverse hyaline marking. R_2 is moderately oblique, approximately as long as R_{3+4}, placed before fork of R_{3+4}; cell M_1 is lacking; m-cu is near 2/3 of cell dm. Abdomen is brown to darker brown except segments 8–9 yellow. Posterior margin of ninth tergite has two small triangular processes; interbase is cylindrical, but stubby at base.

**Description.** Male (*N* = 1): Body length 8.8 mm, wing length 7.2 mm.

Head (Figs 46) brown with long brown setae. Rostrum very short, brownish yellow; palpi brown. Antennal scape brown with brown setae; pedicel brownish yellow; flagellum is broken.

Thorax (Figs 46, 47) brown with long brown setae. Legs: coxae and trochanters brown with long brown setae; femora and tibiae yellow with brown setae; basal two segments of tarsi yellow with brown setae, reminder segments brownish yellow to brown with brown setae. Wing (Figs 46, 48) brownish yellow, anal cells more yellow; anal cells with hyaline markings at base; an oblique transverse hyaline marking from R extended up to CuA in base of wing; origin of Rs with a small hyaline marking; a longer oblique transverse hyaline marking from R extended to wing margin before cord; both sides of R_2 with a hyaline marking; tip of R_1 from Sc to R_3 with an oblique transverse hyaline marking; veins slightly brown, very inconspicuous against ground. Venation: R_2 oblique, approximately as long as R_{3+4}, placed before fork of R_{3+4}; cell M_1 lacking; m-cu near 2/3 of cell dm. Halter (Figs 46, 47) length approximately 1.2 mm, pale brown.

Abdomen (Fig. 46) with brown setae. Segments 1–5 brown, segments 6–7 dark brown, segment 8 yellow.
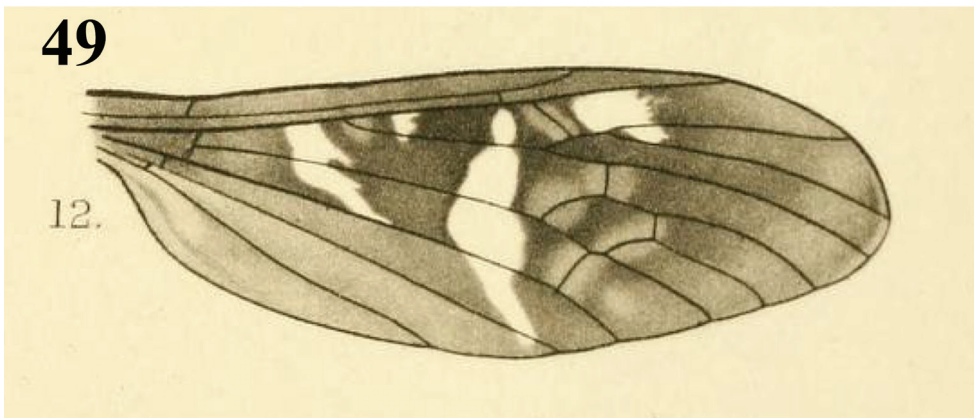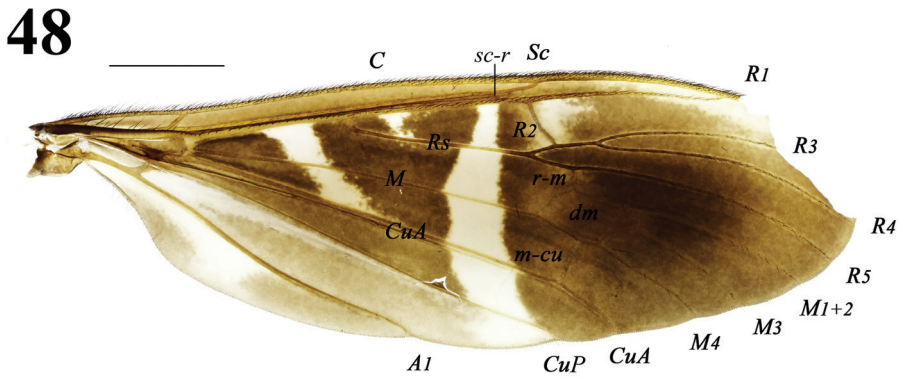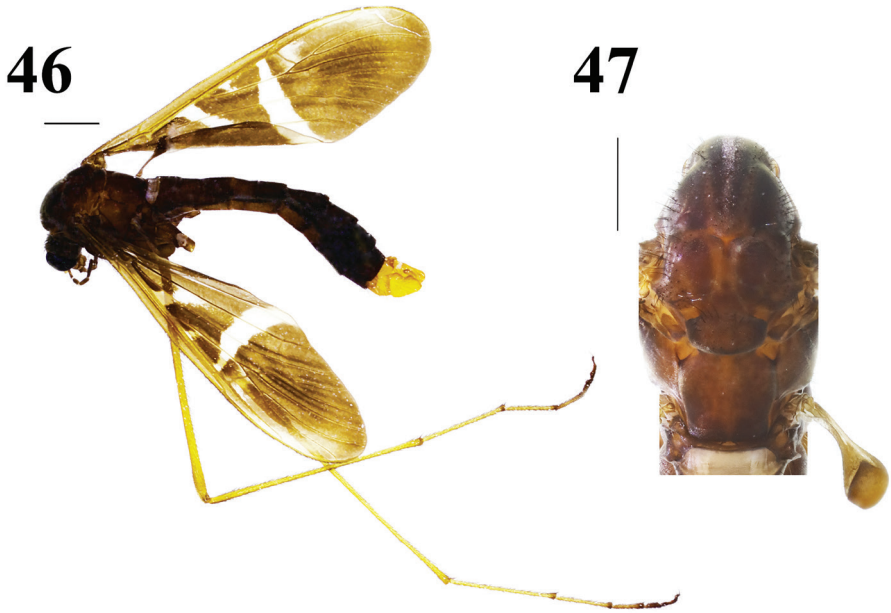
Figures 46–49. 46–48 *Hexatoma* (*Eriocera*) *xizangensis* sp. nov., male **46** habitus, lateral view **47** male thorax, dorsal view **48** right wing **49** wing of *Hexatoma* (*Eriocera*) *decorata* (Brunetti, 1918: plate VII, fig. 12). Scale bars: 1.0 mm (46–48).
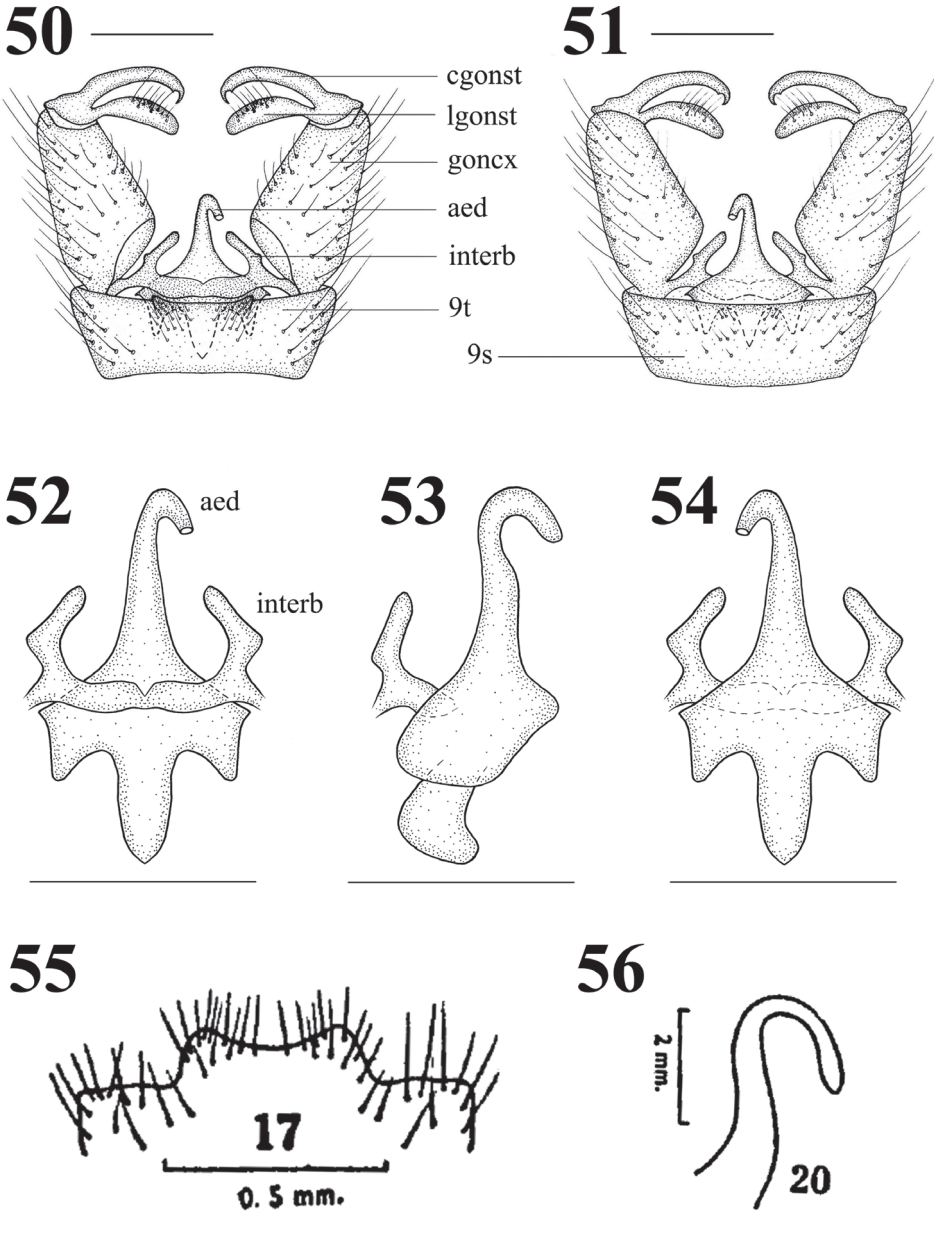
Figures 50–56. 50–54 *Hexatoma* (*Eriocera*) *xizangensis* sp. nov., male **50** terminalia, dorsal view **51** terminalia, ventral view **52** aedeagal complex, dorsal view **53** aedeagal complex, lateral view **54** aedeagal complex, ventral view **55–56** *Hexatoma* (*Eriocera*) *decorata* (Brunetti, 1918), male. **55** ninth tergite (Joseph, 1977: 427, fig. 17) **56** aedeagus (Joseph, 1977: 427, fig. 20). Scale bars: 0.5 mm (50–54).

Male terminalia (Figs 46, 50–54) yellow with brownish yellow setae. Posterior margin of ninth tergite with two small triangular processes, with abundant brown setae; gonocoxite moderately stubby; clasper of gonostylus slender, terminal spine

decurved; lobe of gonostylus short and stout, middle margin swollen with setae; interbase cylindrical, stubby at base; aedeagus longer, apically directed ventrally.

Female. Unknown.

Distribution. China (Xizang).

Etymology. The species is named after Xizang Autonomous Region, where the type locality is located.

Remarks. This new species is very similar to *H.* (*E.*) *decorata* (Brunetti, 1918) from India (W Bengal) in having similar wing markings, but can be separated from it by the wing with a longer oblique transverse hyaline marking from *R* extended to wing margin before cord (Figs 46, 48) and the posterior margin of the ninth tergite with two small triangular processes (Fig. 50). In *H.* (*E.*) *decorata*, the oblique transverse hyaline marking from *R* extends to the *CuP* before the cord (Fig. 49 i.e., Brunetti, 1918: plate VII. fig. 12; Edwards, 1924: 304; Joseph, 1977: 427, fig. 16) and the posterior margin of the ninth tergite is produced, its margin concave (Fig. 55 i.e., Joseph, 1977: 427, fig. 7). These two species are very special within the subgenus *Eriocera*, because of their unique position and slope of vein R_2 (Fig. 46, 48–49): it contacts vein R_{3+4} (and not vein R_3 as is common in all *Eriocera* with a short vein R_{2+3+4}), and is sloping forwards (also a very uncommon feature in *Eriocera*).

Acknowledgements

References

Alexander CP (1933) New or little-known Tipulidae from eastern Asia (Diptera). XV. Philippine Journal of Science 52: 131–166.

Alexander CP (1948) Notes on the tropical American species of Tipulidae (Diptera). V. The specialized Hexatomini: *Limnophila*, *Shannonomyia*, *Gynoplistia*, *Hexatoma*, *Atarba*, *Elephantomyia*, and allies. Revista de Entomologia 19: 509–556.

Alexander CP (1963) Classification and synonymy of the crane-flies described by Enrico Brunetti (Diptera: Families Ptychopteridae, Trichoceridae and Tipulidae). Records of the Indian Museum 59: 19–34.

Alexander CP (1968) The crane flies (Trichoceridae and Tipulidae: Diptera). Khumbu Himal 3: 82–100.

Alexander CP (1971) New exotic crane-flies (Tipulidae: Diptera). Part XXI. Entomological News 82: 113–120.

Alexander CP (1973) Undescribed species of crane flies from the Himalaya mountains (Diptera: Tipulidae). XXI. Journal of the New York Entomological Society 81: 3–9.

Alexander CP, Byers GW (1981) Tipulidae. In: McAlpine JF, Peterson BV, Shewell GE, Teskey HJ, Vockeroth JR, Wood DM (Eds) Manual of Nearctic Diptera. Vol. 1. Biosystematics Research Institute, Ottawa, Ontario, Monograph 27: 153–190.

Alexander CP, Lloyd JT (1914) The biology of the North American crane-flies (Tipulidae, Diptera). I. The genus *Eriocera* Macquart. Journal of Entomology and Zoology 6: 12–34. https://doi.org/10.5962/bhl.part.26522

Brunetti E (1918) Revision of the Oriental Tipulidae with descriptions of new species, Part 2. Records of the Indian Museum 15: 255–344.

de Jong H (2017) Limoniidae and Tipulidae (crane flies). In: Kirk-Spriggs AH, Sinclair BJ (Eds) Manual of Afrotropical Diptera. Volume 2. Nematocerous Diptera and Lower Brachycera. Suricata 5. South African National Biodiversity Institute, Pretoria 427–477.

Edwards FW (1921) The Old-World species of *Eriocera* in the British Museum collection (Diptera, Tipulidae). Annals and Magazine of Natural History (9)8: 67–99. https://doi.org/10.1080/00222932108632559

Edwards FW (1924) Notes on the types of Diptera Nematocera (Mycetophilidae and Tipulidae), described by Mr. E. Brunetti. Records of the Indian Museum 26: 291–307.

Joseph ANT (1977). The Brunetti types of Tipulidae (Diptera) in the collection of the Zoological Survey of India. Part IX. The genera *Limnophila*, *Hexatoma* and *Atarba*. Oriental Insects 11: 421–448. https://doi.org/10.1080/00305316.1977.10433825

Men Q, Yu D (2015) One new species of the subgenus *Hexatoma* (*Eriocera*) Macquart (Diptera, Limoniidae) from China, with a key to Chinese species. ZooKeys 477: 157–171. https://doi.org/10.3897/zookeys.477.7570

Mitra B, Lahiri AR, Mukherjee M (2006) Insecta: Diptera: Nematocera. State Fauna Series 13, Fauna of Arunachal Pradesh 2: 225–255.

Oosterbroek P (2021) Catalogue of the Craneflies of the World, (Diptera, Tipuloidea, Pediciidae, Limoniidae, Cylindrotomidae, Tipulidae). http://ccw.naturalis.nl/. Accessed on: 2020-05-07.

Podenas S, Geiger W, Haenni JP, Gonseth Y, (2006) Limoniidae & Pediciidae de Suisse. Fauna Helvetica 14: 1–375.

Podeniene V, Gelhaus JK (2015) Review of the last instar larvae and pupae of *Hexatoma* (*Eriocera*) and *Hexatoma* (*Hexatoma*) (Diptera, Limoniidae, Limnophilinae). Zootaxa 4021: 93–118. https://doi.org/10.11646/zootaxa.4021.1.4

Ribeiro GC (2006) Homology of the gonostylus parts in crane flies, with emphasis on the families Tipulidae and Limoniidae (Diptera: Tipulomorpha). Zootaxa 1110: 47–57. https://doi.org/10.11646/zootaxa.1110.1.5

Ribeiro GC (2008) Phylogeny of the Limnophilinae (Limoniidae) and early evolution of the Tipulomorpha (Diptera). Invertebrate Systematics 22: 627-694. https://doi.org/10.1071/IS08017

Savchenko EN (1986) Komary-limoniidy [Limoniid-flies]. (General description, subfamilies Pediciinae and Hexatominae). Fauna Ukrainy 14(2): 1–380.

Walker F (1848) List of the specimens of dipterous insects in the collection of the British Museum. London 1: 1–229.

Westwood JO (1836) Insectorum nonnullorum novorum (ex ordine Dipterorum) descriptiones. Annales de la Société Entomologique de France (1) 4: 681–685.

RESEARCH ARTICLE

New genetic data reveals a new species of *Zospeum* in Bosnia (Gastropoda, Ellobioidea, Carychiinae)

Thomas Inäbnit[1], Adrienne Jochum[2,3,4], Raijko Slapnik[5], Eike Neubert[2,3]

1 *Institute for Biochemistry & Biology, University of Potsdam, Karl-Liebknecht-Strasse 24-25, House 26, 14476, Potsdam, Germany* **2** *Natural History Museum of the Burgergemeinde Bern, Bernastrasse 15, 3005, Bern, Switzerland* **3** *Institute of Ecology and Evolution, University of Bern, Baltzerstrasse 6, 3012, Bern, Switzerland* **4** *Senckenberg Research Institute and Natural History Museum, Senckenberganlage 25, 60325 Frankfurt/M, Germany* **5** *Drnovškova pot 2, Mekinje, SI - 1240 Kamnik, Slovenia*

Corresponding author: Thomas Inäbnit (inaebnit.thomas@gmail.com)

Citation: Inäbnit T, Jochum A, Slapnik R, Neubert E (2021) New genetic data reveals a new species of *Zospeum* in Bosnia (Gastropoda, Ellobioidea, Carychiinae). ZooKeys 1071: 175–193. https://doi.org/10.3897/zookeys.1071.66417

Abstract

Recent integrative investigations of the terrestrial ellobiid genus, *Zospeum*, have revealed significant findings concerning its Alpine-Dinaric evolution and taxonomy. Due to the expected discrepancy between the useful, but limited, 1970s' classification system based on shell data and the results of recent genetic analyses in the latest investigation, a revision of the entire radiation was undertaken, and a new classification system was devised by the present authors in an earlier paper. Concurrent to this work, molecular sequences from two Austrian caves were published independently of our revision by another research group. By incorporating these genetic data within our phylogenetic framework here, we show that the Austrian individuals are genetically most similar to *Zospeum amoenum* and consequently, classify them within that species. We additionally reveal two new genetic lineages from the largely under-sampled southern extension of *Zospeum's* known distributional range. The first lineage, deriving from the region of Dubrovnik, Croatia, is a potential candidate for genetically clarifying *Zospeum troglobalcanicum*. The second lineage derives from the municipality of Tomislavgrad, Bosnia-Herzegovina and is herein, described a new species: *Zospeum simplex* Inäbnit, Jochum & Neubert, sp. nov.

Keywords

Dinarides, microsnails, molecular phylogenetics, shell variability, subterranean ecology, troglobitic microsnails

Introduction

The carychiid genus, *Zospeum*, consists of tiny (0.9–2.6 mm), troglobitic snail species that are distributed in two disjunct areas: a western zone, comprising the western Pyrenees and the Cantabrian mountains of Spain and France (Jochum et al. 2015a, 2019) and an eastern zone, encompassing the southeastern Alps and Dinarides of northeastern Italy, southern Austria, Slovenia, Croatia, Bosnia-Herzegovina and Montenegro (see Inäbnit et al. 2019). This work addresses the species rich, eastern radiation of *Zospeum*.

Until recently, the eastern radiation of *Zospeum* was largely classified using a scheme devised by Bole (1974), based solely on shell morphology. More recent studies (Weigand et al. 2011; Weigand et al. 2013; Jochum et al. 2015b), however, found Bole's (1974) scheme, though effective for its time, now incongruent with genetic data, leading to a thorough revision by Inäbnit et al. (2019). They subdivided the eastern *Zospeum* radiation into 25 species that could be divided genetically into five species groups: the *Z. spelaeum* group (northeastern Italy, Slovenia, north-western Croatia; five species), the *Z. alpestre* group (Slovenian Alps and adjacent regions in Italy and Austria; four species), the *Z. obesum* group (southwestern Slovenia and adjacent Croatia; two species), the *Z. pretneri* group (Croatia, more or less close to the Adriatic coast; four species), and the *Z. frauenfeldii* group (southern Slovenia, northwestern Croatia, northwestern Bosnia-Herzegovina; five species); five species could not be assigned to any of the five groups due to lack of molecular data.

One of the issues raised in Inäbnit et al. (2019) is that *Zospeum*'s eastern distribution has been unevenly sampled throughout its history. Most studies covered almost only Slovenian (e.g., Frauenfeld 1854, 1856; Freyer 1855; Bole 1974; Weigand et al. 2013), Italian (Pezzoli 1992 and papers cited therein) and northwestern Croatian populations (Slapnik and Ozimec 2004; Inäbnit et al. 2019). The consequence of this sampling disparity is that we have very limited records from southern Croatia, Bosnia-Herzegovina and Montenegro (see Inäbnit et al. 2019: fig. 1a), none of which include genetic data. In fact, the only species described from the southern half of the *Zospeum*'s distribution range is *Zospeum troglobalcanicum* Absolon 1916. Shells that obviously belong to different species exist in museum collections (see Inäbnit et al. 2019: fig. 10W-Z; Gittenberger 1975), but genetic data from these southernmost populations is still lacking for a contemporary, integrative taxonomic assessment. In the current study, we add new sequences from 12 specimens, collected in southern Croatia and Bosnia-Herzegovina to the existing genetic dataset.

Approximately the same time as the revision by Inäbnit et al. (2019) was published, Kruckenhauser et al. (2019) published the results of a small barcoding study of specimens from Austria (for locations see Fig. 1). Due to this unfortunate overlap, their results could not be incorporated into the classification system proposed by Inäbnit et al. (2019). We have however, included these results in our work here.

Materials and methods

Material is housed in the following collections:

AJC   Adrienne Jochum Collection, Kelkheim, Germany;
MCSMNH Malacological Collection of the Slovenian Museum of Natural History (former CSR SASA, MZBI & SMNH) Ljubljana, Slovenia;
NHMW Naturhistorisches Museum Wien, Wien, Austria;
NMBE   Naturhistorisches Museum der Burgergemeinde Bern, Bern, Switzerland;
RSC   Rajko Slapnik Collection, Kamnik, Slovenia;
SMF   Senckenberg Forschungsinstitut und Naturmuseum, Frankfurt am Main, Germany.

In order to preserve the shell from dissolution during the extraction, our DNA extraction protocol was based on a method initially described in Schizas et al. (1997) and partially modified after Böttger-Schnack and Machida (2011). DNA extraction was conducted on 12 ethanol-preserved individuals (NMBE 568052-568063). Each specimen was inserted into a 0.2-ml PCR-tube and dried at room temperature. Eight µl ddH$_2$O and 2 µl 5× PCR-buffer (Promega 5× Colorless GoTaq Reaction Buffer) were added and the mixture was heated at 94 °C for 2 min. whereby 1.3 µl proteinase K solution (from the DNEasy Blood and tissue kit, Qiagen) were then added and the solution was homogenised and then incubated in a PCR-thermocycler at 55 °C for 15 min., afterwards at 70 °C for 10 min. The incubation was repeated once. Ten µl of Gene Releaser (Bioventures Inc.) were then added and the mixture was inserted into a thermocycler with the following protocol: 65 °C for 30 s, 8 °C for 30 s, 65 °C for 1.5 min., 97 °C for 3 min., 8 °C for 1 min., 65 °C for 3 min., 97 °C for 1 min., 65 °C for 1 min., 80 °C for 5 min. The mixture, including the intact shell, was centrifuged for 1 min. using a table centrifuge and the clear phase with the DNA was transferred to another 0.2 mL PCR-tube, where 15 µl of AE-Buffer (DNeasy Kit, Qiagen) was added. The shell was cleaned from the remains of the Gene Releaser chemicals by rinsing with 80% EtOH.

We used five markers, two mitochondrial (COI (658 bp), 16S (483 bp)) and three nuclear markers (H3 (330 bp), ITS2 (809 bp), 28S (590 bp)) with a total length of 2870 bp (for primers, see Table 1).

The PCR-solution included the following admixture: 2 µl template, 12.5 µl GoTaq (Promega) polymerase, 8.5 µl of nuclease-free water, and 1 µl of both forward and reverse primer (10 µmol) respectively. In cases where the PCR signal was judged too weak, the reaction was repeated using 3 µl template DNA, 3 µl of the previous PCR product, and 5.5 µl of nuclease-free water. The amount of GoTaq and primers remained the same. The amplification was conducted using the following cycling protocols: For COI, the admixture was first heated up to 95 °C for 1 min, followed by 30 cycles of 30 s (of denaturation at 95 °C for 30 s, annealing at 52 °C for 30 s, extension
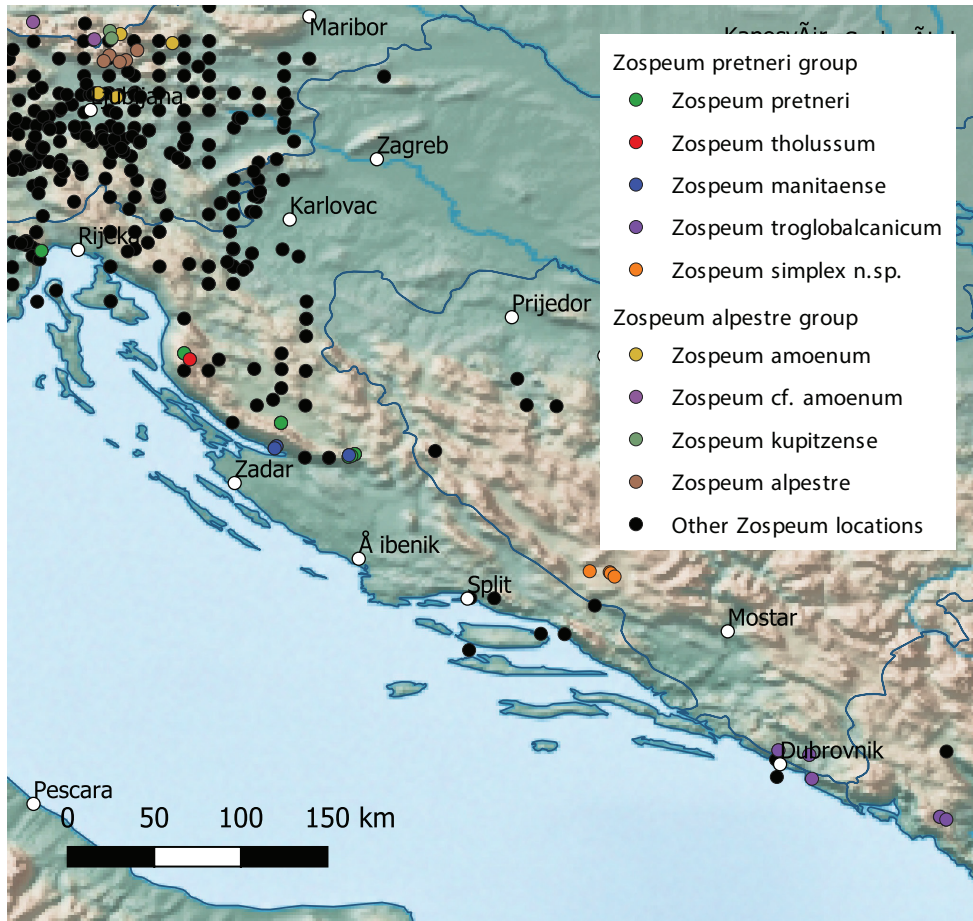
Figure 1. Map showing the distribution of the *Zospeum pretneri* group and the *Zospeum alpestre* group (except *Z. isselianum*). Austrian specimens from Kruckenhauser et al. (2019) are labelled as "*Z.* cf. *amoenum*".

at 72 °C for 1 min), and a final extension at 72 °C for 3 min. For 16S, the protocol started with 2:30 min at 90 °C, followed by 10 cycles of 30 s at 92 °C, 30 s at 44 °C, and 40 s at 72 °C, followed again by 30 s at 92 °C, 40 s at 48 °C, and 40 s at 48 °C. The protocol for 28S started with 1 min at 96 °C, then went into 35 cycles of 30 s at 94 °C, 30 s at 50 °C, and 1 min at 72 °C, finishing with 10 min at 72 °C. The ITS2 protocol started with 1 min at 96 °C, followed by 35 cycles of 30 s at 94 °C, 30 s at 44 °C, and 1 min at 72 °C, ending with 10 min at 72 °C. For H3, the admixture was first heated up to 95 °C for 3 min, followed by 40 cycles of 45 s at 94 °C, 45 s at 50 °C, and 2 min at 72 °C, finishing with 10 min at 72 °C. The protocols for COI and H3 could be used for both markers. The PCR products were sequenced at the LGC Genomics GmbH (Berlin, Germany) using their standard protocol.

Sequences received from LGC were imported into the Geneious 5.4.7 software (Kearse et al. 2012). The forward and reverse sequences for each gene and individual

Table 1. Primers used in this study.

Marker	Primer Name	Primer sequence	Reference
COI	LCO1490 (F)	5'-GGTCAACAAATCATAAAGATATTGG-3'	Folmer et al. (1994)
COI	HCO2198 (R)	5'-TAAACTTCAGGGTGACCAAAAAATCA-3'	Folmer et al. (1994)
16S	16S F	5'-CGGCCGCCTGTTTATCAAAAACAT-3'	Palumbi et al. (1991)
16S	16S R	5'-GGAGCTCCGGTTTGAACTCAGATC-3'	Palumbi et al. (1991)
28S	LSU-2 (F)	5'-GGGTTGTTTGGGAATGCAGC-3'	Wade and Mordan (2000)
28S	LSU-4 (R)	5'-GTTAGACTCCTTGGTCCGTC-3'	Wade and Mordan (2000)
ITS2	ITS2ModA (F)	5'-GCTTGCGGAGAATTAATGTGAA-3'	Bouaziz-Yahiatene et al. (2017)
ITS2	ITS2ModB (R)	5'-GGTACCTTGTTCGCTATCGGA-3'	Bouaziz-Yahiatene et al. (2017)
H3	H3-F	5'-ATGGCTCGTACCAAGCAGAC(ACG)GC-3'	Colgan et al. (1998)
H3	H3-R	5'-ATATCCTT(AGGGCAT(AG)AT(AG)GTG-3'	Colgan et al. (1998)

were combined and edited. In addition to the sequences that were generated during this study, we used the sequences previously used and generated in Inäbnit et al. (2019), as well as those generated by Kruckenhauser et al. (2019). The name of some of the Spanish specimens were updated based on the results of Jochum et al. (2019). A total list of samples can be found in Table 2. For each marker, sequences were aligned in Geneious using the MAFFT multiple sequence alignment plugin version 1.3.6 (based on MAFFT v7.308; Katoh et al. 2002; Katoh and Standley 2013), allowing the program to choose the most appropriate algorithm. The sequence length of each alignment was standardised to the length mentioned above.

Topologies were estimated using two different phylogenetic methods: Maximum Likelihood (**ML**) and Bayesian Inference (**BI**). The five markers were set as partitions in both of these methods, using a distinct model for the third codon in protein-coding genes (COI, H3). The maximum likelihood (ML) topology was estimated using the RAxML 7.2.8 (Stamatakis 2014) plugin of Geneious with the GTR gamma nucleotide model and 1000 bootstrap replicates. An additional ML tree was calculated for the *Z. pretneri* group (with *Z. robustum* NMBE 548777 as an outgroup) without H3 and 28S.

The Bayesian tree was reconstructed with MrBayes 3.2.6 (Huelsenbeck and Ronquist 2001) using the substitution models suggested by PartitionFinder (Lanfear et al. 2016, Lanfear et al. 2012, Guindon et al. 2010), a Markov Chain Monte Carlo (MCMC) chain length of 10000000 generations, a subsampling frequency of every 4000 generations, the first 100000 generations were discarded as burn-in, four heated chains and a chain temperature parameter of 0.2. Calculations were performed on the UBELIx (http://www.id.unibe.ch/hpc), the HPC cluster at the University of Bern.

The single gene alignments of COI, 16S, and ITS2 were imported into MEGA X 10.1.7 (Kumar et al. 2018) and the various sequences grouped into species. The average evolutionary divergence between sequence pairs within species (subsequently referred to as within-species divergence) was estimated where possible (only for species with more than one sequence present) using the Maximum Composite Likelihood model (Tamura et al. 2004) on standard settings. The Maximum Composite Likelihood model was also used to estimate the average evolutionary divergence between sequence pairs between species (subsequently referred to as between-species divergence). The focus of the analyses lay on the *Z. pretneri* group (as defined by Inäbnit et al. 2019;

Table 2. Specimens used in this study. Italicised accession numbers indicate sequences taken from BOLD, not italicised numbers are from GenBank.

Species	Source	Collection number	Locality	Coordinates	COI	16S	H3	28S	ITS2
Carychium tridentatum (Risso, 1826)	Inäbnit et al 2019	NMBE 549936	Taunus, Eppstein, Germany	50.1601, 8.3846	MH383001	MH382969	MH383018	MH382989	MH383038
Z. vasconicum Prieto, De Winter, Weigand, Gómez & Jochum, 2015	Weigand et al. 2013	AJC 1875a	Cueva del Cráneo, Dima, Bizkaia, Spain	43.1287, -2.7348	*BAR-CA206-12*	KC206116	KC206249	—	—
	Weigand et al. 2013	AJC 1874b	Cueva Silibranka II, Manaria, Bizkaia, Spain	43.287, -2.945	*BAR-CA206-12*	KC206117	KC206248	—	—
	Weigand et al. 2013	AJC 1847c	Cueva de Ermita de Sandaili, Valle de Araotz, Bizkaia, Spain	42.9994, -2.4381	KM281092	KC206119	KC206247	—	—
Z. cf. *schaufussi*	Weigand et al. 2013	AJC 1878a	Cueva de Las Paúles, Monte Santiago, Castilla y León, Spain	43.1282, -2.7362	*BAR-CA194-12*	KC206113	KC206252	—	—
	Weigand et al. 2013	AJC 1844b	Cueva de los Cuervos, Barranco de Aranaga, Bizkaia, Spain	43.2829, -3.2588	*BAR-CA192-12*	KC206120	KC206246	—	—
Z. praetermissum Jochum, Prieto & De Winter 2019	Weigand et al. 2013; Romero et al. 2017	AJC 1842a	Cueva del Bosque, Inguanzo, Asturias, Spain	43.3123, -4.8724	KM281091	KC206121	KC206245	KM281051	—
Z. zaldivarae Prieto, De Winter, Weigand, Gómez & Jochum, 2015	Weigand et al. 2013	AJC 1876c	Cueva de Las Paúles, Monte Santiago, Castilla y León, Spain	43.1282, -2.7362	*BAR-CA209-12*	KC206114	KC206251	—	—
	Weigand et al. 2013	AJC 1876b	Cueva de Las Paúles, Monte Santiago, Castilla y León, Spain	43.1282, -2.7362	*BAR-CA208-12*	KC206115	KC206250	—	—
Z. costatum Freyer, 1855	Weigand et al. 2013	NMBE 553383	Jama 2 pri Jabljah, Loka pri Mengšu, Slovenia	46.1426, 14.5533	HQ171599	KC206158	KC206208	—	—
	Weigand et al. 2013	NMBE 553383	Jama 2 pri Jabljah, Loka pri Mengšu, Slovenia	46.1426, 14.5533	HQ171601	KC206159	KC206207	—	—
Z. spelaeum (Rossmaessler, 1838)	Weigand et al. 2013	NMBE 553316	Grotte Bac, Trieste Municipality, Trieste Prov., Italy	45.6361, 13.8717	*BAR-CA182-12*	KC206110	KC206255	—	—
	Weigand et al. 2013	AJC 1898a	Grotte Bac, Trieste Municipality, Trieste Prov., Italy	45.6361, 13.8717	*BAR-CA184-12*	KC206108	KC206257	—	—
	Weigand et al. 2013	NMBE 553316	Grotte Bac, Trieste Municipality, Trieste Prov., Italy	45.6361, 13.8717	—	KC206109	KC206256	—	—
	Weigand et al. 2013	NMBE 553314	Grotte d'Ercole, near Gabrovizza, Trieste Prov., Italy	45.731, 13.7261	*BAR-CA181-12*	KC206111	KC206254	—	—
	Weigand et al. 2013	NMBE 553311	Velika Pasica, Gornji Ig, Slovenia	45.9189, 14.4934	*BAR-CA179-12*	KC206135	KC206231	—	—
Z. iselianum Pollonera, 1887	Inäbnit et al. 2019	NMBE 554396	Horiške Ponikve, Horičina, Slovenia	45.5735, 14.0309	MH382992	MH382954	MH383022	MH382974	MH383024
	Weigand et al. 2013	NMBE 553389	Turjeva jama, Robič, Kobarid, Slovenia	46.2435, 13.5046	HQ171594	KC206097	KC206268	—	—
Z. amoenum (Frauenfeld, 1856)	Inäbnit et al. 2019	RS 2037	Ihanščica, Ihan, Ljubljana, Slovenia	46.1216, 14.6476	MH383003	MH382971	MH383020	—	—
	Weigand et al. 2013	NMBE 553378	Konečka zijalka, Šmihel nad Mozirjem, Mozirje, Slovenia	46.4024, 14.9393	*BAR-CA123-10*	KC206179	KC206187	—	—
	Weigand et al. 2013	NMBE 553378	Konečka zijalka, Šmihel nad Mozirjem, Mozirje, Slovenia	46.4024, 14.9393	*BAR-CA124-10*	KC206178	KC206188	—	—
	Jochum et al. 2015	MCSMNH 40600a	Potočka zijalka, Olševa, Slovenia	46.4493, 14.6693	*BAR-CA211-13*	—			—

Species	Source	Collection number	Locality	Coordinates	COI	16S	H3	28S	ITS2
Z. amoenum (Frauenfeld, 1856)	Jochum et al. 2015	MCSMNH 40600a-2	Potočka zijalka, Olševa, Slovenia	46.4493, 14.6693	BAR-CA212-13	—	—	—	—
Z. cf. amoenum	Kruckenhauser et al. 2019	NHMW109000/AL/01821/8139	Steiner Lehmhöhle, Austria	46.42228, 14.53462	AMOL570-19	—	—	—	—
	Kruckenhauser et al. 2019	NHMW109000/AL/01821/8140	Steiner Lehmhöhle, Austria	46.42228, 14.53462	AMOL571-19	—	—	—	—
	Kruckenhauser et al. 2019	NHMW109000/AL/01822/8141	Hafnerhöhle, Austria	46.51200, 14.21623	AMOL572-19	—	—	—	—
	Kruckenhauser et al. 2019	NHMW109000/AL/01822/8142	Hafnerhöhle, Austria	46.51200, 14.21623	AMOL573-19	—	—	—	—
Z. alpestre (Freyer, 1855)	Weigand et al. 2013	NMBE 553391	Jama pod Mokrico, Kamniška Bistrica, Slovenia	46.3093, 14.5832	HQ171593	KC206099	KC206266	—	—
	Inäbnit et al. 2019	MCSMNH 40651a	Jelenska zijalka, Raduha, Slovenia	46.3656, 14.7567	MH383002	MH382970	MH383019	MH382990	MH383039
Z. kupitzense A. Stummer, 1984	Weigand et al. 2013; Romero et al. 2017	NMBE 553393	Ložekarjeva zijalka, Solčava, Slovenia	46.4268, 14.624	BAR-CA125-10	KC206150	KC206216	KM281049	—
Z. exiguum Kuščer, 1932	Inäbnit et al. 2019	NMBE 548774	Jama Borušnjak 3, Lupoglav, Čičarija, Istra	45.3702, 14.1841	MH382994	MH382959	MH383009	MH382979	MH383030
	Weigand et al. 2013	NMBE 553384	Križna jama, Lož, Cerknica, Slovenia	45.7452, 14.4673	HQ171582	KC206162	KC206204	—	—
	Weigand et al. 2013	NMBE 553384	Križna jama, Lož, Cerknica, Slovenia	45.7452, 14.4673	HQ171585	KC206163	KC206203	—	—
Z. obesum (Frauenfeld, 1854)	Weigand et al. 2013	NMBE 553409	Krška jama, Krška vas, Slovenia	45.8899, 14.7711	BAR-CA177-12	KC206136	KC206230	—	—
	Weigand et al. 2013	NMBE 553409	Krška jama, Krška vas, Slovenia	45.8899, 14.7711	BAR-CA175-12	KC206137	KC206229	—	—
Z. pretneri Bole, 1960	Weigand et al. 2013	AJC 1370	Donja Cerovačka špilja, Kesići, Gračac, Croatia	44.2701, 15.8855	HQ171595	KC206151	KC206215	—	—
Z. tholussum Weigand, 2013	Weigand 2013	SMF 341633	Lukina jama – Trojama, Krasno, Croatia	44.7621, 15.0296	BAR-CA120-10	—	—	—	—
Z. manitaense Inäbnit, Jochum & Neubert 2019	Inäbnit et al. 2019	NMBE 548800	Manita peć, Starigrad, Croatia	44.311, 15.4792	—	MH382963	MH383012	MH382983	—
	Inäbnit et al. 2019	NMBE 548811	Manita peć, Starigrad, Croatia	44.311, 15.4792	MH383000	MH382968	MH383017	MH382988	MH383037
Z. aff. troglobalcanicum Absolon 1917	This work	NMBE 568052	Špilja Jezero, Cavtat, Konavle, Croatia	42.5858, 18.2569	MW786768	—	MW796484	MW784525	MW784537
	This work	NMBE 568053	Špilja Jezero, Cavtat, Konavle, Croatia	42.5858, 18.2569	MW786767	—	MW796485	MW784524	MW784536
Z. simplex sp. nov. Inäbnit, Jochum & Neubert	This work	NMBE 568054	Špilja Dahna, Omerovići, Bosnia and Herzegovina	43.6572, 17.2078	—	—	MW796475	—	—
	This work	NMBE 568055	Jama u kamenolomu, Cebara, Bosnia and Herzegovina	43.6517, 17.2133	MW786764	MW784509	MW796481	MW784526	MW784530
	This work	NMBE 568056	Jama u kamenolomu, Cebara, Bosnia and Herzegovina	43.6517, 17.2133	MW786765	MW784510	MW796478	MW784521	MW784532
	This work	NMBE 568057	Jama u kamenolomu, Cebara, Bosnia and Herzegovina	43.6517, 17.2133	MW786766	MW784511	MW796476	MW784520	MW784531
	This work	NMBE 568058	Jama u kamenolomu, Cebara, Bosnia and Herzegovina	43.6517, 17.2133	MW786763	MW784512	MW796477	—	MW784529

Species	Source	Collection number	Locality	Coordinates	COI	16S	H3	28S	ITS2
Z. simplex sp. nov. Inäbnit, Jochum & Neubert	This work	NMBE 568059	Vranjača, Grabovica, Bosnia and Herzegovina	43.6625, 17.1039	MW786762	MW784513	MW796486	MW784522	—
	This work	NMBE 568060	Jama Dobravljevac, Gornji Brišnik, Bosnia and Herzegovina	43.6347, 17.2328	MW786761	MW784515	MW796482	MW784527	MW784535
	This work	NMBE 568061	Jama Dobravljevac, Gornji Brišnik, Bosnia and Herzegovina	43.6347, 17.2328	MW786760	MW784516	MW796479	MW784523	MW784533
	This work	NMBE 568062	Jama Dobravljevac, Gornji Brišnik, Bosnia and Herzegovina	43.6347, 17.2328	MW786759	MW784514	MW796483	—	MW784534
	This work	NMBE 568063	Jama Dobravljevac, Gornji Brišnik, Bosnia and Herzegovina	43.6347, 17.2328	MW786758	MW784517	MW796480	MW784519	MW784528
Z. subobesum Bole, 1974	Weigand et al. 2013	NMBE 553326	Tounjčica, Tounj, Ogulin, Croatia	45.2439, 15.3253	HQ171602	KC206152	KC206214	—	—
	Weigand et al. 2013	NMBE 553326	Tounjčica, Tounj, Ogulin, Croatia	45.2439, 15.3253	HQ171604	KC206153	KC206213	—	—
	Weigand et al. 2013	NMBE 553328	Jopićeva špilja, Brebovnica, Krnjak, Karlovac, Croatia	45.2951, 15.5939	BAR-CA172-12	KC206125	KC206241	—	—
Z. frauenfeldii (Freyer, 1855)	Weigand et al. 2013	NMBE 553388	Podpeška jama, Podpeč, Dobrepolje, Slovenia	45.8393, 14.6863	HQ171587	KC206160	KC206206	—	—
	Weigand et al. 2013	NMBE 553388	Podpeška jama, Podpeč, Dobrepolje, Slovenia	45.8393, 14.6863	HQ171589	KC206161	KC206205	—	—
	Inäbnit et al. 2019	NMBE 548771	Hrustovača špilja, Hrustovo, Sanski Most, Bosnia and Herzegovina	44.6607, 16.7285	—	—	MH383006	MH382976	MH383027
Z. bucculentum Inäbnit, Jochum & Neubert 2019	Inäbnit et al. 2019	NMBE 548801	Jama na Škrilama, Netretić, Croatia	45.5277, 15.3476	MH382997	MH382964	MH383013	MH382984	MH383033
	Inäbnit et al. 2019	NMBE 548772	Pivnica špilja, Žakanje, Croatia	45.6108, 15.3617	—	MH382957	MH383007	MH382977	MH383028
	Inäbnit et al. 2019	NMBE 548806	Vrelić špilja, Donje Dubrave, Ogulin, Croatia	45.3114, 15.352	—	MH382966	MH383015	MH382986	MH383035
Z. pagodulum Inäbnit, Jochum & Neubert 2019	Inäbnit et al. 2019	NMBE 548805	Kučka jama, Lovran, Učka, Istra, Croatia	45.2985, 14.2135	MH382998	MH382965	MH383014	MH382985	MH383034
	Inäbnit et al. 2019	NMBE 548807	Grnjača špilja, Lovran, Učka, Istra, Croatia	45.2835, 14.2381	MH382999	MH382967	MH383016	MH382987	MH383036
Z. robustum Inäbnit, Jochum & Neubert 2019	Inäbnit et al. 2019	NMBE 554397	Tonkovića špilja, Ogulin, Croatia	45.3359, 15.2541	—	MH382953	MH383004	MH382973	MH383023
	Inäbnit et al. 2019	NMBE 548773	Budina špilja, Studenci, Croatia	44.7121, 15.3639	MH382993	MH382958	MH383008	MH382978	MH383029
	Inäbnit et al. 2019	NMBE 548777	Markov ponor, Lipovo polje, Croatia	44.7606, 15.1797	MH382995	MH382961	MH383010	MH382981	MH383032
	Inäbnit et al. 2019	NMBE 548787	Markov ponor, Lipovo polje, Croatia	44.7606, 15.1797	MH382996	MH382962	MH383011	MH382982	—
	Inäbnit et al. 2019	NMBE 548776	Vrlovka, Kamanje, Croatia	45.6319, 15.3934	—	MH382960	—	MH382980	MH383031
	Inäbnit et al. 2019	RS 2210a	Vrlovka, Kamanje, Croatia	45.6319, 15.3934	—	MH382972	MH383021	MH382991	MH383040
	Inäbnit et al. 2019	NMBE 554399	Židovske kuće, Cerovica, Žumberak, Croatia	45.8, 15.48	—	MH382955	—	MH382975	MH383025
	Inäbnit et al. 2019	NMBE 554400	Pušina jama, Jezemice, Žumberak, Croatia	45.7369, 15.3606	—	MH382956	MH383005	—	MH383026

all markers) and the *Z. alpestre* group (only COI, with the Austrian specimens from Kruckenhauser et al. 2019) classified as separate species or included in *Z. amoenum*.

Additionally, an Automatic Barcode Gap Discovery (**ABGD**; Puillandre et al. 2011; https://bioinfo.mnhn.fr/abi/public/abgd/abgdweb.html) analysis was performed on the COI alignments of the *Z. pretneri* group and of the *Z. alpestre* group using the default settings (Pmin = 0.001, Pmax = 0.1, Steps = 10, X = 1.5, Nb bins = 20, distance = Jukes-Cantor).

A map (Fig. 1) was constructed using the Natural Earth dataset in QGIS 3.16.3. Most locality data was taken from Inäbnit et al. (2019), and the coordinates for the Austrian sites were taken from Kruckenhauser et al. (2019). Locality data of the specimens sequenced in this study were provided by the various collectors.

Results

Phylogenetic trees

Both the ML and the BI trees (see Fig. 2 for the latter) are more or less identical. The specimens sequenced in this study clustered with *Z. pretneri*, *Z. tholussum,* and *Z. manitaense*. In both trees they form a badly supported monophyletic group that splits again into two groups in accordance with their geographical distribution (see Fig. 1) and could be separated at the species level: the two specimens from the region of Dubrovnik, Croatia (Špilja Jezero; referred to as *Z.* aff. *troglobalcanicum*), and the remaining specimens from Bosnia-Herzegovina (Jama u kamenolomu, Vranjača, Jama Dobravljevac; described as *Z. simplex* sp. nov. herein). The latter group is not supported in either tree but recovered in both. An additional specimen (NMBE 568054, Špilja Dahna), from which we were only able to amplify H3, didn't cluster with any species within the *Z. pretneri* group. The two groups were also recovered, though here with high node support, in the additional ML tree (Suplementary tree 1) calculated for the *Z. pretneri* group. The Austrian specimens from Kruckenhauser et al. (2019) form a strongly supported monophyletic group within *Z. amoenum*.

Divergences

For most markers, intraspecific divergences among the species in the *Z. pretneri* group are clearly smaller than the interspecific divergences (Table 3). This indicates that these species comprise separate lineages, especially the specimens classified as *Z.* aff. *troglobalcanicum* and those collected in Bosnia (henceforth referred to as *Z. simplex* sp. nov.), which were not included in previous genetic studies (see Inäbnit et al. 2019).

Zospeum amoenum shows a high intraspecific divergence when compared to other members of the *Z. alpestre group* (see Table 4), though other species (such as *Z.* aff. *troglobalcanicum*, see Table 3) show similarly high intraspecific divergence. When the Austrian populations from Kruckenhauser et al. (2019) are aligned within *Z. amoe-*

Table 3. The number of base substitutions per site from averaging over all sequence pairs within (within-species divergences) and between (between-species divergences) species within the *Z. pretneri* group. Results shown for each marker separately. Between-species distances are listed below the black, empty boxes, the Standard errors above.

COI								
Species	No. of sequences	Within-species divergences		Between-species divergences				
		Divergence	Standard Error	*Z. tholussum*	*Z. pretneri*	*Z. manitaense*	*Z. simplex* sp. nov.	*Z.* aff. *troglobalcanicum*
Z. tholussum	1	—	—		0.0126	0.0152	0.0148	0.0142
Z. pretneri	1	—	—	0.0602		0.0123	0.0148	0.0123
Z. manitaense	1	—	—	0.0849	0.0618		0.0161	0.0167
Z. simplex sp. nov.	9	0.0034	0.0018	0.0765	0.0779	0.0882		0.0133
Z. aff. *troglobalcanicum*	2	0.0288	0.0078	0.0777	0.0628	0.0974	0.0724	
16S								
Species	No. of sequences	Within-species divergences		Between-species divergences				
		Divergence	Standard Error	*Z. pretneri*		*Z. manitaense*		*Z. simplex* sp. nov.
Z. pretneri	1	—	—			0.0079		0.0097
Z. manitaense	2	0.0045	0.0031	0.0302				0.0078
Z. simplex sp. nov.	9	0.005	0.0022	0.0389		0.0301		
ITS2								
Species	No. of sequences	Within-species divergences		Between-species divergences				
		Divergence	Standard Error	*Z. simplex* sp. nov.		*Z. manitaense*		*Z.* aff. *troglobalcanicum*
Z. simplex sp. nov.	8	0.012	0.003			0.0055		0.0056
Z. manitaense	1	—	—	0.0226				0.0074
Z. aff. *troglobalcanicum*	2	0.0072	0.0035	0.0219		0.0278		

num, the interspecific divergence within the *Z. alpestre* group ranges between 0.0564–0.067. The between-group divergence amongst *Z. amoenum* sensu Inäbnit et al. (2019) and the specimens from Kruckenhauser et al. (2019) was smaller (0.0348±0.0071) than that amidst the other species within the *Z. alpestre* group, but still higher than the within-group divergence in both *Z. amoenum* and the Austrian specimens.

Automatic Barcode Gap Discovery (ABGD)

The ABGD run on the *Z. pretneri*-group COI alignment yielded two different possible subdivision schemes: one where the alignment was subdivided into five groups (five groups scheme; prior maximal distance P = 7.74e^{-03}; barcode gap distance: 0.043) and a second where the alignment was subdivided into seven groups (seven groups scheme; prior maximal distance P = 4.64e^{-03}; barcode gap distance: 0.003). Both subdivision schemes considered the previously published sequences of *Z. pretneri*, *Z. tholussum,* and *Z. manitaense* as separate groups. The five-group scheme separated the individuals sequenced in this study into a Croatian group (Špilja Jezero) and a Bosnian group (Jama Dobravljevac, Jama u kamenolomu, Vranjača), while the seven-group scheme separated those individuals into two Croatian groups (one for each of the two specimens from Špilja Jezero) and two Bosnian groups (1: specimens from Jama u kamenolomu; 2: specimens from Jama Dobravljevac and Vranjača).

Table 4. The number of base substitutions per site from averaging over all sequence pairs within (within-species divergences) and between (between-species divergences) species within the *Z. alpestre* group for the marker COI. Shown are results, where the four Austrian specimens were considered a separate species and where the Austrian specimens were considered conspecific with *Z. amoenum*. Between-species distances are listed below the black, empty boxes, the Standard errors above.

Species	No. of sequences	Within-species divergences		Between-species divergences				
Austrian populations treated as a separate species								
		Divergence	Standard Error	Z. amoenum	Austrian pops.	Z. alpestre	Z. isselianum	Z. kupitzense
Z. amoenum	5	0.0203	0.0048		0.0071	0.0105	0.0104	0.0118
Austrian pops.	4	0.0062	0.0026	0.0348		0.0117	0.0107	0.0126
Z. alpestre	2	0.0098	0.0039	0.0564	0.0629		0.0133	0.013
Z. isselianum	1	—	—	0.0554	0.0524	0.0693		0.0131
Z. kupitzense	1	—	—	0.067	0.0704	0.075	0.0718	
Austrian populations included in Z. amoenum								
Species	No. of sequences	Divergence	Standard Error	Z. amoenum	Z. alpestre	Z. isselianum	Z. kupitzense	
Z. amoenum	9	0.02599	0.0055		0.0109	0.0099	0.0112	
Z. alpestre	2	0.0098	0.004	0.0593		0.013	0.0129	
Z. isselianum	1	—	—	0.0541	0.0693		0.0127	
Z. kupitzense	1	—	—	0.0685	0.075	0.0718		

The ABGD run on the *Z. alpestre*-group COI alignment yielded one subdivision scheme with seven groups (prior maximal distance P = 4.64e^{-03}; barcode gap distance: 0.016): *Z. isselianum*, *Z. alpestre*, *Z. kupitzense*, *Z. amoenum* from Ihanščica, *Z. amoenum* from Konečka zijalka, *Z. amoenum* from Potočka zijalka and *Zospeum sp.* from Austria.

Taxonomic implications

Zospeum simplex Inäbnit, Jochum & Neubert, sp. nov.
http://zoobank.org/0B924616-1AC1-49B8-BE5F-531286EACE63
Figures 1, 3

Type specimens. *Holotype*: NMBE 568060, Jama Dobravljevac, 25.08.2019, leg. R. Slapnik & J. Valentinčič; *Paratypes*: NMBE 568061–568063; SMF 349425, 4 shells; RSC 3760, 6 shells; Jama Dobravljevac, 25.08.2019, leg. R. Slapnik & J. Valentinčič.

Specimens examined. NMBE 568054, Špilja Dahna, 03.09.2009, leg. A. Schoenhoffer; NMBE 568055–568058, Jama u kamenolomu, 24.08.2019, leg. R. Slapnik & J. Valentinčič; NMBE 568059, Vranjača, 24.08.2019, leg. R. Slapnik & J. Valentinčič.

Diagnosis. Shell usually ca. 1.3 mm in height, transparent, conical, peristome thickened, roundish, with a differentiated parietal shield, lamellae not present.

Measurements (n = 9): Shell height: 1.26–1.42 mm (mean: 1.378 $\pm$ 0.047 mm); shell width: 0.93–1.04 mm (mean: 0.976 $\pm$ 0.035 mm); aperture height: 0.54–0.67 mm (mean: 0.6 $\pm$ 0.037); aperture width: 0.54–0.65 mm (mean: 0.601 $\pm$ 0.033 mm); number of whorls: 5–5.5.
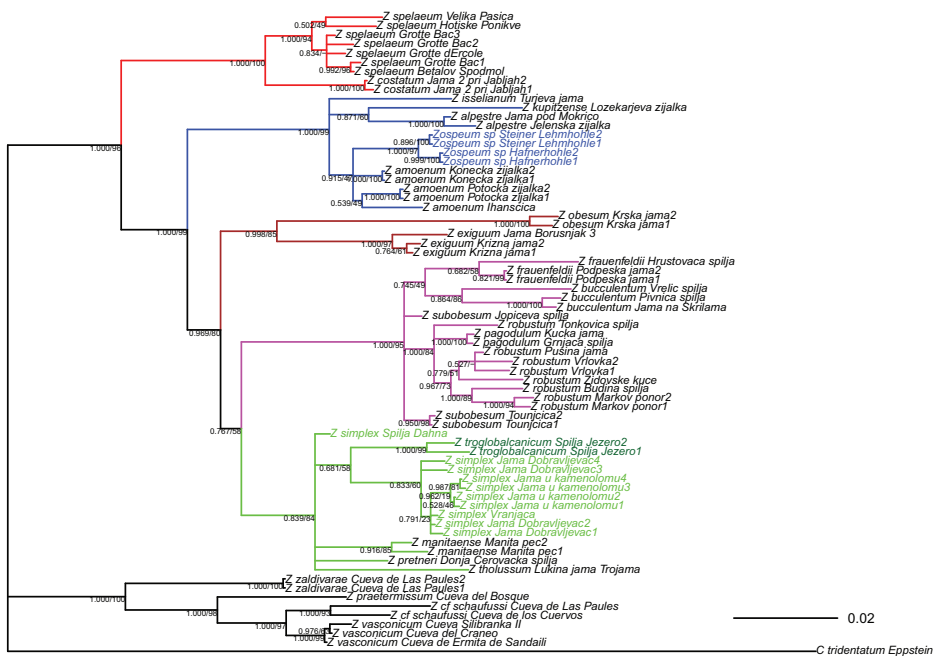
Figure 2. Bayesian tree of the genus *Zospeum*. Node support values of both the Bayesian Inference (front) and the Maximum Likelihood analysis (back) are given. Branches are coloured to denote the informal species groups within the eastern radiation of *Zospeum* following Inäbnit et al. (2019). Coloured sample names indicate specimens not included in the tree in Inäbnit et al. (2019): blue: Austrian specimens from Kruckenhauser et al. (2019); dark green: *Zospeum troglobalcanicum*; light green: *Zospeum simplex* sp. nov.

Description. Shell conical, translucent when fresh; suture deep; aperture somewhat roundish to reniform; parietal shield clearly differentiated from the rest of the lip, straight and thin; no lamellae present.

Differing from *Z. pretneri* and *Z. tholussum* by its broader shell and the differentiated parietal shield; differs from *Z. manitaense* by the absence of a visible parietalis in the aperture; barely differs from *Z.* aff. *troglobalcanicum* morphologically, on average with reduced shell broadness and a slightly deeper suture (see Remarks).

Distribution. Known from four caves (Jama Dobravljevac, Špilja Dahna, Jama u kamenolomu, Vranjača) in the municipality of Tomislavgrad in Bosnia-Herzegovina.

Etymology. Named *simplex* (= simple, unsophisticated) due to the lack of any form of shell sculpture or lamellae.

Remarks. Difficult to separate from *Z. troglobalcanicum* without genetic data (which is not uncommon in *Zospeum*; see Inäbnit et al. 2019). Both species have a nondescript shell without prominent shell sculpture or lamellae within the aperture. Absolon's (1916) description of *Z. troglobalcanicum* consisted out of a photograph
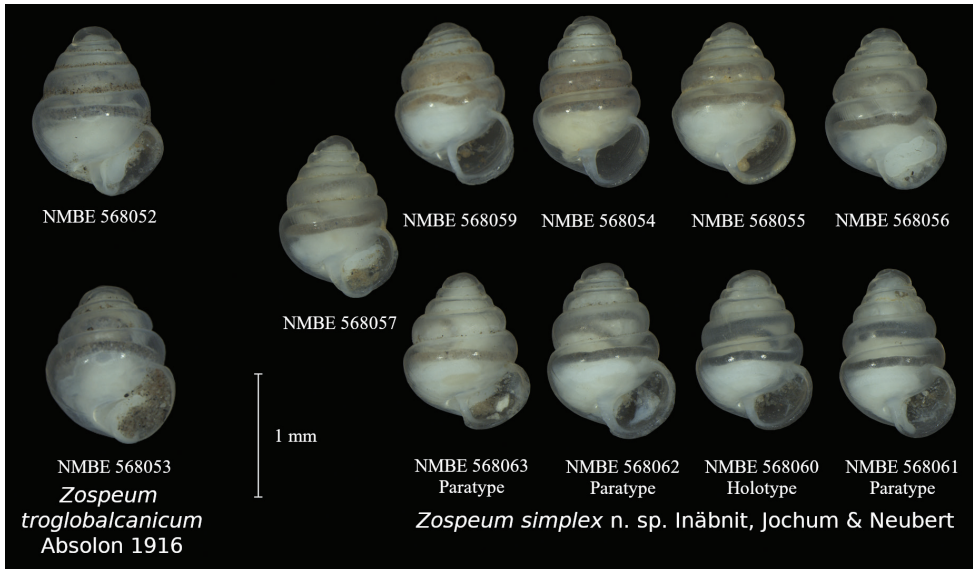
Figure 3. Specimens sequenced in this study. *Zospeum troglobalcanicum*: NMBE 568052 & 568053 (both from Špilja Jezero); *Zospeum simplex* sp. nov.: NMBE 568054 (Špilja Dahna), NMBE 568055–568057 (Jama u kamenolomu), NMBE 568059 (Vranjača), NMBE 568060 (Holotype, Jama Dobravljevac), NMBE 568061–568063 (Paratypes, Jama Dobravljevac)

depicting multiple specimens haphazardly clustered together in various positions and a legend that established the name and type locality. The lack of a written characterisation of the species in the original description and the fact that the specimens in the photograph weren't depicted in any standardised position makes a characterisation of the species fairly challenging (putative syntype specimen, collected by K. Absolon from the type locality, was only located very recently by AJ in Vienna (NHMW Mol.Coll.Edlauer 32.749) and couldn't be studied yet). From the photograph in Absolon (1916), the species can be characterised as similar to *Z. manitaense* in shell shape, without any visible lamella in the aperture and with a comparatively large parietal shield. The larger parietal shield might serve as a distinguishing character between *Z. simplex* and *Z. troglobalcanicum*, though the illustration of a topotypic specimen in Bole (1974; fig. 3h) might indicate that this character is variable within the population. The two specimens we preliminarily assigned to *Z. troglobalcanicum* (Fig. 3, NMBE 568052; Inäbnit et al. 2019: fig. 7u) only have a small parietal shield. As of now, the shell height:shell width ratio seems to be the most effective way of separating the two specimens from *Z. simplex* (*Z. simplex*: generally higher than 1.3 (one exception); *Z.* aff. *troglobalcanicum*: below 1.3), but that might just be due to the low sample sizes. Investigation of the inner aspects of the shells will be presented in a later work.

Discussion

The phylogenetic tree reconstructions (Fig. 2) agree mostly with those figured in Inäbnit et al. (2019). The main difference is that the node support values within the *Z. pretneri* group and in that of *Z. amoenum* are now fairly low and the topology is different. This can be explained by the high number of new specimens that sometimes are only represented by one marker (especially in *Z. amoenum*). It should also be noted that our current trees resolve *Z. robustum*, for which we didn't have any new specimens, with a significant node support as a monophyletic group (node support was not significant in Inäbnit et al. 2019, but the classification as an independent species could be justified via species delimitation methods). Since its position was not resolved with significant node support in either tree, the specimen from Tonkovića špilja is not included in *Z. robustum* in this tree, as was the case in Inäbnit et al. (2019). Due to lack of additional material, the classification within *Z. robustum* remains unchanged in this work.

The 12 *Zospeum* individuals from Bosnia-Herzegovina and Croatia, are the first to be molecularly assessed from the greatly understudied, southern extension of *Zospeum*'s distribution. Within the phylogenetic trees (Fig. 2, Suppl. material1), these specimens form a monophyletic group with a deep split between the two specimens from Croatia and nine of the ten specimens from Bosnia-Herzegovina (the remaining specimen from Špilja Dahna is only represented by a sequence of the conservative histone H3 gene, which doesn't usually resolve to species level).While recovered in all phylogenetic trees calculated for this work, this arrangement only has high node support values in the Suppl. material1, which was calculated without the conservative H3 and 28S nuclear markers. This result might indicate that conservative markers may have a destabilising effect on species level phylogeny within this group. Both ABGD schemes support the separation of the Croatian and Bosnia-Herzegovina individuals from each other at species level, though the seven-group scheme further subdivided the specimens from both geographical regions. We prefer to use the five-group scheme for the following reasons here: a) The barcode gap of the seven-group scheme is much lower (0.003) than the barcode gap (0.032) that was detected in the Carychiidae alignment in Weigand et al. (2011), while the barcode gap in the five-group scheme was slightly higher (0.043) than in Weigand et al. (2011); b) both individuals from Croatia (considered separate groups in the seven-group scheme) derive from the same cave and are unambiguously recovered as monophyletic and closely related in all trees, making their status as separate taxa unlikely. The divergence analysis further corroborates the results of the ABGD five-group scheme whereby the between-group divergence between the Croatian and the Bosnian groups (see Table 3) was within the general range of interspecific divergence within the *Z. pretneri* group. We thus, propose separating the individuals sequenced in this study into two species:

•   A species encompassing all ten specimens from Bosnia-Herzegovina. This species is described as *Z. simplex* sp. nov. above. Since we do not have enough molecular and morphological data for the individual from Špilja Dahna, we cannot confidently place it within *Z. simplex* right now. However, due to its close geo-

graphical proximity (less than 1 km) to one of the caves with genetically identified specimens (Jama u kamenolomu), we expect it could well be assignable to *Z. simplex* as no external morphological inconsistencies separate it from other *Z. simplex* specimens in our study.

• A species comprising two specimens from Špilja Jezero in the region of Dubrovnik. This locality is fairly close (around 22 km) to the type locality (Benetina pećina) of *Z. troglobalcanicum* Absolon, 1916. The sequenced specimens do not show any major external morphological differences from the specimen identified as *Z. troglobalcanicum* (as figured in Bole 1974: fig. 3h) and from those imaged in Inäbnit et al. 2019: fig. 7u), though the adult specimen clearly has a smaller parietal shield than the specimens figured in Absolon (1916). We propose tentatively classifying those specimens within *Z. troglobalcanicum* until genetic material from the type locality can clarify its status and the morphological investigation of the singular syntype (NHMW Mol.Coll.Edlauer 32.749) of this species can be taxonomically and nomenclaturally clarified in a separate work.

Even if it is not as large as the between-group divergence of other species pairs within the *Z. alpestre* group, our divergence analysis revealed that the between-group divergence between *Z. amoenum* and the two Austrian populations is greater than the within-group divergence of either lineage. Our analysis also found that the within-group divergence in *Z. amoenum* is only slightly increased if the Austrian populations are included within this species. These results agree with the tree reconstruction published in Kruckenhauser et al. (2019), which resolved the Austrian population as the sister group of *Z. amoenum*. Our trees, as mentioned above, lack the resolution to separate the Austrian populations from *Z. amoenum* and can thus, not confirm this conclusion. The ABGD scheme for the *Z. alpestre* group recovers the Austrian population as a separate group from *Z. amoenum* and splits the latter species into three groups. The barcode gap in this scheme is, however, much lower (0.016) than the one proposed for Carychiidae in Weigand et al. (2011), which was used for species classification within the *Z. alpestre* group before (e.g., in Weigand et al. 2013). We are thus, reluctant to draw conclusions regarding *Z. amoenum* and the Austrian specimens from the ABGD scheme. It may indicate some large intraspecific genetic variability within *Z. amoenum* (with the possibility of the presence of several species) that might coincide with the large morphological variation found in this species (Inäbnit et al. 2019), which would need to be addressed in a separate study with better sampling.

Zospeum amoenum described in Inäbnit et al. (2019) bears either a small parietalis that does not expand within the shell or it is lacking completely. Kruckenhauser et al. (2019) did not figure a specimen in which the configuration of the parietalis within the last whorl could be seen, but Gittenberger (1982) figured one specimen from the Hafnerhöhle (one of the two caves sampled by Kruckenhauser et al. 2019), where the parietalis was exposed. The parietalis of this specimen is slightly broadened three quarters of a whorl into the shell and seems to decrease expansion again further into the shell. Though the syntype of *Z. amoenum* (see Inäbnit et al. 2019: fig. 6L) shows a similar configuration of the parietalis, it is not congruent with the description of this structure in *Z. amoenum* assessed in Inäbnit et al. (2019).

Our study suggests that a final species assignment for the two Austrian populations is not possible until further supporting information becomes available. Until then, we classify these two Austrian populations as *Z. amoenum*, avoiding the now outdated classification of these populations with *Z. isselianum* (as was done in Kruckenhauser et al. 2019).

Acknowledgements

References

Absolon K (1916) Z výzkumných cest po krasech Balkánu. O balkánské temnostní zvířeně. Zlatá Praha 33: 574–576.

Bole J (1960) Novi vrsti iz rodu *Zospeum* Bourg. (Gastropoda). Biološki vestnik 7: 61–64.

Bole J (1974) Rod *Zospeum* Bourguignat 1856 (Gastropoda, Ellobiidae) v Jugoslaviji. Die Gattung *Zospeum* Bourguignat 1886 (Gastropoda, Ellobiidae) in Jugoslawien. Razprave – Slovenska akademija znanosti in umetnosti. Razred za naravoslovne vede 17: 249–291.

Böttger-Schnack R, Machida RJ (2011) Comparison of morphological and molecular traits for species identification and taxonomic grouping of oncaeid copepods. Hydrobiologia 666: 111–125. https://doi.org/10.1007/s10750-010-0094-1

Bouaziz-Yahiatene H, Pfarrer B, Medjdoub-Bensaad F, Neubert E (2017) Revision of *Massylaea* Möllendorff, 1898 (Stylommatophora, Helicidae). ZooKeys 694: 109–133. https://doi.org/10.3897/zookeys.694.15001

Bourguignat JR (1856) Aménités Malacologiques. § LI. Du genre *Zospeum*. Revue et Magasin de Zoologie pure et appliquée 8: 499–516.

Colgan DJ, McLauchlan A, Wilson GDF, Livingston SP, Edgecombe GD, Macaranas J, Cassis G, Gray MR (1998) Histone H3 and U2 snRNA DNA sequences and arthropod molecular evolution. Australian Journal of Zoology 46: 419. https://doi.org/10.1071/ZO98048

Folmer O, Black M, Hoeh W, Lutz R, Vrijenhoek R (1994) DNA primers for amplification of mitochondrial cytochrome c oxidase subunit I from diverse metazoan invertebrates. Molecular Marine Biology and Biotechnology 3: 294–299.

Frauenfeld von G (1854) Über einen bisher verkannten Laufkäfer beschrieben von L. Miller; und einen neuen augenlosen Rüsselkäfer, beschrieben von F. Schmidt; ferner einige von Schmidt in Schischka neu entdeckte Höhlentiere. Verhandlungen des Zoologisch-Botanischen Vereins in Wien 4: 23–34.

Frauenfeld von G (1856) Die Gattung *Carychium*. Sitzungsberichte der mathematisch-naturwissenschaftlichen Classe der Kaiserlichen Akademie der Wissenschaften 19: 70–93.

Freyer H (1855) Über neu endeckte Conchylien aus den Geschlechtern *Carychium* und *Pterocera*. Sitzungsberichte der mathematisch-naturwissenschaftlichen Classe der kaiserlichen Akademie der Wissenschaften 5: 18–23.

Gittenberger E (1975) Cave snails found in southern Crna Gora. Glasnik Republ. Zavoda zast. Prirode. Prirodnjackog muzeja 8: 21–37.

Gittenberger E (1982) Nachweis der Höhlenschnecke *Zospeum alpestre* (Freyer, 1855) in der Hafnerhöhle, Karawanken – Kärnten. Carinthia II 172: 351–354.

Guindon S, Dufayard J-F, Lefort V, Anisimova M, Hordijk W, Gascuel O (2010) New Algorithms and Methods to Estimate Maximum-Likelihood Phylogenies: Assessing the Performance of PhyML 3.0. Systematic Biology 59: 307–321. https://doi.org/10.1093/sysbio/syq010

Huelsenbeck JP, Ronquist F (2001) MRBAYES: Bayesian inference of phylogenetic trees. Bioinformatics 17: 754–755. https://doi.org/10.1093/bioinformatics/17.8.754

Inäbnit T, Jochum A, Kampschulte M, Martels G, Ruthensteiner B, Slapnik R, Nesselhauf C, Neubert E (2019) An integrative taxonomic study reveals carychiid microsnails of the troglobitic genus *Zospeum* in the Eastern and Dinaric Alps (Gastropoda, Ellobioidea, Carychiinae). Organisms Diversity & Evolution 19: 135–177. https://doi.org/10.1007/s13127-019-00400-8

Jochum A, de Winter AJ, Weigand AM, Gómez B, Prieto C (2015a) Two new species of *Zospeum* Bourguignat, 1856 from the Basque-Cantabrian Mountains, Northern Spain (Eupulmonata, Ellobioidea, Carychiidae). ZooKeys 483: 81–96. https://doi.org/10.3897/zookeys.483.9167

Jochum A, Prieto CE, Kampschulte M, Martels G, Ruthensteiner B, Vrabec M, Dörge DD, de Winter AJ (2019) Re-evaluation of *Zospeum schaufussi* von Frauenfeld, 1862 and *Z. suarezi* Gittenberger, 1980, including the description of two new Iberian species using Computer Tomography (CT) (Eupulmonata, Ellobioidea, Carychiidae). ZooKeys 835: 65–86. https://doi.org/10.3897/zookeys.835.33231

Jochum A, Slapnik R, Klussmann-Kolb A, Páll-Gergely B, Kampschulte M, Martels G, Vrabec M, Nesselhauf C, Weigand AM (2015b) Groping through the black box of variability: An integrative taxonomic and nomenclatural re-evaluation of *Zospeum isselianum* Pollonera, 1887 and allied species using new imaging technology (Nano-CT, SEM), conchological, histological and molecular data (Ellobioidea, Carychiidae). Subterranean Biology 16: 123–165. https://doi.org/10.3897/subtbiol.16.5758

Katoh K (2002) MAFFT: a novel method for rapid multiple sequence alignment based on fast Fourier transform. Nucleic Acids Research 30: 3059–3066. https://doi.org/10.1093/nar/gkf436

Katoh K, Standley DM (2013) MAFFT Multiple Sequence Alignment Software Version 7: Improvements in Performance and Usability. Molecular Biology and Evolution 30: 772–780. https://doi.org/10.1093/molbev/mst010

Kearse M, Moir R, Wilson A, Stones-Havas S, Cheung M, Sturrock S, Buxton S, Cooper A, Markowitz S, Duran C, Thierer T, Ashton B, Meintjes P, Drummond A (2012) Geneious Basic: An integrated and extendable desktop software platform for the organization and analysis of sequence data. Bioinformatics 28: 1647–1649. https://doi.org/10.1093/bioinformatics/bts199

Kruckenhauser L, Plan L, Mixanig H, Slapnik R (2019) Verwandtschaftsbeziehungen von Kärntner Populationen der Höhlenschnecke *Zospeum isselianum*. Die Höhle 70: 139–147.

Kumar S, Stecher G, Li M, Knyaz C, Tamura K (2018) MEGA X: Molecular Evolutionary Genetics Analysis across Computing Platforms. Battistuzzi FU (Ed.). Molecular Biology and Evolution 35: 1547–1549. https://doi.org/10.1093/molbev/msy096

Kuščer L (1932) Höhlen- und Quellenschnecken aus dem Flussgebiet der Ljubljanica. Archiv für Molluskenkunde 64: 60–61.

Lanfear R, Calcott B, Ho SYW, Guindon S (2012) PartitionFinder: Combined Selection of Partitioning Schemes and Substitution Models for Phylogenetic Analyses. Molecular Biology and Evolution 29: 1695–1701. https://doi.org/10.1093/molbev/mss020

Lanfear R, Frandsen PB, Wright AM, Senfeld T, Calcott B (2016) PartitionFinder 2: New Methods for Selecting Partitioned Models of Evolution for Molecular and Morphological Phylogenetic Analyses. Molecular Biology and Evolution: msw260. https://doi.org/10.1093/molbev/msw260

Palumbi S, Martin A, Romano S, McMillan WO, Stice L, Grabowski G (1991) The simple fool's guide to PCR version 2.0. University of Hawaii, Honolulu.

Pezzoli E (1992) Il genere *Zospeum* Bourguignat, 1856 in Italia (Gastropoda Polmonata Basommatophora). Censimento delle stazioni ad oggi segnalate. Natura Bresciana 27: 123–169.

Pollonera C (1887) Note malacologiche. I. Molluschi della Valle del Natisone (Friuli). Bullettino della Società Malacologica Italiana 12: 204–208.

Puillandre N, Lambert A, Brouillet S, Achaz G (2012). ABGD, automatic barcode gap discovery for primary species delimitation. Molecular Ecology, Vol.21: 1864–1877. https://doi.org/10.1111/j.1365-294X.2011.05239.x

Risso JA (1826) Histoire naturelle des principales productions de l'Europe méridionale et particulièrement de celles des environs de Nice et des Alpes Maritimes. Tome quatrième. F.G. Levrault, Paris, 439 pp. https://doi.org/10.5962/bhl.title.58984

Rossmässler EA (1838) Iconographie der Land- und Süsswasser-Mollusken, mit vorzüglicher Berücksichtigung der europäischen noch nicht abgebildeten Arten. 1: 2 (3/4). Arnoldische Buchhandlung, Dresden, Leipzig.

Schizas NV, Street GT, Coull BC, Chandler GT, Quattro JM (1997) An efficient DNA extraction method for small metazoans. Molecular Marine Biology and Biotechnology 6: 381–383.

Stamatakis A (2014) RAxML version 8: a tool for phylogenetic analysis and post-analysis of large phylogenies. Bioinformatics 30: 1312–1313. https://doi.org/10.1093/bioinformatics/btu033

Stummer A (1984) Eine neue Unterart der Höhlenschnecke *Zospeum alpestre* (Freyer) aus der Kupitzklamm bei Eisenkappel, Kärnten (Basommatophora: Ellobiidae). Heldia 1: 13–14.

Tamura K, Nei M, Kumar S (2004) Prospects for inferring very large phylogenies by using the neighbor-joining method. Proceedings of the National Academy of Sciences 101: 11030–11035. https://doi.org/10.1073/pnas.0404206101

Wade CM, Mordan PB (2000) Evolution within the gastropod molluscs; using the ribosomal RNA gene cluster as an indicator of phylogenetic relationships. Journal of Molluscan Studies 66: 565–570. https://doi.org/10.1093/mollus/66.4.565

Weigand A (2013) New *Zospeum* species (Gastropoda, Ellobioidea, Carychiidae) from 980 m depth in the Lukina Jama–Trojama cave system (Velebit Mts., Croatia). Subterranean Biology 11: 45–53. https://doi.org/10.3897/subtbiol.11.5966

Weigand AM, Jochum A, Pfenninger M, Steinke D, Klussmann-Kolb A (2011) A new approach to an old conundrum–DNA barcoding sheds new light on phenotypic plasticity and morphological stasis in microsnails (Gastropoda, Pulmonata, Carychiidae). Molecular Ecology Resources 11: 255–265. https://doi.org/10.1111/j.1755-0998.2010.02937.x

Weigand AM, Jochum A, Slapnik R, Schnitzler J, Zarza E, Klussmann-Kolb A (2013) Evolution of microgastropods (Ellobioidea, Carychiidae): integrating taxonomic, phylogenetic and evolutionary hypotheses. BMC Evolutionary Biology 13: e18. https://doi.org/10.1186/1471-2148-13-18

Supplementary material 1

Figure S1
Authors: Thomas Inäbnit, Adrienne Jochum, Raijko Slapnik, Eike Neubert
Data type: phylogenetic tree
Copyright notice: This dataset is made available under the Open Database License (http://opendatacommons.org/licenses/odbl/1.0/). The Open Database License (ODbL) is a license agreement intended to allow users to freely share, modify, and use this Dataset while maintaining this same freedom for others, provided that the original source and author(s) are credited.
Link: https://doi.org/10.3897/zookeys.1071.66417.suppl1